THE MECHANISMS OF METABOLIC REGULATION OF THE CLONED EQUIVALENT OF THE VASCULAR K_{ATP}/K_{NDP} CHANNEL

Tabasum Farzaneh

A thesis submitted to University College London, the University of London, in part fulfilment for the degree of DOCTOR OF PHILOSOPHY

Centre for Clinical Pharmacology
Department of Medicine
University College, London

September 2007

ProQuest LLC
789 East Eisenhower Parkway
P.O. Box 1346
Ann Arbor, MI 48106-1346

Abstract

At the molecular level, K_{ATP} is an octameric protein complex composed of an inwardly rectifying K^+ channel subunit (Kir6.*x*) which forms the channel pore and a regulatory sulphonylurea receptor subunit (SUR). By sensing intracellular nucleotide concentrations, K_{ATP} channels couple the membrane potassium conductance of a cell to its metabolic state.

To understand the molecular basis of metabolic regulation of the K_{ATP}/K_{NDP} channel Kir6.1/SUR2B, the cell-based Rubidium-86 ($^{86}Rb^+$) efflux assay was employed, using HEK293 cells as the expression system. $^{86}Rb^+$ efflux was activated on the addition of 10μM levcromakilim and metabolic poisoning (induced by 20mM 2-deoxyglucose and 2.5mM sodium cyanide), and inhibited by 10μM glibenclamide. The subsequent $^{86}Rb^+$ distribution between intracellular and extracellular space was determined via the measurement of Cherenkov radiation, the relative amount of $^{86}Rb^+$ in the cell supernatant being a direct measure of channel activity. The functionality of selected mutants was also investigated under physiological conditions by the perforated patch-clamp method, whereby currents were evoked via voltage clamp recordings over 1000ms voltage steps between -150mV and +50mV from a holding potential of -80mV.

ΔN-Kir6.1-ΔC truncations were made in an attempt to understand the role of the pore-forming subunit pharmacologically in channel gating, as has previously been shown for Kir6.2ΔC26. Mutants for which the RXR motif was removed were surface expressed (as shown via immunofluorescent staining using an anti-HA-fluorescein conjugated antibody), and showed increased basal efflux in the absence of SUR2B which was reduced by inhibitors which bind to the pore-forming subunit (1mM $BaCl_2$ or 100μM PNU-37883A). However, these mutants did not display intrinsic ATP sensitivity, as for ΔN-Kir6.2-ΔC, and for Kir6.1ΔC48/ΔN13 this was confirmed by perforated patch clamping.

When Kir6.1ΔC48/ΔN13 was expressed with SUR2B, glibenclamide was able to reverse efflux induced on metabolic inhibition, but it was suspected that under this condition the sterical conformation of the channel changed which prevented Kir6.*x*-specific inhibitors from binding (since they were not able to reverse metabolically induced efflux). In contrast, application of either 1mM $BaCl_2$ or 100μM PNU-37883A was able to reverse metabolically induced efflux for Kir6.2ΔC26/SUR2B. On the introduction of mutations into NBD1 or NBD2 (K708A and K1349M respectively) of SUR2B, Kir6.1/SUR2B K708A/K1349M was shown to be non-functional, whereas Kir6.2/SUR2B K708A/K1349M displayed normal pharmacology on the addition of KCOs and metabolic inhibitors.

In conclusion, Kir6.1/SUR2B is sensitive to metabolic poisoning in an analogous fashion to Kir6.2/SUR2B, but the Kir6.1 pore-forming subunit does not display intrinsic metabolic sensitivity, unlike Kir6.2. Metabolic sensitivity of Kir6.1/SUR2B is determined by both nucleotide binding domains of SUR2B, and finally the pharmacology of metabolically attenuated currents is different from those activated by a K_{ATP} channel opener.

Commonly used Abbreviations

ΔN	N-terminal deletion
ΔC	C-terminal deletion
$[ATP]_i$	intracellular ATP
2-DG	2-deoxy-glucose
$^{86}Rb^+$	86-rubidium
ABC	ATP-binding cassette
AMPK	5'-AMP-activated protein kinase
ATP	adenosine triphosphate
ADP	adenosine diphosphate
$BaCl_2$	barium chloride
CHO	chinese hamster ovary cells
cDNA	complementary DNA
DMSO	dimethylsulphoxide
DNA	deoxyribonucleic acid
E.coli	*Escherichia coli*
E_K	equilibrium potential for K^+ ions
GFP	green fluorescent protein
HBS	HEPES (4-(2-hydroxyethyl) piperazine-1-acid Buffered Saline
HEK293	Human Embryonic Kidney 293 cell line
IC_{50}	half maximal inhibitory concentration
K^+	potassium ion
K_{ATP}	potassium-ATP ion channel
KCB	potassium channel blocker
KCO	potassium channel opener
kbp	kilo base pairs
Kir	inwardly rectifying K^+ channel subunit

K_{NDP}	potassium-NDP ion channel
MgADP	magnesium adenosine diphosphate
MI	metabolic inhibition
NaCN	sodium cyanide
NBDs	nucleotide binding domains
PCR	polymerase chain reaction
PKA	protein kinase A
PKC	protein kinase C
PNU-37883A	4-morpholinecarboximidine-N-1-adamantyl-N'-cyclohexylhydrochloride
SEM	standard error of the mean
SUR	sulphonylurea receptor
VSM	vascular smooth muscle
W_A	walker A motif
W_B	walker B motif
CL	cytosolic loop
TM	transmembrane domain

Amino acids are abbreviated according to the standard one and three letter code

Acknowledgements

I would like to give my thanks to the following:

My primary supervisor, Professor Andrew Tinker, for his guidance, enthusiasm and optimism throughout my studies.

To Professors Lucie Clapp and Gordon Stewart for their critical appraisal of my work.

To Drs Philippe Behe, Jatinder Ahluwalia and Brian Tennant and for their valuable expertise and help with the patch-clamping.

To members of the Tinker Laboratory, past & present: Drs Alison Thomas, Sean Brown, Kathryn Quinn, Jon Giblin, Morris Muzyamba, Muriel Nobles, Steve Harmer, and Dr Keat-Eng Ng for their friendship and advise.

My Ph.D. was sponsored by the British Heart Foundation, without whom this work would not have been possible.

Special thanks to my parents, Mansour and Christine Farzaneh, and to my sisters Taraneh and Afsaneh Farzaneh for their support and encouragement.

Contents

List of Tables

List of Figures

Chapter One

Chapter Two

Chapter Three

Chapter Four

Chapter Five

Chapter One

Introduction

Chapter One: Introduction

1.1 Importance of Potassium Channels and the existence of Superfamilies

A typical excitable cell contains an intracellular potassium concentration of approximately 150mM, while the extracellular concentration lies in the range of 3-5mM (Hille 1992). This dis-equilibrium exists because of the differences that occur between the plasmalemmal permeabilities of Na^+, K^+, Ca^{2+} and Cl^-, and together with the activities of electrogenic pumps (principally the Na^+/K^+ ATPase), the activity of co-transporters (such as the Na^+/Ca^{2+} exchanger) and the synthesis of large, non-diffusable ions, a resting or basal membrane potential in the region of -60mV is generated. This varies according to the tissue concerned. The membrane potential (E_K) at which $[K^+]_i$:$[K^+]_o$ would be in equilibrium is around -90mV, and the modulation of K-channel gating offers the cell a method of altering its excitability status. When K^+ channels are opened, the membrane is hyperpolarised towards E_K, and its excitability decreases. Conversely, there is a significant K^+-conductance at resting membrane potentials, and K^+-channel closure results in membrane depolarisation and an increase in its excitability (Hille 1992).

K^+ channels play a crucial role in basic cellular functions such as excitability, secretion, proliferation and volume regulation. They occur in virtually every eukaryotic and prokaryotic cell, and with enormous advances made in the elucidation of their architecture and function, they are undoubtedly one of the best understood ion channels. The growing number of mutations in potassium channel genes that have been linked with disease illustrates the fundamental importance of K^+ channels to an organism: Bartter's syndrome (a rare disorder manifested by primary inherited renal tubular hypokalaemic metabolic alkalosis) long-QT syndrome (a heart disease in which is there is an abnormally long delay between depolarisation and repolarisation of the ventricles of the heart) and familial persistent hyperinsulinaemic hypoglycaemia of infancy (whereby the secretion of insulin is unregulated resulting in profound

hypoglycemia), are examples of diseases arising from mutations in K^+ channels or via altered K^+ channel function (Cohen 2003; Kleta and Bockenhauer 2006; Weese-Mayer, Ackerman et al. 2007).

The combination of electrophysiological and structural information has enabled the classification of K^+ channels into three superfamilies: (1) Kv channels (activated by a change in transmembrane voltage), (2) inward rectifier channels (Kirs) and (3) twin-pore inward rectifier channels.

Superfamily 1: K_V, K_A, and BK_{Ca}

The first K^+ channel subunit cloned was the *Shaker Drosophila* K^+ channel, and is thought to be related to this superfamily (Butler, Wei et al. 1989). Here the K^+ channels include the delayed rectifier (Kv), the 'A'-channel (K_A) and the large conductance, Ca^{2+} sensitive channel (BK_{Ca}). The α-subunits of the K_V channels consist of six transmembrane segments (S1 to S6), and one potential pore-forming region (H5) between S5 and S6 (*Figure 1.4*). The S4 region is positively charged, and is thought to act as a voltage sensor, and the amino (N-) and carboxy (C-) termini are located intracellularly. This structure is thought to be similar to that of the voltage-dependent Na^{2+} and Ca^{2+} channels, although the latter are formed by a single molecule, whereas K_V channels are formed of an aggregate of 4 subunits. The gating properties of the α-subunits can also be modulated by β-subunits (Isomoto, Kondo et al. 1997). Electrophysiologically, they are activated upon depolarisation, with typically outwardly-rectifying current-voltage relationships when measured under whole cell voltage-clamp conditions. They exhibit a wide range of time-dependent inactivation properties, ranging from very rapid (K_A) to essentially none (BK_{Ca}) (Isomoto, Kondo et al. 1997).

Superfamily 2: Kir and K_{ATP}

In 1993, the expression cloning of cDNAs encoding distinct inwardly rectifying K^+ channels (Kir) was reported (Ho, Nichols et al. 1993; Kubo, Baldwin et al. 1993), which led to the identification of the structure and function of the Kir subfamily. A variety of cells possess Kir channels, which stabilize the resting potential near the K^+ equilibrium potential, controlling cellular excitability. Their name is derived from the fact that inward currents evoked by hyperpolarisation are greater than currents elicited by depolarisation of the same amplitude. They also play a role in the maintenance of resting membrane potential, the regulation of action potential duration, in the secretion and absorption of K^+ ions across the membrane and in receptor-dependent inhibition of cellular excitability. Cells expressing a sufficient quantity of Kir channels are expected to have a resting potential near to E_K and may not excite automatically, but when stimulated exhibit action potentials with a long-lasting plateau when the abundance of voltage-gated outward K^+ channels is less frequent.

The inwardly rectifying K^+ channel proteins so far identified vary from ~ 360 to 500 amino acids long, and the amino acid homology is ~40% between members belonging to different subfamilies and ~60% between individual members within each subfamily (Nichols and Lopatin 1997). *Figure 1.1* details the seven subfamilies have now been identified, designated Kir 1.0-7.0.

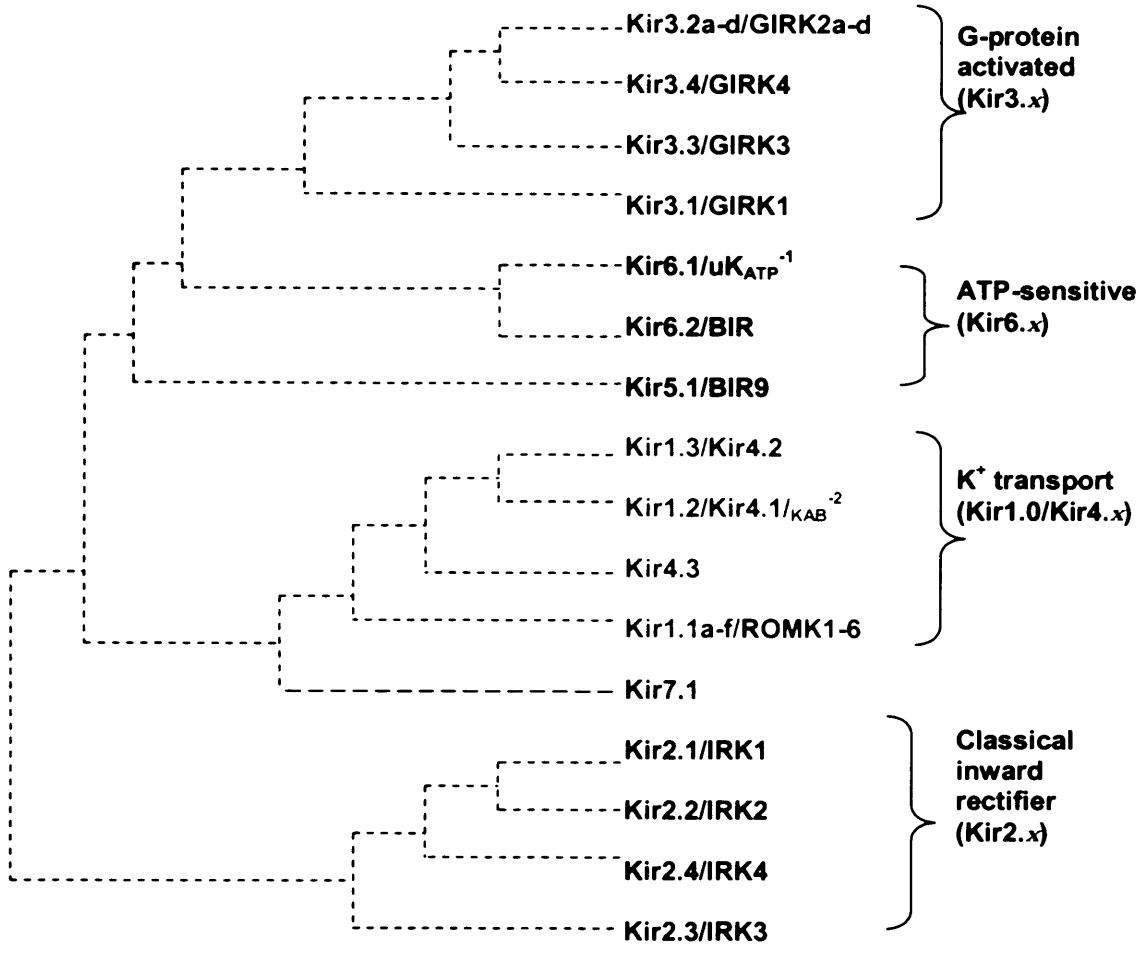

Figure 1.1: The evolutionary tree of the inward rectifying K^+-channel family with two-membrane-spanning domains (adapted from *Fujita & Kurachi; 2000*).

In contrast to the Kv superfamily, they comprise only two hydrophobic transmembrane-spanning segments separated by the conserved H5 region that determines K^+ selectivity (*Figure 1.3*). The classic Kir channels such as Kir2.*x* conduct modest currents at physiological potentials, but exhibit a markedly-enhanced current flow negative to E_K. This inwardly-rectifying behaviour, illustrated in *Figure 1.2*, is a function of the membrane potential and $[K^+]_0$. The Kir6.*x* family members are unique in that they form a heteromultimeric K^+ channel/receptor complex together with sulphonyl urea receptor subunits to exert K^+ channel function, i.e. form the K_{ATP}

channel (Inagaki and Seino 1998; Aguilar-Bryan and Bryan 1999). K_{ATP} channels are "weak" inward rectifiers; they are modulated by changes in intracellular ATP, $[ATP]_i$, and as the $[ATP]_i$ increases, K_{ATP} closes, while channel opening is associated with a lowering of $[ATP]_i$. $I_{k(ATP)}$ currents show no time-dependent activation, and I-V relationships show some evidence of inward rectification, but this effect is small compared with K_{ir} channels (Ashcroft and Ashcroft 1990).

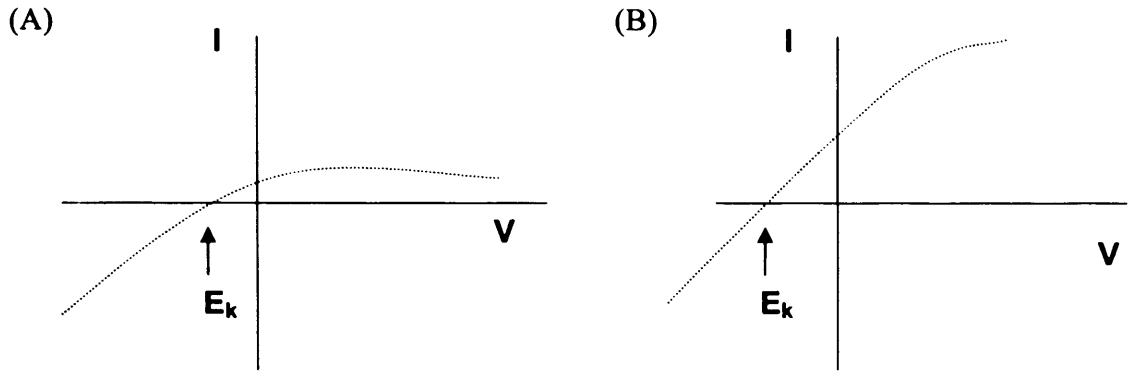

Figure 1.2: A theoretical current/voltage relationship for (A) a strong and (B) a weak inward rectifier (such as K_{ATP}) generated during a ramp protocol.

Superfamily 3: Twin-Pored Inward Rectifier Channels

A novel yeast K^+ channel subunit (TOK1), structurally equivalent to a Kir subunit in tandem with a six-transmembrane domain K_V subunit and which expressed outwardly rectifying K^+ currents in *Xenopus* oocytes has been described (Ketchum, Joiner et al. 1995), as has the cloning and expression of a mammalian channel (TWIK-1), which consists of two transmembrane domain channels in tandem (Lesage, Reyes et al. 1996). Since the expressed currents through TWIK-1 channels appear to be weakly inwardly rectifying, similar to those expressed by Kir1.1 channels, it is possible that a generation of novel Kir channels arose from a gene duplication (Lesage, Reyes et al. 1996). They play an important role in the background potassium conductance of a wide range of tissues with poor pharmacology.

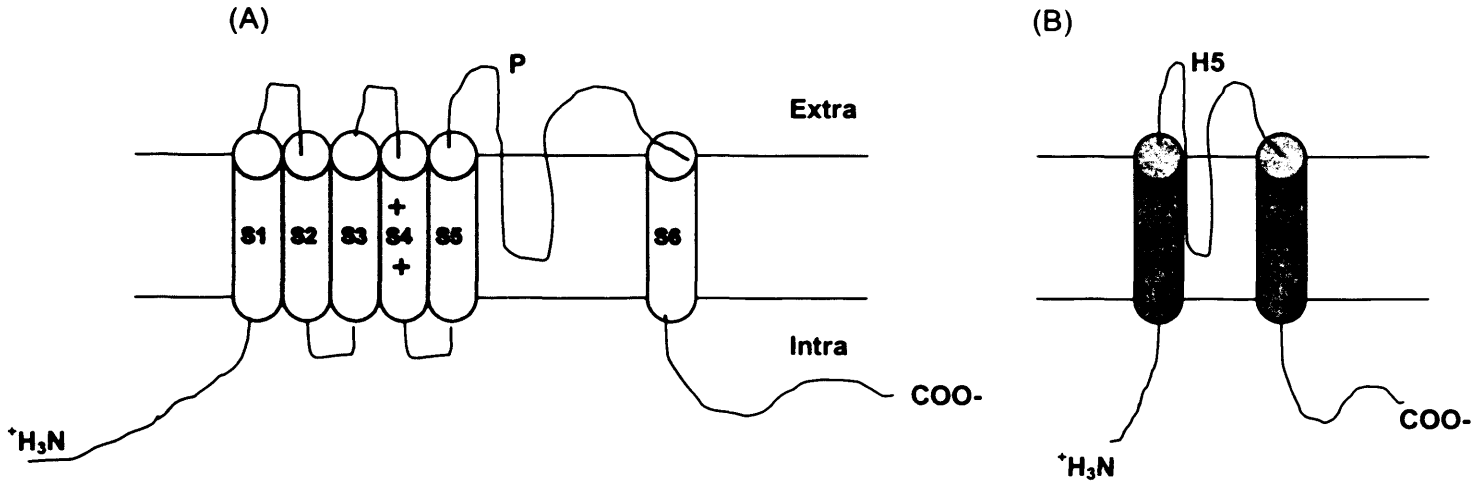

Figure 1.3: Structures of a pore-forming subunit of an α-subunit of K_V channels (A) and Kir channels (B). Putative transmembrane segments are numbered. H5 and P are pore-forming regions. S4 is the voltage-sensitive segment.

The ATP-binding cassette (ABC) Superfamily

The ABC transporter superfamily is one of the largest groups of proteins involved in active transport across cell membranes, their characteristic feature being the highly conserved ATP-binding cassette in the molecules (Hyde, Emsley et al. 1990). Existing in all species, with 29 members known in yeast, 69 in *E.coli* (accounting for 5% of its genomic coding capacity) and 48 in human, they couple the transport of various compounds to ATP-binding and hydrolysis (Dean, Hamon et al. 2001). Many have great clinical significance: MDR1 confers cancer resistance to chemotherapeutic drugs (Gottesman 1988), and mutations of ABCR, CFTR and cMOAT cause Stargardt macular dystrophy of eyes (Allikmets, Gerrard et al. 1996), cystic fibrosis (Riordan, Rommens et al. 1989) and Dubin-Johnson (Paulusma, Bosma et al. 1996) syndrome respectively all of which are caused by the failure to export a specific ligand across a lipid bilayer. ABC proteins can be regarded as active transporters, using the energy of ATP hydrolysis: many regulate ion channels. CFTR is a Cl^- channel itself and regulates the outwardly rectifying Cl^- channel (ORCC) and the epithelial sodium channel (ENaC) (Stutts, Canessa et al. 1995). MDR1 has been considered to be a regulator of the

volume-sensitive chloride channel (Miwa, Ueda et al. 1997). The clinically relevant and atypical ABC proteins in human are shown in *Table 1.1*.

ABC Protein	Ligand(s)/Function	Associated Disease(s)
ABC1	Cholesterol	Tangier disease
ABCR	Retinal	Various eye diseases (Stargardt)
TAP1/2	Peptides	Bare lymphocyte syndrome
ABC7	Iron	Anemia and XLSA
MRP6	?	Pseudoxanthoma elasticum
ALD	vlcFA	Adrenoleukodystrophy
Sterolin ½	Sterols	Sitosterolemia
PGY3/MDR3	Phosphatidylcholine	Liver disease: PFIC3, OC
BSEP/SPGP	Bile acids	Liver disease: PFIC2
MRP2	Conjugated bilirubin	Liver disease: D-J syndrome
MDR1	Hydrophobic drugs	Failure of chemotherapy
BCRP/MXR	Hydrophobic drugs	
MRP1	Conjugated drugs	
MRP4	Conjugated nucleosides	
	Atypical ABC proteins (Nontransporter)	
CFTR	Chloride ion channel	Cystic fibrosis
SUR	Regulation of K_{IR} channel	PHHI
SMC1-6	Chromosome maintenance	
Rad50	DNA, telomere repair	
MutS	DNA mismatch repair	
MSH2/6	DNA mismatch repair	
Elf1p	mRNA trafficking	

Abbreviations: XLSA, X-linked sideroblastomic anemia; PFIC, progressive familial intrahepatic cholestasis; OC, obstetric cholestasis; D-J, Dubin-Johnson syndrome; PHHI, persistent hyperinsulinemic hypoglycemia of infancy

Table 1.1: The clinically relevant and atypical ABC proteins in humans with their corresponding ligands/functions and associated diseases (adapted from *Linton; 2007 & Higgins & Linton; 2004*).

In bacteria, both complete and partial structures of ABC transporters have been determined (Oswald, Holland et al. 2006), revealing that they are dimeric and consist of two transmembrane domains (TMDs), which form the ligand binding sites and provide specificity, and two nucleotide binding domains (NBDs) which bind and hydrolyse ATP to drive the translocation of the bound ligand. The NBDs are well conserved in both

sequence and structure throughout the family, and have several characteristic motifs, including the W_A and W_B motifs an intervening linker motif (LSGGQ) which is unique to all ABC proteins and is thus known as the ABC signature, and stacking aromatic D, H, and Q loops. The W_A and W_B motifs are specifically involved in nucleotide binding and hydrolysis, but the function of the signature sequence is less clear, and is thought that the linker serines are involved in transducing nucleotide binding into channel activation. Via these conserved regions, ATP binding and hydrolysis is often coupled to changes in protein activity in all ABC proteins. The transmembrane domain sequences, on the other hand, are poorly preserved. The exact order of the TMDs and NBDs varies and can be encoded on different polypeptides or fused together in any combination. These domains are often separate subunits that co-assemble to produce a functional ABC protein in prokaryotes, whereas in eukaryotes a single gene usually encodes both NBDs and TMDs (Linton and Higgins 1998; Campbell, Sansom et al. 2003).

Functional studies involving both bacterial and eukaryotic ABC proteins have indicated that the two NBDs of ABC proteins interact and operate as a functional unit (Kerr 2002). It would appear that the NBDs dimerize in a nucleotide-sandwich conformation, with the signature sequence (linker) of one NBD monomer located close to the W_A motif of the other. Crystallographic and functional studies of ABC proteins have provided experimental evidence in favour of this conformation (Locher, Lee et al. 2002).

A model of the SUR1-NBD dimer with bound ATP is shown in *Figure 1.4.* ATP lies in the binding pocket formed by the W_A and W_B motifs of one NBD and the linker motif of the other. An aspartate in the W_B motif co-ordinates the Mg^{2+} ion of Mg-ATP and is required for nucleotide binding. A lysine in the W_A motif interacts with the γ and β phosphate groups of ATP, and is essential for ATP hydrolysis (Higgins 1992). Aside from the established role of each of the NBDs in nucleotide hydrolysis, the signature linker sequence is thought to be critical for transduction (Kerr 2002). The model depicts that the W_A and W_B of NBD1 associate with the linker sequence of NBD2, and

vice versa. The nucleotide-binding pockets are referred to as 'site 1' (Walker motifs of NBD1, linker NBD2) and 'site 2' (Walker motifs of NBD2, linker NBD1). The structural details of the ATPase cycle and the interaction between the two NBDs of ABC transporters are still controversial however (Matsuo, Dabrowski et al. 2002).

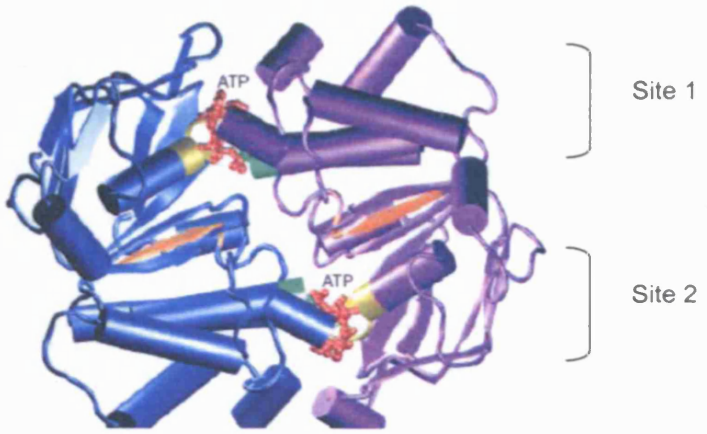

Figure 1.4: A model of the NBDs of SUR1, showing the nucleotide-sandwich dimer and the conserved motifs. The W_A motif (yellow), W_B motif (orange) and the signature sequence (green) are shown. NBD1 is blue, and NBD2 is purple, and sites 1 and 2 are indicated. The binding pocket thought to be formed by the MgATP molecule (red) is also depicted (taken from *Campbell et al., 2003*).

The strong conservation of sequence and structure in the NBD of ABC proteins with diverse functions suggests that this domain may be the site at which a common mechanism occurs to power a variety of cellular processes in a similar fashion.

1.2 General features of ATP-sensitive K^+ channels

ATP-sensitive K^+ (K_{ATP}) channels were originally discovered in the heart (Noma 1983), and are widely distributed in many cells and tissues including pancreatic ß-cells (Ashcroft, Harrison et al. 1984; Cook and Hales 1984; Rorsman and Trube 1985) brain (Ashford, Sturgess et al. 1988; Amoroso, Schmid-Antomarchi et al. 1990), skeletal (Spruce, Standen et al. 1985), smooth muscles (Standen, Quayle et al. 1989) and kidney (Hunter and Giebisch 1988). They are inhibited by intracellular ATP and activated by MgADP (Noma 1983; Ashcroft 1988), and by sensing changes in intracellular adenine nucleotide concentration, couple the altered metabolic state of the cell, for example

with hyperglycemia, hypoglycaemia, ischemia and hypoxia, to membrane potential (Yokoshiki, Sunagawa et al. 1998). K_{ATP} channels exhibit characteristic pharmacological properties. Antidiabetic sulfonylurea derivatives, e.g. glibenclamide and tolbutamide, selectively inhibit them, whereas agents such as pinacidil, levcromakalim and nicorandil activate them. *Table 1.2* shows that heterologous expression of two types of Kir6.*x* subunit and three main SUR subunits in differing combinations reconstitutes different types of K_{ATP} channel with distinct electrophysiological properties and nucleotide and pharmacological sensitivities, reflecting the various K_{ATP} channels in native tissues.

Subunit composition	Type
Kir6.2/SUR1	Pancreatic ß-cell (*Inagaki et al., 1995; Sakura et al., 1995*)
Kir6.2/SUR2A	Cardiomyocyte (*Inagaki et al., 1996*)
Kir6.2/SUR2B	Non-vascular smooth muscle? (*Isomoto et al., 1996*)
Kir6.1/SUR2B	Vascular smooth muscle (*Yamada et al., 1997*)

Table 1.2: Subunit composition of K_{ATP} channels in various tissues

The physiological role of K_{ATP} channels has been best characterised in insulin-secreting pancreatic ß-cells (Cook, Satin et al. 1988; Ashcroft and Rorsman 1989), whereby an increase in glucose metabolism leads to an increase in ATP concentration which closes the K_{ATP} channels. This closure results in depolarization of the ß-cell membrane, leading to opening of the voltage-dependent calcium channels (VDCCs) allowing calcium influx. The subsequent rise in intracellular calcium concentration in the ß-cell triggers exocytosis of insulin-containing granules. It is therefore apparent that K_{ATP} channels in ß-cells are critical in the regulation of glucose-induced insulin secretion.

The K_{ATP} channel is a hetero-octameric complex comprising either Kir6.1 or Kir6.2 and a regulatory Sulphonylurea Receptor (SUR) subunit, so named because it binds sulphonylureas (that are used for the treatment of type 2 diabetes mellitus) with high

affinity (Ashcroft and Gribble 1998; Aguilar-Bryan and Bryan 1999; Seino 1999). There is roughly 70% amino acid identity between Kir6.1 and Kir6.2 (Inagaki, Tsuura et al. 1995). In inwardly rectifying K^+ channels there is a highly conserved Gly-Tyr-Gly motif in the H5 region, critical for ion selectivity. However, in Kir6.*x* members this is Gly-Phe-Gly. Sulphonylurea receptors belong to members of the ABC protein superfamily (Higgins 1992) and two isoforms, SUR1 and SUR2, exist. The partial amino acid sequence of [^{125}I]-iodoglibenclamide binding to purified protein was used to obtain the first clone of SUR1 from the pancreatic ß-cell cDNA libraries (Aguilar-Bryan, Nichols et al. 1995). SUR2, now renamed SUR2A, was subsequently cloned by homology screening using SUR1 as a probe (Inagaki, Gonoi et al. 1996). There is a major variant of SUR2A, SUR2B, resulting from alternative splicing (Chutkow, Simon et al. 1996; Isomoto, Kondo et al. 1996; Chutkow, Makielski et al. 1999). These splice variants differ by 42 amino acids in the C-terminus, and consequently the C-terminus of SUR2B is similar to SUR1. A further splice variant of SUR2A, SUR2C, which has a deletion of 35 amino acids in the intracellular loop between the 11th and 12th membrane spanning domains has also been cloned, but its function is not clear (Chutkow, Simon et al. 1996; Ashcroft and Gribble 1998). Further alternative splicing events have also been observed for SUR2, and a total of six splice variants of SUR1 have been identified to-date (Shi, Ye et al. 2005). Studies with membrane-impermeable biotinylating reagents (Conti, Radeke et al. 2001) have confirmed that the sulfonylurea receptor is composed of three transmembrane domains, TMD0, TMD1 and TMD2, each of which consists of five, six and six membrane spanning regions respectively. This topographical arrangement is illustrated in *Figure 1.5*. SURs also have two nucleotide binding folds (NBD1 and NBD2) with W_A and W_B motifs on the cytoplasmic side of the cell. They are located in the loop between TMD1 and TMD2 and in the C-terminus respectively (Conti, Radeke et al. 2001). The Walker motifs are crucial for stimulation of K_{ATP} gating by ATP and NDPs in the presence of Mg^{2+}. Biochemical studies have indicated that the molecular mass of the glycosylated complex of Kir6.2/SUR1 to be 950kDa (Clement, Kunjilwar et al. 1997), indicating that the K_{ATP} channel is likely to be a hetero-octameric complex of

Kir6.2 and SUR1 in a 4:4 stoichiometry (Clement, Kunjilwar et al. 1997; Inagaki, Gonoi et al. 1997; Shyng, Ferrigni et al. 1997).

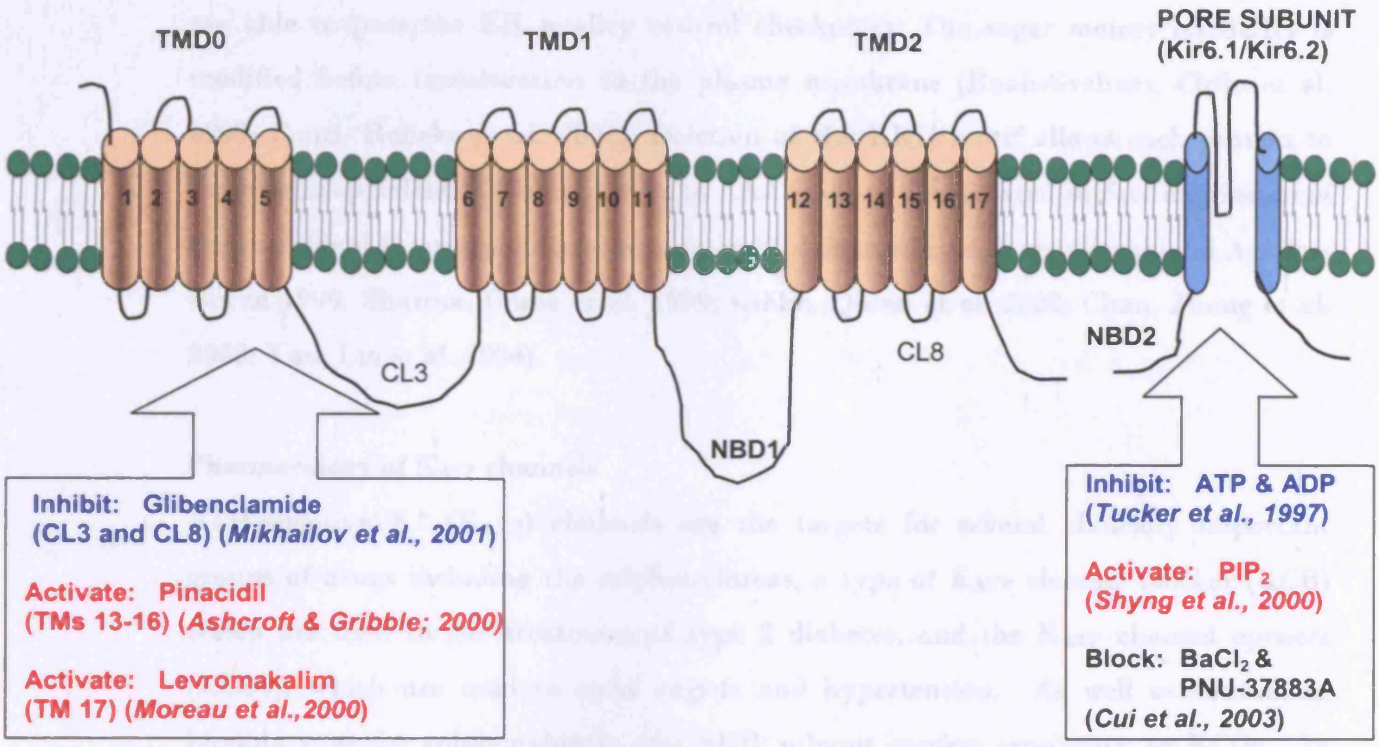

Figure 1.5: Transmembrane topology of a single SUR (left) and Kir6.*x* (right) subunit of a K_{ATP} channel. The sites of channel activators and inhibitors, including the suspected sites of action of the KCOs and KCBs used in this thesis, are shown.

Co-expression of Kir6.*x* and SUR is necessary to generate significant plasmalemmal currents, and aside from functional regulation, both subunits are required for cell surface expression of the channel. There is a wealth of evidence to suggest that Kir6.2 and SUR1 contain small tripeptide Arg-Lys-Arg motifs (RKR) that act as a quality control mechanism, ensuring surface expression of only properly assembled octameric proteins (Zerangue, Schwappach et al. 1999). In smooth muscle-type K_{ATP} channels, it remains elusive as to which of the many factor(s) modify the expression of K_{ATP} channel components in the cell plasma membrane, although the RKR motif is

considered to play an important role here too (Zerangue, Schwappach et al. 1999). It has been proposed that in partially and preassembled channel proteins, the RKR motif is exposed and that this either prevents export of the protein from the ER and/or retrieves it from the golgi. Upon complete assembly of the channel complex, the RKR motifs become shielded to allow the channel to traffic to the plasma membrane as they are able to pass the ER quality control checkpoint. The sugar moiety on SUR1 is modified before translocation to the plasma membrane (Raab-Graham, Cirilo et al. 1999; Conti, Radeke et al. 2001). Deletion of the RKR motif allows each protein to express independently, and mutation to AAA leads to unregulated surface expression of the individual subunits and partially assembled channel complexes (Bryan and Aguilar-Bryan 1999; Sharma, Crane et al. 1999; Giblin, Quinn et al. 2002; Chan, Zhang et al. 2003; Yan, Lin et al. 2004).

Pharmacology of K_{ATP} channels

ATP-sensitive K^+ (K_{ATP}) channels are the targets for several clinically important groups of drugs including the sulphonylureas, a type of K_{ATP} channel blocker (KCB) which are used in the treatment of type 2 diabetes, and the K_{ATP} channel openers (KCOs), which are used to treat angina and hypertension. As well as containing binding sites for sulphonylureas, the SUR subunit confers sensitivity to KCOs. In general, channel activation by KCOs leads to hyperpolarisation of the cell membrane, with the functional consequences obviously depending on the tissue involved.

A chimaeric approach has been used to localize the binding sites for KCOs within SUR2, based on the fact that openers such as pinacidil, cromakilim and P1075 are highly effective on SUR2 but not SUR1-containing K_{ATP} channels. TMD2 was implicated as critical for KCO action. Activation by pinacidil was conferred by the transfer of TMs 13-16 from SUR2A into SUR1, whereas the reverse swap impaired pinacidil sensitivity (Ashcroft and Gribble 2000).

Chimerical studies in which regions within TMD2 were swapped between SUR1 and SUR2, have shown that part of CL7 and TMs 16-17 are important for both P1075 binding and channel activation by openers, although there are differences depending on the KCO used (Reimann, Proks et al. 2001). Using a cromakilim analogue, it was shown that transfer of TM17 from SUR2A was sufficient to confer opener sensitivity to SUR1, and that amino acids L1249 and T1253 of TM17 of SUR2 are critical for opener action (Moreau, Jacquet et al. 2000). Diazoxide activates Kir6.2/SUR1 and Kir6.2/SUR2B channels when MgATP is present and Kir6.2/SUR2A channels when MgADP is present. Transfer of TMs 6-11 together with NBD1 from SUR1 conferred diazoxide sensitivity on SUR2A, suggesting that these regions are involved in diazoxide action. It has been suggested that diazoxide may occupy the same binding site as other KCOs, but that TMs 6-11 and NBD1 couple diazoxide to the gating mechanism for Kir6.2 (Babenko, Gonzalez et al. 2000).

Nucleotides are also important for the action of KCOs. It has been proposed that nucleotide binding or hydrolysis at the NBDs act allosterically to increase the affinity of the KCO binding site, and allosteric effects can act in the opposite direction to alter channel-nucleotide interactions in response to KCOs. Pinacidil, for example, can stabilize MgADP binding to Kir6.1/SUR2B (Satoh, Yamada et al. 1998). Pinacidil also increases ATP hydrolysis by NBD2, and contributes to channel activation via stabilization of the Mg-nucleotide bound state (Zingman, Alekseev et al. 2001).

The sulphonylurea and glinide drugs bind to SUR1 of the β-cell K_{ATP} channel to cause channel closure and initiate insulin secretion. Chimeric and mutagenesis studies have implicated TMD2 as a high affinity binding site in SUR1. In particular the serine residue S1237 within cytoplasmic loop CL8 is critical for high affinity drug binding (Ashfield, Gribble et al. 1999). The L0 linker (CL3) has also been implicated, and it has been suggested that native SUR1 L0 and CL8 lie in close proximity, leading to the formation of the sulphonylurea binding site (Mikhailov, Mikhailova et al. 2001).

Non-selective compounds such as glibenclamide, show high affinity block of SUR2 and SUR1 channels. SUR1-selective agents such as tolbutamide, do not show high affinity block of SUR2 channels and in structural terms contain a non-sulphonylurea region. Aside from the critical Serine 1237 residue found in SUR1 alone, there is a site that binds meglitinide-like structures and which is common to SUR1 and SUR2 (Gribble and Reimann 2003). The effect that MgADP has on channel inhibition by sulphonylureas also differs between SUR1 and SUR2-containing channels. MgADP impairs sulphonylurea inhibition of SUR2-containing K_{ATP} channels, yet enhances inhibition of SUR1-containing K_{ATP} channels (Gribble, Tucker et al. 1998). In the latter, sulphonylurea binding prevents MgADP activation, but weak inhibition at the inhibitory site of Kir6.2 remains, giving an apparent increase in block of the drug (Gribble and Reimann 2003). The regions responsible for this differential effect have been identified as TMs 8-11 of TMD1 and the first part of NBD1 (Reimann, Dabrowski et al. 2003).

There are two novel K_{ATP} channel inhibitors: PNU-37883A and PNU-99963. Both compounds inhibit relaxation of blood vessels and hypotension induced by KCOs. PNU-99963 has demonstrated little selectivity between different K_{ATP} channels and appears to act primarily through the SUR subunit. PNU-37883A blocks K_{ATP} channels of the smooth muscle and appears to act with the pore-forming subunit, with selectivity for Kir6.1 over Kir6.2 (Surah-Narwal, Xu et al. 1999). Chimerical experiments have lead to the suggestion that PNU-37883A sensitivity resides in an 81 amino-acid section of the C-terminus of Kir6.1 (Kovalev, Quayle et al. 2004). Conversely, another study has reported sensitivity for PNU-37883A for SUR2B-containing channels, but little discrimination between Kir6.1/SUR2B and Kir6.2/SUR2B (Cui, Tinker et al. 2003).

1.3 Regulation of the ATP-sensitive K^+ channel by nucleotides

The unusual molecular architecture of K_{ATP} channels is related to their complex gating behaviour. In a nutshell, intracellular ATP, $[ATP]_i$, inhibits K_{ATP} channels by directly binding to the Kir6.*x* subunits, whereas MgADP increases channel activity upon the hydrolysis of ATP to ADP at NBD2 of SUR. The membrane phospholipid phosphoinositol 4,5-bisphosphate, PIP_2, also interacts with the Kir to increase channel open probability and gating. This ATP/ADP dependence allows K_{ATP} channels to link metabolism to membrane excitability; important for many physiological functions, such as insulin secretion.

$[ATP]_i$ is the main regulator of classical K_{ATP} channels and has the dual function of closing the channel and maintaining channel activity in the presence of Mg^{2+} (Trube and Hescheler 1984; Findlay and Dunne 1986; Ohno-Shosaku, Zunkler et al. 1987; Takano, Qin et al. 1990). $[ATP]_i$ demonstrates ligand action and hydrolysis dependent action. $[ATP]_i$ binding to the K_{ATP} channel is assumed to be required for activity, which persists as long as $[ATP]_i$ is bound to the channel. Hydrolysis of $[ATP]_i$ in the presence of Mg^{2+} is also required, whereby when the channel is operative, $[ATP]_i$ inhibits channel opening, and when channels are not operative, treatment with MgATP restores channel opening. NDPs are also major regulators of K_{ATP} channel activity, having two distinct actions: (1) attenuating ATP-induced channel inhibition via competition with the binding of $[ATP]_i$ to the K_{ATP} channels and (2) permitting K_{ATP} channel opening even after channel rundown (Faivre and Findlay 1989; Dunne and Petersen 1991; Tung and Kurachi 1991; Beech, Zhang et al. 1993; Terzic, Tung et al. 1994). However, the absolute concentrations of ATP and ADP are critical in channel regulation. Patch clamping studies have demonstrated very clearly that for the same ATP/ADP ratio, high concentrations of ATP and ADP result in channel inhibition, whereas low concentrations support channel activity, i.e. that nucleotides exert both stimulatory and inhibitory actions on channel activity, and the inhibitory action of ADP dominates at concentrations that are greater than 1mmol/l (Tarasov, Dusonchet et al. 2004).

By varying their open probability in accordance with changes in the [ATP]/[ADP] ratio inside the cell, ATP-sensitive potassium channels link cellular metabolism to membrane excitability (Ashcroft 2006). K_{ATP} channels sense changes in energy metabolism in several ways: (1) via direct interactions between the channel and cell metabolites (producing intermediate and sequential effects on channel activity), (2) via the physiological effects of adenosine and (3) via regulation of K_{ATP} gene expression by energy metabolism (producing a delayed, but more profound affect on channel quantity) (Zhuo, Huang et al. 2005). They may also exert trafficking effects (Zerangue, Schwappach et al. 1999). The underlying question, where K_{ATP} regulation is concerned, has always been which properties of the K_{ATP} channel are intrinsic to Kir and which are endowed by SUR. The primary site at which intracellular free ATP acts to cause K_{ATP} channel inhibition appears to lie on Kir6.2 (Nichols and Lederer 1991; Ashcroft and Gribble 1998; Ribalet, John et al. 2003), whereas the SUR subunit is the primary site for pharmacological agents (Aguilar-Bryan, Nichols et al. 1995; Inagaki, Gonoi et al. 1996). The SUR subunit also mediates the stimulatory effects of intracellular MgADP and enhances channel open probability (Nichols, Shyng et al. 1996; Proks and Ashcroft 1997; Trapp, Tucker et al. 1997; Tucker, Gribble et al. 1997).

Studies involving Kir6.2

Despite the fact that Kir6.2 contains no obvious consensus sequences for nucleotide binding, a single mutation in the subunit (K185Q) significantly reduces the ability of ATP to inhibit channel activity (Tucker, Gribble et al. 1997). This information suggested that the site at which ATP mediates channel inhibition resides on Kir6.2. The ability of ATP in the absence of Mg^{2+}, or non-hydrolysable analogues of ATP to inhibit channel activity, suggests that ATP hydrolysis is not required for channel inhibition, and that binding of the molecule is sufficient for channel closure (Ashcroft and Rorsman 1989). The inhibitory effects of ATP were analysed using Kir6.2ΔC26 and Kir6.2ΔC36 isoforms expressed in the absence of SUR, since this overcomes the problem of the dual ability of nucleotides to both stimulate and inhibit wild-type K_{ATP} channels (Tucker, Gribble et al., 1997). The C-terminal domain of Kir6.2 expressed in *E.coli*

binds the ATP analogue, 2'3'-O-(2,4,6-trinitrophenylcyclo-hexadienylidene), and it therefore became apparent that both the ß-phosphate and moieties within the adenine ring were critical for K_{ATP} channel inhibition by ATP (Tanabe, Tucker et al., 1999). Site-directed mutagenesis studies and changes in single channel patch clamping kinetics identified that regions in the N-terminus immediately preceding TM1 and the C-terminus immediately following TM2 are equally important. Various other mutations at the cytosolic end of TM2 were similarly identified, and found to significantly reduce the frequency of the long closed channel state, suggesting that they impair the ability of the channel to close, and that they form part of an intracellular gate that governs access to the channel pore (Proks, Gribble et al., 1999; Tanabe, Tucker et al., 1999).

Other mutations did not affect single channel kinetics, and may reduce ATP inhibition via interfering with ATP binding or the link between ATP binding and channel closure (Tucker, Gribble et al. 1998). Aside from the K185 mutant, mutations in R50, I182, R201 and G334 reduce the channel ATP sensitivity independently of ATP-binding affinity, by altering the intrinsic stability of the open state. These residues are all close to each other at the inter-subunit interface in the model, but are well separated in the primary sequence (Tucker, Gribble et al. 1997; Drain, Li et al. 1998; Proks, Gribble et al. 1999; Li, Wang et al. 2000; Shyng, Cukras et al. 2000). It has also been suggested that the N and C terminal domains of Kir6.2 are involved in the ATP binding pocket, since both the R50G and K185Q mutations reduced photoaffinity labelling of Kir6.2 by 8-azido-ATP (Tanabe, Tucker et al. 1999). A thiol modification and cysteine substitution study also suggest that R50 interacts with the γ-phosphate and K185 interacts with the ß-phosphate of ATP (Trapp, Haider et al. 2003).

K_{ATP} channel inhibition by ATP and activation by PIP_2 are interrelated because PIP_2 decreases ATP sensitivity. Kinetic analysis indicates that unliganded Kir6.2 subunits are relatively unstable, and therefore will be predominantly bound to either ATP or PIP_2 at any time. In the absence of ATP, wild-type subunits are bound to membrane PIP_2, and are in the 'open' state. Binding of ATP to the unliganded subunit will trap it

in the non-permissive, 'closed', state. Trapping of any one subunit in the closed conformation is sufficient to close the channel (Enkvetchakul, Loussouarn et al. 2000; Markworth, Schwanstecher et al. 2000), yet all four subunits need to be in the 'open' state for the channel to be active; for most cells the expected open probability is negligible without the stimulatory effects of Mg-nucleotides acting at SUR (Nichols 2006).

It has been suggested that competition between ATP and PIP_2 for binding to K_{ATP} channels may account for the decrease in the ATP sensitivity evoked via PIP_2 (Shyng, Cukras et al. 2000; MacGregor, Dong et al. 2002). Potential PIP_2-interacting residues (R54, R176, R177 and R206) are near the ATP binding-site, and appropriately located to interact with PIP_2 headgroups. It has been proposed that 'negative heterotrophic' interaction of these two ligands in channel regulation exists (Shyng and Nichols 1998; Enkvetchakul and Nichols 2003), and overlapping ATP- and PIP_2-binding sites, and biochemical competition of the two ligands for the non-ligand bound state (MacGregor, Dong et al. 2002) would be consistent with this theory. However, other data have suggested that the two ligand binding sites have no common residues (Ribalet, John et al. 2003), therefore would not compete for binding. There are another group of residues, R314 and E229, that are too far away from the membrane to interact with PIP_2 directly, but which may alter protein conformation and allosterically affect the interaction of PIP_2 with the other group of residues. These residues are thought to form inter-subunit interactions between the C-tails of the Kir tetramer. A model has been proposed whereby these subunit interactions stabilise the tetramer, which in turn facilitates channel interaction with PIP_2 in order to achieve a high channel open probability (Lin, Jia et al. 2003). In line with this model, PIP_2 has previously been shown to affect the interaction of SUR1 with Kir6.2, causing functional uncoupling between the two subunits, as manifested by loss of channel inhibition to glibenclamide and reactivation by MgADP (Ribalet, John et al. 2000). The proposed nucleotide regulation of K_{ATP} channel activity and the proposed involvement of PIP_2 activity is depicted in *Figure 1.6.*

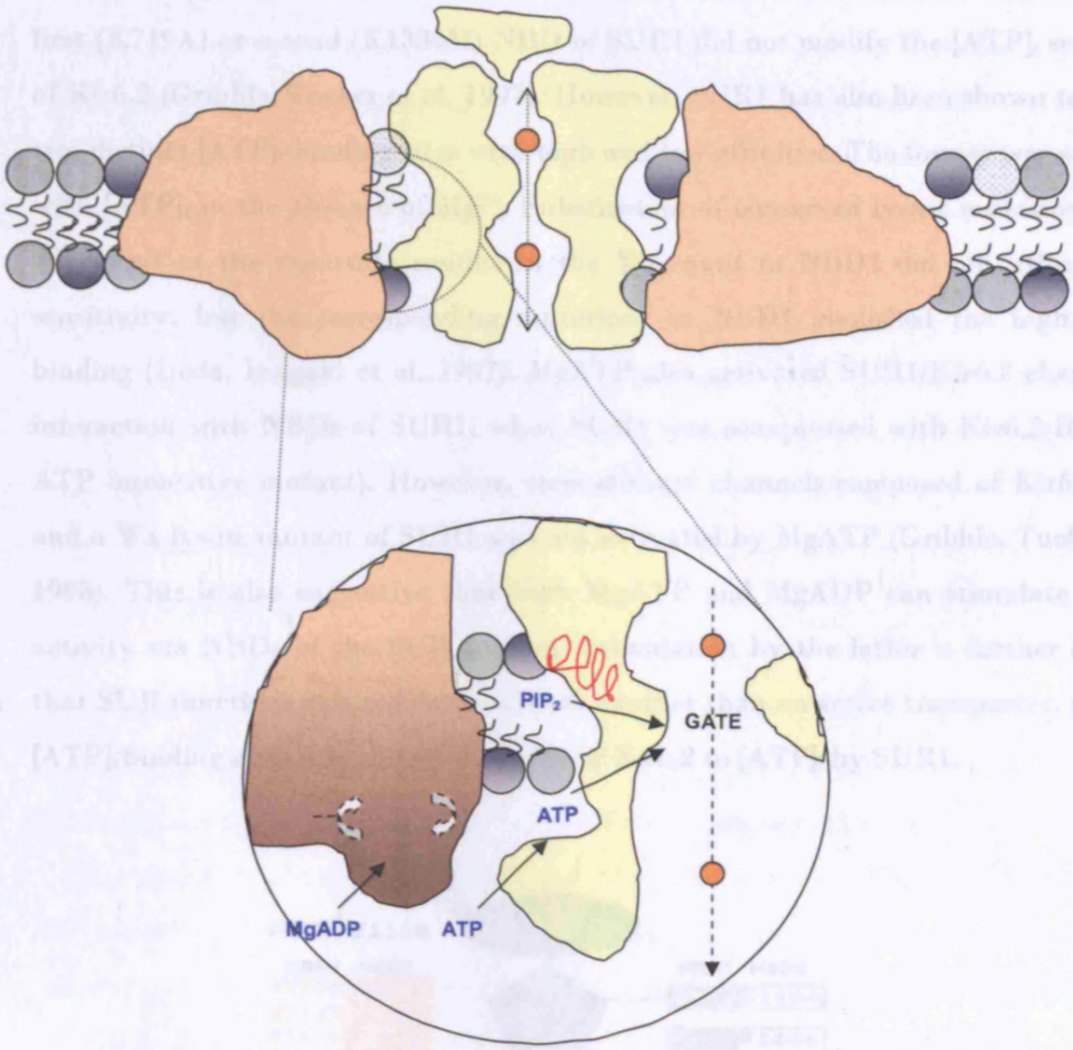

Figure 1.6: Nucleotide regulation of K_{ATP} activity. The cytoplasmic end of the inner channel cavity is where the metabolically controlled gate is located. PIP_2 serves to open the channels and ATP binding serves to close the ligand-operated gate, possibly by the physical link provided by the side helix (red). At the interface between NBD1 and NBD2 of SUR are ATP-binding sites to which MgATP binds. ATP hydrolysis at NBD2 results in a conformational 'activated' state that overrides ATP inhibition at the Kir6.2 subunit. MgADP dissociation maintains this activated state, and can be maintained by MgADP rebinding (adapted from *Nichols C; 2006*).

Studies involving SUR subunits

Mutations on either or both of the two conserved lysine residues in the W_A motif in the first (K719A) or second (K1384M) NBD of SUR1 did not modify the $[ATP]_i$ sensitivity of Kir6.2 (Gribble, Tucker et al. 1997). However, SUR1 has also been shown to possess two distinct $[ATP]_i$-binding sites with high and low affinities. The former was saturated with $[ATP]_i$ in the absence of Mg^{2+}. Substitution of conserved lysine mutations in the W_A motif or the aspartate residue in the W_B motif in NBD2 did not affect $[ATP]_i$ sensitivity, but the corresponding mutations in NBD1 abolished the high affinity binding (Ueda, Inagaki et al. 1997). MgATP also activated SUR1/Kir6.2 channels by interaction with NBDs of SUR1, when SUR1 was coexpressed with Kir6.2-R50G (an ATP insensitive mutant). However, reconstituted channels composed of Kir6.2-R50G and a W_A lysine mutant of SUR1 was not activated by MgATP (Gribble, Tucker et al. 1998). This is also suggestive that both MgATP and MgADP can stimulate channel activity via NBDs of the SUR subunit. Stimulation by the latter is further evidence that SUR functions as a regulator of Kir6.*x* rather than an active transporter, and that $[ATP]_i$ binding underlies the sensitization of Kir6.2 to $[ATP]_i$ by SUR1.

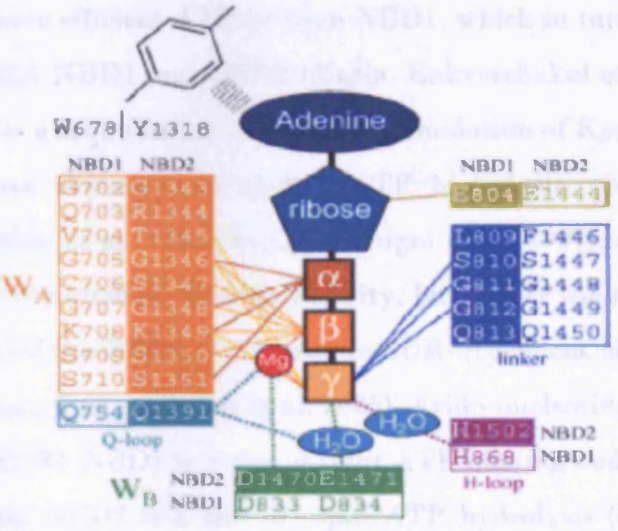

Figure 1.7: Hypothetical coordination of the ATP molecule with SUR. The first binding pocket formed by the W_A motif, Q-loop, W_B motif, H-loop of NBD2 and the linker region of NBD1 is represented by the internal circle of coloured elements. The second binding pocket is represented by the external circle (clear elements) and is composed of the counterparts of NBD1 and NBD2 (taken from *Matsuo et al., 2005*).

$[ATP]_i$ inhibits Kir6.2/SUR2A and Kir6.2ΔC26 (expressed with the sulphonylurea receptor) with similar potencies (Inagaki, Gonoi et al. 1996; Tucker, Gribble et al. 1997; Okuyama, Yamada et al. 1998). Therefore, SUR2A may not significantly increase $[ATP]_i$ sensitivity to Kir6.2. Kir6.2/SUR2A channel is equally sensitive to free MgATP and Mg^{2+}-bound $[ATP]_i$, while Kir6.2/SUR2B channel is more sensitive to free Mg^{2+}. This may be due to the difference in amino acid sequence of the C-terminus between SUR2A and SUR2B (Isomoto, Kondo et al. 1996). The last 42 amino acids in the C terminal of SUR2B is more similar to SUR1 than SUR2A, and may be involved in the discrimination of Mg^{2+}-bound rather than Mg^{2+}-free $[ATP]_i$ by K_{ATP} channels. The second NBD is known to play a crucial role in $[NDP]_i$-induced activation of K_{ATP} channels (Nichols, Shyng et al. 1996), and in SUR1 the binding of [ADP]i to the second NBD potentially antagonises $[ATP]_i$ binding to the first NBD in the presence of Mg^{2+} (Ueda, Inagaki et al. 1997).

The depicted hypothetical coordination of the sulphonylurea receptor with an ATP molecule is illustrated in *Figure 1.7*. In SUR1, it has been reported that NBD2 is generally a more efficient ATPase than NBD1, which in turn is similar in its properties to both SUR2A NBD1 and NBD2 (Masia, Enkvetchakul et al. 2005). ATP hydrolysis at the NBDs is a requirement for MgADP stimulation of K_{ATP} channels. Mutations that abolish, or are expected, to abolish ATP hydrolysis, abolish MgADP stimulation (Gribble, Tucker et al. 1997; Shyng, Ferrigni et al. 1997), and it has been speculated that it is not the intrinsic ATPase activity, but rather the stability of the ADP-bound configuration of the NBDs that underlies SUR-dependent MgADP stimulation of K_{ATP} channels (Masia, Enkvetchakul et al. 2005). Azido-nucleotide labelling studies have also shown that SUR1 NBD1 is a site of tight ATP binding and potentially low hydrolysis rates, whereby NBD2 is a site of rapid ATP hydrolysis (Ueda, Inagaki et al. 1997; Ueda, Komine et al. 1999; Matsuo, Tanabe et al. 2000). SUR1 NBD2 has also been shown to exhibit higher Mg^{2+}-dependence of ATP-binding than SUR2A NBD2 (Matsuo, Tanabe et al. 2000). However, the transduction pathway of SUR-mediated activation of K_{ATP} channels is thought to be too complicated to reduce to isolated

NBDs, and may lie in inter-NBD interactions, since conflicting evidence exists. For example, replacing NBD2 of SUR2A with NBD2 of SUR1 is without effect on MgADP stimulation (Reimann, Dabrowski et al. 2003). SUR photoaffinity labelled with 8-azido-ATP was also digested with trypsin to examine the NBDs in more detail, and the tryptic fragments immunoprecipitated with antibodies against NBD1 or NBD2. The results indicated that NBD1 of SUR binds 8-azido-ATP in a Mg^{2+}-independent manner, and that NBD2 binds in a Mg^{2+}-dependent manner, suggesting that NBD2 is responsible for channel activation by MgADP (Matsuo, Tanabe et al. 2000). The most recent 8-azido-[α-^{32}P]ATP experiments performed suggest that MgADP, either via direct binding to NBD2 or hydrolysis of bound MgATP, is likely to induce a conformational change in NBD2 which transduces another conformational change in NBD1 to stabilize nucleotide binding at NBD1 (Ueda, Komine et al. 1999). Since the C-terminal tail of SURs is very close to the first NBD in primary structure it was speculated that the C-terminal serves to regulate either $[ATP]_i$ hydrolysis or [ADP]i binding to the second NBD in the presence of Mg^{2+}. It may interact with the NBD2 W_A motif (Matsushita, Kinoshita et al. 2002), or may be part of the NBD1-NBD2 dimer interface (Yamada and Kurachi 2004).

The effects of nucleotide binding and Mg^{2+}-nucleotide stimulation of K_{ATP} channel activity, of mutating the invariant serine linker motif of NBD1 (SR1) or NBD2 (SR2) to arginine was examined (the linker motif of NBD1 of SUR*x* being LSGGQ, and that or NBD2 being LSQGQ in SUR1 and LSVGQ in SUR2). Neither MgATP nor MgADP binding was altered by mutation of the linker serine in either NBD1 or NBD2 of SUR1, nor was MgATP hydrolysis abolished. However, SR1 reduced and SR2 abolished activation of Kir6.2/SUR1 and Kir6.2/SUR2B channels by MgATP and MgADP, whereas no effect of mutating SR2 was observed for Kir6.2-SUR2A channels (Matsuo, Dabrowski et al. 2002). This indicates that the linker serines play a critical role in transducing nucleotide binding into channel opening, but how this occurs remains unclear. It is possible that the linker residue interacts with the TMDs of SUR1, inducing a conformational change in the TMDs that would be transmitted to the TMDs

in Kir6.2. It is also possible that the linker either interacts directly/indirectly with the cytosolic domains of Kir6.2. Because the SR2 mutation did not impair transduction in Kir6.2/SUR2A channels, this suggests that the 'tail' of SUR2 may interact with the linker of NBD2 in the transduction process, and that this interaction differs for SUR2A and SUR2B. The C-terminus and the NBD2 linker may co-operate in transducing nucleotide binding into channel stimulation, and the C-terminus of SUR2A is able to compensate for the effect of the linker mutation, either directly or allosterically. It might influence the local structure of NBD2 such that it is able to tolerate the effect of the serine to arginine mutation at residue 1446. Another possibility is that the SR2 mutation abolishes function in SUR1 and SUR2B, but not SUR2A (Matsuo, Dabrowski et al. 2002).

Differences between the SUR subunits on the interaction with adenine nucleotides

The nucleotide-binding properties that are similar among all SUR subtypes are that: (1) NBD1 is a Mg^{2+}-independent nucleotide binding site; (2) NBD2 is a Mg^{2+}-dependent nucleotide binding site; (3) 8-azido-ATP binds to NBD1 stably; (4) MgATP or MgADP binding to NBD2 stabilizes 8-azido-ATP binding at NBD1; (5) NBD2 has ATPase activity, whereas NBD1 has little or no ATPase activity. However, the affinities of NBDs of SUR for MgATP and MgADP differ among subtypes, and are probably related to the differential regulation of K_{ATP} channels and their different physiological roles. The affinities of NBD1 of SUR1 for ADP, and especially ATP, are significantly higher than those of SUR2A and SUR2B. The affinity of NBD1 of SUR2B for ATP, and NBD2 of SUR2B for ATP and ADP are significantly higher than those of SUR2A (Matsuo, Kimura et al. 2005).

SUR as an intracellular ADP sensor and the role of ATP hydrolysis

A model, as summarised in *Figure 1.8*, has recently been proposed for the nucleotide activation of the K_{ATP} channels by SUR subunits. The $[ATP]_i$ concentration is presumed to be several mM, approximately 10 times higher than the $[ADP]_i$ concentration, suggesting that NBD1 of SUR binds MgATP rather than MgADP, since

NBD1 has low ATPase activity. Irrespective of channel open and closed states, NBD1 of SUR binds MgATP. SUR is in an active state when binding MgATP at NBD1 and MgADP at NBD2 to open the pore of the Kir6.2 subunit. Since NBD2 of SUR has ATPase activity, bound MgATP is hydrolysed to MgADP at NBD2. When MgADP dissociates from NBD2 followed by binding of MgATP, the three states of SUR form a cycle (Matsuo, Kimura et al. 2005).

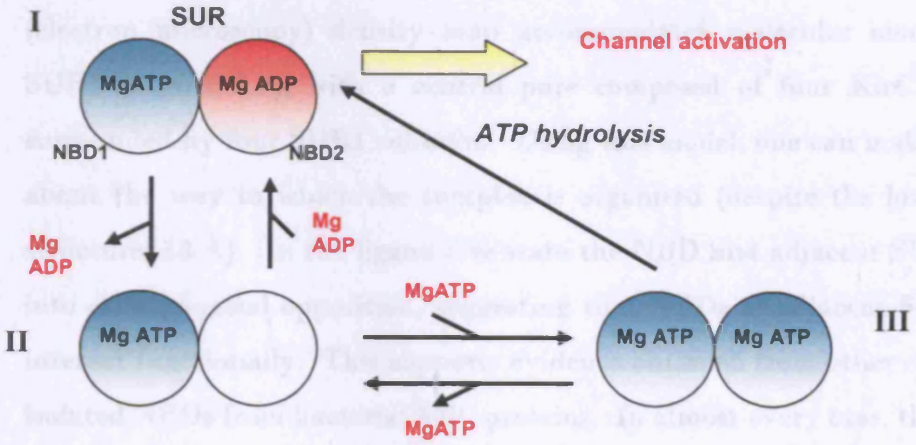

Figure 1.8: Model for nucleotide regulation: State I is the 'active' state in which SUR stimulates channel activity. State II is transient, and states II & III are 'inactive' states in which SUR cannot stimulate channel activity (adapted from *Matsuo et al., 2005*)

Can changes in adenine nucleotides solely regulate K_{ATP} channel activity?

The principle arguments against ATP being the sole regulator of K_{ATP} channel activity, is the obvious difference between ATP sensitivity of channel measured in the inside-out patch (IC_{50}=10-30μmol/l) and that in the intact cell (IC_{50}=0.8mmol/l). Also, in ß-cells exposed to glucose-free solutions, significant channel activity can be recorded from on-cell patches, despite the fact that when $[ATP]_i$ is measured under similar conditions this suggests that the channels should be completely closed (Ghosh, Ronner et al. 1991). PIP_2, (phosphatidylinositol-4,5-bisphosphate), related phosphoinositides (PPIs), long-chain acyl-CoA esters (LC-CoAs) and MgADP all decrease the ability of ATP to close the channel. It is not known whether these agents change the sensitivity of the channel to physiological changes of $[ATP]_i$, by shifting the ATP concentration-inhibition curve

to the right, or whether metabolically generated changes in PIP_2, LC-CoA or MgADP serve to couple metabolism to K_{ATP} channel activation.

1.4 ATP-sensitive K^+ channel structure

Cryoelectron microscopy has recently revealed insight as to the three-dimensional structure of the K_{ATP} channel complex (Mikhailov, Campbell et al. 2005), which is compact in structure, roughly 18 nm in cross-section and 13 nm in height. The EM (electron microscopy) density map accommodates molecular models of Kir6.2 and SUR1 (*Figure 1.9*), with a central pore composed of four Kir6.2 subunits that is surrounded by four SUR1 subunits. Using this model, one can make novel predictions about the way in which the complex is organised (despite the low resolution of the structure; 18 Å). In the ligand-free state the NBD and adjacent SUR1 subunits come into close physical opposition, suggesting that NBDs of adjacent SUR1 subunits may interact functionally. This supports evidence obtained from other crystal structures of isolated NBDs from bacterial ABC proteins. In almost every case, the NBDs crystallise as 'head-to-tail' dimers, and each nucleotide-binding pocket formed at the dimer interface contains elements from both NBDs (Hung, Wang et al. 1998; Hopfner, Karcher et al. 2000; Locher, Lee et al. 2002). Extensive intersubunit interactions between SUR1 and Kir6.2 with both the transmembrane and cytosolic domains as suggested by various studies (Giblin, Leaney et al. 1999; Mikhailov, Mikhailova et al. 2000; Schwappach, Zerangue et al. 2000; Babenko and Bryan 2002; Chan, Zhang et al. 2003; Bryan, Vila-Carriles et al. 2004; Rainbow, James et al. 2004) is also accounted for by the close juxtaposition of Kir6.2 and SUR1 subunits in these regions (Mikhailov, Campbell et al. 2005). It further suggests that nucleotide binding/hydrolysis causing movement of the NBDs of SUR1 (Higgins and Linton 2004; Vergani, Lockless et al. 2005) may influence the opening and closing of the pore via the TMDs and via the cytosolic domains of Kir6.2. ATP may access its binding site on Kir6.2 through a cleft running between adjacent SUR1 subunits just below the membrane, and this may explain how the sulphonylurea receptor enhances the affinity of Kir6.2 for ATP (Tucker, Gribble et al. 1997). With reference to *Figures 1.9-1.11*, a combination of

molecular modelling and site-directed mutagenesis has led to speculation that the ATP binding site on Kir6.2 is approximately 2nm below the membrane and at the interface between adjacent Kir6.2 subunits (Antcliff, Haider et al. 2005). It is not yet certain how ATP binding to the Kir6.2 tetramer is translated into pore closure.

There have been various speculations as to the location of TMD0 of SUR1 in the K_{ATP} channel complex. Initially it was thought to be outside the complex (Zerangue, Schwappach et al. 1999; Schwappach, Zerangue et al. 2000). It was then suggested that TMD0 was sandwiched between Kir6.2 and TMDs 1 & 2 of SUR1 (Bryan, Vila-Carriles et al. 2004) when subsequent studies showed that Kir6.2 and TMD0 interact both physically and functionally (Babenko and Bryan 2002; Chan, Zhang et al. 2003). However, recent insertion of the homology models into the EM density map indicates that the five TMD0 helices are more likely to lay between adjacent SUR subunits, and interface with TM1 of Kir6.2. In this position residues 76-78 in TM1 of Kir6.2 which specify physical assembly with SUR1 (Schwappach, Zerangue et al. 2000) are well placed to interact with TMD0 (Mikhailov, Campbell et al. 2005), and is consistent with functional studies showing that the N-terminus of Kir6.2 lies in close proximity to the cytosolic loop (L0) between TMDs 0 and 1 of SUR1 (Babenko and Bryan 2002; Chan, Zhang et al. 2003).

Mutations that abolish ATP hydrolysis without affecting MgATP or MgADP binding would be an invaluable tool to test that idea that MgATP does not activate the channel directly, but must first be hydrolysed to MgADP (Zingman, Alekseev et al. 2001). Unfortunately, none have been identified to date, but current evidence suggests that most ATP hydrolysis occurs at Site 2 (Zingman, Alekseev et al. 2001; Masia, Enkvetchakul et al. 2005) which is formed largely from NBD2 with contributions from the linker region of NBD1 (Campbell, Sansom et al. 2003). Although the ATPase-activity of the Kir6.2/SUR1 tetramer has not been determined previously, it has been determined for isolated NBDs by fusing them to maltose-binding protein (Masia, Enkvetchakul et al. 2005). Since the rate of ATP hydrolysis and affinity for ATP were

significantly higher for the K_{ATP} channel complex (Mikhailov, Campbell et al. 2005) than for isolated NBDs (Masia, Enkvetchakul et al. 2005), this may be reflective of the fact that there is a requirement for heterodimerization of the NBDs for concerted nucleotide binding (Chan, Zhang et al. 2003; Vergani, Lockless et al. 2005). Additionally, it may be due to Kir6.2 influencing the ATPase activity of the NBDs of SUR1, or due to cooperative interactions between SUR1 subunits of the same tetramer (Ashcroft 2006). We can be confident in concluding that at Å resolution, cardiac, skeletal, and vascular smooth muscle K_{ATP} channels will share structural features similar to the β-cell SUR1-Kir6.2 channel, due to the extensive sequence similarity between Kir6.*x* and SUR*x* families (Seino and Miki 2003).

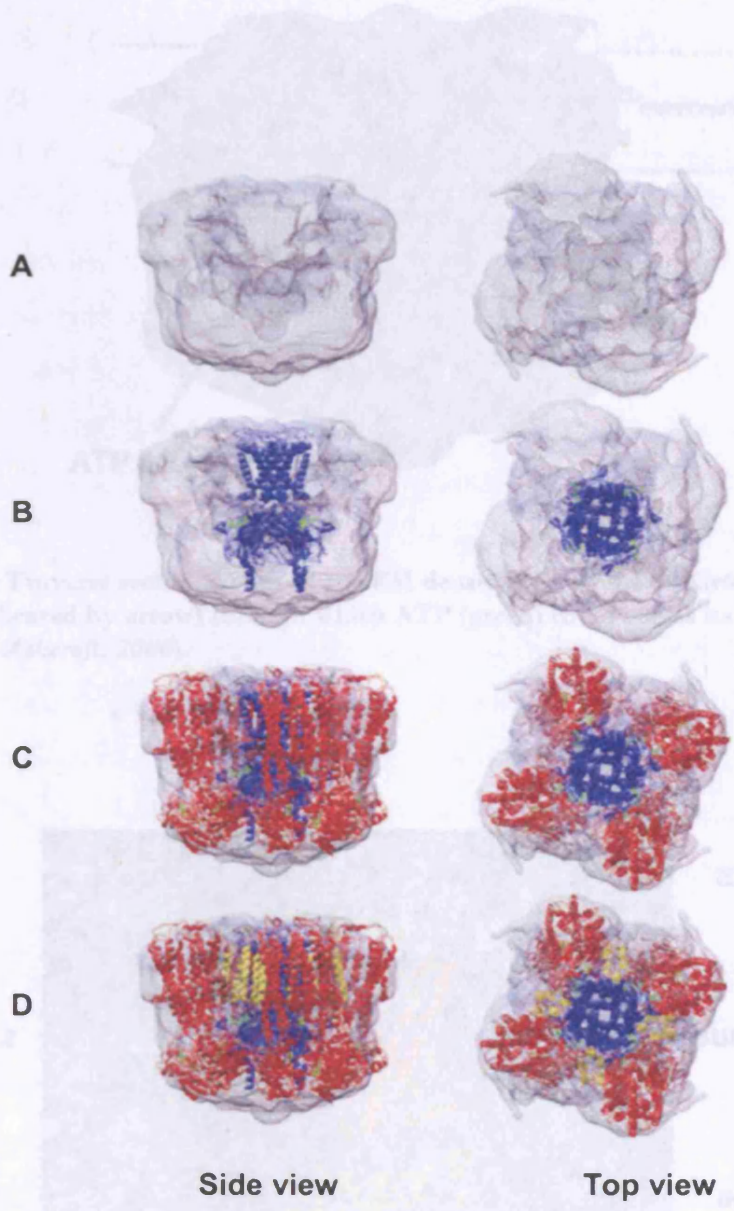

Figure 1.9: Location of molecular models within the 3D Kir6.2-SUR1 structure. (A-D) respective top and side views of the EM density with models of Kir6.2 (blue), SUR1 minus the first five transmembrane domains TMD0 (red), and TMD0 (yellow) inserted sequentially from (B) to (D). ATP molecules are shown in green (taken from *Mikhailov et al., 2005*).

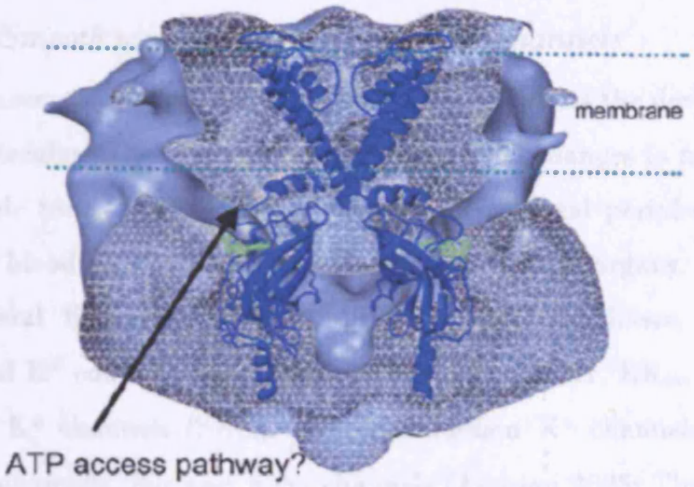

Figure 1.10: Traverse sectional view of the EM density of a model of Kir6.2 (dark blue) showing clefts (as indicated by arrow) through which ATP (green) could access its binding site on Kir6.2 (taken from *Ashcroft; 2006*).

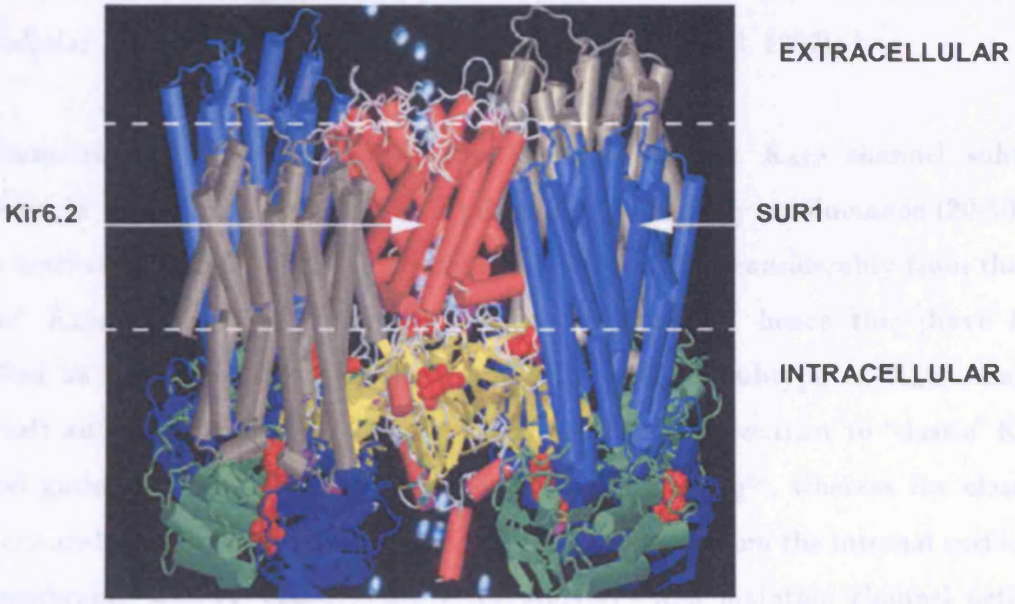

Figure 1.11: Another model of how SUR1 and Kir6.2 might assemble to for the K_{ATP} channel. This model illustrates that the channel complex contains 4 ATP-binding sites on Kir6.2 and 8 Mg nucleotide-binding sites on SUR1 (taken from *Ashcroft; 2005*).

1.5 Vascular Smooth muscle ATP-sensitive K^+ channels

It is generally accepted that K^+ channel activation prevents the development of action potentials in vascular smooth muscles, allowing graded changes in membrane potential to regulate their tone. As such they play a role in total peripheral resistance, the distribution of blood flow between and within tissues and organs, and microvascular exchange. Several K^+ channels, with different molecular bases, contribute to the regulatory basal K^+ conductance in smooth muscle cells: K_V, BK_{Ca}, small conductance Ca^{2+}-activated K^+ channels (SK_{Ca}), two-pore domain K^+ channels (TASK), stretch-dependent K^+ channels, Kir and K_{ATP} channels (Jackson 2005; Thorneloe and Nelson 2005).

The predominant Kir channel isoform expressed in smooth muscle is Kir2.1 (Bradley, Jaggar et al. 1999). These channels are blocked by Ba^{2+} ions at micromolar concentrations and are activated by increases in extracellular K^+, acting as sensors for increases in K^+, leading to membrane hyperpolarisation and vasodilation when extracellular K^+ is elevated from 5-15mM (Quayle, Nelson et al. 1997).

In symmetric KCl recording conditions, the predominant K_{ATP} channel subtype expressed in smooth muscle cells has a relatively low unitary conductance (20-50pS), and is activated by NDPs. The nucleotide sensitivity differs considerably from that of 'classic' K_{ATP} channels of pancreatic ß-cells, for example, hence they have been classified as a functionally distinct NDP-sensitive, K_{NDP} subtype of K_{ATP} channel (Ashcroft and Ashcroft 1990; Zhang and Bolton 1996). In contrast to 'classic' K_{ATP}, channel gating is observed in the presence of NDPs and Mg^{2+}, whereas the classical K_{ATP} channels open spontaneously when $[ATP]_i$ is removed from the internal surface of the membrane. MgATP can substitute for MgNDPs and maintain channel activity (Zhang and Bolton 1996; Teramoto, McMurray et al. 1997). K_{NDP} channels are also inhibited by ATP and glibenclamide, but inhibition by ATP occurs at much higher, and more variable concentrations compared to pancreatic ß-cell or cardiac K_{ATP} channels (Babenko, Aguilar-Bryan et al. 1998). Additionally, inhibition is bell shaped, and

maximal activity occurs between 0.1 and 1mM. Inhibition occurs in the absence and >1mM $[ATP]_i$. In other words, the K_{NDP} channel is activated rather than inhibited by $[ATP]_i$ (Yamada and Kurachi 2005).

Medium conductance (50-70 pS) K_{ATP} channels also exist in vascular smooth muscle (VSM), although they have a more limited distribution, an example being the cardiac-like LK channel of rat portal vein myocytes. These channels exhibit spontaneous activity in inside-out patches in the absence of nucleotides, are activated by metabolic inhibition and are inhibited by glibenclamide and also ATP in the micromolar range (with an approximate IC_{50} of 20μM). They partially mimic classic K_{ATP} channels in terms of their unitary conductance, activity in the absence of nucleotides and a lack of sensitivity to KCOs, when applied at concentrations that increase K_{NDP} gating (Zhang and Bolton 1996; Cole, Malcolm et al. 2000). Large-conductance (> 100 pS) channels that display sensitivity to ATP, KCOs and glibenclamide also exist in vascular myocytes, but it is debatable whether these channels should be categorised as a distinct K_{ATP} channel subtype (Standen, Quayle et al. 1989; Zhang and Bolton 1995).

Evidence that Kir6.1/SUR2B Represent K_{NDP} of VSM

The Kir6.1/SUR2B channel is similar to the K_{ATP} channel in VSM cells (i.e. the K_{NDP} channel), especially in terms of single channel conductance and ATP sensitivity, and is similarly responsive to MgADP. The relatively small conductance ~35pS and the bell-shaped relation for the ATP action on the channel are closely related to those of VSM (20-40pS conductance). However, channels containing Kir6.2 have a 70-80pS conductance in symmetrical 140mM K^+ conditions (Teramoto, Tomoda et al. 2006). Whereas the single-channel conductance of heteromeric Kir6.1-Kir6.2 channels containing one or two Kir6.2 subunits is within the range of values reported for K_{NDP}, they are dissimilar in that the latter are activated by PKC, and exhibit spontaneous activity in the absence of nucleotides (Babenko and Bryan 2001; Cole and Clement-Chomienne 2003). Pig urethral K_{ATP} channels have a conductance of 43 pS (an intermediate conductance between that of Kir6.1 and Kir6.2 subunits) (Teramoto,

Creed et al. 1997), suggesting that the nature of the pore region of urethral channels differs from that of vascular K_{ATP} channels. Even though different experimental recording conditions could be responsible for the different channel conductances observed, the latter provides evidence for a heteromeric channel structure, with the channel pore composed of Kir6.1 and Kir6.2 subunits (Teramoto 2003). The difference in conductance between Kir6.1 and Kir6.2 is determined by a chain of amino acids in the M1-H5 extra-cellular link and a single amino acid in the H5-M2 link (N123-V124-R125 and M148 in Kir6.1 and S113-I114-H115 and V138 in Kir6.2) (Repunte, Nakamura et al. 1999). Steric effects at Kir6.1 M148 or Kir6.2 V138 may directly influence K^+ diffusion, and structural constraints between Kir6.1 N123 and R146 or Kir6.2 S113 and R136 may influence the configuration of the permeation pathway (Repunte, Nakamura et al. 1999).

The K_{ATP} channel Kir6.1/SUR2B is dose dependently stimulated by 0.1-100μM ATP and inhibited by 1-3mM ATP in the presence of pinacidil, with maximal activity at ~1mM ATP. Spontaneous activity of this channel is not observed on patch excision to the inside-out configuration unless nucleoside diphosphates or triphosphates and Mg^{2+} are present, as was described for K_{NDP} channels (Zhang and Bolton 1996). This requirement for NDPs is not observed for heteromeric Kir6.1-Kir6.2/SUR1 channels, or channels containing Kir6.2 subunits expressed with SUR1, SUR2A or SUR2B. Since there is evidence to suggest that the presence of only one Kir6.2 subunit in heteromeric Kir6.1-Kir6.2/SUR1 channels permits gating in the absence of Mg^{2+} and nucleotides (Babenko, Gonzalez et al. 2000), this indicates that only homomeric Kir6.1 channels mimic the nucleotide regulation characteristic of VSM K_{NDP}.

Kir6.1/SUR2B channels exhibit a SUR and KCO pharmacology consistent with that of VSM K_{NDP} channels, i.e. are activated by pinacidil and diazoxide, whereas SUR1-containing channels are not affected by pinacidil and SUR2A-containing channels exhibit a low sensitivity to diazoxide in the absence of intracellular MgADP (D'Hahan, Moreau et al. 1999). Kir6.1/SUR2B channels exhibit around four-fold higher

glibenclamide sensitivity than Kir6.2/SUR2B channels (Hambrock, Loffler-Walz et al. 1999) and this difference in sensitivity is comparable to the high glibenclamide sensitivity ascribed to the low-conductance K_{NDP} channel compared to the medium-conductance cardiac-like K_{ATP} channel subtype of rat portal vein (Zhang and Bolton 1996). The similar reciprocal allosteric coupling of KCO, glibenclamide and nucleotide action reported for Kir6.1/SUR2B has also been reported for K_{NDP} channels (Zhang and Bolton 1996). In a recent study it was shown that isoflurane (a volatile anaesthetic) activates Kir6.1/SUR2B channels but not Kir6.2/SUR2A channels expressed in HEK293 cells, which was consistent with experiments using mouse perfused heart and vascular smooth muscle cells whereby coronary vasodilation was achieved (Fujita, Ogura et al. 2006).

The regulation by PKC demonstrated for native VSM K_{NDP} and whole-cell K_{ATP} currents is mimicked by Kir6.1/SUR2B (purified PKC applied to inside-out patches in the presence of ATP and MgADP inhibits Kir6.1/SUR2B channel gating, as does activation of PKC due to exposure to a phorbol ester or angiotensin II). The presence of a single Kir6.2 subunit in heteromeric Kir6.1-Kir6.2/SUR2B channels abolishes inhibition of gating by PKC observed for K_{NDP} (Thorneloe, Maruyama et al. 2002; Quinn, Cui et al. 2003).

Studies using a gene knockout strategy also provide strong evidence that Kir6.1, but not Kir6.2, is essential for the formation of VSM K_{ATP} channels. $Kir6.1^{-/-}$ mice (generated via disruption of the gene *KCNJ8*) exhibit sudden death as the result of myocardial ischemia due to abnormal regulation of coronary arteriolar vascular tone and presence of coronary vasospasm (Miki, Suzuki et al. 2002), indicated by spontaneous elevation of ST segments followed by AV blocks of various degrees on the electrocardiogram. Kir6.2 knockout mice, however, were unaffected (Suzuki, Sasaki et al. 2002).

In another knockout study employing aortic smooth muscle cells, pinacidil was shown to stimulate significant K^+ currents that were blocked by glibenclamide in wild type

and Kir6.2 knockout mice, but not in Kir6.1$^{-/-}$ mice, indicating that Kir6.1 is an essential component of K_{ATP} in vascular smooth muscles (Miki, Suzuki et al. 2002; Suzuki, Sasaki et al. 2002).. The lack of vasodilatation response to pinacidil was confirmed *in vitro* by measuring the isometric tension of aortic rings isolated from Kir6.1$^{-/-}$ mice. Methylergometrine, a diagnostic compound for vasospastic angina (also known as Prinzmetal angina in humans) was used to induce vasospasms in Kir6.1$^{-/-}$ mice both *in vivo* and *in vitro*. Disruption of SUR2 also produces the phenotype of Prinzmetal angina (Chutkow, Pu et al. 2002) and SUR2-null mice demonstrate ST elevation, coronary vasospasm and sudden cardiac death, as well as narrowing of the coronary arteries and elevated blood pressure (Chutkow, Pu et al. 2002). The cumulative evidence therefore suggests that the Kir6.1/SUR2B channel is critical in the regulation of vascular smooth muscle, especially in the coronary arteries.

RT-PCR was used to demonstrate the presence of Kir6.1 transcript in rat pulmonary artery (Cui, Tran et al. 2002), Kir6.1 was detected in the mouse aorta using the Northern blot technique (Suzuki, Li et al. 2001), and transcripts of Kir6.1 in rat aorta, tail artery, pulmonary artery and mesenteric artery tissues have been identified (Cao, Tang et al. 2002). The use of an anti-Kir6.1 antibody (generated using GST-tagged Kir6.1C fusion protein) has also identified Kir6.1 proteins in four rat vascular smooth muscle tissues, including mesenteric artery, tail artery, pulmonary artery and aorta (Sun, Cao et al. 2004). The differential expression of Kir6.1 and SUR2B subunits has become apparent due to *in situ* hybridization studies, which have shown that both subunits are expressed in the smooth muscle layer of arterioles as well as small and intermediate arteries. Since these blood vessels are known to determine blood pressure and circulation resistance (Wilson 1989), this is suggestive that the Kir6.1/SUR2B channel is the mediator of vascular diameter in accordance with the change of physiological and pathophysiological conditions. Such experiments are also suggestive that the ion channel believed to be responsible for the fast endothelial response to Ca^{2+} signals and mediate the release of endothelium-derived relaxing factor is

Kir6.1/SUR2B, since the mRNA of each subunit are abundantly expressed in the capillaries of the skeletal muscle and renal glomerulus (Li, Wu et al. 2003).

Recent experiments using sensitive quantitative LightCycler technology in combination with SYBR Green Dye chemistry have allowed for accurate quantification of K_{ATP} channel mRNA subunits in rat basilar and middle cerebral artery RNA preparations (Ploug, Edvinsson et al. 2006). In agreement with the in situ hybridisation experiments performed in the rat by Li and colleagues, it was found that Kir6.1 and SUR2B were the predominant transcripts in both rat basilar and middle cerebral artery. However, this data indicated that Kir6.1 mRNA levels were higher than SUR2B mRNA levels, especially in the cerebral arteries. Since this is not in accordance with the known 4:4 Kir6.*x*/SUR stoichiometry, it was suggested that a minor population of Kir6.1/SUR1 octamers may exist, based on the available evidence from such studies (Li, Wu et al. 2003; Ploug, Edvinsson et al. 2006). It is a valid assumption that not all proteins forming K_{ATP} channels are expressed at the same concentration, and that the protein least expressed is the one that determines the number of K_{ATP} channels, and it has been shown that the level of Kir6.2 protein in anti-SUR2 immunoprecipitate accurately reflects the number of K_{ATP} channels (Ranki, Crawford et al. 2002). With this in mind, a recent study using real-time RT PCR revealed that SUR2A mRNA levels are lower than the concentration of mRNA of any other K_{ATP} channel-forming protein in the heart; overexpression of the SUR2A protein generated a cardiac phenotype with more sarcolemmal K_{ATP} channels (composed of pore-forming Kir6.2 and regulatory SUR2A subunits) with increased resistance to hypoxia and ischemia-reperfusion (Du, Jovanovic et al. 2006).

It is therefore apparent that the K_{NDP} channel represents the K_{ATP} channel Kir6.1/SUR2B. This vascular K_{ATP} channel is readily activated during metabolic stress such as hypoxia, ischemia and hypoglycaemia. Channel activation results in hyperpolarization and a decrease in cellular excitability. In turn, the voltage-activated Ca^{2+} channels are inhibited with hyperpolarization, lowering intracellular Ca^{2+} concentration. As a result VSM contractility decreases. In principle, this vasodilation allows a better perfusion within local tissues and reverses hypoxic ischemia.

1.6 Regulation of the ATP-sensitive K^+ channels via metabolically active proteins

The K_{ATP} channel complex as a component of the cellular energetic network

Some accessory proteins such as adenylate kinase (AK) and creatine kinase (CK), physically associate with the K_{ATP} channel and regulate its activity, and may be acting as integral parts of the K_{ATP} channel complex *in vivo* (Bienengraeber, Alekseev et al. 2000; Carrasco, Dzeja et al. 2001; Crawford, Budas et al. 2002; Crawford, Ranki et al. 2002; Selivanov, Alekseev et al. 2004). Mitochondria are responsible for the production of the majority of cellular ATP, and respond rapidly to metabolic stress by the release of signaling molecules. They contribute to metabolic oscillations that drive fluctuations of membrane current, and via the regulation of K_{ATP} channels, help set membrane excitability. With high intracellular ATP levels however, K_{ATP} channels may not sense bulk cytosolic, but rather local submembrane nucleotide concentrations set by membrane ATPases and phosphotransfer enzymes. As such, cells with high and fluctuating energy demands, such as cardiomyocytes, possess well-defined phosphotransfer systems to facilitate energetic signaling between sites of ATP production and ATP utilization and sensing, thus coupling channel behavior with cellular energetic state (Selivanov, Alekseev et al. 2004). There is a wide distribution of adenylate kinase (AK: $2ADP \leftrightarrow ATP + AMP$) and creatine kinase (CK: $ADP + CrP \leftrightarrow ATP + Cr$) in cell membranes and compartments, and a known physical association with the K_{ATP} channel subunits which ensures their functional and structural interactions with the channel (Carrasco, Dzeja et al. 2001; Crawford, Ranki et al. 2002).

In knockout mice lacking the creatine kinase gene M-CK, the observed ATP-induced K_{ATP} channel closure is lost (Abraham, Selivanov et al. 2002), and in cardiomyocytes lacking the adenylate kinase AK1 gene, ATP-induced K_{ATP} channel closure is lost (Carrasco, Dzeja et al. 2001; Selivanov, Alekseev et al. 2004). The involvement of AK phosphotransfer in linking mitochondrial events with K_{ATP} channels has been demonstrated, whereby pharmacological inhibition of AK phosphotransfer has been shown to impede delivery of mitochondrial signals to the K_{ATP} channel site. The AK system is also capable of modulating changes in the ATP/ADP ratio. *Figure 1.12* illustrates that under severe metabolic challenge, provided that glycolysis maintains submembrane ATP levels, AK catalysis may facilitate K_{ATP} channel opening by elevating AMP flux into the submembrane compartment, and promoting generation of submembrane ADP levels (ATP + AMP → 2ADP) (Carrasco, Dzeja et al. 2001; Selivanov, Alekseev et al. 2004).

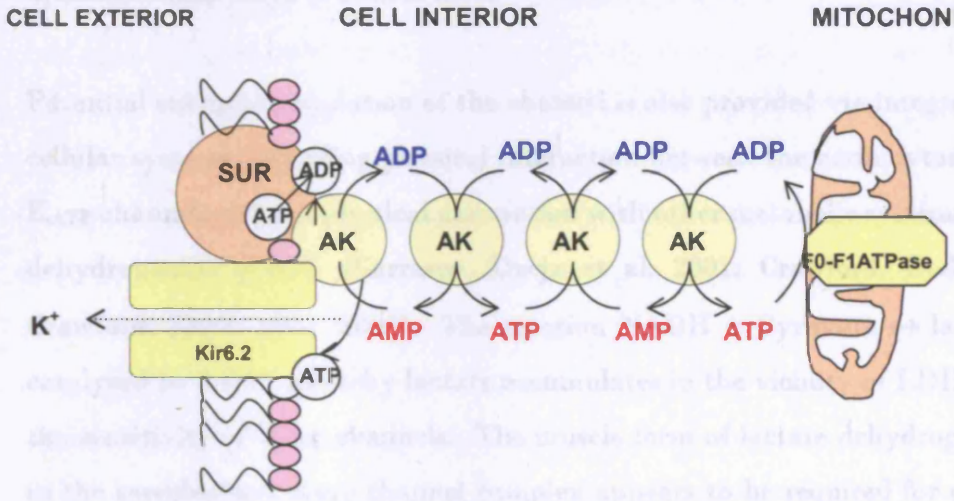

Figure 1.12: AK phosphotransfer communicates mitochondria-generated signals to K_{ATP} channels. A phosphorelay network of AK molecules is formed, and connects mitochondria with the cell membrane. Mitochondrial F_1-F_0-ATPase consumes cellular ATP generating ADP under hypoxic stress, and this is delivered to the K_{ATP} channel through the chain of sequential AK-catalysed phosphotransfer reactions (adapted from *Carrasco et al., 2001*).

In the heart, the observation that elevating extracellular glucose concentration to supraphysiologic levels reversed shortening of the action potential during hypoxia suggested that glycolytic ATP may be preferentially used to preserve membrane function (McDonald and MacLeod 1973). Glycolysis has been shown to be a preferential source of ATP for cardiac ATP-sensitive K^+ channels, and has been shown to be related to the close physical proximity of key glycolytic enzymes to the channels (Weiss and Lamp 1989). The preferential dependence of the channels on ATP derived from anaerobic glycolysis is an attractive mechanism linking the metabolism of glucose directly to the activity of K_{ATP} channels. Glycolytic flux is composed of both exogenous glucose utilization and glycogenolysis. It has long since been reported that glycolytic flux increases during early ischemia (Rovetto 1979). Even though it is unlikely that K_{ATP} channels would be activated as a consequence, it may be necessary for both glycogenolytic and glycolytic enzymes to be associated with K_{ATP} channels for their activation during ischemia once ATP production from exogenous glucose utilization falls below a critical level.

Potential energetic regulation of the channel is also provided via integration with other cellular systems, including physical interaction between the actin cytoskeleton and the K_{ATP} channel, and via physical association with other metabolic systems such as lactate dehydrogenase (LDH) (Carrasco, Dzeja et al. 2001; Crawford, Budas et al. 2002; Crawford, Ranki et al. 2002). The reaction NADH + Pyruvate $\leftrightarrow$ lactate + NAD is catalysed by LDH, whereby lactate accumulates in the vicinity of LDH and modulates the sensitivity of K_{ATP} channels. The muscle form of lactate dehydrogenase (M-LDH) in the sarcolemmal K_{ATP} channel complex appears to be required for early opening of K_{ATP} channels during ischemia and cellular resistance against metabolic stress (Crawford, Budas et al. 2002). The integrity of the microenvironment surrounding K_{ATP} channel proteins, in particular the actin filament network, may play an important role in modulating the channel activity of K_{ATP} channels (Van Wagoner and Lamorgese 1994). In cardiomyocytes, the actin microfilament disrupter DNase I has been shown to stimulate the activity of K_{ATP} channels (Terzic and Kurachi 1996). Similarly, the

activity of native K_{ATP} channels in smooth muscle was enhanced by cytochalasin B (Teramoto, Tomoda et al. 2002). The actin filament network and its related proteins might be involved in signal transduction between the inhibitory regulatory proteins and K_{ATP} channels. Regulation by the signaling pathways discussed below, direct channel effects of G protein subunits (Terzic, Tung et al. 1994), pH effects via protonation of channel proteins (Vivaudou and Forestier 1995), and changes in membrane phospholipids that interact with Kir6.2 to modulate pore function (Baukrowitz, Schulte et al. 1998) are other systems that synchronize K_{ATP} channel function with changes in cellular energetic state.

K_{ATP} channels involved in insulin release from the pancreatic β-cell associate with Rim, Piccolo, Epacs and Ca^{2+} channel subunits, which confer regulation of insulin release by cytosolic ATP, Ca^{2+} and cAMP (Shibasaki, Sunaga et al. 2004). The coordination of exocytosis and ionic events leading to secretion may also occur via interaction of the K_{ATP} channel with the vesicle docking protein, syntaxin-1 (Pasyk, Kang et al. 2004). It has also been demonstrated that key glycolytic enzymes such as glyceraldehyde-3-phosphate (GAPDH), triose phosphate isomerase (TP), and phosphoglycerate kinase (PK) can associate with Kir6.2 subunits of cardiac sarcolemmal ATP-sensitive K_{ATP} channels, that they are components of the K_{ATP} channel complex and that their activity regulates K_{ATP} channel opening by allowing fast-sensing of glucose levels (Dhar-Chowdhury, Harrell et al. 2005; Jovanovic, Du et al. 2005).

Regulation by Cellular signalling pathways

Aside from the role of nucleotides in K_{ATP} channel regulation, K_{ATP} channels in vascular smooth muscle are also regulated by a wide range of vasoconstrictors and vasodilators, which are thought to form an important part of their control under physiological conditions. Small arteries play a major role in the control of luminal flow, intravascular pressure, and responsiveness to local metabolites. As such, they have a high density of K_{ATP} channels.

The vasodilators known to activate Kir6.1/SUR2B include calcitonin gene-related peptide (CGRP), prostacyclin, adenosine, and ß-adrenoreceptor agonists. There is evidence to suggest that they act through the classical adenyl cyclase-protein kinase A pathway, i.e. activate PKA through the formation of cyclic AMP. Intracellular application of either cyclic AMP or the catalytic subunit of PKA also activates the channel, whereby low intracellular ATP suppresses tonic activation (i.e. activation that does not require the presence of receptor agonists), which is reversed by increasing ATP towards physiological levels. This may be important for the tonic contribution of the channels to resting blood flow. The molecular mechanism via which PKA activates the channel may be via a conserved consensus site in Kir6.1 at T234 (Brayden 2002; Standen 2003). By employing the cloned equivalent of vascular K_{ATP}, Kir6.1/SUR2B, evidence was provided that PKA activation involves phosphorylation of both subunits; at S385 in Kir6.1 and T633 and S1465 in SUR2B (Quinn, Giblin et al. 2004). For substantial channel activation to occur, it was deduced that a large number of these sites need to be phosphorylated.

Adenosine is a mediator of metabolic distress. It is ubiquitously released, being formed in the extracellular space by the breakdown of ATP, and in hypoxic tissues it accumulates to high levels. Adenosine acts physiologically on specific cell surface G-protein coupled receptors, four of which (A_1, A_{2A}, A_{2B} and A_3) have been cloned and described pharmacologically. Collectively, their expression is widespread, such that adenosine controls the function of virtually every organ and tissue. A_1 and A_3 receptors interact with pertussis toxin-sensitive G proteins of the G_i and G_0 family, whereas A_{2A} and A_{2B} receptors stimulate adenylyl cyclase via Gs. In addition, A_{2B} receptors can activate phospholipase C, and this is thought to be mediated via activation of Gq (Klinger, Freissmuth et al. 2002). Since they are able to couple to G_i and G_0 proteins, they mediate a broad range of signalling responses, and aside from adenylate cyclase and phospholipase C, regulate several other membrane and intracellular proteins upon activation, including Ca^{2+} channels and K^+ channels (Fredholm, AP et al. 2001; Klinger, Freissmuth et al. 2002).

There is a high expression of A_{2B} receptors in smooth muscle cells, with high levels in the cecum, colon, bladder and blood vessels. Through A_{2B} receptors, adenosine also regulates the growth of smooth muscle cell populations in blood vessels, cell growth, intestinal function, inhibition of Tumour Necrosis Factor (TNF-α), vascular tone and inflammatory processes (Baraldi, Romagnoli et al. 2006). It has been shown that agonists specific for the A_1 receptor increase the activity of the high-affinity Na^+-dependent adenosine transporter (CNT2) by a mechanism which is completely dependent on K_{ATP} channel function, since the K_{ATP} channel mediates the link between adenosine retrieval and uptake into the cell, where it may contribute to replenishing the nucleotide pool (Duflot, Riera et al. 2004). It has also been shown that under brief ischemic conditions, adenosine receptors are activated, which in turn activate PKC and which phosphorylates the K_{ATP} channel. The phosphorylation alters the sensitivity of K_{ATP} channels in such a way that these channels open earlier and/or more intensely during prolonged ischemia (Liu, Gao et al. 1997).

Vasoconstrictors that inhibit the channel include angiotensin II, endothelin I, vasopressin, serotonin, phenylephrine, neuropeptide Y and histamine and several of these have been shown to inhibit the channel via PKC (Kubo, Quayle et al. 1997) resulting in depolarisation and contraction (Quayle, Nelson et al. 1997; Cole, Malcolm et al. 2000). PKC has been shown to directly inhibit recombinant channels comprising Kir6.1/SUR2B, and this inhibition is consistent with the inhibition of whole-cell vascular K_{ATP} currents by vasoactive agonists. However, the phosphorylation sites have not been identified (Thorneloe, Maruyama et al. 2002). In many tissues, including vascular smooth muscle, AngII receptors (AT_1 and AT_2) have been shown to couple several cellular signalling pathways. The binding of Ang II to pertussis toxin-insensitive G protein ($G_q/11$)-coupled Ang II receptors activates the phospholipase C (PLC) cascade, initiating the conversion of phosphatidylinositol bisphosphate to inositol trisphosphate, which evokes Ca^{2+} release from intracellular stores, and 1,2-diacylglycerol, which activates PKC (Park, Kim et al. 2006). PKC has been shown to inhibit nucleotide diphosphate-sensitive K_{ATP} channels when applied to inside-out

membrane patches excised from rabbit or rat pulmonary vein, and it was suggested that molecular modulation of activity may occur via the conserved threonine (T190) in Kir6.1. This was shown to be the case for the corresponding residue on Kir6.2 (Light, Bladen et al. 2000). It was recently shown that in small-diameter coronary arterial smooth muscle cells, Ang II inhibits the Kir channel through activation of PLC and Ca^{2+}-dependent PKCα by acting at the AT_1 receptor (Hayabuchi, Standen et al. 2001; Park, Kim et al. 2006). Ang II receptors also cause inhibition of cyclic AMP-dependent protein kinase (PKA) through the inhibition of adenylyl cyclase and reduction in cyclic AMP (Unger, Chung et al. 1996). Interestingly, when the intracellular concentration of ATP is high, steady state K_{ATP} channel activation by PKA is observed (Hayabuchi, Standen et al. 2001), whereby Ang II acts via the AT_1 receptor to inhibit PKA (to reduce this steady-state activation) and through the activation of PKC. It was suggested that the PKCε isoform mediates this effect (Hayabuchi, Standen et al. 2001). Therefore, the background activity of K_{ATP} channels may be set by steady-state activation of PKA, and an additional pathway for the actions of some vasodilators to act through PKC may be due to reduction in this PKA activation by inhibition of adenylyl cyclase.

Work in aortic smooth muscle has also indicated that calcium-sensitive protein phosphatase 2B (calcineurin) affects K_{ATP} channel activity via regulation of intracellular Ca^{2+} concentration. Calcineurin may regulate the degree of phosphorylation of a site that causes channel activation, either on the channel itself or on an accessory regulatory protein, which may be the same site at which PKA activates the channel (Wilson, Jabr et al. 2000).

There is also strong evidence for a key role of an A-kinase anchoring protein (AKAP) in PKA-K_{ATP} channel signalling. Some types of AKAP can also bind PKC and PP2B, and essentially form multi-enzyme complexes that act synergistically to regulate the phosphorylation state of cellular substrates. Since PKA, PKC and PP2B are all involved in K_{ATP} channel regulation, it has been proposed that all of these enzymes

might be localised by the same AKAP, and that by anchoring into a signalling complex their functions in regulating the K_{ATP} channel might be integrated. *Figure 1.13* is a hypothetical scheme of factors that regulate vascular K_{ATP} channels (Standen 2003).

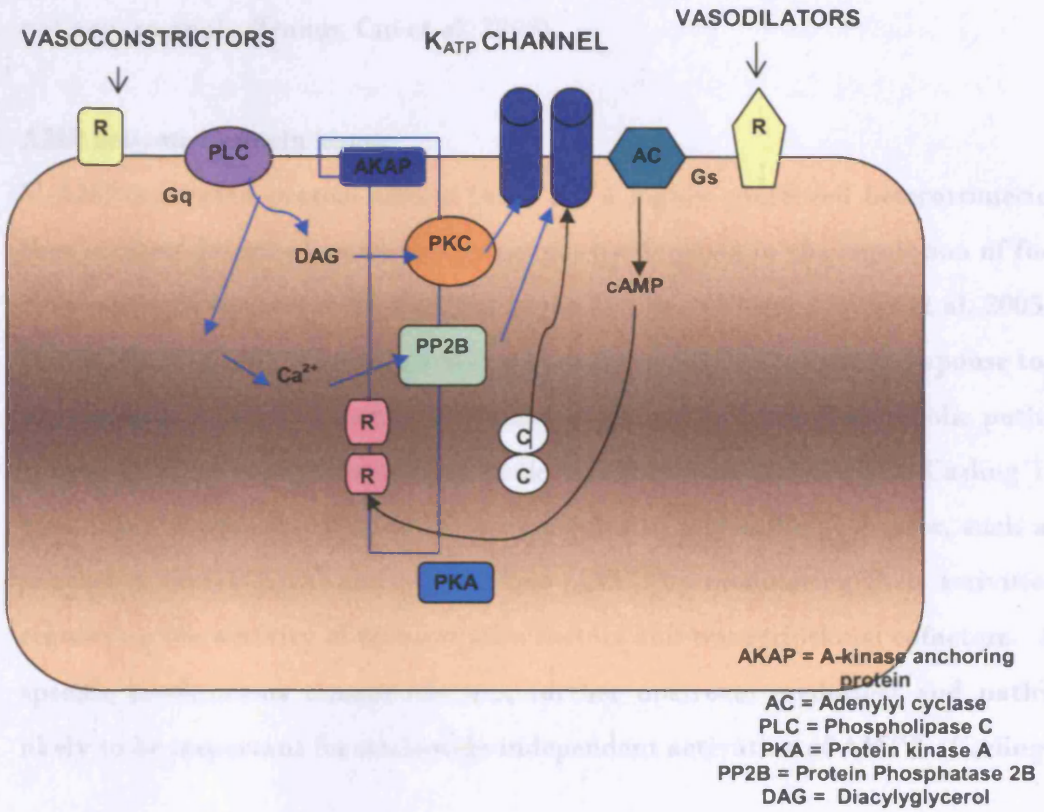

Figure 1.13: Factors that regulate vascular K_{ATP} channels. Black arrows represent activation pathways, and blue arrows represent inhibitory pathways. AKAP is thought to be important in localising key regulatory enzymes close to the channel to form a regulatory complex. Many vasodilators act through AC and PKA to cause channel activation. Vasoconstrictors act through PLC and inhibit the channel through PKC, and may further do so via activation of PP2B or via inhibition of AC (adapted from *Standen; 2003*).

The ATP-sensitivity of K_{ATP} channels is also modulated by membrane inositol phospholipids; an increase in PIP_2 or PIP_3 concentration shifting the ATP-inhibition curve to higher ATP concentrations, and so increasing the open probability (Hilgemann and Ball 1996; Baukrowitz, Schulte et al. 1998; Shyng and Nichols 1998; Baukrowitz and Fakler 2000). PIP_2 breakdown by phospholipase has also been shown to reduce

K_{ATP} channel activity in recombinant systems. It is not clear whether changes in phospholipid concentration serve to regulate the activity of native channels, or to provide a background reduction in ATP-sensitivity. It is possible that PKA may increase the PIP_2 affinity for Kir6.2 resulting in channel activation, however Kir6.1 already has a very high affinity for anionic phospholipids and the same mechanism is unlikely to apply (Quinn, Cui et al. 2003).

AMP activated protein kinase

5'-AMP-activated protein kinase (AMPK), a highly conserved heterotrimeric enzyme that is often described as an energy gauge, participates in the regulation of fuel supply in response to the metabolic needs of organ systems (Kahn, Alquier et al. 2005; Hardie, Hawley et al. 2006). Upon its activation during metabolic stress in response to elevated intracellular AMP/ATP ratios, a number of energy producing metabolic pathways are turned on, and energy consuming pathways inhibited (Hardie and Carling 1997). It does this via phosphorylation of key enzymes in metabolic pathways, such as acetyl-enzyme A (acetyl-CoA) and carboxylase (ACC), by modulating their activities and by regulating the activity of transcription factors and transcriptional cofactors. Although specific mechanisms remain obscure, further upstream mediators and pathways are likely to be important for nucleotide-independent activation of AMPK (Carling 2004).

Recent studies suggest that AMPK plays an important role in regulating insulin release from β-cells of the pancreas, and this may occur via activation of K_{ATP} channels. Both the Kir6.2 and the SUR1 subunits of the K_{ATP} channel, along with the voltage-sensitive Ca^{2+} channel isoform expressed in β-cells, contain potential consensus AMPK-phosphorylation sites (Rutter, Da Silva Xavier et al. 2003). The potential role of AMPK in modulating this response needs to be further investigated, despite characterization of the direct activating and inhibitory effects of ADP and ATP on the channel respectively (Ashcroft and Gribble 1998).

In wild type cells, preconditioning increases sarcolemmal/cytosolic Kir6.2 ratio, confirming previous findings that preconditioning stimulates the recruitment of sarcolemmal K_{ATP} channels (Budas, Jovanovic et al. 2004; Sukhodub, Jovanovic et al. 2007). A dominant negative form of the α2 AMPK subunit (an α subunit isoform specifically expressed in the liver, cardiac and skeletal muscle) was overexpressed in cardiomyocytes to analyse the role that AMPK plays in preconditioning in the heart, yet channel recruitment was not observed, suggesting that α2 AMPK catalytic activity is essential for preconditioning-induced stimulation of K_{ATP} channel trafficking to the sarcolemma (Sukhodub, Jovanovic et al. 2007).

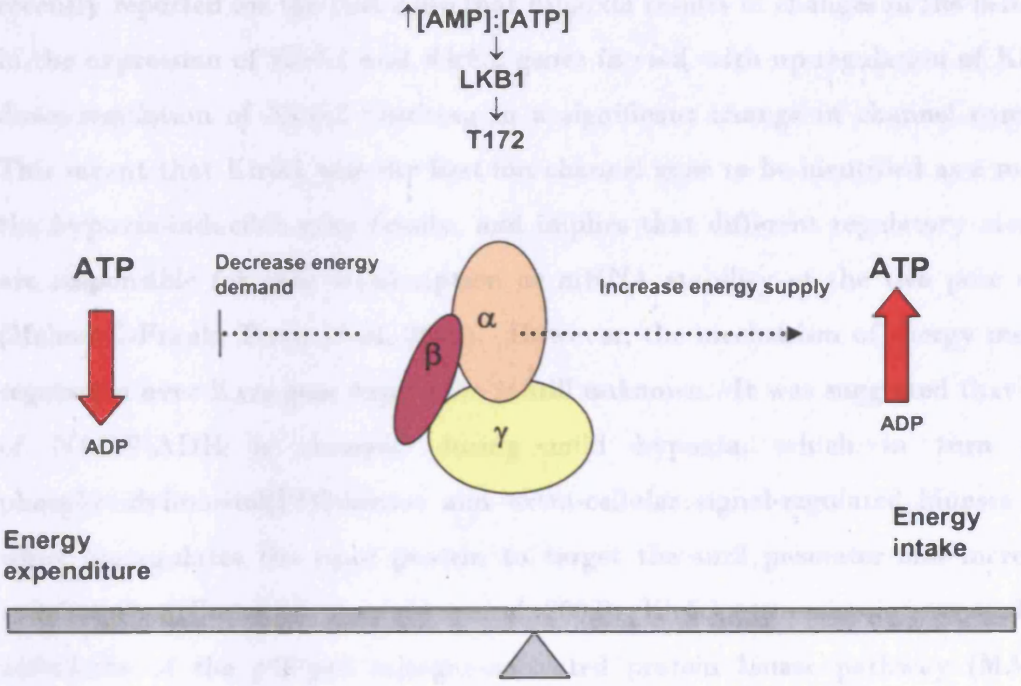

Figure 1.14: Energy levels are regulated by AMPK. AMPK is activated by a rise in the AMP:ATP ratio. When threonine 172 (T172) of the α subunit is phosphorylated (catalysed by serine-threonine tumor-suppressor kinase, LKB1) AMPK is activated. ATP generating pathways are as such switched-on, and ATP utilizing pathways are switched-off. The combined roles of AMPK ensure that the energy status of the cell is finely balanced (adapted from *Carling; 2005*).

Cell energy metabolism regulates K_{ATP} gene expression

As well as the described interaction of K_{ATP} channels with nucleotides and cell metabolites, K_{ATP} gene expression is also regulated by energy metabolism, whereby alterations in metabolism will lead to changes of K_{ATP} channel number. In rat pancreatic islets, a decrease of Kir6.2 mRNA level was induced by high glucose, which was reversed by exposure to low glucose (Moritz, Leech et al. 2001), and Kir6.1 mRNA was specifically upregulated in both ischemic and non-ischemic regions of the rat heart after ischemia followed by reperfusion (Akao, Otani et al. 1997). Conversely, K_{ATP} channel number was increased, and resistance conferred against Ca^{2+} loading in heart cells following the induction of acute hypoxia (Crawford, Jovanovic et al. 2003). It was recently reported for the first time that hypoxia results in changes in the mRNA level in the expression of Kir6.1 and Kir6.2 genes *in vivo*, with up-regulation of Kir6.1 and down-regulation of Kir6.2 resulting in a significant change in channel composition. This meant that Kir6.1 was the first ion channel gene to be identified as a member of the hypoxia-inducible gene family, and implies that different regulatory mechanisms are responsible for gene transcription or mRNA stability of the two pore sub-units (Melamed-Frank, Terzic et al. 2001). However, the mechanism of energy metabolism regulation over K_{ATP} gene expression is still unknown. It was suggested that the ratio of NAD/NADH is changed during mild hypoxia, which in turn activates phosphotidylinositol(PI)3-kinase and extra-cellular signal-regulated kinases (ERKs), which upregulates the *c-jun* protein to target the sur2 promoter and increase gene transcription (Crawford, Jovanovic et al. 2003). Kir6.1 expression is increased through activation of the p42/p44 mitogen-activated protein kinase pathway (MAPK) via urocortin (Lawrence, Chanalaris et al. 2002), and hyperglycemia decreases Kir6.2 mRNA levels via inhibition of mRNA stability (Moritz, Leech et al. 2001). The control of K_{ATP} channel number via genetic regulation has a significant impact on channel function. There is a direct link between the levels of cell resistance to oxidative stress and channel number (Crawford, Jovanovic et al. 2003), and enhanced sensitivity to hypoxia or ischemia of cardiac cells is induced by inhibition of K_{ATP} gene expression in diabetes (Ren, Xu et al. 2003).

1.7 Physiological and pathophysiological roles of the vascular smooth muscle ATP-sensitive K^+ channel

Resting membrane potential and basal tone

Various *in vitro* studies have shown that glibenclamide causes depolarisation and increases muscle tone in the vascular smooth muscle of rabbit mesenteric artery and canine saphenous vein (Nelson, Huang et al. 1990; Nakashima and Vanhoutte 1995) and in guinea-pig trachea, dog bronchial and pig urethra non-vascular smooth muscle (Kamei, Yoshida et al. 1994; Teramoto, Creed et al. 1997). *In vivo* studies have also shown that glibenclamide significantly increases vascular resistance and decreases arterial diameter (Quayle, Nelson et al. 1997). Presumably there is a low density, or a low open probability of native K_{ATP} channels, since direct recordings of channel activity showed that they opened briefly in the absence of channel openers (Teramoto, McMurray et al. 1997). Therefore the resting membrane potential of smooth muscle may be regulated by K_{ATP} channels with a low level of channel activity.

Endotoxins and Septic Shock

Since K^+ channel blockers reduce vasodilation (Clapp and Tinker 1998), it follows that activation of potassium channels in the peripheral circulation might be important in the refractory vasodilation of shock, the characteristics of which are vascular hyporesponsiveness to vasoconstrictors, inadequate tissue perfusion, low systemic resistance and hypotension. The first evidence for a role of K_{ATP} channels in the vasodilatation induced by shock showed that the blood pressure in dogs with endotoxic hypotension could be restored via the vasoconstrictive action of glibenclamide (Landry and Oliver 2001). Since then, a wealth of evidence has accumulated to suggest that the activity of K_{ATP} channels is increased in circulatory shock. Studies in rat and pig models in which shock is induced by bacterial endotoxins (lipopolysaccharides) have shown that glibenclamide can partially restore arterial pressure (Salzman, Vromen et al. 1997; Sorrentino, d'Emmanuele di Villa Bianca et al. 1999). There is substantial evidence that increased synthesis of nitric oxide (NO) contributes to the hyporeactivity of shock and

vascular hypotension (Garland and McPherson 1992; Miyoshi, Nakaya et al. 1994; Murphy and Brayden 1995; Wu, Thiemermann et al. 1995), and it has been suggested that endotoxaemia can reduce K_{ATP} channel sensitivity to glibenclamide, maybe through the action of NO (O'Brien 2002). The requirement of Kir6.1 in securing coronary vasoreactivity has been demonstrated in a model of severe sepsis with acute endotoxic shock. Knockout of the *KCNJ8* gene (encoding for Kir6.1) interrupted a vital vasodilatory adaptive mechanism in LPS-induced endotoxemia, resulting in premature death and producing deficits in ischemic cardiac dysfunction and coronary flow (Kane, Lam et al. 2006).

Vasodilator Responses to Metabolic Demand and Exercise

Blood flow is closely correlated to metabolic demand in many vascular beds. Metabolically active tissue releases local vasodilator signals, such as prostacyclin and adenosine, in response to a fall in oxygen tension and pH. Blood vessel diameter and thus blood flow is subsequently altered. In the coronary circulation and several other vascular beds, K_{ATP} channel activation is important in hypoxic vasodilation. It has been suggested that K_{ATP} channels play an important role in post-ischaemic vasodilation from studies of reactive hyperaemia in both human forearm and guinea-pig (Bank, Sih et al. 2000; Kingsbury, Robinson et al. 2001). Endogenous substances that hyperpolarize and relax cerebral vascular smooth muscle such as endothelium-derived hyperpolarizing factor (EDHF), prostacyclin, opioids and adenosine, appear to do this via K_{ATP} channels, which in turn may contribute to cerebral vasodilation in response to hypoxia and to cerebral vascular autoregulation (Lee, Kwon et al. 1993; Reid, Paterson et al. 1993; Faraci and Sobey 1998).

K_{ATP} channels may be involved in circulatory responses to the increased metabolic demands induced by exercise, as indicated by their role in metabolic vasodilation. In exercising dogs, resting coronary blood flow was reduced via K_{ATP} channel blockade with glibenclamide, as was the reactive increase in blood flow due to ischaemia. However, exercise-induced vasodilation was not prevented (Duncker, Van Zon et al.

1993). However, blockade of K_{ATP} channels hindered exercise-induced coronary vasodilation when adenosine receptors were inhibited (Duncker, van Zon et al. 1995) and this effect became more severe when NO synthase activity was also inhibited (Ishibashi, Duncker et al. 1998). Since both adenosine and NO were unaffected by blockade of both pathways, neither appear essential for maintaining either resting coronary flow or the increase in coronary flow on exercise. This in turn suggests that, under normal conditions, K_{ATP} channels are important for maintaining coronary vasodilation during exercise, but that when they are blocked, adenosine and NO can act to increase coronary blood flow (Ishibashi, Duncker et al. 1998). An increased dependence on K_{ATP} channel opening to increase coronary blood flow in exercise is also seen in hypertrophied hearts, whereby glibenclamide alone diminished the exercise-induced increase in flow (Melchert, Duncker et al. 1999). A recent study involving exercising pigs has shown that even though K_{ATP} channel activation was not essential for exercise-induced vasodilation, it contributes to vasodilation both at rest and during exercise in both the systemic and coronary circulations. However, pulmonary vascular conductance was unaffected by glibenclamide either at rest or during exercise (Duncker, Oei et al. 2001).

Proposed mechanism by which hypoxia triggers vasodilatation

In smooth muscle cells, K_{ATP} channels are thought to be either directly activated by hypoxia, or activated by receptor-coupled signal transduction pathways via the release of vasodilator metabolites from surrounding tissue or endothelial cells. At the tissue and organ level the role that K_{ATP} channels play in hypoxic vasodilation is well established, but this is not the case at the cellular level. In arteries supplying rat cremaster muscle, a lack of effect of hypoxia on K_{ATP} current was reported (Jackson 2000) and in a recent experiment K_{ATP} current was undetectable in hypoxic cells from arteries supplying rat skeletal muscle (Quayle, Turner et al. 2006). Conversely, in smooth muscle cell from pig coronary arteries, K_{ATP} current was shown to be activated by hypoxia (Dart and Standen 1995).

Even though the latter study would suggest that hypoxia vasodilation in the heart results in changes in intracellular nucleotide levels and direct activation of smooth muscle K_{ATP} channels, it is unclear whether this is actually the case. They may be regulated by oxygen tension independently of cell metabolism. The recent data suggests that, at the cellular level, changes in cell metabolism during hypoxia do not activate vascular K_{ATP} channels since anoxia but not hypoxia activated K_{ATP} current in femoral artery myocytes, and because inhibition of cellular energy production was insufficient to activate K_{ATP} current, with current activation requiring energy consumption. Furthermore, a relaxant effect of hypoxia on rat femoral artery was observed, and it was suggested that this was mediated by changes in $[Ca^{2+}]_i$ through modulation of calcium channel activity (Quayle, Turner et al. 2006).

1.8 Aims and hypotheses

It was hypothesized that the intrinsic metabolic sensitivity of Kir6.1/SUR2B demonstrated in my initial experimental analysis could be accounted for by an increase in intracellular MgADP upon metabolic poisoning, and subsequent depletion of the glycolytic and oxidative phosphorylation pathways. However, I wanted to determine if the channel pore or the sulphonylurea receptor was primarily responsible for this apparent intrinsic metabolic sensitivity. Therefore, I set out to deduce:

(1) If protein kinases or variations in nucleotide concentration have a predominant role in the regulation of the channel *in vitro*

(2) If the pore of the channel displays any intrinsic ATP sensitivity, and to create a constitutively active channel at the membrane in the absence of SUR

(3) The role of the NBDs of the sulphonylurea receptor in the regulation of Kir6.1/SUR2B

(4) Any differences in metabolic regulation between Kir6.1/SUR2B and Kir6.2/SUR2B

(5) If there are any differences in pharmacology between metabolically activated currents, and those activated upon the addition of a K_{ATP} channel opener

Chapter Two

Materials and Methods

Chapter Two: Materials and Methods

2.1 General Molecular Biology

It will become apparent that in my thesis several powerful molecular biology techniques were used throughout my experimentation, since the majority of my data was reliant on my ability to manipulate cloned cDNA encoding the K_{ATP} channel Kir6.1 and SUR2B channel subunits. Due to its length and chemical monotony, DNA was an extremely difficult molecule to analyse before the 1970s. The discovery of prokaryotic enzymes that cut and join specific base-pair sequences in double stranded DNA, and those that replicate DNA and reverse transcribe RNA, revolutionised molecular biology. The second major advance was the finding that complementary single-stranded nucleic acid chains can hybridise to form double-stranded molecules at around 65°C (this can occur between DNA/DNA, DNA/RNA and RNA/RNA). Additionally, the powerful technique we refer to as the Polymerase Chain Reaction (PCR) was introduced in the 1970s as was the discovery of a heat-resistant DNA polymerase isolated from thermophilic bacteria, which together allow the amplification of a particular sequence of DNA in the test tube. This is in turn possible, because methods were developed in the 1970s to determine the sequence of any nucleotide fragment, making it possible to determine the complete DNA sequences of thousands of genes. Finally, advances in microbial genetics found application in molecular biology, such as the extensive use of bacterial plasmids to package and deliver recombinant DNA molecules into host cells and viral enzymes to reverse transcribe mRNA into cDNA.

Plasmids exist in many bacterial species: circular double-stranded DNA molecules that act as accessory chromosomes that replicate themselves and drive mRNA transcription independently of the host genome. However, they require the transcription and translation machinery of the host cell. To allow the efficient delivery of foreign genetic material into either bacterial or eukaryotic cells, such plasmids have been modified to

allow them to be used as vectors. Many are now commercially available, such as the pcDNA3.1 family (*Invitrogen, Paisley, UK*) employed in this thesis, the main features of which are shown in *Figure 2.1.* These vectors are designed for high level stable or transient expression of the encoded gene in mammalian cells, and the efficient propagation of the plasmid vector in many strains of *E.coli.*

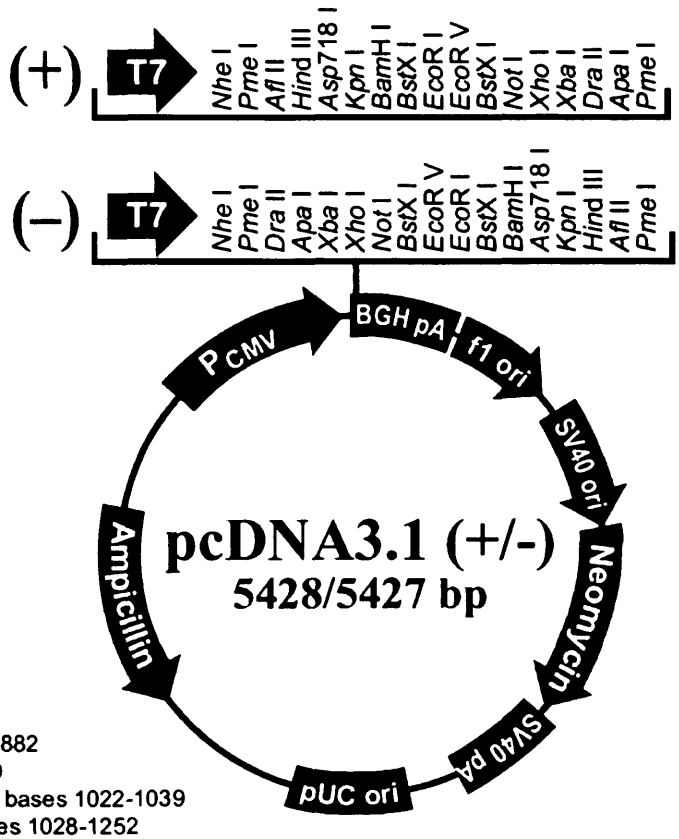

Comments for pcDNA3.1 (+)
5428 nucleotides

CMV promoter: bases 232-819
T7 promoter/priming site: bases 863-882
Multiple cloning site: bases 895-1010
pcDNA3.1/BGH reverse priming site: bases 1022-1039
BGH polyadenylation sequence: bases 1028-1252
f1 origin: bases 1298-1726
SV40 early promoter and origin: bases 1731-2074
Neomycin resistance gene (ORF): bases 2136-2930
SV40 early polyadenylation signal: bases 3104-3234
pUC origin: bases 3617-4287 (complementary strand)
Ampicillin resistance gene (*bla*): bases 4432-5428 (complementary strand)
ORF: bases 4432-5292 (complementary strand)
Ribosome binding site: bases 5300-5304 (complementary strand)
bla promoter (P3): bases 5327-5333 (complementary strand)

Figure 2.1 Diagram to show main features of pcDNA3.1, including the multiple cloning site

Restriction digestion of DNA molecules

The restriction endonuclease activity of restriction enzymes can be used to manipulate double stranded DNA. They hydrolyse DNA at specific palindromic nucleotide sequences (Sambrook 1989). Some types create blunt ends via cleaving the DNA at the axis of symmetry (e.g. Eco47III), while some create cohesive ends, i.e. protruding 5' or 3' single-stranded overhangs (e.g. EcoRI) via cleaving on the opposite sides of the symmetrical axis. A specific condition is required for the optimal activity for each restriction enzyme. A specific incubation buffer (provided by the manufacturer) and bovine serum albumin (BSA), ensure maximal activity. The components of a typical restriction digest are listed below:

5μl DNA
2μl 10× BSA stock solution (final concentration 100μg/ml)
2μl 10× Reaction buffer
10.5μl molecular biology grade water (*Sigma, Poole, UK*)
0.5μl Restriction enzyme (2-10 units)

A unit of enzyme is typically defined as the amount required for complete digestion of 1μg λDNA in 16 hours at 37°C. Digests were generally incubated for 1-3 hours. In the majority of cases, two restriction enzymes were used in a digest in order to subclone DNA from one plasmid vector to another, whereby a compatible buffer was used such that each enzyme had greater than 50% of its maximal activity.

Agarose gel electrophoresis

DNA fragments can be separated from each other on the basis of size using agarose gel electrophoresis. This works on the principle that the phosphate groups of DNA are negatively charged at neutral pH, and therefore migrate under the influence of an electric field. The gel forms a matrix, and effectively sieves the DNA, whereby the migration rate of linear double stranded DNA molecules through the gel is proportional to the logarithm of the number of base pairs (Helling and Boyer 1974). The migration

rate differs depending on the conformation of the DNA – supercoiled, nicked circular and linearised DNA molecules all migrate at different rates (Thorne 1966). DNA was visualised using ethidium bromide. This is a dye that intercalates between base pairs so that DNA bands can be visualised under ultraviolet light. In the majority of cases a 0.7% (w/v) agarose gel was made, since the effective range of size separation is between 0.8 and 10 kilobase pairs (kB) (Sambrook 1989). For a 0.7% (w/v) gel, 420mg electrophoresis grade agarose (*Invitrogen, UK*) was added to 60ml 1× Tris-Acetate-EDTA (TAE) solution. A 50× TAE stock solution was made using 2M Tris Base (*Sigma Aldrich, UK*), 50mM EDTA pH8.0 and 5.71% (v/v) glacial acetic acid (*BDH, UK*). The mixture was microwaved until completely dissolved, and then ethidium bromide (*Sigma Aldrich, UK*) was added upon cooling from a 10mg/ml aqueous solution to a final concentration of 0.5μg/ml. The agarose-TAE mixture was poured into a plastic tray, sealed securely with autoclave tape and plastic combs placed in the appropriate slots to create wells. The gel was allowed to set at room temperature, and then placed into an electrophoresis tank containing the running buffer 1× TAE.

DNA was loaded via the addition of gel loading buffer. A 6× buffer was made from 0.25% (w/v) bromophenol blue, 0.25% (v/v) xylene cyanol FF and 30% (v/v) glycerol (all reagents supplied from *Sigma Aldrich, Poole, UK*). Typically 4μl of 6× gel loading buffer was added to 20μl sample. DNA samples were loaded into their designated wells along with the standard DNA molecular weight marker VII (*Roche Labs, UK*) to determine the size of DNA fragments. A gel was typically run for one hour at 100mV , then viewed under ultra-violet (UV) light at 312nm wavelength in a UVP dual intensity transilluminator (*Upland, California, USA*), equipped with digital video camera and monitor (*Sony SSM-121CE*). Photographs of the gel image were printed by a video graphic printer.

Extraction and purification of DNA fragments from agarose gels

A commercial kit is available from Qiagen (QiaEX II agarose gel extraction kit, *Qiagen, Crawley, Sussex*) that is able to purify DNA from an agarose gel with high efficiency. This is able to solubilise agarose, and under high salt concentrations bind DNA fragments via a resin of silica-gel particles. Contaminants are removed via a series of washes, and purified DNA eluted from the resin using distilled water.

The DNA fragment of interest was excised from the agarose gel with a scalpel, weighed in an eppendorf tube then 3 volumes of buffer QX1 added to one volume of DNA fragment (100bp-4kb) to dissolve the gel at 50°C for approximately 10 minutes. 10μl of QIAEX II resin was added to the solubilised mixture to bind the DNA, and binding was allowed to proceed for a further 10 minutes at 50°C with regular vortexing to keep the resin in suspension. Subsequently, the resin was pelleted at ~17, 900×g in a micro-centrifuge for 30 seconds and the supernatant removed. The pellet was washed via resuspension and subsequent pelleting with 500μl of buffer QX1, followed by two additional washes in 500μl buffer PE (a buffer containing ethanol to remove residual salt). After air drying the pellet at room temperature, the sample was centrifuged with 20μl distilled water to elute the DNA, which was collected in a clean eppendorf tube. Elution was repeated, and the elutates combined to increase the yield of DNA.

Ligation of DNA fragments

In a ligation reaction, a DNA fragment and a vector digested with the same restriction enzymes can be spliced together. Compatible cohesive sticky ends were produced by digesting the vector and DNA fragment of interest with the same restriction enzymes. The cleaved phosphodiester bonds were therefore easily resealed via the DNA ligase, an enzyme that catalyses the formation of new phosphodiester bonds between residues located at the 5' terminus of the DNA fragment and hydroxyl groups located at the 3'end. The 5' phosphate groups of the vector were removed with the enzyme calf intestinal phosphatise (CIP), (*New England Biolabs, UK*) to prevent re-ligation of the vector termini. In these experiments Bacteriophage T4 DNA ligase (*NEB, UK*) was

used which requires the co-factors ATP and Mg^{2+} (Weiss 1968). The buffer provided from the same manufacturer contained 66mM trisHCl, 5mM $MgCl_2$, 1mM Dithiothreitol and 1mM ATP, pH7.5. A control reaction for self-ligation of the CIP-treated vector was set up in parallel with each ligation reaction. A typical reaction was set up as below;

Control reaction	*Ligation reaction*
5µl CIP-treated digested vector	5µl CIP-treated digested vector
12µl distilled water	12µl digested DNA fragment
2µl 10x ligation buffer	2µl 10x ligation buffer
1µl T4 DNA ligase (1 unit)	1µl T4 DNA ligase (1 unit)

It was generally necessary to adjust the molar ratio of insert to vector DNA to obtain a successful ligation; generally this was 3:1 (insert: vector), i.e.

Mass insert(ng) = 3 × (mass (ng) /length (bps) vector) × mass vector (ng)

Ligation reactions were incubated overnight at 16°C, and the ligated DNA subsequently transformed into competent *E.coli*.

Procedure for making competent *E.coli* for transformation

The process of introducing foreign DNA into bacteria is known as transformation. For practical reasons, chemical transformation was used, whereby bacteria first need to be treated with a series of ice-cold buffers containing either $CaCl_2$ or RbCl to make them competent. Competent bacteria are in a state whereby they can more readily take up foreign DNA. Two different strains of competent *E.coli* were used in my transformation experiments: DH5α and Top10. The Top10 strain was preferentially used since it allows stable replication of high copy number plasmids, the original glycerol stock of which was purchased from Invitrogen (*Groningen, Netherlands*) and stored at -80°C.

To replenish competent *E.coli* stocks, cells from the glycerol stock were streaked onto LB broth (Luria) agar plates using a sterile inoculating loop, incubated at 37°C overnight and stored at 4°C thereafter for a maximum of four weeks. LB broth also served as the culture medium for *E.coli*, composition per litre: 10g Tryptone, 5g Yeast extract and 5g NaCl, and was supplied in tablet form (*Sigma, Aldrich, Poole, UK*). LB agar plates were made via the addition of 1.5g agar (*Sigma, Aldrich, Poole, UK*) per 100mls broth, which was microwaved to dissolve then poured into 90mm Petri dishes (*VWR, Merck House, UK*) upon cooling. Plates were left to set at room temperature and stored at 4°C.

With reference to Top10 *E.coli* cells, individual colonies were picked using a sterile pipette tip and grown in 3mls LB broth for 7-9 hours in a shaking incubator set at 400×g and 37°C. 1ml of starter culture was transferred into a sterile 2L flask containing 200ml of LB broth and the cells incubated until the $O.D._{550}$ was between 0.450 and 0.550nm. The cells were transferred into sterile 250ml centrifuge bottles and allowed to cool on ice, before being centrifuged at 4000×g for 15 minutes. The supernatants were discarded, and the cells resuspended in 20ml ice-cold RF1 buffer (100mM RbCl, 50mM $MnCl_2.4H_20$, 30mM potassium acetate, 10mM $CaCl_2.2H_20$, 15% (w/v) glycerol, pH adjusted to 5.8 with 0.2M acetic acid and filter sterilised) and incubated on ice for 15 minutes before centrifugation at 2500×g for a further 9 minutes. The supernatant was again discarded and the cells resuspended in 3.5mls ice-cold RF2 buffer (10mM RbCl, 10mM MOPS, 75mM $CaCl_2.2H_20$, 15% glycerol, pH adjusted to 6.8 with 0.2M NaOH and filter sterilised). All cells were pooled and incubated on ice for 15 minutes. Cells were aliquoted into sterile eppendorf tubes and flash frozen using liquid nitrogen, then stored in the -80°C freezer.

Transformation of plasmid DNA

100µl of pre-thawed Top10 *E.coli* cells were incubated with 1µl purified plasmid DNA or 10µl of a ligation reaction, incubated on ice for 30 minutes then heat-shocked at 42°C for 90 seconds to introduce the DNA into the bacterium. Immediately after heat-

shocking, cells were cooled on ice for 2 minutes, before the addition of 800µl LB broth, then, incubated at 37°C for 30 minutes. This allowed the expression of the antibiotic resistance gene encoded by the plasmid DNA. The transformation mixture was plated onto LB plates containing the desired antibiotic (either 30-100µg/ml carbenicillin or 30µg/ml kanamycin). Low carbenicillin plates were used with the mutagenesis kit. 100µl plasmid DNA was normally transformed, but when transforming ligation mixtures the cells were pelleted then resuspended in 100µl fresh LB before plating. The plates were incubated at 37°C for 12-16 hours after which time discrete colonies were observed that were assumed to have arisen from a single transformed bacterium.

Plasmid DNA purification

After transformation of plasmid DNA into bacteria, it needs to be purified so that it can be sequenced and digested to ensure that the cDNA has been manipulated correctly. Upon confirmation of the sequence, the plasmid DNA is usually retransformed so that it can be amplified in a large scale culture, in turn providing large yields of plasmid DNA. QIAGEN plasmid purification kits were used, which are based on a modified alkaline lysis procedure and the use of an anion-exchange resin (whereby the positively charged DEAE groups on the surface resin interact with the negatively charged phosphates of the DNA backbone) to bind plasmid DNA. The salt concentration and pH conditions of the buffers used determine whether DNA is bound or eluted from the column. Low molecular weight impurities, dyes, RNA and proteins are removed by a medium-salt wash, plasmid DNA is eluted in a high salt buffer and then concentrated and desalted by isopropanol precipitation. The type of QIAGEN kit employed depends on the yield of purified DNA required. Generally 10-20µg DNA are obtained using the QIAprep Miniprep system, 100µg of high-or-low copy plasmid/cosmid DNA using the midi kit system and up to 500µg DNA using the maxi kit. The QIAGEN plasmid midi kit was generally employed, as elaborated.

A single colony derived from transformed bacterium was picked and a starter culture of 3mls of LB medium, containing the appropriate selective antibiotic, inoculated and

incubated for ~8 hrs at 37°C at ~450×g. The starter culture was diluted in 50mls (in a flask of at least 4 times the volume) and grown for a further 12-16 hrs. The cells were harvested by centrifugation at 6000×g for 15 minutes at 4°C, and the pellet resuspended in 4 ml of buffer P1 (resuspension buffer: 50mM Tris.Cl, pH 8.0; 10mM EDTA; 100μg/ml RNase A). To lyse the pellet, 4 ml of buffer P2 (lysis buffer: 200mM NaOH, 1% SDS (w/v)) were added, the lysate mixed gently by inverting the tube and incubated at room temperature for 5 minutes. The DNA was precipitated by adding 4mls of chilled buffer P3 (neutralization buffer: 3M potassium acetate, pH 5.5), and via gentle inversion and incubation on ice for 15 minutes. The samples were centrifuged at 20,000×g for 30 minutes at 4°C, and meanwhile a QIAGEN-tip 100 equilibrated by applying 4 ml of buffer QBT (equilibration buffer: 750mM NaCl; 50mM MOPS, pH 7; 15% isopropanol (v/v); 0.15% Triton X-100 (v/v)), and allowing the column to empty by gravity flow. The sample was filtered to remove the supernatant, which was applied to the tip and allowed to enter the resin by gravity flow. The tip was washed twice with buffer QC (wash buffer: 1M NaCl; 50mM MOPS; pH 7; 15% isopropanol (v/v)) to remove the contaminants in the plasmid DNA preparation, then the DNA eluted with 5 ml buffer QF (elution buffer: 1.25M NaCl; 50mM Tris.Cl, pH 8.5; 15% isopropanol (v/v)) and collected in an oakridge tube. The DNA was further precipitated with 3.5 ml room-temperature isopropanol, mixed and centrifuged immediately at 15,000×g for 30 minutes at 4°C. The supernatant was decanted, and the DNA pellet resuspended in 500μl ddH_20 and transferred to a 1.5ml eppendorf tube, to which 1ml 100% ethanol and 50μl 3M pH 5.2 sodium acetate were added. The mixture was vortexed then incubated at -80°C for 20 minutes. Finally, the samples were spun at 18,000×g for 30 minutes at 4°C, the supernatant removed and 1ml 70% ethanol added to the pellet, and the samples spun again under the same conditions for a further 10 minutes. The supernatant was removed, the pellet left to air-dry for ~ 15 minutes, and then resuspended in 250μl ddH_20.

The Polymerase chain reaction (PCR)

Cloned cDNA was manipulated using PCR for eventual use in biochemical and electrophysiological analysis. PCR results in the selective amplification of a chosen region of a DNA molecule (Sambrook 1989). It works on the basis that short oligonucleotides can hybridise to the DNA molecule, one on either side of the double helix, and act as primers for DNA synthesis reactions, delimiting the region to be amplified. Amplification is usually carried out via a temperature resistant DNA polymerase (*Taq* or *Vent* DNA polymerase), which when added to the primed DNA and incubated, synthesises new complementary strands. The mixture is heated to 94°C so that the newly synthesised strands detach from the template (denaturation), and cooled to approximately 55°C, enabling the primers to hybridise to their respective positions, including positions on the newly synthesised strands (hybridisation). The DNA polymerase then synthesises a new strand at 72°C (extension). This cycle of denaturation-hybridisation-extension is repeated, usually 25-30 times, resulting in the eventual synthesis of several hundred million copies of the amplified DNA fragment via logarithm amplification. The annealing temperature for individual PCR experiment is determined via calculating the melting temperature (T_m) for each primer - i.e. a temperature that is low enough to enable hybridization, but high enough to prevent mismatched hybrids from forming;

$$T_m = (4\times[G+C] + (2\times[A+T])°C$$

A feature of PCR is that nucleotide sequences can be added to the 5'end of primer molecules, which during the PCR are incorporated into the DNA sequence. In this way, PCR fragments can be engineered to contain restriction enzyme sites for insertion into a particular cDNA sequence. The components of a typical reaction mixture are as follows;

Component	*Amount*
DNA template	~50-100ng
Forward primer	5.0 pmoles
Reverse primer	5.0 pmoles
Thermopolymerase buffer	10μl
dNTP mixture*	2μl
Taq DNA polymerase**	2 units
$MgCl_2$	2μl
ddH_20	to 100μl

* dNTP mixture = 25mM dATP, dCTP, dTTP, dGTP (purchased separately from *New England Biolabs, Hitchin, UK* as 100mM solutions and mixed in 1:1 ratios to produce a 25mM primer stock)

** Obtained from *New England Biolabs*

The cycling steps were conducted using a programmable thermal cycler (*Flexigene, Techne*) and typical cycling steps are as below;

Step 1	94°C, 4 minutes	Initial denaturation
Step 2	94°C, 1 minute	Denaturation
Step 3	55°C, 1 minute	Annealing of primers to ssDNA
Step 4	72°C, 1 minute	Elongation of nascent DNA
Step 5	72°C, 10 minutes	Final elongation
Step 6	Hold at 4°C	

Cycle from step 2 to step 4 for 30 cycles

The primers used in the standard PCR procedures are as follows:

Delta C48 5'-TCTTCTAGACTACTGGTGCGACAGTTCACTCTT-3'

Delta C61 5'-TCTTCTAGACTAGATGGAAGGTTTCTCGTCCAG-3'

Delta N13 5'-GGAGGATCCATGCTGGCCCGCATCGCGGCGGAG-3'

Delta N33 5'-GGAGGATCCATGGCCCGCTTCATCGCCAAG-3'

61R 5'-AAGAAGCTTTCATGATTCTGATG-3'

61F 5'-GGAGGATCCCTGGCCAGGAAGAGCATCATC-3'

Delta C48 and C61 were used to truncate the C-terminus of Kir6.1 by 48 and 61 amino acids respectively, Delta N13 and N33 were used to truncate the N-terminus by 13 and 33 amino acids respectively, and 61R and 61F were used to clone full length Kir6.1. Refer to section Chapter 4, *Figure 4.1.*

PCR Purification

This protocol purifies single- or double-stranded DNA fragments from PCR and other enzymatic reactions, since it is necessary to remove any contaminating proteins that may interfere with subsequent enzymatic steps. Again, a commercially available QIAquick kit was employed (*Qiagen, Crawely, Sussex*). 5 volumes of Buffer PB (exact formulation disclosed; contains hydrochloride and isopropanol) were added to 1 volume of PCR sample, mixed and placed in a spin column, and, to bind DNA, centrifuged for 30 seconds and the flow-through discarded. To wash the DNA, 0.75 ml of Buffer PE (formulation disclosed) was added to the column, which was centrifuged twice for 30 seconds and the flow-through discarded. To elute the DNA, 30µl dH_20 was added to the QIAquick membrane, the column centrifuged and the supernatant (purified DNA) collected in an eppendorf tube.

Site-directed mutagenesis

The commercially available *in vitro* QuikChange site-directed mutagenesis kit (*Stratagene, California, USA*) was used to make single amino acid point mutations in double-stranded DNA templates. The desired mutation was introduced via a PCR-based approach using temperature cycling and two synthetic oligonucleotide primers. The high fidelity *Pfu Turbo* DNA polymerase was used to replicate both DNA strands by extending the mutant oligonucleotide primers. Incorporation of the mutant primers into the newly synthesised DNA resulted in a mutated plasmid containing staggered nicks. Following temperature cycling, the products are treated with *Dpn* I. This is an

endonuclease enzyme that specifically digests methylated and hemimethylated DNA, with the target sequence 5'-Gm^{6}ATC-3'. Since DNA isolated from most strains of *E.coli* is dam methylated, *Dpn* I treatment will selectively digest the parental template, thus selecting for mutation-containing synthesised DNA. The nicked vector DNA containing the desired mutations is then transformed into *Epicurian coli* XLI-Blue competent bacterial cells. These repair the nicked DNA and amplify the mutated DNA construct. Transformed XLI-Blue competent cells were spread onto agar plates containing 30μg carbenicillin (since the DNA mutated was contained in pcDNA3.1), or 50μg ampicillin for the control reactions, and the DNA was prepared using standard molecular biology techniques. It was necessary to commercially sequence the cDNA to determine whether the desired mutation was incorporated into the sequence (performed by *Cytomyx, Cambridge, UK*).

The mutagenic oligonucleotide primers were designed individually according to the desired mutation. Both the forward and reverse primers contained the desired mutation, annealing to the same sequence on opposite strands. The mutation was in the middle of the primer, and they had a minimum GC content of 40% and terminated in one or more G/C bases. Primers were between 25 and 45 bases in length with a T_m of ≥78°C, whereby for a primer of length *N* bases:

$T_m = 81.5 + 0.41(\%GC) - 675/N - \%mismatch$

A typical mutagenesis reaction was prepared as below in a thin-walled PCR tube:

5μl 10× reaction buffer

Xμl (5-50ng) of dsDNA template

Xμl (125ng) of olignucleotide primer 1

Xμl (125ng) of oligonucleotide primer 2

1μl of dNTP mix

dd$H_2$0 to a final volume of 50μl

1μl PfuTurbo DNA polymerase (2.5U/μl)

For the control reaction, 2μl (10ng) of pWhitescript 4.5kb control plasmid (5ng/μl) was used as the template.

Reactions were subjected to the following cycling parameters:

Step 1: 94°C for 30 seconds	Initial denaturation
Step 2: 95°C for 30 seconds	Denaturation
Step 3: 55°C for 1 minute	Annealing of mutant primers to ssDNA
Step 4: 68°C for 2 minutes per kB of plasmid length	Elongation of mutant oligonucleotide primers
Cycle from Step 2 to Step 4 for 18 cycles	
Hold at 4°C	

Following temperature cycling, 1μl *Dpn* I (10 units/μl) was added to each mutagenesis reaction, mixed gently, spun in a micro-centrifuge for 1 minute and then incubated at 37°C for 1 hour to digest the parental supercoiled dsDNA.

Before transformation, the DNA was glycogen precipitated to increase DNA concentration (important because >5 kb templates were used). Briefly, 2.4 volumes 100% ethanol, 0.1 volumes 3M sodium acetate, 1μl glycogen were added to the reaction mixture, which was vortexed then incubated at -80°C ≥ 30 minutes. The mixture was then thawed and centrifuged at 20,000g for 30 minutes at 4°C to pellet the DNA. The supernatant was discarded and the pellet washed once with 250μl 70% ethanol and recentrifuged. The resultant pellet was resuspended in 5μl molecular biology grade water. 3μl DNA was used to transform XLI-Blue competent cells according to the manufacturer's instructions. The expected colony number for the control reactions was between 50-800 colonies and that of the sample transformations 10-1000 colonies (dependent of the base composition and length of the DNA template employed).

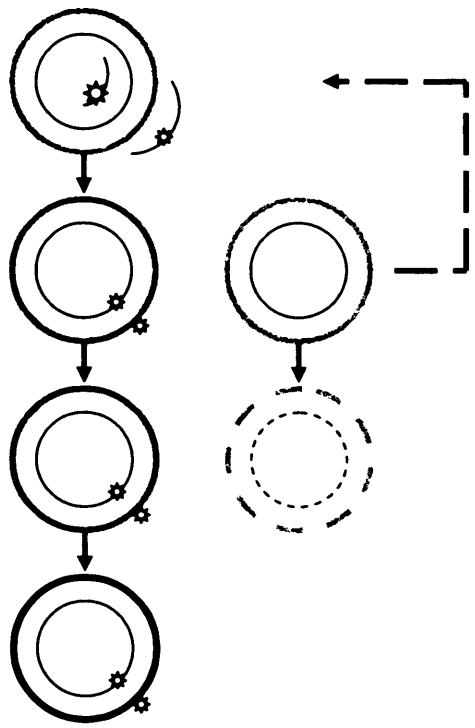

Mutant strand synthesis
DNA template denatured, mutagenic primers containing desired mutation anneal and extended

Dpn1 Digestion of Template
Parental methylated and hemimethylated DNA digested with Dpn1

Transformation
Mutant molecules transformed into competent cells for nick repair

Figure 2.2: The principles of site-directed mutagenesis

The following primers were used in site-directed mutagenesis to create point mutations in the sulphonylurea receptor of the reconstituted vascular smooth muscle K_{ATP} channel, Kir6.1/SUR2B:

T1345N F 5'-GGTGGGCATCTGTGGTCGAAATGGCAGTGGGAAGTCCTCC-3'
T1345N R 5'-GGAGGACTTCCCACTGCCATTTCGACCACAGATGCCCACC-3'

K1349R F 5'-GGTCGAACTGGCAGTGGGAGGTCCTCCTTATCCCTGG-3'
K1349R R 5'-CCAGGGATAAGGAGGACCTCCCACTGCCAGTTCGACC-3'

R816Q F 5'-GAGTGGGGGTCAGAGGCAGCAAATCTGCGTGGCACGGGCAC-3'
R816Q R 5'-GTGCCCGTGCCACGCAGATTTGCTGCCTCTGACCCCCACTC-3'

R816K F 5'-GAGTGGGGGTCAGAGGCAGAAAATCTGCGTGGCACGGGCAC-3'
R816K R 5'-GTGCCCGTGCCACGCAGATTTTCTGCCTCTGACCCCCACTC-3'

K708A F 5'-GGCAAGGAGAAGAGATGATGCTCCACAACCCACTTGGCC-3'
K708A R 5'-GGCAGGGAGAAGAGATGATGCTCCACAACCCACTTGGCC-3'

K1349M F 5'-GCTCGAACTGGCAGTGGGATGTCCTCCTTATCCCTGGC-3'
K1349M R 5'-GCCAGGGATAAGGAGGACATCCCACTGCCAGTTCGACC-3'

DNA Sequencing

To check that the nucleotide sequence was not altered through manipulating the cDNA, sequencing of plasmid DNA was achieved through a procedure based on the dideoxy nucleotide-mediated chain-termination method (Sanger, Nicklen et al. 1977). A minimum of 500ng purified plasmid DNA per sequencing reaction or 100ng/kb purified product per reaction was sent to the DNA Sequencing Service, CYTOMYX, along with the necessary pre-designed sequencing primers. The results were sent via email and the chromatogram files viewed using Chromas Version 2.31.

Primers to sequence single point mutations SUR2B:
R816Q/K seq: 5'-GGCTTACGCTGCCCAGAAGCC-3'
T1345N/K1349R seq: 5'-GCAGTGAAGAAAGTGAACAG-3'

Primers to sequence double point mutation in SUR2B:
K708A seq: 5'-GGATACTTCTCATGGGGC-3'
K1349M seq: 5'-CGATCTGTGTGTCAGATATG-3'

2.2 Cell culture

The majority of my studies were performed on immortalised eukaryotic cell lines. The HEK293 cell line (*obtained from Dr L Y Jan, UCSF*) is an immortalised human cell line derived from primary embryonic kidney cells transformed with sheared adenovirus type 5 DNA.

The HEK293 cell line

Growth conditions and method of subculture and maintenance

Cells were grown and cultured in Minimum Essential Medium (MEM) containing Earle's salts and L-Glutamine (*Invitrogen, UK*) supplemented with 1% Penicillin-Streptomycin (from a stock of 1mg/ml streptomycin and 10,000 units/ml penicillin) and 10% Foetal Bovine Serum (*Invitrogen, UK*). Cells were usually grown in a T75 ($75cm^2$) tissue culture flask (*VWR, Merck House, UK*) in a humidified atmosphere of 95% oxygen and 5% CO_2 and typically subcultured when 90% confluent. To passage cells, the culture medium was removed and the cells washed twice with Ca^{2+}, Mg^{2+} free Dulbeccos' phosphate buffered saline (*Invitrogen, Paisley, UK*). Cells were detached from the flask via incubation for 2 minutes at room temperature with 1ml 0.25% Trypsin (*Invitrogen, Paisley, UK*) in PBS. To inhibit the tryptic activity, 3mls of growth medium was added and the cell suspension collected in 15ml falcon tubes (*Sarstedt, UK*), and centrifuged at 340g for 3 minutes. Pelleted cells were resuspended in 10mls of fresh medium, and 1ml of the resuspension used to seed a new T75 flask. During log phase growth, the doubling time of HEK293 cells was around 24-36 hours, and therefore it was necessary to subculture once weekly. Fresh culture medium was applied every 3 days.

Production/revival of frozen stocks

Cells at 80-100% confluence were subcultured as described, but resuspended in culture medium containing 10% sterile Dimethyl Sulfoxide (*Sigma, Poole, UK*), and 1ml aliquots placed in cryogenic vials (*VWR, Merck house, UK*). Cells were gradually cooled. A Nalgene freezing jar (*VWR, Merck house, UK*) containing room temperature

isopropanol was initially used, and then the cryovials were placed in a -80°C freezer for 6-12 hours before being transferred to liquid nitrogen for long-term storage. Cells were revived by rapidly thawing an aliquot at 37°C before inoculation of a T25 ($25cm^2$) tissue culture flask (*VWR, Merck House, UK*) containing pre-warmed culture medium, which was replaced after 18-24 hours.

HEK293 cells subcloned with the K_{ATP} channel Kir6.1/SUR2B or Kir6.2/SUR2B

The cDNA constructs encoding the K_{ATP} channel pore-forming subunits Kir6.1 or Kir6.2 were previously subcloned in pcDNA3.1/zeo, likewise, the cDNA encoding for SUR2B was previously subcloned into pcDNA3.1. Since these vectors contain a gene encoding for resistance to Zeocin and Neomycin respectively, cells made to stably express the K_{ATP} channel were doubly selected with both Zeocin and Geneticin (G418). Geneticin was employed since it is an analogue of neomycin sulphate. The zeocin resistance gene encodes a protein that binds stoichiometrically to Zeocin and inhibits its DNA strand cleavage ability, thus death only occurs in cells that are non-resistant. The stable lines were cultured in the same manner as described, except that MEM containing 10% FBS, 344μg Zeocin (*Invitrogen, Paisley, UK*) and 727μg/ml Geneticin (G418) (*Invitrogen, Paisley, UK*) was applied. Frozen stocks of cells were produced and revived as previously described, but the culture medium of those revived was replaced with G418/Zeocin medium 18-24 hours after revival.

CHO-K1 cell line

The CHO-K1 cell line was derived as a subclone from the parental CHO cell line initiated from the biopsy of an ovary of an adult Chinese hamster (Puck 1957)and was obtained from the American Type Culture Collection (ATCC). Cells were grown in (Hams) F12 media (*Invitrogen, Paisley, UK*), supplemented with 10% fetal calf serum and 1% penicillin/streptomycin and cultured, frozen and revived as described for the HEK293 cell line.

C2C12 cell line

This is a subclone of the mouse myoblast cell line (Blau, Webster et al. 1985), as established by *D. Yaffe and O. Saxel* in *1977* (Yaffe and Saxel 1977). The C2C12 cell line differentiates rapidly, forming contractile myotubes and producing characteristic muscle proteins. Treatment with the bone morphogenic protein 2 (BMP-2) causes a shift in the differentiation pathway from myoblastic to osteoblastic. Cells were cultured as described, but it was important that they were passaged before reaching confluency as this would deplete the myoblastic population in the culture. Cells were grown in MEM supplemented with 10% FBS and 1% P/S.

Aortic and Cardiac Smooth Muscle Cell lines (AOSMC and CASMC)

These are primary human cell lines, comprised of either normal aortic or cardiac cells, purchased in the third or fourth passage (for references refer to www.lonza.com). Medium and reagents were obtained from Clonetics from CAMBREX. Smooth muscle cell basal medium (500ml) was supplemented with 0.5ml hEGF, 0.5ml insulin, 1ml hFGF-B, 25ml FBS, 0.5ml giberellic acid (GA)-1000. Cells were subcultured when 70% to 80% confluent and contained many mitotic figures throughout the flask (since they became irreversibly contact inhibited if allowed to reach confluence). For a T25 flask, the medium was aspirated, and cells were rinsed with 5 ml of room temperature HEPES Buffered Saline Solution (HEPES-BSS). Following aspiration, cells were covered with 2ml Trypsin/EDTA solution and trypsinisation allowed to occur until at least 90% of the cells were spherical. The trypsin was neutralized with 4ml room temperature Trypsin Neutralising Solution (TNS) and the cells transferred to sterile 15ml centrifuge tubes. The flask was given a final rinse with 2ml HEPES-BSS to collect residual cells, which were added to centrifuge tube. Harvested cells were centrifuged at 220×g for 5 minutes to pellet the cells, all bar 100-200µl of supernatant was aspirated. The remaining was used to resuspend pellet, then the cells diluted in 4-5ml growth medium (1ml per $5cm^2$). $1ml/5cm^2$ of growth medium were added to subsequent flasks, into which the desired volume of cells were dispensed then incubated at 37°C (5% CO_2). Growth medium was changed the day after seeding and every other day thereafter.

Cells under 25% confluency were fed with 1ml/5cm^2, from 25-45% confluency 1.5ml/5cm^2, and over 45% confluency 2ml/5cm^2. Cells were not cultured beyond eight passages.

Cells were cryopreserved in 80% Clonetics growth media, 10% FBS and 10% DMSO, which had been filter sterilised with a 0.2μm filter. Cells were harvested and centrifuged, and the pellet resuspended at 500,000 to 2,000,000 cells per ml. 1ml aliquots were pipetted into freezing vials and insulated in an isopropanol freezing canister. Cells were stored at -70°C overnight, and within 12-24 hours placed in liquid nitrogen for long term storage. Cells were revived and returned to culture as quickly as possible with minimal handling.

HL-1 Cardiomyocytes

The HL-1 cell line is derived from the AT-1 mouse atrial cardiomyocyte tumor lineage (Claycomb, Lanson et al. 1998). This was maintained in Claycomb Medium (*JRH Biosciences*), which when supplemented with 0.1mM norepinephrine (*Sigma*), 10% FBS, 1% P/S and 4mM L-glutamine (*Gibco Life Technologies, Paisley, UK*) will maintain the mature cardiomyocyte behaviour and differentiated phenotype.

Norepinephrine was made up in 30mM L-ascorbic acid. 80mg norepinephrine was added to 25ml acid, and the mixture filter sterilised with a 0.2μM syringe filter, aliquoted into 1ml volumes and stored at -20°C. A 1ml aliquot was added per 100ml medium for a 0.1mM final concentration. Soybean trypsin inhibitor was made from 25mg inhibitor (*Gibco Life Technologies, Paisley, UK*) dissolved in 100ml PBS, which was filter sterilised.

Flasks were pre-coated with gelatin/fibronectin (*Difco, UK & Sigma, UK* respectively) before culturing cells (2ml/T25). A sterile 0.02% solution of gelatin was made, of which 199ml was added to 1ml of fibronectin and mixed gently. 6ml aliquots were frozen at -

20°C. Coated flasks were incubated at 37°C overnight, and the gelatin/fibronectin removed before adding cells to flasks.

Cultures were split after full confluence. A T25 flask was rinsed with 3ml 0.05% trypsin/EDTA (*Gibco Life Technologies, Paisley, UK*), then aspirated. An additional 1.3ml trypsin EDTA was added, the culture incubated for 2 minutes at 37°C, then incubated for a final 5-8 minutes with fresh tryspin/EDTA. The trypsin was inactivated with 1.3ml soybean trypsin inhibitor, and the cells transferred to a centrifuge tube. The empty flask was additionally washed with 5ml of Claycomb Medium (10% FBS, 1% P/S, 4mM L-glutamine, 0.1mM norepinephrine) and added to the tube, which was spun at 140×g for 5 minutes. The subsequent pellet was resuspended in 3ml medium, and 1ml was transferred into each of three T25 flasks containing 4mls of medium. Cultures were fed with 5ml medium/T25 flask every day.

When freezing cells, those harvested from a T75 were resuspended in 1.5ml freezing medium (95% FBS and 5% DMSO), transferred to a cryovial which was placed in a Nalgene freezing jar containing room temperature isopropanol, which in turn was incubated at -80°C. 6-12 hours later, the vial was transferred to liquid nitrogen. When reviving cells, aliquots were quickly thawed, then centrifuged for 5 minutes at 1400×g and resuspended in 5ml medium before transfer to a T75 flask.

Transfections

The process of introducing foreign DNA into a cell line is known as a transfection. It was necessary to transfect K_{ATP} channel subunits into a heterologous system, such as the HEK293 cell line, since once in the cytoplasm, DNA is transported to the nucleus and, using the host cell's transcriptional and translational machinery, the encoded proteins are over-expressed. In the majority of cells, the DNA is maintained transiently, since eventually the plasmid is lost as the cells continue to divide. In my studies, liposome mediated gene transfer was used (Itani 1987) to transfect cells transiently, whereby complexes form between positively charged lipids and negatively

charged DNA which can then fuse to the cell plasma membrane, facilitating the uptake of DNA via endocytosis. Serum-free medium is used throughout, since serum proteins can interfere with the formation of complexes. This method is well characterised, and efficient transfections can be achieved with relatively small quantities of DNA (0.5-1.5μg).

Liposome based transient transfection procedure

Cells were subcultured as previously described, and seeded into 6 well tissue culture plates (with wells of 35mm diameter) (*Triple Red, UK*) at the necessary cell density to reach 70% confluence within 24 hours. For individual transfections 5μl of 2mg/ml lipofectamine (a 3:1 w/w ratio of the polycationic lipid DOSPA and the neutral lipid DOPE in sterile water) (*Gibco Life Technologies, Paisley, UK*) preincubated for 15 minutes with 100μl Optimem serum free medium (*Gibco Life Technologies, Paisley, UK*) was added to a mixture of 0.8μg-2.0μg plasmid DNA in 100μl Optimem. The combined DNA-lipid mixture was incubated at room temperature for 30 minutes to allow complex formation, and then a further 800μl Optimem added (final volume 1ml). Cells were washed twice with optimem to remove contaminating serum proteins, incubated in the transfection mixture for at least 5 hours (typically overnight), before the transfection mixture was replaced with normal culture medium.

2.3 Immunohistochemistry and immunofluorescence microscopy

Immunofluorescence microscopy involves the labelling of antigens by antibodies labelled with fluorescent groups, and was developed by Coons and Colleagues in 1941. The fluorescent microscope employed illuminated the sample using epi-illumination, i.e. the specimen was illuminated from the same side as the objective lens, and required a dichroic mirror to reflect the excitatory light onto the specimen, whilst transmitting the emitted light to the eyepieces. It is only when employing epi-illumination that we can make quantitative analysis of fluorescence. It omits the disadvantage of reabsorption of emitted light by the specimen, thus lowering the observed fluorescence intensity (which is possible at high fluorophore concentrations). Depending upon the fluorophore being studied, the excitatory and emitted light can be filtered by optical filters that only allow transmission of light of certain wavelengths, whereby the emission filter ensures that only light emitted from the sample reaches the eyepiece, and the excitation filter ensures that only light of the appropriate wavelength is incident on the sample in question. Slides were viewed under epi-fluorescence illumination using a Zeiss Axiovert 100M microscope (*Zeiss Instruments, Jena, Germany*). Samples were viewed at 400× magnification using a Zeiss 40× (*Plan-Neofluar oil immersion*) objective with 10× eyepieces. The objective had a numerical aperture of 1.41. The microscope was equipped with a filter set (*XF66-1 multiband filter, Omega Optical, Brattleboro, Vermont, USA*), comprising a dichroic mirror and emission and excitation filters, which allowed the observation of specimens double labelled with rhodamine and fluorescein conjugated fluorophores. The emission filter was fitted into a filter wheel (*LUDL, Hawthorne, New York, USA*), and the microscope was equipped with a monochrome digital camera (*C4742-95, Hamamatsu, Japan*) with the facility to divert the light path fully to the camera aperture. Specimens were illuminated by a Xenon short arc lamp (*Ushio Inc., Japan*) integrated with a Polychrome II monochromator (*T.I.L.L., Photonics GMBH, Planegg, Germany*) linked to the microscope via a specially designed epi-fluorescence condenser. The wavelength of excitatory light was controlled via analogue voltage.

A standard procedure for antibody staining of cells for immunofluorescence microscopy was employed. The cells to be stained were subcultured and transfected as previously described and re-seeded onto 13mm glass coverslips (*VWR, Merck house, UK*) in 6 well dishes, such that they were approximately 70% confluent for staining. All subsequent steps were performed at 4°C, and washes with PBS were of 10 minutes duration, unless otherwise stated. Cells were quickly washed twice with PBS (10mM phosphate buffer, 2.7mM KCl, 137mM NaCl, pH 7.4, obtained in tablet form from *Sigma, Poole, UK*) and then fixed with 4% (v/v) paraformaldehyde solution for 20 minutes. The purpose of fixation is to immobilise antigens whilst maintaining cellular structure and architecture. Formaldehyde creates a network of interlinked antigens, via the reaction of aldehyde with amino groups. Cells were further washed twice with PBS, and then cells requiring permeabilisation (to allow access of the antibody to the intracellular epitope) were incubated with PBS + 0.2% Triton X-100 (*Sigma, Poole, UK*) for 20 min. Cells were aspirated then incubated in blocking solution (2% BSA, 5% goat serum in PBS) for 1hr to block non-specific protein binding sites, with the addition of 0.1% Triton-X to permeabilised cells. Cell-coated cover slips were transferred to humidified chambers. Primary and secondary antibodies were diluted in blocking solution (containing 0.1% Triton-X for incubation with permeabilised cells) and aggregated material removed via centrifugation at 20,800×g. Cells were incubated with a 1:500 dilution of mouse monoclonal HA primary antibody (*Covance, UK*) for 1hr, then washed four times with PBS. Cells were then incubated with a 1:300 dilution of goat anti-mouse IgG fluorescein conjugated secondary antibody (*Chemicon International*) in the dark at room temperature for 1hr. After a final set of four washes with PBS at room temperature, the cover slips were air-dried in the dark and mounted with Vectrashield (*Vector Laboratories*). Slides were stored at 4°C and viewed using a computer-based image analysis system (*OPENLAB 3.1; Improvision, Cambridge, U.K.*).

The immunohistochemistry results obtained are based on the use various derivatives of the anti-HA antibody to optimize surface staining. Initially double staining, involving the rat anti-HA (3F10, *Roche*) antibody followed by either Fluorescein (FITC)-

conjugated AffiniPure goat anti-rat IgG (*Jackson ImmunoResearch Labs, inc.*) or Alexa Fluor 488 goat anti-rat IgG (*Molecular Probes*) was employed to detect over-expressed HA-tagged protein. In an attempt to optimize staining the second generation mouse monoclonal HA.11 antibody (*Covance*) followed by a goat anti-mouse IgG fluorescein conjugated secondary antibody (*Chemicon International*) was employed, as was a anti-HA-Fluorescein high affinity (3F10) conjugate (*Roche*). The later, (a monoclonal antibody whose high affinity and low working concentrations resulted in less cross-reactivity than other antibodies to the HA-epitope) was found to give preferable staining. Thus, all immunohistochemistry was repeated with this conjugate and confirmed the results obtained from prior staining.

2.4 Procedure for Rubidium-86 ($^{86}Rb^+$) efflux in cultured cells

Rb^+ is an ideal tracer for potassium channels as it is similar in size, has the same charge as potassium and potassium channels are permeable to it. Since it is not present in biological systems, it is an easy target to detect adding no residual background noise to the experiment. The cell-based $^{86}Rb^+$ efflux assay for the functional analysis of native and recombinant ion channels works on the basis that, when cells are loaded for rubidium (a tracer for potassium), the rubidium distribution between intracellular and extracellular space subsequent to channel activation can be determined via the measurement of Cherenkov radiation. The relative amount of rubidium in the cell supernatant is a direct measure of channel activity. Thus this assay can provide a simple and relatively inexpensive screening assay for K^+ conductance in cultured cells to assess the effects of agonist, blockers, or genetic manipulations.

Experiments were conducted in an area designated for handling $^{86}Rb^+$, behind a shield designed to minimise exposure to ß- radiation and whole body dosimeters were worn to measure cumulative $^{86}Rb^+$ exposure per month. The risk of contamination via spillage was monitored throughout each experiment using a Geiger-Mueller detector and waste was isolated in sealed, shielded containers for decay. All experimental manipulations were conducted at room temperature. HEK293 cells were subcultured and seeded in 6-well plates, then transfected (when around 70% confluent) as previously described. It was necessary to obtain a transfection efficiency of at least 80%, and this was monitored by simultaneous transfection with eGFP. The cells were loaded with culture medium (2mls/well) containing 0.037MBq ml^{-1} $^{86}Rb^+$ overnight in a perspex box at 37°C (Shyng, Ferrigni et al. 1998). The following day, the loading medium was removed and the cells washed 3 times with 2ml of HEPES Buffered Saline (HBS) assay medium (10mM HEPES, 10mM Glucose, 130mM NaCl, 7mM KCL, 2mM $CaCl_2$ and 1mM $MgCl_2$), pH 7.4. For the time course assays, 2ml of HBS containing either an opener/inhibitor of the K_{ATP} channel were added per well, the timer immediately started, and at each desired time point 300µl aliquots of assay medium removed and placed into 6ml polyethylene scintillation vials (*Packard Biosciences*). For experiments

whereby one time point was examined, the entire 2ml of medium was removed. At the end of each experiment, the reaction was stopped via the addition of 1ml of HBS plus 2% triton to each well for 2 minutes. The lysates were collected and placed in scintillation vials. It should be noted that when investigating the effect of AMPK inhibitors and activators, PKA inhibitors and adenosine receptor antagonists on the response of the K_{ATP} channel under metabolic inhibition (*Fig 3.13*), cells were initially incubated for 15 minutes with the activator/inhibitor, then incubated for an additional 15 minutes in combination with the metabolic inhibitors (activators/inhibitors of signalling pathways are relatively slow-acting). NaCN and 2-DG were added from a concentrated stock to the total volume of incubation buffer, so as not to affect the final concentrations of activators/inhibitors.

All vials were assayed for $^{86}Rb^+$ content by measurement of Cherenkov radiation in a liquid scintillation counter (*TriCarb, Packard 2000CA*). Cherenkov radiation is refers to the electromagnetic radiation emitted when a charged particle passes through an insulator at a speed which exceeds that at which light passes through a vacuum. This can be expressed as:

$v > v_t = c/n$,

n = refractive index of the medium

c = velocity of light in the medium

v_t = threshold velocity

The percentage efflux at each time point was calculated as the cumulative counts in the aspirated solution divided by the total counts from the solutions and the cell lysates, i.e.

$$\frac{^{86}Rb^+ \text{ content of the medium}}{(^{86}Rb^+ \text{ content of the medium} + ^{86}Rb^+ \text{ content of the cells})}$$

Readings obtained from the scintillation counter were initially transferred to and analysed in Microsoft Office Excel 2003, then further analysed in GraphPad Prism 4 (refer to general analysis section).

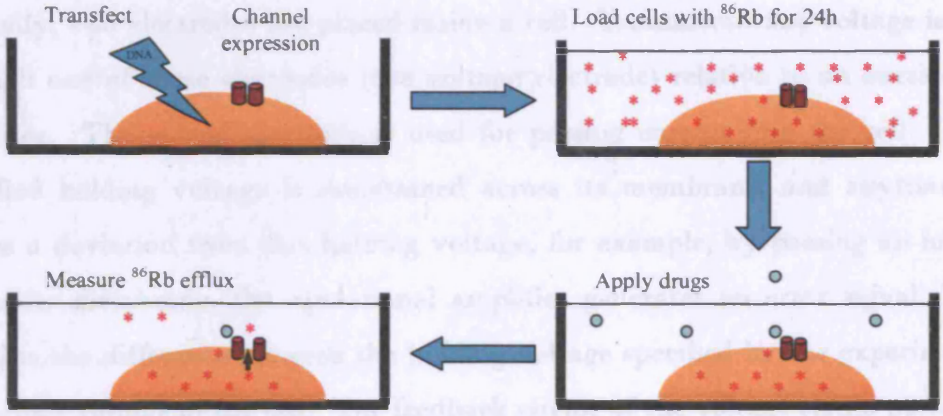

Figure 2.3: Measurement of $^{86}Rb^{+}$ efflux of transfected HEK293 cells. Cells were loaded overnight with 0.037MBq ml^{-1} Rubidium-86 in six-well plates. The following day, cells were washed several times with HBS and incubated with the relevant drug for 15 minutes. The $^{86}Rb^{+}$ content of the supernatant and the cell lysate was assayed by measurement of Cherenkov radiation in a liquid scintillation counter.

2.5 The Patch Clamp technique

Electrophysiology

Experiments using the voltage clamp technique have revealed many of the properties of ion channels. This was first developed by Cole, and Hodgkin and Katz in 1949 to allow an electrophysiologist to measure the ion currents flowing across a cells membrane using two electrodes and a feedback circuit. The squid giant axon was the first preparation that could be used to do this.

Basically, two electrodes are placed inside a cell. Transmembrane voltage is recorded through one of these electrodes (the voltage electrode) relative to an outside, ground reference. The second electrode is used for passing current into the cell. Briefly, a specified holding voltage is maintained across its membrane, and anytime the cell makes a deviation from this holding voltage, for example, by passing an ion current across its membrane, the operational amplifier generates an error signal. The error signal is the difference between the holding voltage specified by the experimenter and the actual voltage of the cell. The feedback circuit of the voltage clamp passes current into the cell (via the current electrode) in the polarity needed to reduce the error signal to zero. Thus, the current is applied in the polarity opposite the current that the cell is passing across its membrane, and the clamp circuit provides a current that is the mirror image of the cellular current. This mirror or clamp current can be easily measured, giving an accurate reproduction of the currents flowing across the cell's membrane (albeit in the opposite polarity).

Several variations of the voltage clamp technique were developed to accommodate biological cells that were too small to accept giant electrode assemblies used in the squid giant axon. The development of the *gigaseal* and *patch-clamp* methods by Erwin Neher and Bert Sakmann in 1975, contributed to a profound advance in electrophysiology. They discovered that a clean fire-polished glass pipette could fuse with a clean cell membrane, creating a seal of great mechanical stability and exceptionally high electrical resistance (Hamill, Marty et al. 1981).

The patch clamp technique

This technique is a variation of the single electrode voltage clamp, whereby a single electrode is placed in contact with the intracellular compartment of a cell. That single electrode serves both the voltage-recording and current-passing duties that are performed by two separate electrodes in two-electrode clamp. A miniature glass micro-pipette (the patch-clamp electrode) is pressed against the cell membrane, and a piece of membrane (the 'patch') is positioned within the pipette orifice. A tight seal of gigaohm electrical resistance (a 'gigaseal') is formed between the pipette rim and the cell membrane, and if the patch contains ion channels movement of ions through these channels is measured as tiny (picoampere) currents. Due to the high resistance of the gigaseal, the leak current across the seal is insignificant.

Specifically, five configurations may be employed:

(1) *Cell-attached (on-cell)*: the pipette makes a gigaseal with the intact cell allowing measurements of single-channel currents.

(2) *Inside out*: upon cell-attached configuration the pipette is withdrawn while the gigaseal is maintained. The inside (cytoplasmic) side of the membrane is facing the bath fluid. This configuration is used for single-channel recordings with the ability to change the intracellular solution.

(3) *Whole-cell*: The average current across the entire surface area of one cell is measured; whereby upon cell-attached configuration vigorous suction (or brief high-voltage pulses) is applied to the pipette causing the patch to break. The cytoplasm and the pipette solution are subsequently in direct contact, and after a short time diffusion of cytoplasmic constituents (molecules and cell organelles) results in identical (unphysiological) chemical composition of the fluids in the cell and in the pipette. In this configuration the activity of all membrane ion channels are measured.

(4) *Outside out*: from whole-cell configuration the pipette is gently withdrawn. This causes the membrane to break outside the sealing zone. The membrane fragments subsequently flip over, reseal, and constitute an inverted membrane patch exposing the extracellular side to the bath fluid. This configuration is used for single-channel recordings.

(5) *Perforated whole-cell*: cell-attached configuration is achieved with pore-forming compounds (amphotericin B, nystatin) in the pipette solution, which cause perforation of the patch allowing small molecules and ions, but not larger compounds, to cross the patch. Consequently, larger molecules and cell organelles remain within the cell. As with conventional whole-cell patch clamp the sum of all ion channel currents is measured.

In my experiments, *whole cell patch clamping and perforated whole cell patch clamping* techniques were implemented to measure the average current across the entire surface area of one cell, as exemplified in *figure 2.4*.

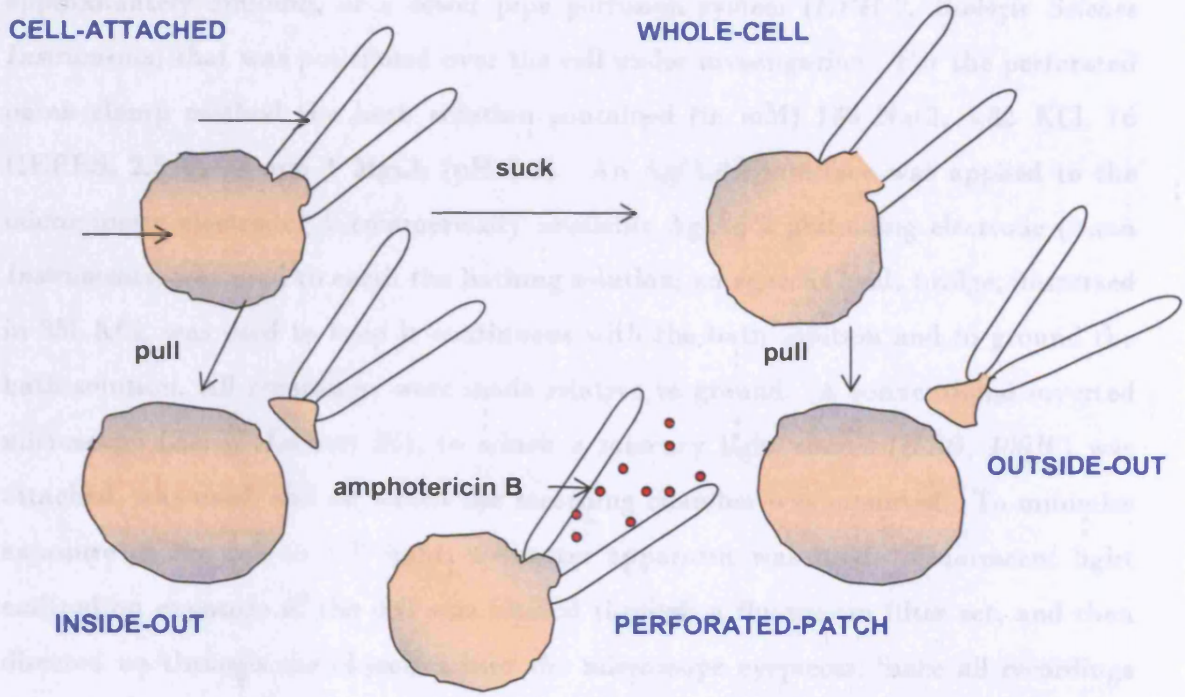

Figure 2.4: The five configurations of the patch-clamp technique. All methods start with the formation of a gigaohm seal between a fire polished patch pipette and the cell membrane. Unitary currents may be recorded in this cell-attached configuration. Further manipulation of the patch pipette allows recordings from a small patch of the membrane in the inside-out or outside-out configurations, or from the whole cell under voltage clamp. The inclusion of amphotericin B in the patch pipette solution of a cell-attached patch leads to the formation of small pores in the membrane beneath the patch pipette which will pass anions and cations, but not of larger molecules, permitting voltage clamp of the whole cell (adapted *from Hille; 1992*).

The patch-clamp recording setup used in my experiments

Non-electronic equipment for the recording of whole-cell currents was mounted on an anti-vibration table (a platform with minimal mechanical interference), and electrically shielded by a cage. Cells were subcultured onto glass coverslips (*10mm diameter, borosilicate glass; VWR, Poole, UK*) that were transferred to the recording chamber (*15mm diameter; Series 20 Perfusion chamber; Warner Instruments Inc., Hamden, USA*). For whole cell patch clamping, this was continuously perfused to a depth of 1.5-2.5mm with high K^+ external solutions (140mM KCl, 2.6mM $CaCl_2$, 1.2mM $MgCl_2$, 5mM HEPES, pH 7.4) by a standard gravity-driven perfusion system at a rate of

approximately 3ml/min, or a sewer pipe perfusion system (*EVH-9, Biologic Science Instruments*) that was positioned over the cell under investigation. For the perforated patch clamp method the bath solution contained (in mM) 130 NaCl, 5.42 KCl, 16 HEPES, 2.5 $CaCl_2$ and 1 $MgCl_2$ (pH 7.4). An Ag/AgCl interface was applied to the micropipette electrode. A commercially available Ag/AgCl grounding electrode (*Axon Instruments*) was used to earth the bathing solution; an agar/KCl salt bridge, immersed in 3M KCl, was used to keep it continuous with the bath solution and to ground the bath solution. All recordings were made relative to ground. A conventional inverted microscope (*Zeiss, Axiovert 25*), to which a mercury light source (*HBO, 100W*) was attached, was used, and on which the recording chamber was mounted. To minimise exposure of the cell to UV light, a shutter apparatus was used. Fluorescent light emitted on exposure of the cell was filtered through a fluorescein filter set, and then directed up through the objective into the microscope eyepieces. Since all recordings were of whole-cell membrane current, the electrode was connected to a unitary voltage gain headstage amplifier (*HS-2; Axon Instruments, Union City, CA, USA*) containing a 10MΩ resistor. Signals were further amplified by an Axopatch 200B amplifier (*Axon Instruments*), converted from analogue to digital signals by a Digidata 1200B converter, and captured and analysed using pClamp software (*version 6.0; Axon Instruments*). Voltage commands were generated using pClamp6 software.

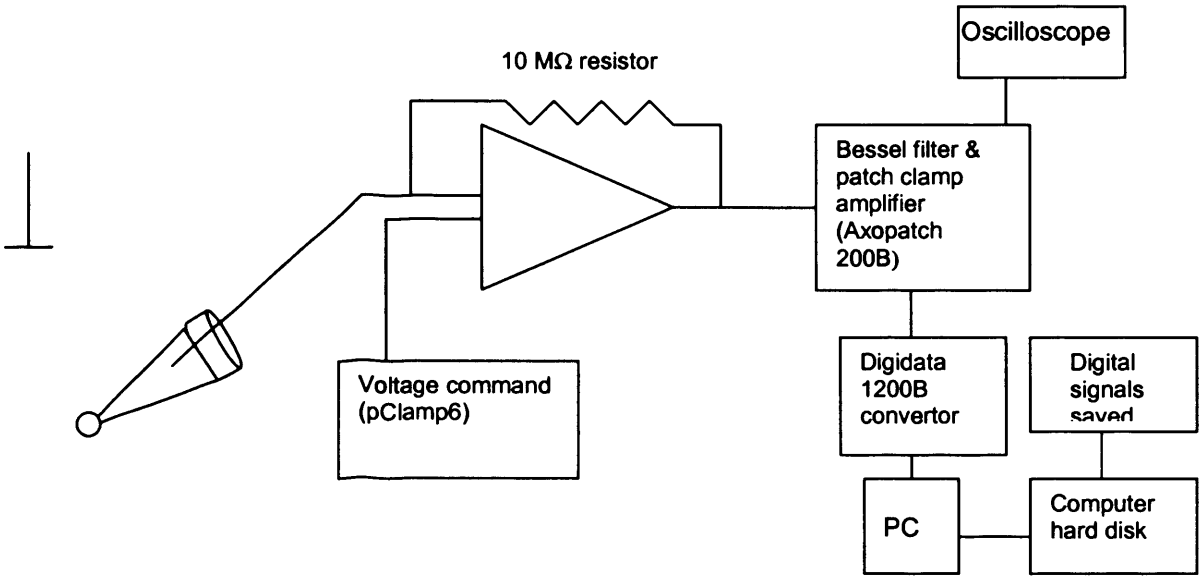

Figure 2.5: Configuration of patch-clamp recording setup. For whole cell recordings, the electrode was connected to the headstage amplifier, and the current resolution was determined by resistance feedback via a 10MΩ resistor in the headstage. Voltage commands were performed via pClamp6 software. Signals were further amplified by an Axopatch 200B amplifier, and filtered at 500 Hz. Signals were sampled at 1 kHz by a Digidata 1200B converter before capture on a computer hard disk.

Application of the whole-cell configuration of the patch clamp

Using a horizontal pipette puller (*DMZ-Universal Puller; Zeitz Instruments, Munich, Germany*) patch pipettes were pulled from filamented 1.5mm O.D.×1.17mM I.D. borosilicate glass (*Clark Electromedical; Harvard Apparatus, Edenbridge, UK*) and each micropipette tip fire-polished. Micropipette tips had resistances of 2.5-3.5 MΩ when back-filled with pipette solution (107mM KCl, 1.2mM $MgCl_2$, 1mM $CaCl_2$, 10mM EDTA, 5mM HEPES, 0.5mM UDPNa salt, 1mM ATPMg salt). The pH of the pipette solution was adjusted to 7.2 using KOH, resulting in a total K^+ concentration of ~140mM. 100mls were made up at a time, filter-sterilised and stored at -20°C as 1ml aliquots. A fresh aliquot was defrosted on the day of each experiment and incubated on ice to prevent the breakdown of ATP. After filling, the tips of the patch pipettes were coated with Parafilm/mineral oil suspension to reduce the capacitance of the tip. The patch pipette was positioned and lowered over the cell under investigation in the

recording chamber using a fine micromanipulator (*Sutter Instruments, Navato, CA, USA*) until the polished tip came into contact with the cell membrane. Gentle suction was applied via a 2ml syringe until a seal of high electrical resistance (2-10GΩ) was obtained. Following a 30-60 second equilibration period, sharp suction was applied and the membrane patch consequently ruptured, bringing the contents of the pipette solution into contact with the cell cytoplasm. Cell capacitive transients, indicative of a successful breakthrough, were cancelled via the patch clamp amplifier (whereby a good cell capacitance in combination with a low series resistance resulted in a large, quick transient). Current-voltage relationships were immediately performed to establish that the currents were present. Reversal potential was applied by exposing the cell to symmetrical K^+ solutions and maintaining a holding potential of 0mV at which no net current was passed. Current-voltage relationships were monitored over an equilibration period of approximately 10 minutes, during which time leaky cells were discarded. Thereafter cells were voltage clamped at -100mV and agonist/antagonist induced currents measured at this holding potential. All recordings of membrane current were made at room temperature.

Application of the perforated whole-cell configuration

The same basic procedure was followed as for the whole cell configuration, however after a seal (of around 2GΩ or above) was obtained, the amphotericin in the patch pipette was responsible for perforation of the cell and to achieve the whole cell configuration (without any additional suction). On adjusting the pH with KOH, the pipette solution contained (in mM) ~135 KCl, 5 NaCl, 10 EGTA, 10 HEPES, 1 $CaCl_2$ and 2 $MgCl_2$ (pH 7.4). 6mg of purified amphotericin B from streptomyces species (*Sigma*) was dissolved in 100µl fresh DMSO, of which 3.3µl was diluted in 1ml of pipette solution to obtain a working concentration of (+/- 20%) 120µg.ml^{-1}. This was sonicated before use to ensure complete dilution of the amphotericin. Pipettes were pre-dipped in regular pipette solution for around 10 seconds, then back-filled with amphotericin-containing pipette solution. A seal was obtained at 0mV (as previously described) and around ten minutes allowed for the amphotericin to perforate the cell. A ramp protocol

was subsequently employed to obtain recordings, at which agonist/antagonist induced currents were logged at +50mV. Again, all recordings were made at room temperature.

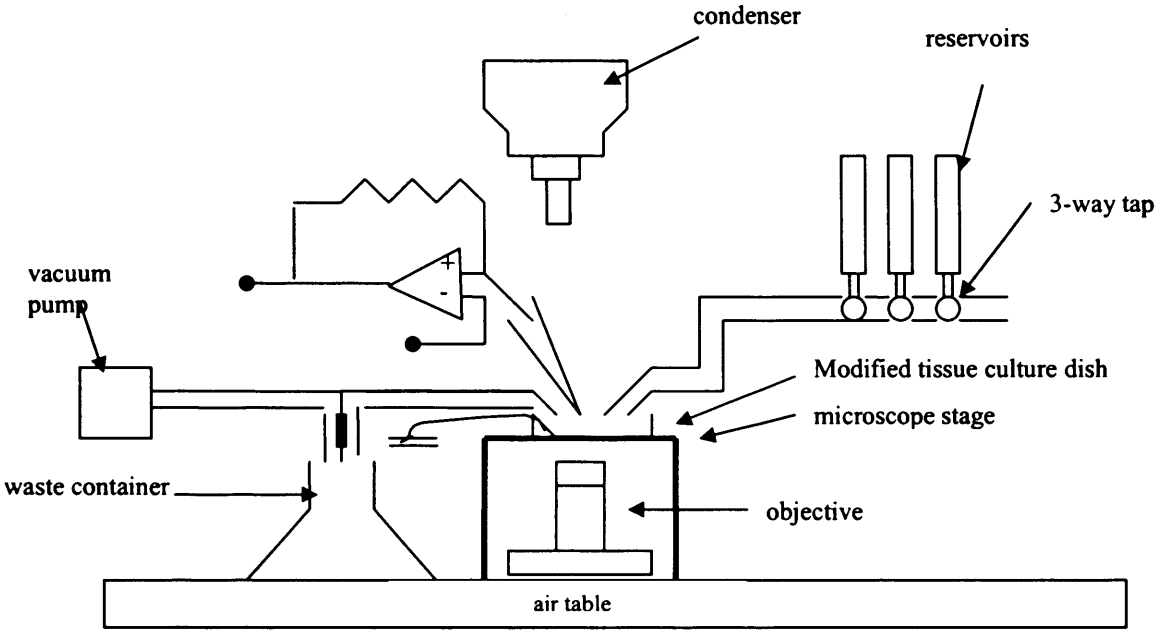

Figure 2.6: Perfusion of the patch-clamp recording setup. Solutions were supplied by both a standard gravity-driven and fast perfusion system, which was positioned over the cell of interest. A vacuum pump was used to remove solutions from the chamber, which was earthed by an Ag/AgCl electrode to a waste container. An electrode with an Ag/AgCl interface was also used to make recordings of whole cell currents.

Whole cell capacitance and Series Resistance Compensation

The cell membrane acts as an efficient capacitator, and a significant current injection is required to charge the membrane capacitance and to step the membrane to a new potential. The time course of the membrane potential change in response to a step in current is given by the membrane time constant (τ_M). If the series resistance is known, (the resistance in series with the cell membrane and current-passing electrode, in addition to the resistance of the cell membrane), the cell membrane capacitance (C_M) can be calculated as follows:

$$C_M = \tau_M / Ra,eff$$

Ra refers to the access resistance of the pipette (the sum of the micropipette resistance and residual resistance of the ruptured membrane patch and the cytoplasm) and Ra, eff refers to the effective value of Ra after series resistance compensation. An estimate of the membrane area (A) can be made from the value of the cell membrane capacitance in picofarads (as read from the amplifier), since most biological membranes have a capacitance close to 1.0$\mu F/cm^2$. In the subsequent experiments, all current amplitudes were corrected for cell size, and are expressed in picoamperes per picofarads (pA/pF).

A potential difference of Ip×Ra,eff is generated when a current (I_p) flows from the pipette into the cell through the series resistance. A true potential of the cell membrane can only be obtained on extraction of this potential difference from the command potential, since series resistance can contribute a considerable error in whole-cell recordings, particularly when currents are large. When either the current or voltage is clamped, both series resistance and membrane resistance (hence membrane capacitance), can be directly calculated; for example:

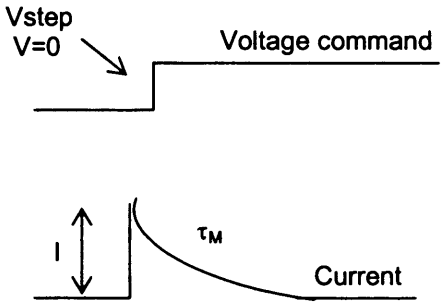

$$Ra,eff = Vstep/I \qquad C_M = \tau_M/Ra,eff$$

In the voltage clamp mode, this represents the current response to a small voltage step. The current transient decays exponentially with a time constant, τ_M, and therefore, Ra,eff and C_M can be calculated. Ra,eff also affects the time resolution of the whole-cell patch clamp, whereby in voltage-clamp, application of a small voltage step will generate a transient current that decays exponentially. This is equal to the product of the series resistance and membrane capacitance ($\tau_M = Ra,eff \times C_M$).

In these studies, the series resistance compensator on the amplifier was used to add 70% of Ip×Ra,eff to the voltage command, and to partly rectify the error (since the compensation circuitry is prone to self-amplifying destabilisation, this degree of compensation was a good result). As described, the whole-cell capacitance was also measured using the analogue circuitry of the amplifier by cancelling out a current transient in response to a step in voltage.

Nernst Equilibrium Potential and Reversal Potential

In a biological membrane, the *reversal potential* (or Nernst potential) of a particular ion is the membrane voltage at which there is no net flow of ions from one side of the membrane to the other. For a single-ion system only, reversal potential is synonymous with *equilibrium potential*, and their numerical values are identical. The two terms simply refer to the two aspects of that potential difference. *Equilibrium* refers to the fact that the net ion flux at that voltage is zero (that is, the outward and inward rates are the same; the flux is in equilibrium). *Reversal* implies that perturbation of the membrane potential on either side of the equilibrium potential reverses the net direction of the ion flux. The Nernst Equilibrium Potential is given by:

$$E_K = (RT/ZF)\,(\ln[ion^+]_0/[ion^+]_i)$$

where R is the gas constant (8.315 $JK^{-1}mol^{-1}$), T is the absolute temperature on the Kelvin scale, F is the Faraday constant (9.648×10^4 $Cmol^{-1}$), Z is the valency of the ion (for K^+ this is 1), ln is the natural logarithm, and [ion] is the extra or intra-cellular concentration of the ion concerned. For K^+ the potential will be named E_K.

The $[K^+]_0$ is around 5mM in physiological extracellular solution, and the $[K^+]_i$ is approximately 130mM. The calculated E_K value at 25°C is -83.7mV and at 37°C is -87.1mV. In the whole cell patch clamp studies, symmetrical K^+ ion concentrations were used: $[K^+]_0$ = 140mM and $[K^+]_i$ = 140mM. The calculated E_K value at 25°C is 0mV. In many excitable cells, since the membrane is permeable to many other ions, the reversal potential (E_{rev}) may not be the same as the equilibrium potential. However, for electrically quiescent HEK293 cells stably expressing the K_{ATP} channel, $E_K = E_{rev}$. This is because the cells are over-expressing a channel that is selective to one species of ion (K^+), and the voltage inside the cell will equilibrate to the reversal potential of K^+. In perforated patch clamp studies, physiological conditions were applied, i.e. $[K^+]_i$ = 135mM and $[K^+]_0$ = 5.42mM, and the calculated E_K value at 25°C is -82.6mV.

2.6 General data analysis

All data are presented as mean +/- SEM, whereby n indicates the number of cells from which a recording was taken. The mean, μ, is given by: $\Sigma\chi$ /N

where χ is the value of each sample, and N is the size of the sample. The standard deviation σ is given by: $\sqrt{(\Sigma(\chi-\mu)^2/N)}$

The standard error of the mean is given by: $\sigma / \sqrt{N}$

Data were analysed using GraphPad Prism 4 for windows (*GraphPad Software, San Diego California USA, www.graphpad.com*).

Since three or more groups of data were compared, significant differences were tested for by employing the one-way ANOVA, and where appropriate either the Dunnett's or Bonferroni post-test. ANOVA depends on the assumption that the populations all have the same variance (the Bartlett's test for equal variances was used to test this assumption using GraphPad Prim). The decision to apply a post test was conditional on the reported value of the Bartlett's statistic, and secondly on whether the reported value was less than 0.05. Both are modifications of the t test that account for multiple comparisons. The Dunnett's test was widely used in my analyses to compare the various data sets to the control data set of any given experiment. The Bonferroni test for 'selected pairs of columns' was used less frequently on comparison of selected data sets. Significant differences are indicated as follows: * indicates $P \leq 0.05$, ** indicates $P \leq 0.01$ and *** indicates $P \leq 0.001$.

Traces obtained from patch clamp recordings were initially opened and analysed using Clampfit 9.0, Axon Laboratory pClamp9.0 to visualise both variations in current and voltage with time for the individual sweeps. Representative IV plots for individual

experiments were produced in pClamp9. Representative traces for individual experiments were produced by importing data from pClamp9 into Microcal Origin 6.0, whereby current (nA) was plotted against time (ms). Traces were then opened with Adobe Photoshop Elements 3.0 and further manipulated. For perforated patch clamp and whole cell patch clamp data, current density was calculated at +50mV (pA/pF) and -100mV (pA/pF) respectively. This was measured for individual sweeps (determined on opening data in pClamp 9.0) under any given condition, and data analysed as described in GraphPad Prism 4.

Chapter Three

Characterization of K_{ATP} channel current in response to metabolic inhibition and signalling pathways

Chapter Three: Results

Characterization of K_{ATP} channel current in response to metabolic inhibition and signalling pathways

The rubidium flux assay was one of the principle techniques employed in this thesis as a screening tool for K_{ATP} channel functionality. Flux assays utilize ion channel kinetics to measure tracer element movement, in order to demonstrate functional compound interactions, and are becoming increasingly popular as tools for screening compounds. In an optimized flux assay, modulation of ion channel activity may produce readily detectable changes in radio labeled ionic flux. In fact, technologies based on flux assays are currently available in fully automated, high throughput format for efficient screening. Industrial application of this assay has shown to be sensitive and precise; giving reproducible measurements and accurate drug rank orders which match those of patch clamp data. $^{86}Rb^+$ is an ideal tracer for potassium channels as it is similar is size, has the same charge as potassium and is permeable in potassium channels. $^{86}Rb^+$ is not present in biological systems, and is therefore an easy target to detect adding no residual background noise to the experiment. For more detail please refer to methodology chapter.

Since this assay has been well characterized (Koster, Sha et al. 1999; Mattheakis and Savchenko 2001; Xu, Wang et al. 2001), it was employed to gain more insight into the function of the K_{ATP} channel. Initial experiments involved optimization of the assay in relation to the cell system employed. It was necessary to determine optimal concentrations of drugs to establish differences in functionality of mutated versions of the channel, to establish an utilizable degree of sensitivity of the assay, and to establish a time point at which differences in pharmacology of the channel would be optimal after the addition of isotope to the cells. HEK293 cells stably expressing Kir6.2/SUR2B and Kir6.1/SUR2B were initially employed to achieve these aims. Time course assays were conducted, in which the $^{86}Rb^+$ efflux was measured in assay medium

extracted from cells every 5 minutes for a total of 30 minutes from the addition of the drug, to establish the linear phase of efflux. Both known KCOs and KCBs were applied to the cells to assess pharmacological activity. Response of the channel to metabolic inhibition was also assessed (since one objective of this thesis was to assess any difference in channel regulation under metabolic depletion). Instead of removing oxygen and glucose from cultures, pharmacologic blockade of metabolism was used to stimulate ischemic conditions, providing a rapid and controllable loss of ATP. Sodium cyanide (NaCN) and 2-deoxy-glucose (2-DG) were used in combination to induce metabolic inhibition.

The toxicity of NaCN results from the high affinity of cyanide for certain sulfur compounds and metallic complexes. The cyanide ion can rapidly combine with iron in cytochrome oxidase a_3 (a component of the cytochrome aa_3 or cytochrome oxidase complex IV of the electron transport chain in mitochondria) to inhibit this enzyme, thus uncoupling mitochondrial oxidative phosphorylation and inhibiting cellular respiration, even in the presence of adequate oxygen stores. Cellular metabolism shifts from aerobic to anaerobic, with the consequent production of lactic acid (Ray, Monroe et al. 1991). 2-DG abolishes ATP generation through the glycolytic pathway. 2-DG is an analogue of glucose and is able to bind to and suppress hexokinase II, an enzyme that catalyses the initial metabolic step in the conversion of glucose to glucose-6-phosphate during glycolysis. Inhibition of this rate-limiting step by 2-DG causes a depletion of $[ATP]_i$ and leading to blockage of cell cycle progression and cell death *in vitro* (Xu, Pelicano et al. 2005). This may also involve insufficient ATP supply for Na^+-K^+ pump activity. Glycolysis has been shown to preferentially provide ATP for the Na^+-K^+ pump, and when ATP supply is inhibited with 2-deoxyglucose, Na^+-K^+ pump activity is reduced (Glitsch and Tappe 1993).

The resultant decrease in intracellular ATP on the addition of metabolic inhibitors opens K_{ATP} channels. Pinacidil was the KCO applied to the Kir6.2/SUR2B stable cell line, and levcromakalim to Kir6.1/SUR2B expressed in HEK293 cells since these have

found to be the most effective agonists for each (refer to Introduction, section 1.2). The results represent the cumulative data obtained from three experiments, and each drug was applied to three wells (of a six well plate) per experiment, therefore the average $^{86}Rb^{+}$ efflux deducted at each time point for each drug is effectively taken from 9 samples.

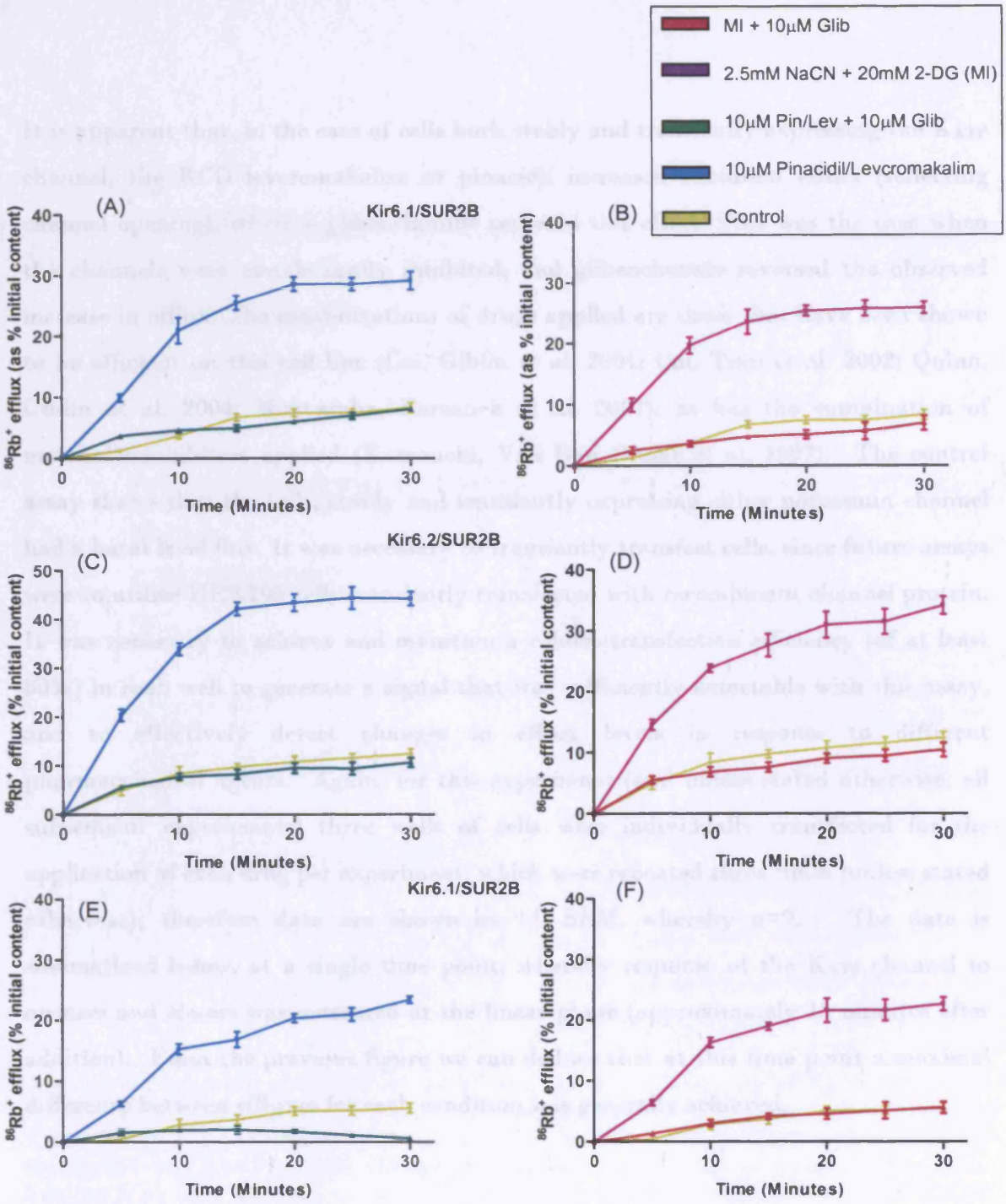

Figure 3.1: $^{86}Rb^{+}$ efflux time course assay on HEK293 cells stably transfected with the potassium channel Kir6.1/SUR2B (A) & (B), stably transfected with Kir6.2/SUR2B (C) & (D) and transiently transfected with Kir6.1/SUR2B (E) & (F). Efflux was measured every 5 minutes from the addition of the drug, for a total of 30 minutes, and was calculated as % efflux of initial $^{86}Rb^{+}$ content. The KCOs pinacidil and levcromakalim were applied to the Kir6.2/SUR2B and Kir6.1/SUR2B cell lines respectively. The control represents DMSO diluted in HBS. The same control is shown for each pair of results, which represent data obtained from the same experiment. Data are shown as +/- SEM, whereby n= 9.

It is apparent that, in the case of cells both stably and transiently expressing the K_{ATP} channel, the KCO levcromakalim or pinacidil increased rubidium efflux (reflecting channel opening), whereas glibenclamide reversed this effect. This was the case when the channels were metabolically inhibited, and glibenclamide reversed the observed increase in efflux. The concentrations of drugs applied are those that have been shown to be efficient on this cell line (Cui, Giblin et al. 2001; Cui, Tran et al. 2002; Quinn, Giblin et al. 2004; Muzyamba, Farzaneh et al. 2007), as has the combination of metabolic inhibitors applied (Kamouchi, Van Den Bremt et al. 1997). The control assay shows that the cells, stably and transiently expressing either potassium channel had a basal level flux. It was necessary to transiently transfect cells, since future assays were to utilize HEK293 cells transiently transfected with recombinant channel protein. It was necessary to achieve and maintain a robust transfection efficiency (of at least 80%) in each well to generate a signal that was sufficiently detectable with this assay, and to effectively detect changes in efflux levels in response to different pharmacological agents. Again, for this experiment (and unless stated otherwise, all subsequent experiments) three wells of cells were individually transfected for the application of each drug per experiment, which were repeated three times (unless stated otherwise), therefore data are shown as +/- SEM, whereby n=9. The data is summarized below, at a single time point, whereby response of the K_{ATP} channel to openers and closers was measured at the linear phase (approximately 15 minutes after addition). From the previous figure we can deduce that at this time point a maximal difference between effluxes for each condition was generally achieved.

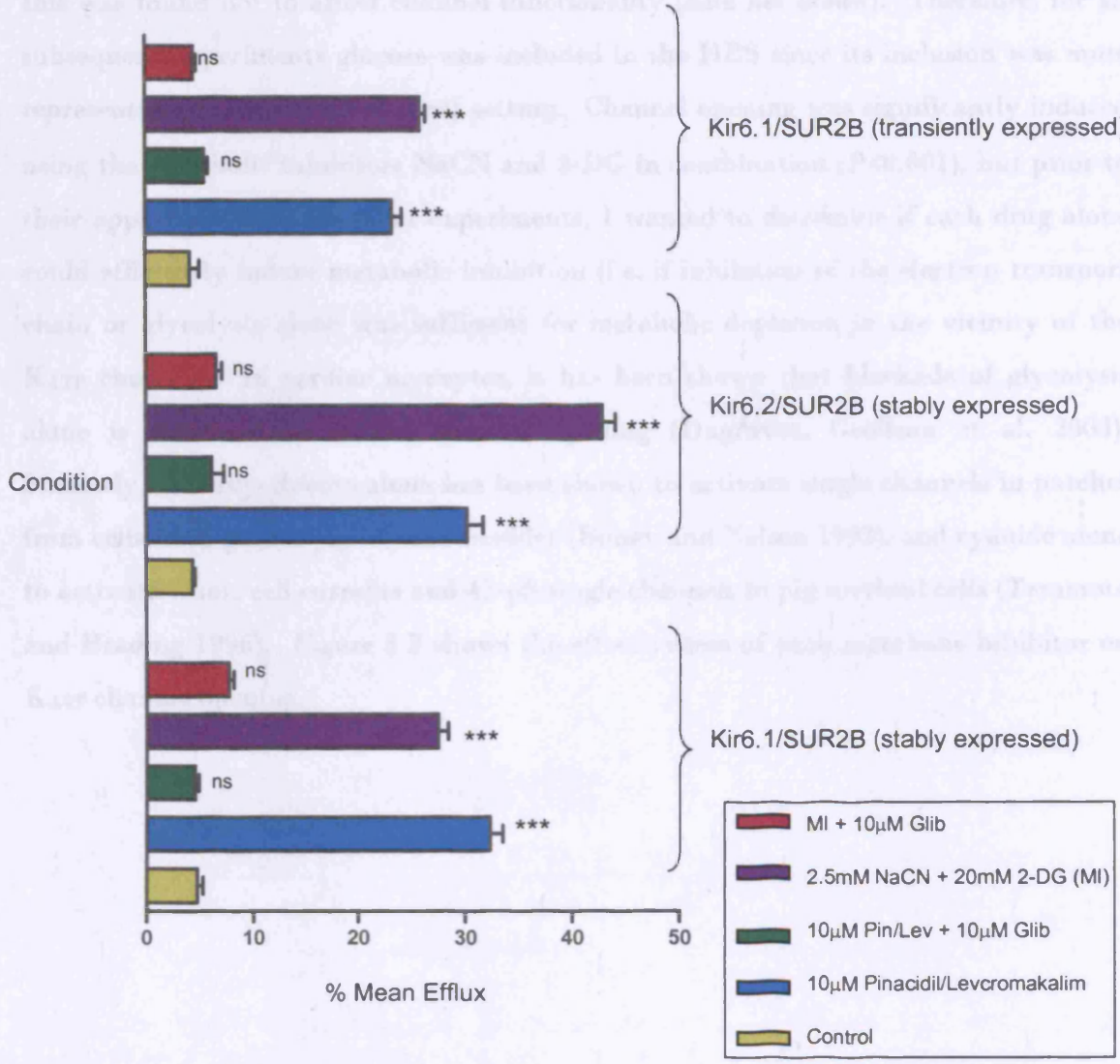

Figure 3.2: Summary of the effects of variation in pharmacology on the K_{ATP} channel, 15 minutes after application of the K_{ATP} channel opener/closer. $^{86}Rb^{+}$ efflux was measured in Kir6.1/SUR2B and Kir6.2/SUR2B stable lines, and on cells HEK293 cells transiently transfected with Kir6.1/SUR2B. Efflux was calculated as % efflux of initial $^{86}Rb^{+}$ content. The KCOs pinacidil and levcromakalim were applied to the Kir6.2/SUR2B and Kir6.1/SUR2B cell lines respectively. The control represents DMSO diluted in HBS. Data are shown as +/- SEM, whereby n=9. *** $P<0.001$ compared to control, (ns) $P>0.05$ compared to control.

It is apparent that after 15 minutes, significant differences in channel pharmacology are observed in both HEK293 cells where the channel is expressed stably and transiently. Therefore, for all future experiments, $^{86}Rb^{+}$ efflux was measured at this time point to assess pharmacology. In initial experiments, glucose was omitted from the HBS, but

this was found not to affect channel functionality (*data not shown*). Therefore, for all subsequent experiments glucose was included in the HBS since its inclusion was more representative of the physiological setting. Channel opening was significantly induced using the metabolic inhibitors NaCN and 2-DG in combination ($P<0.001$), but prior to their application in subsequent experiments, I wanted to determine if each drug alone could efficiently induce metabolic inhibition (i.e. if inhibition of the electron transport chain or glycolysis alone was sufficient for metabolic depletion in the vicinity of the K_{ATP} channel). In cardiac myocytes, it has been shown that blockade of glycolysis alone is sufficient to induce channel opening (Dugravot, Grolleau et al. 2003). Similarly, 2-deoxy-glucose alone has been shown to activate single channels in patches from cells from guinea pig urinary bladder (Bonev and Nelson 1993), and cyanide alone to activate whole cell currents and 43-pS single channels in pig urethral cells (Teramoto and Brading 1996). *Figure 3.3* shows the effectiveness of each metabolic inhibitor on K_{ATP} channel opening.

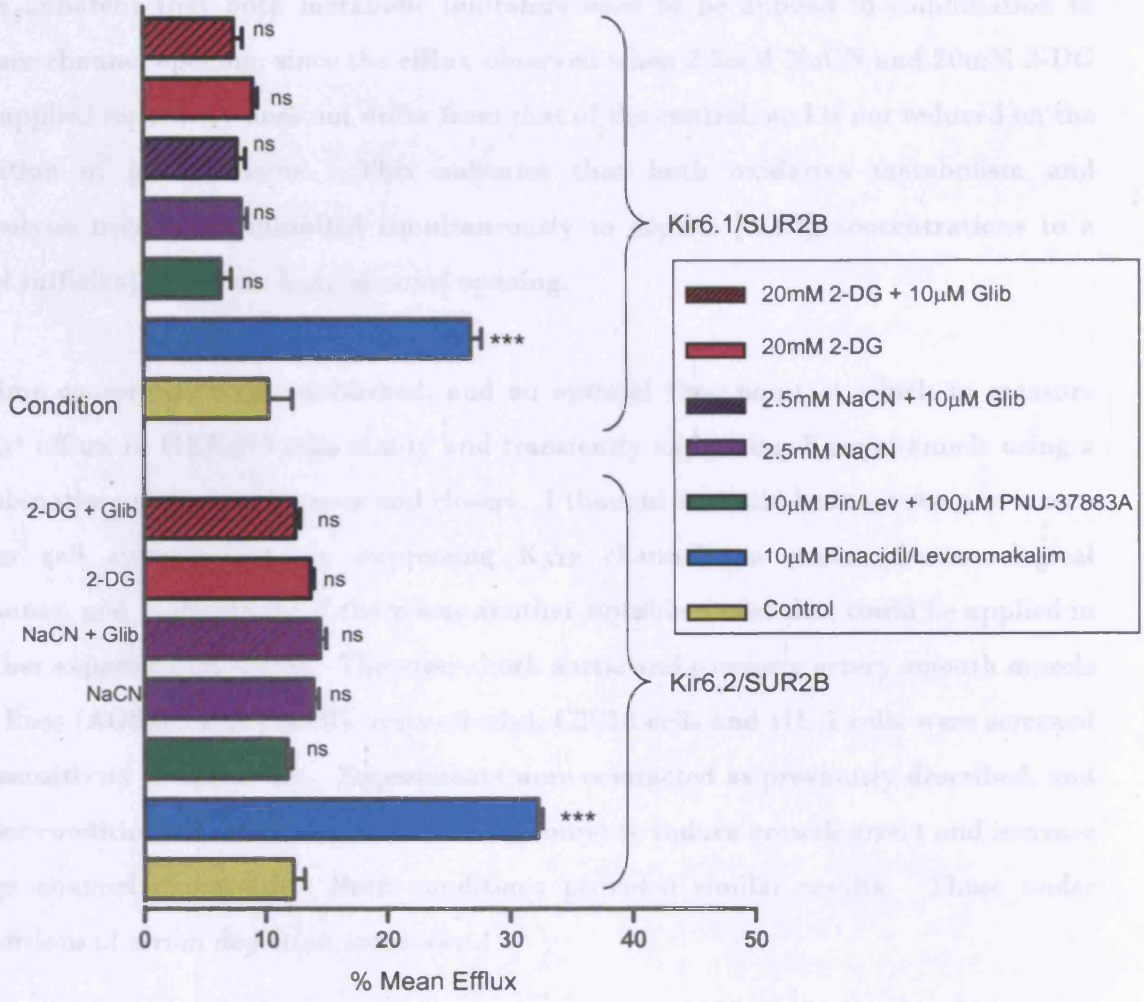

Figure 3.3: The effect of Metabolic Inhibitiors on the K_{ATP} channels Kir6.1/SUR2B and Kir6.2/SUR2B (expressed stably). 2.5mM NaCN and 20mM 2-DG were applied individually, and with 10μM Glibenclamide. Response was measured 15 minutes after addition of the drugs, and efflux was calculated as % efflux of initial $^{86}Rb^{+}$ content. The KCOs pinacidil and levcromakalim were applied to the Kir6.2/SUR2B and Kir6.1/SUR2B cell lines respectively. The control represents DMSO diluted in HBS. Data are shown as +/- SEM, whereby n=9. *** $P<0.001$ compared to control, (ns) $P>0.05$ compared to control.

It is apparent that both metabolic inhibitors need to be applied in combination to induce channel opening, since the efflux observed when 2.5mM NaCN and 20mM 2-DG are applied separately does not differ from that of the control, and is not reduced on the addition of glibenclamide. This indicates that both oxidative metabolism and glycolysis need to be inhibited simultaneously to deplete $[ATP]_i$ concentrations to a level sufficient to induce K_{ATP} channel opening.

A time course has been established, and an optimal time point at which to measure $^{86}Rb^+$ efflux in HEK293 cells stably and transiently expressing K_{ATP} channels using a combination of channel openers and closers. I thought it would be interesting to screen other cell systems natively expressing K_{ATP} channels to assess pharmacological response, and to determine if there was another suitable model that could be applied in further experimental design. Therefore, both aortic and coronary artery smooth muscle cell lines (AOSMC and CASMC respectively), C2C12 cells and HL-1 cells were screened for sensitivity to this assay. Experiments were conducted as previously described, and under conditions of serum depletion (for 24 hours) to induce growth arrest and increase K_{ATP} channel expression. Both conditions provided similar results. Those under conditions of serum depletion are shown.

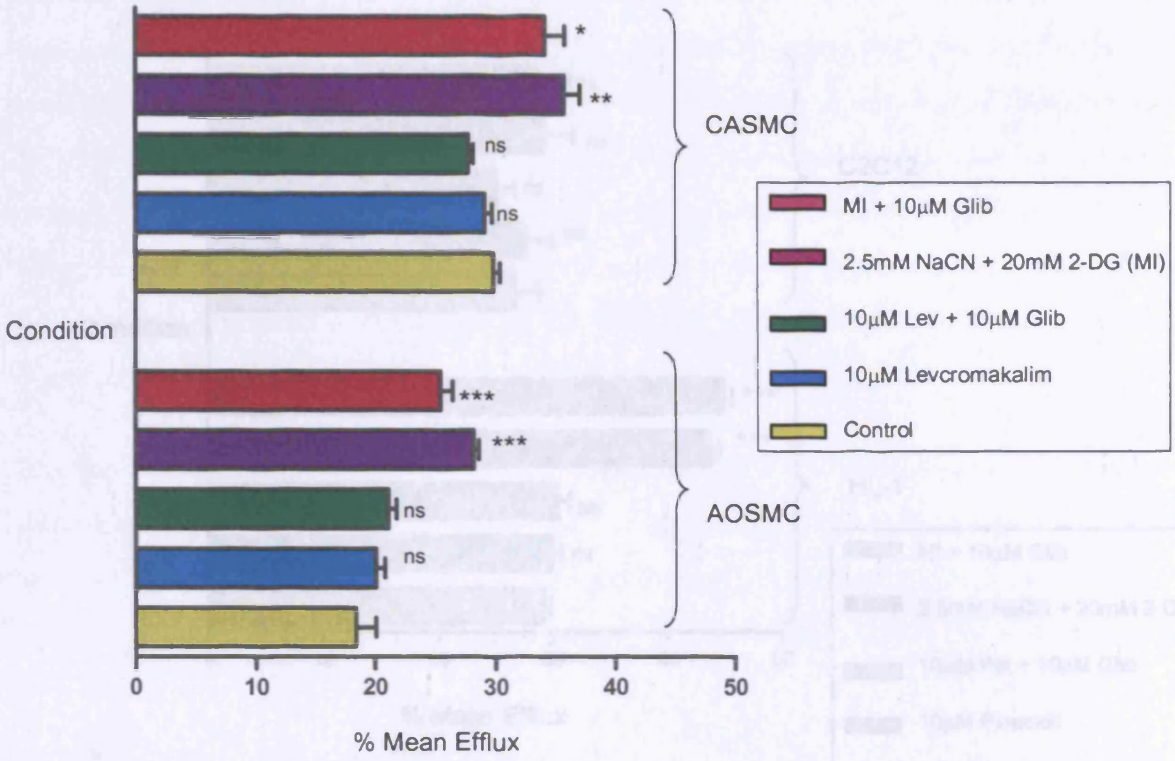

Figure 3.4: Measurement of $^{86}Rb^{+}$ efflux of native potassium channels (principally Kir6.1/SUR2B) in AOSMC and CASMC systems after 24 hours serum depletion. Efflux was measured 15 minutes after addition of the drugs, and was calculated as % efflux of initial $^{86}Rb^{+}$ content. The control represents DMSO diluted in HBS. Data are shown as +/- SEM, whereby n=9. *** P<0.001 compared to control, ** P=0.001-0.01 compared to control, * P=0.01-0.05 compared to control, (ns) P>0.05 compared to control

It is apparent that only metabolic inhibition had a significant effect on smooth muscle channel opening, the effect of which is not reversed via glibenclamide. Background efflux is also high (especially in the coronary smooth muscle cells) indicating detection of efflux from other potassium channel families, and implying that the result is not unique to the K_{ATP} channel. The same experiment was repeated for the C2C12 and HL-1 cell lines, which the lab has expertise in culturing, and which express endogenous K_{ATP} channels.

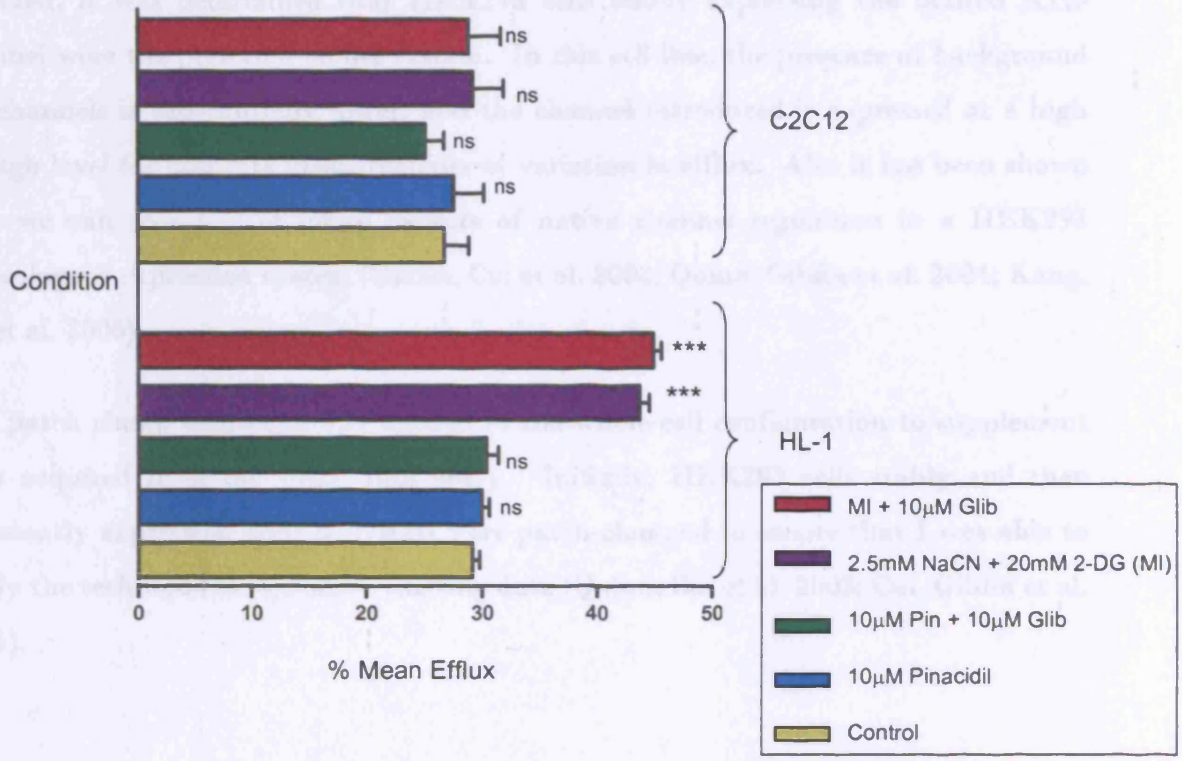

Figure 3.5: Measurement of $^{86}Rb^{+}$ efflux of native potassium channels in HL-1 and C2C12 cell systems. Efflux was measured 15 minutes after addition of the drugs, and was calculated as % efflux of initial $^{86}Rb^{+}$ content. The control represents DMSO diluted in HBS. Data are shown as +/- SEM, whereby n=9. *** P<0.001 compared to control, (ns) P>0.05 compared to control.

For the C2C12 cell line, there is no significant change in efflux compared to the control, and again basal efflux is relatively high, indicating the detection of a varied population of potassium channels. For the HL-1 cell line, metabolic inhibition again induced channel opening, but glibenclamide was unable to reverse this effect and no response to pinacidil was observed. C2C12 cells are thought to predominantly express Kir6.2/SUR1 and Kir6.2/SUR2A (Liu, Gao et al. 1996) and HL-1 cells Kir6.2/SUR2A (Fox, Jones et al. 2005) hence the KCO of choice.

Since no significant difference in pharmacology was detected in these native cell systems using the employed assay, and since a high level of noise (i.e. bassal efflux) was detected, it was determined that HEK293 cells stably expressing the desired K_{ATP} channel were the preferred model system. In this cell line, the presence of background K^+ channels is substantially lower, and the channel introduced is expressed at a high enough level for accurate measurements of variation in efflux. Also it has been shown that we can recapitulate many aspects of native channel regulation in a HEK293 heterologous expression system (Quinn, Cui et al. 2003; Quinn, Giblin et al. 2004; Kang, Ng et al. 2006).

The patch clamp technique was applied in the whole-cell configuration to supplement data acquired from the $^{86}Rb^+$ flux assay. Initially, HEK293 cells stably and then transiently expressing Kir6.1/SUR2B were patch-clamped to ensure that I was able to apply the technique to reproduce existing data (Quinn, Cui et al. 2003; Cui, Giblin et al. 2001).

(A)

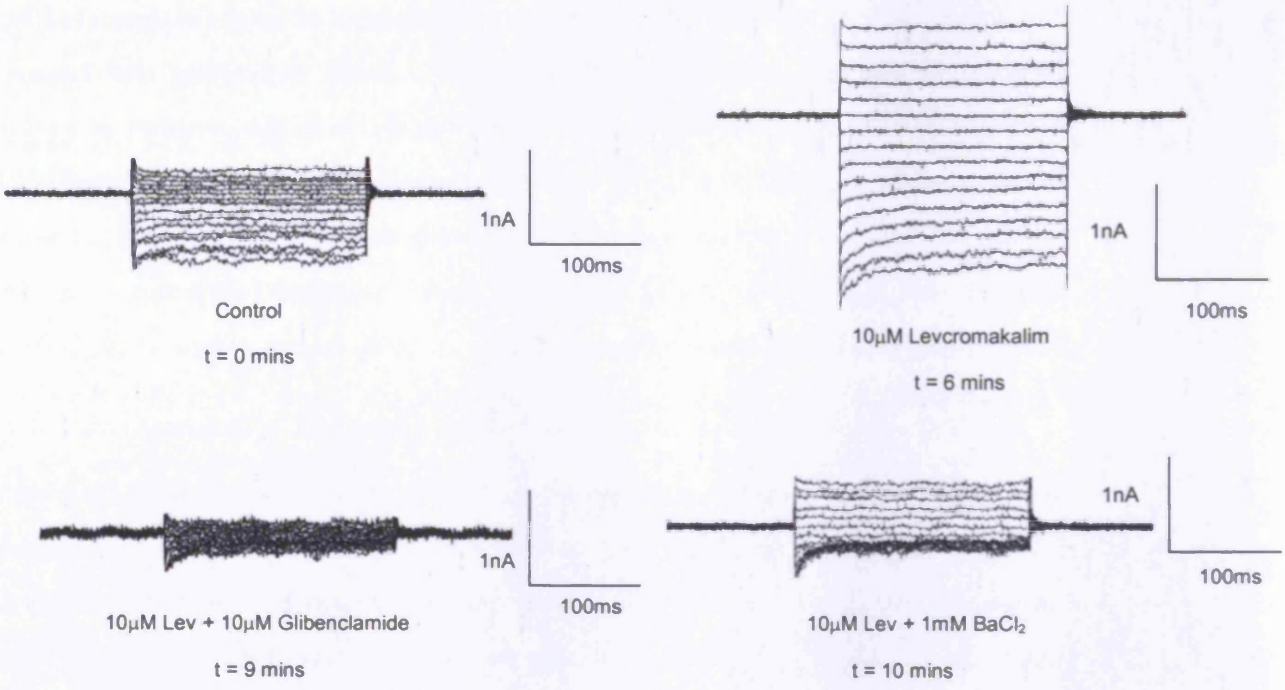
1nA
100ms
Control
t = 0 mins
1nA
100ms
10μM Levcromakalim
t = 6 mins
1nA
100ms
10μM Lev + 10μM Glibenclamide
t = 9 mins
1nA
100ms
10μM Lev + 1mM BaCl2
t = 10 mins

(B)

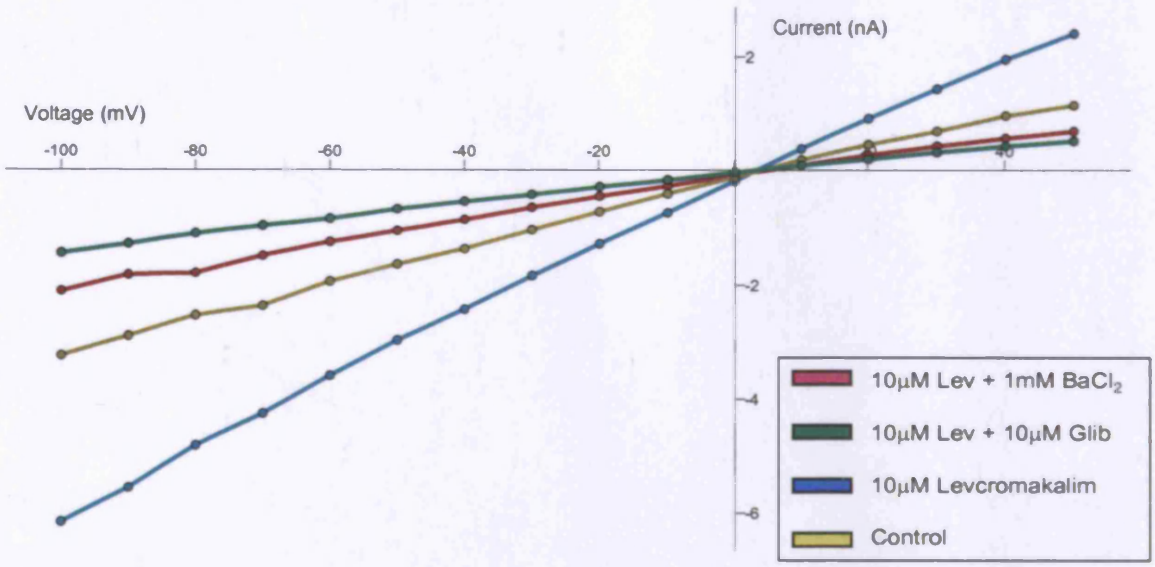
Current (nA)
Voltage (mV)
-100
-80
-60
-40
-20
2
-2
-4
-6
10μM Lev + 1mM BaCl2
10μM Lev + 10μM Glib
10μM Levcromakalim
Control

(C)

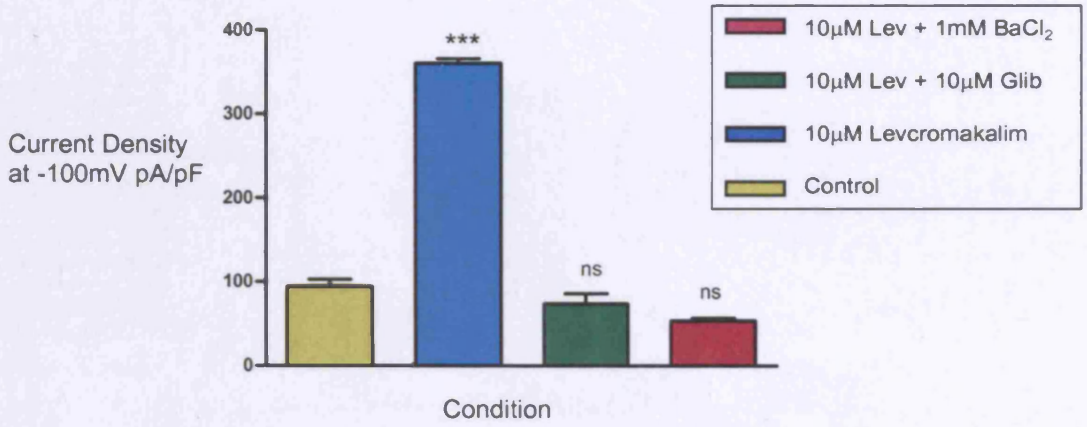

Figure 3.6: Examples of Kir6.1/SUR2B currents in stably transfected HEK293 cells as recorded by the whole-cell patch clamp configuration. Voltage clamp recordings were obtained under symmetrical K^+ conditions, and were evoked during 200ms voltage steps between -100mV and +50mV in 10mV increments from a holding potential of 0mV (A) Representative traces for each of the conditions: control (external solution with DMSO), 10μM levcromakalim, 10μM levcromakalim with 10μM glibenclamide and 10μM levcromakalim with 1mM barium chloride. All effects were reversible with subsequent washout, and all currents were recorded in symmetrical 140mM K^+, and with 0.5mM UDP in the patch pipette. The time taken to achieve a response in relation to the control is given (B) Representative I/V traces for each of the conditions (pA/pF), whereby each trace reverses at 0mV (C) Current/Density bar chart to represent mean data for the response of Kir6.1/SUR2B to the KCO and KCBs *** $P<0.001$ compared to control, (ns) $P>0.05$ compared to control (n=5).

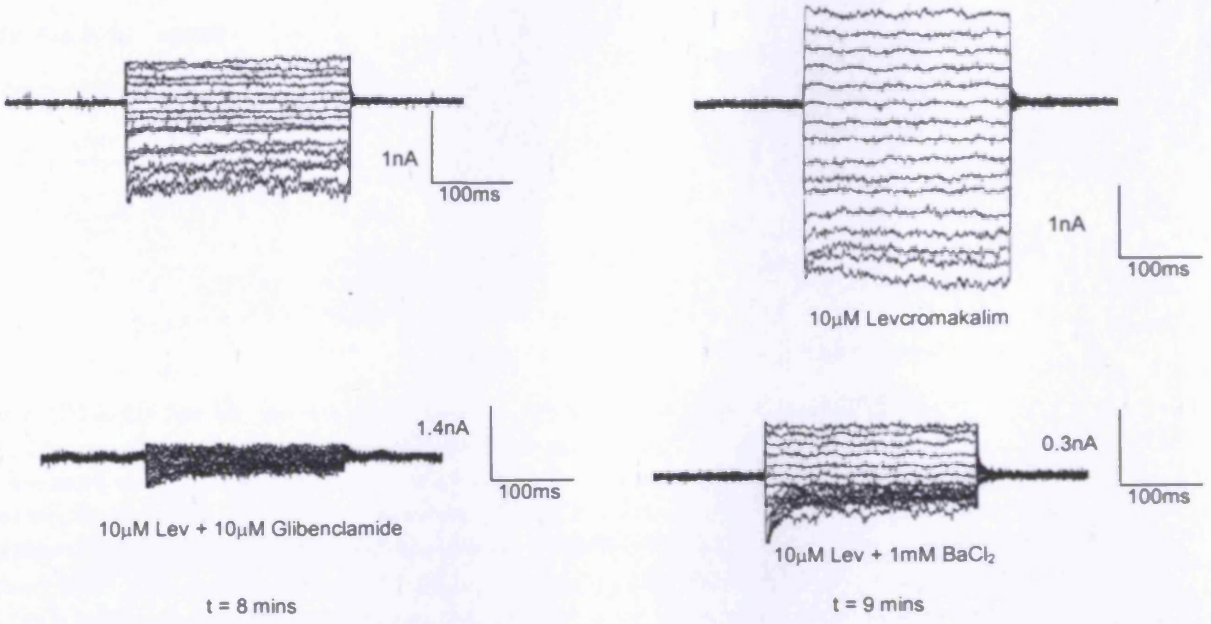
1nA
100ms
1nA
100ms
10μM Levcromakalim
1.4nA
100ms
10μM Lev + 10μM Glibenclamide
t = 8 mins
0.3nA
100ms
10μM Lev + 1mM BaCl2
t = 9 mins

(B)

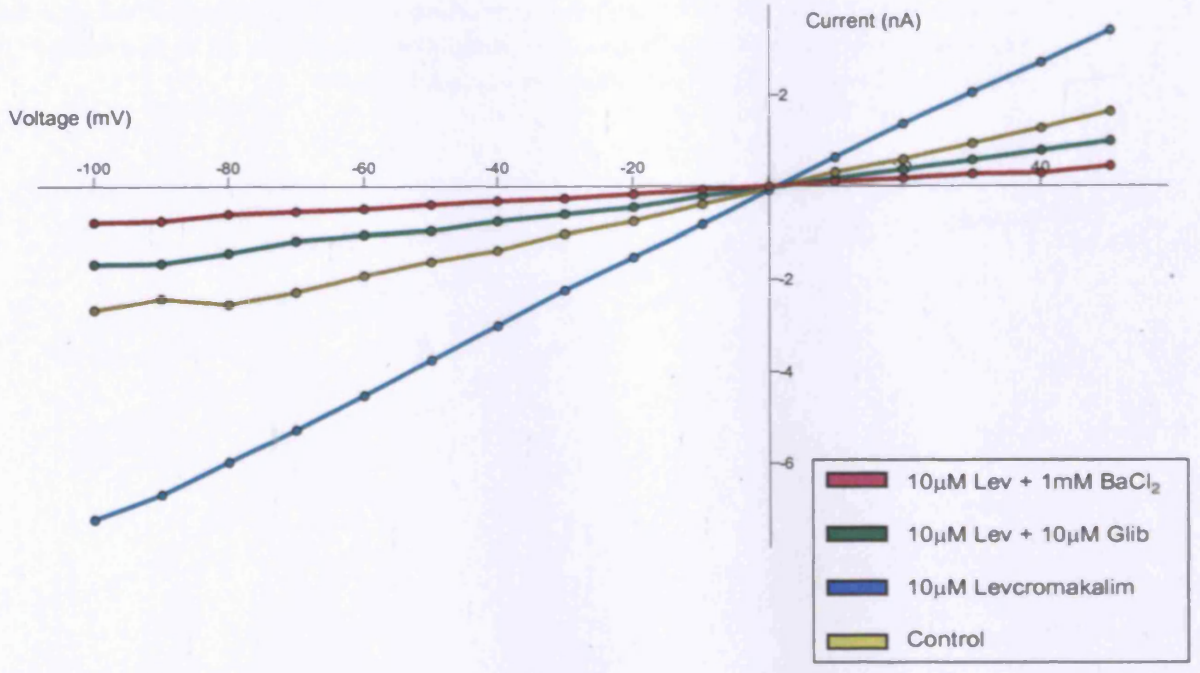
Current (nA)
Voltage (mV)
-100
-80
-60
-40
-20
2
-2
-4
-6
10μM Lev + 1mM BaCl2
10μM Lev + 10μM Glib
10μM Levcromakalim
Control

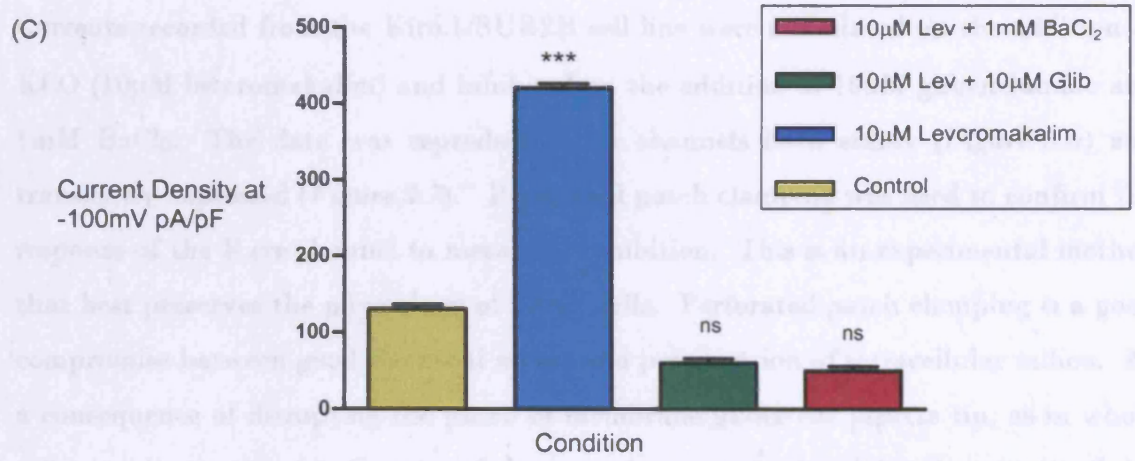

Figure 3.7: Examples of Kir6.1/SUR2B currents in transiently transfected HEK293 cells as recorded by the whole-cell patch clamp configuration. Voltage clamp recordings were obtained under symmetrical K^+ conditions, and were evoked during 200ms voltage steps between -100mV and +50mV in 10mV increments from a holding potential of 0mV (A) Representative traces for each of the conditions: control (external solution with DMSO), 10μM levcromakalim, 10μM levcromakalim with 10μM glibenclamide and 10μM levcromakalim with 1mM barium chloride. All effects were reversible with subsequent washout, and all currents were recorded in symmetrical 140mM K^+, and with 0.5mM UDP in the patch pipette. The time taken to achieve a response in relation to the control is given (B) Representative I/V traces for each of the conditions (pA/pF), whereby each trace reverses at 0mV (C) Current/Density bar chart to represent mean data for the response of Kir6.1/SUR2B the KCO and KCBs *** $P<0.001$ compared to control, (ns) $P>0.05$ compared to control (n=7).

Currents recorded from the Kir6.1/SUR2B cell line were stimulated on the addition of KCO (10μM levcromakalim) and inhibited on the addition of 10μM glibenclamide and 1mM $BaCl_2$. The data was reproducible for channels both stably (*Figure 3.6*) and transiently expressed (*Figure 3.7*). Perforated patch clamping was used to confirm the response of the K_{ATP} channel to metabolic inhibition. This is an experimental method that best preserves the physiology of intact cells. Perforated patch clamping is a good compromise between good electrical access and preservation of intracellular milieu. As a consequence of disrupting the patch of membrane under the pipette tip, as in whole cell recordings, the components of the cytoplasm are replaced by the pipette fluid. There are various situations where replacement of the cytoplasm is undesirable, for example if the subject of study involves intracellular signalling, whereby classic whole-cell recording could dilute or wash out crucial elements in the signalling cascade. It was necessary to apply the perforated patch method to study metabolic inhibition of the channel, since the result observed may be either at the level of the channel or be an indirect effect involving various signalling factors. It was also necessary to maintain the intracellular nucleotide concentrations so the effects of metabolic inhibition on the channel could be accurately assessed. The perforated patch method allowed this because the perforations created by amphotericin B were too small for larger molecules, such as nucleotides, to pass. Therefore, any change in nucleotide concentration within the cytoplasm was due to the effects of metabolic inhibition, and not due to interchange between the cytoplasm and the cell exterior.

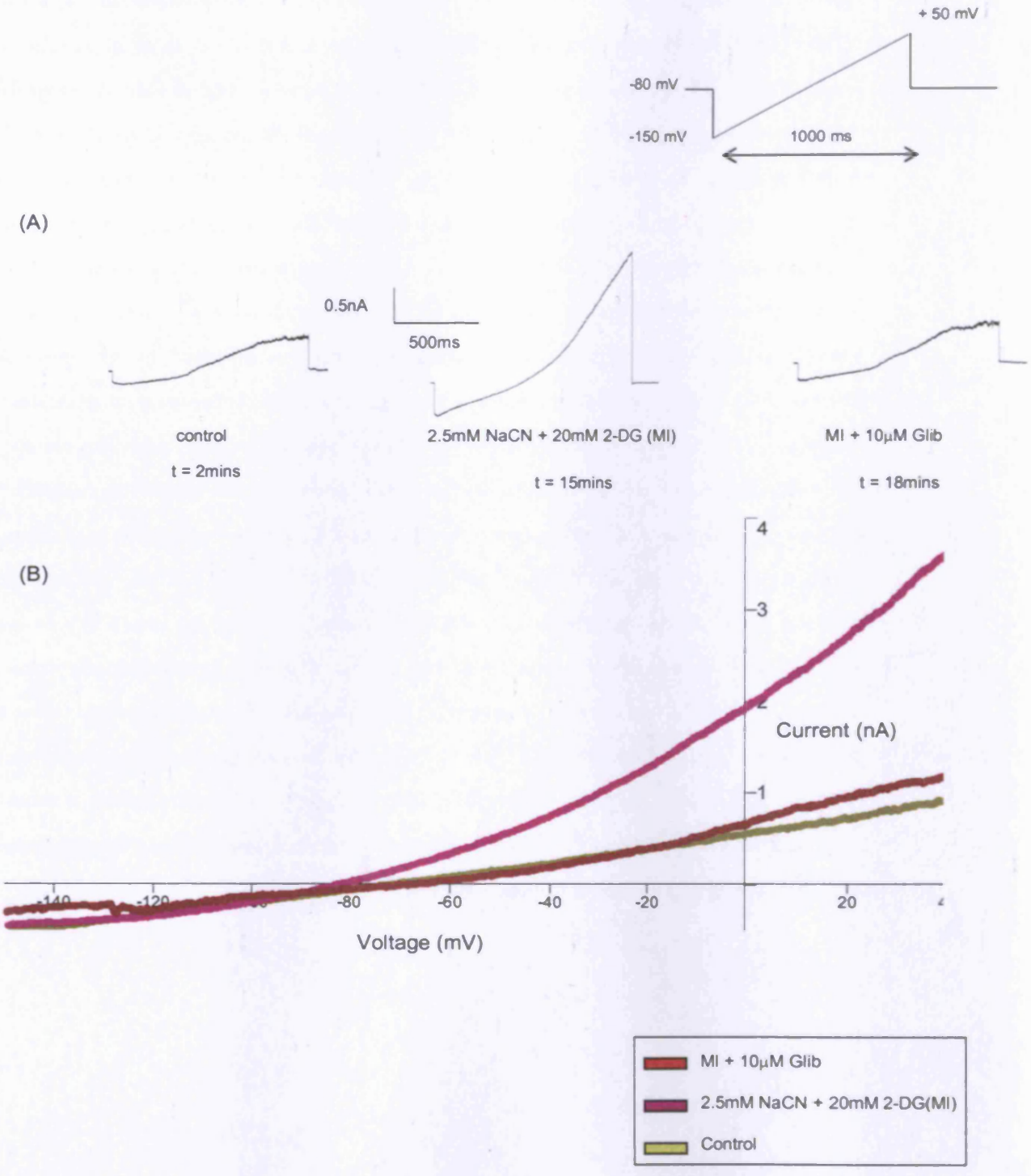
+ 50 mV
-80 mV
-150 mV
1000 ms
(A)
0.5nA
500ms
control
t = 2mins
2.5mM NaCN + 20mM 2-DG (MI)
t = 15mins
MI + 10μM Glib
t = 18mins
(B)
4
3
2
1
Current (nA)
-140
-120
-80
-60
-40
-20
20
Voltage (mV)
MI + 10μM Glib
2.5mM NaCN + 20mM 2-DG(MI)
Control

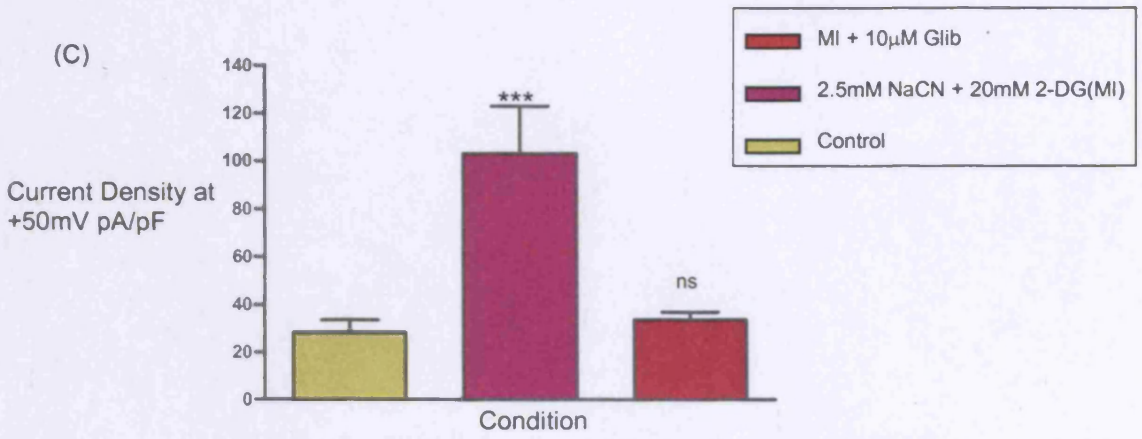

Figure 3.8: Effect of metabolic inhibition on the K_{ATP} channel Kir6.1/SUR2B current as demonstrated by the perforated patch-clamp method. Currents were evoked under asymmetrical conditions via voltage clamp recordings over 1000ms voltage steps between -150mV and +50mV from a holding potential of -80mV, with 15s between sweep starts (A) Representative traces for each of the conditions: external solution with DMSO, metabolic inhibitors (2.5mM NaCN and 20mM 2-DG) and metabolic inhibitors with glibenclamide. The time taken from perforation to the current recorded under each condition is given (B) Representative I/V traces for each of the conditions (pA/pF), whereby each trace reverses at -80mV (C) Current/Density bar chart to represent mean data for metabolic inhibition of the Kir6.1/SUR2B channel currents. *** $P<0.001$ compared to control. (ns) $P>0.05$ compared to control (n=7).

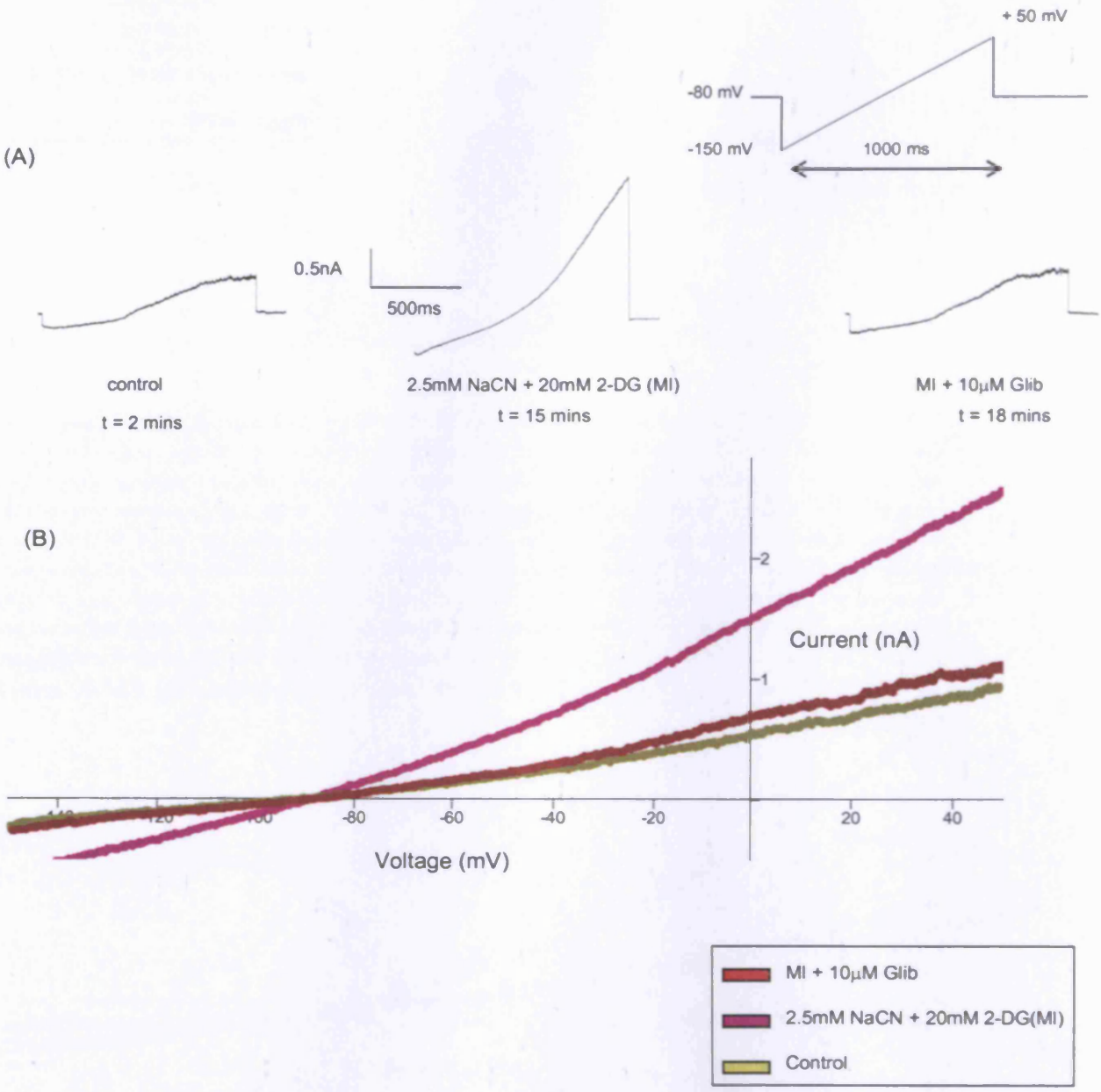
(A)
+ 50 mV
-80 mV
-150 mV
1000 ms
0.5nA
500ms
control
t = 2 mins
2.5mM NaCN + 20mM 2-DG (MI)
t = 15 mins
MI + 10μM Glib
t = 18 mins

(B)
Current (nA)
Voltage (mV)
-80
-60
-40
-20
20
40
MI + 10μM Glib
2.5mM NaCN + 20mM 2-DG(MI)
Control

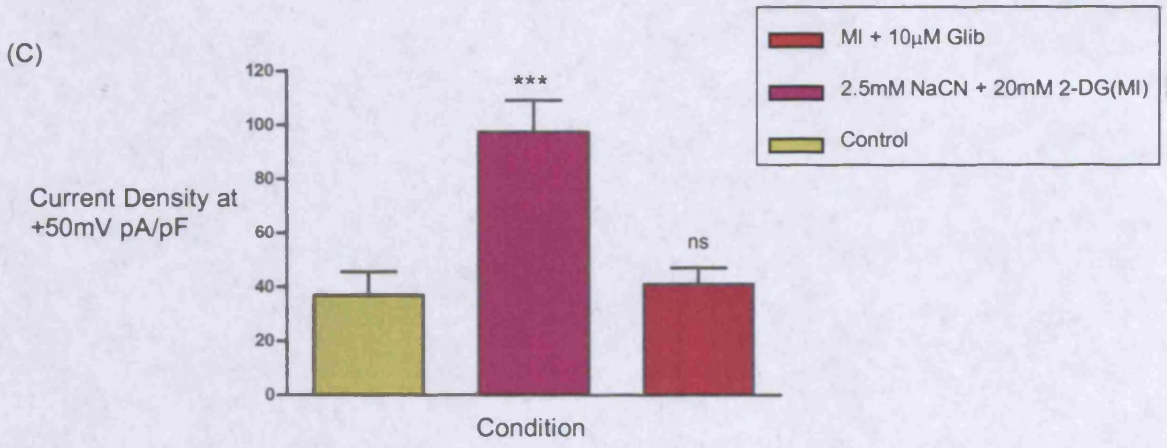

Figure 3.9: Effect of metabolic inhibition on the K_{ATP} channel Kir6.2/SUR2B current as demonstrated by the perforated patch clamp method. Currents were evoked under asymmetrical conditions via voltage clamp recordings over 1000ms voltage steps between -150mV and +50mV from a holding potential of -80mV, with 15s between sweep starts (A) Representative traces for each of the conditions: external solution with DMSO, metabolic inhibitors (2.5mM NaCN and 20mM 2-DG) and metabolic inhibitors with glibenclamide. The time taken from perforation to the current recorded under each condition is given, whereby control represents DMSO in bath solution (B) Representative I/V traces for each of the conditions (pA/pF), whereby each trace reverses at -80mV (C) Current/Density bar chart (to represent mean data for metabolic inhibition of the Kir6.1/SUR2B channel currents. *** $P<0.001$ compared to control, (ns) $P>0.05$ compared to control (n=7).

The data obtained is consistent with that obtained by the $^{86}Rb^{+}$ flux assay. The K_{ATP} channels Kir6.1/SUR2B and Kir6.2/SUR2B open in response to metabolic inhibition, the effect of which is reversed by glibenclamide. This confirms that the assay is a valuable tool for screening for their functionality, and assessing K_{ATP} channel current in response to depletion of ATP.

The importance that cellular signalling pathways are thought to play in K_{ATP} channel regulation was discussed in the introduction. A series of preliminary experiments were conducted to determine whether external signalling factors, such as AMPK, play a role in the response of the channel to variation in intracellular nucleotide concentration; specifically to the depletion of ATP levels that are induced by metabolic inhibition.

I initially thought it would be interesting to look at the role that PKA and adenosine may play in the regulation of Kir6.1/SUR2B. Aside from variation in ATP/ADP ratio, the phosphorylation of ion channels by protein kinases is an important mechanism by which membrane excitability is regulated by cell signalling pathways. It has previously been established that HEK293 cells possess the relevant cellular signalling machinery for PKA-mediated channel modulation. It has been shown that that forskolin, a direct activator of adenylate cyclase, is able to elevate cAMP in HEK293 cells, and that cAMP binds to the regulatory subunit of PKA which activates Kir6.1/SUR2B. It was confirmed that PKA activates Kir6.1/SUR2B by the application of Rp-cAMPS, which competes for cAMP binding to the regulatory subunit of PKA. In whole-cell patch clamp experiments, when Rp-cAMPS was included in the patch pipette and forskolin in the bath solution, forskolin no longer stimulated Kir6.1/SUR2B current (Quinn, Giblin et al. 2004).

It has also been shown that the vasodilator adenosine plays an indirect role in the regulation of K_{ATP} channels to cause membrane hyperpolarisation, and that it acts through the adenylyl cyclase (AC)-protein kinase A (PKA) pathway (Bruch, Rubel et al. 1998). In smooth muscle cells isolated from rabbit or rat mesenteric or porcine

coronary arteries, adenosine activated glibenclamide-sensitive K_{ATP} currents and the AC-PKA pathway was implicated (Dart and Standen 1993: Kleppisch and Nelson 1995).

To determine any involvement of adenosine and PKA in the metabolic regulation of the K_{ATP} channel, the ability of the PKA inhibitors, H-89 and KT5720, and adenosine receptor antagonists, Quinoxaline and SCH58261, to reverse the efflux observed on the application of forskolin and metabolic inhibitors to Kir6.1/SUR2B was compared. 10μM forskolin was applied as this has previously been shown to be effective in the activation of Kir6.1/SUR2B currents (Quinn, Giblin et al. 2004). 250nM H-89 and 6.5μM of KT 5720 of the PKA inhibitors were applied. These are commonly used, and the IC_{50} values have been established, these being 135nM for H-89 and 3.3μM for KT5720 (Davies, Reddy et al. 2000). The adenosine receptor antagonists, SCH58261 and Quinoxaline, were chosen on the basis of literature searches, as were the doses applied (60nM and 100nM respectively) (Belardinelli, Shryock et al. 1996; Belardinelli, Shryock et al. 1998; Baraldi, Tabrizi et al. 2003; Novellino, Cosimelli et al. 2005).

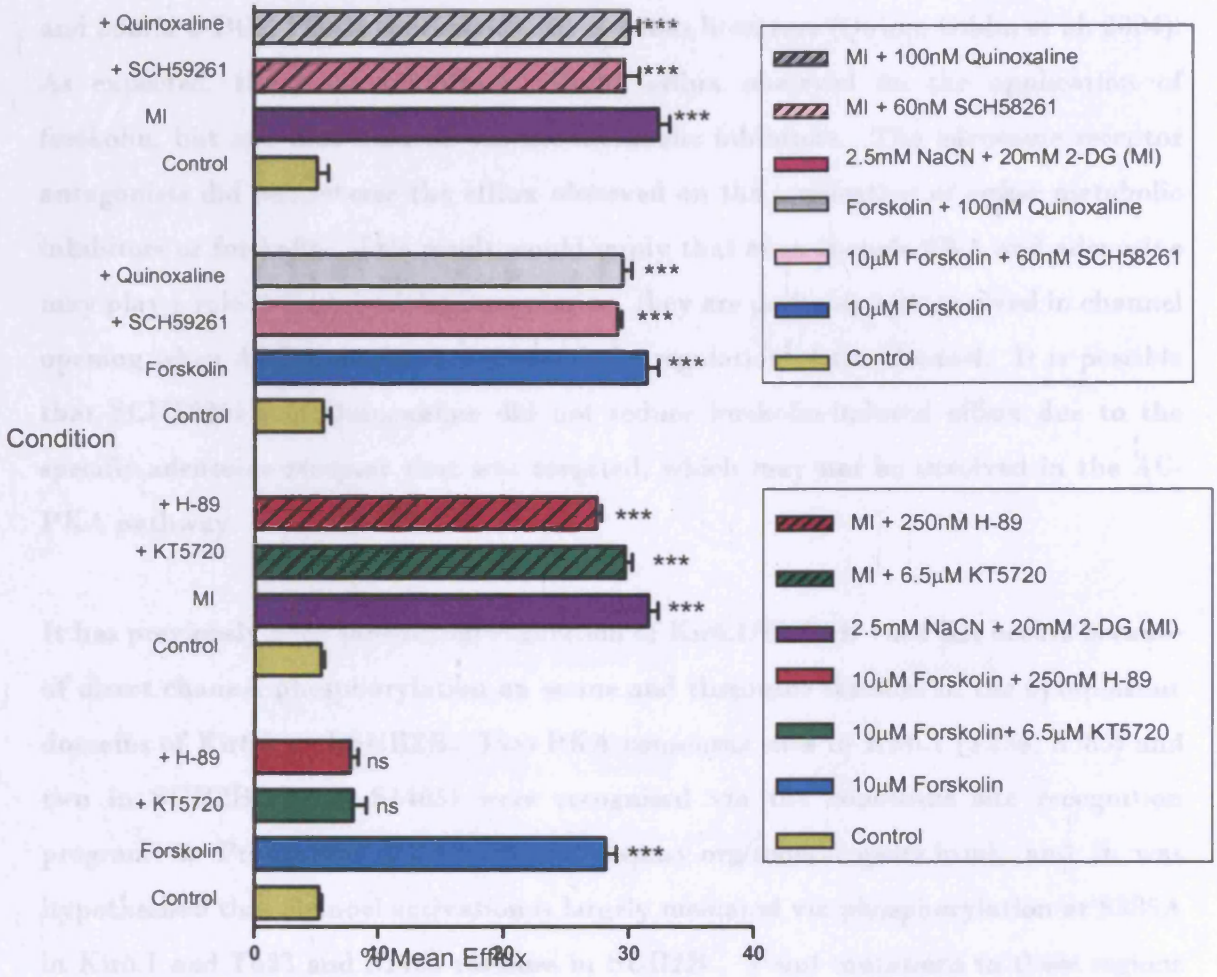

Figure 3.10: The effect of PKA inhibitors (H-89 & KT5720) and adenosine receptor antagonists (Quinoxaline & SCH58261) in response to increased $^{86}Rb^{+}$ efflux observed on the application of either metabolic inhibitors or forskolin to the K_{ATP} channel Kir6.1/SUR2B. Efflux was measured 30 minutes after the addition of drugs, and was calculated as % efflux of initial $^{86}Rb^{+}$ content. The control represents DMSO diluted in HBS. Data are shown as +/- SEM, whereby n=5. *** $P<0.001$ compared to control, (ns) $P>0.05$ compared to control.

In this setting, 10μM forskolin increased Kir6.1/SUR2B efflux significantly beyond the basal level ($P<0.001$), and to a similar degree as the metabolic inhibitors 2.5mM NaCN and 20mM 2-DG. This is consistent with previous literature (Quinn, Giblin et al. 2004). As expected, the PKA inhibitors reduced efflux observed on the application of forskolin, but not that induced via the metabolic inhibitors. The adenosine receptor antagonists did not reverse the efflux observed on the application of either metabolic inhibitors or forskolin. This result would imply that even though PKA and adenosine may play a role in Kir6.1/SUR2B regulation, they are probably not involved in channel opening when ATP is depleted, i.e. metabolic regulation of the channel. It is possible that SCH58261 and Quinoxaline did not reduce forskolin-induced efflux due to the specific adenosine receptor that was targeted, which may not be involved in the AC-PKA pathway.

It has previously been shown that regulation of Kir6.1/SUR2B via PKA occurs because of direct channel phosphorylation on serine and threonine residues in the cytoplasmic domains of Kir6.1 and SUR2B. Two PKA consensus sites in Kir6.1 (T234, S385) and two in SUR2B (T633, S1465) were recognised via the consensus site recognition program in Prosite for PKA: http://ca.expasy.org/tools/scnpsite.html, and it was hypothesised that channel activation is largely mediated via phosphorylation at S385A in Kir6.1 and T633 and S1465 residues in SUR2B. Point mutations in these regions removed the stimulation observed by PKA and forskolin (a direct activator of adenylate cyclise, able to elevate cAMP in HEK293 cells) in an electrophysiological setting. The $^{86}Rb^{+}$ assay was conducted to compare the effect of mutation of these phosphorylation sites on the metabolic stimulation of the channel. These mutants (previously generated within the lab) were transiently transfected with Kir6.1 (in the case of SUR2B mutants) or SUR2B (in the case of Kir6.1 mutants) into HEK293 cells, so that each channel complex contained one point mutation. The assay was applied as described previously.

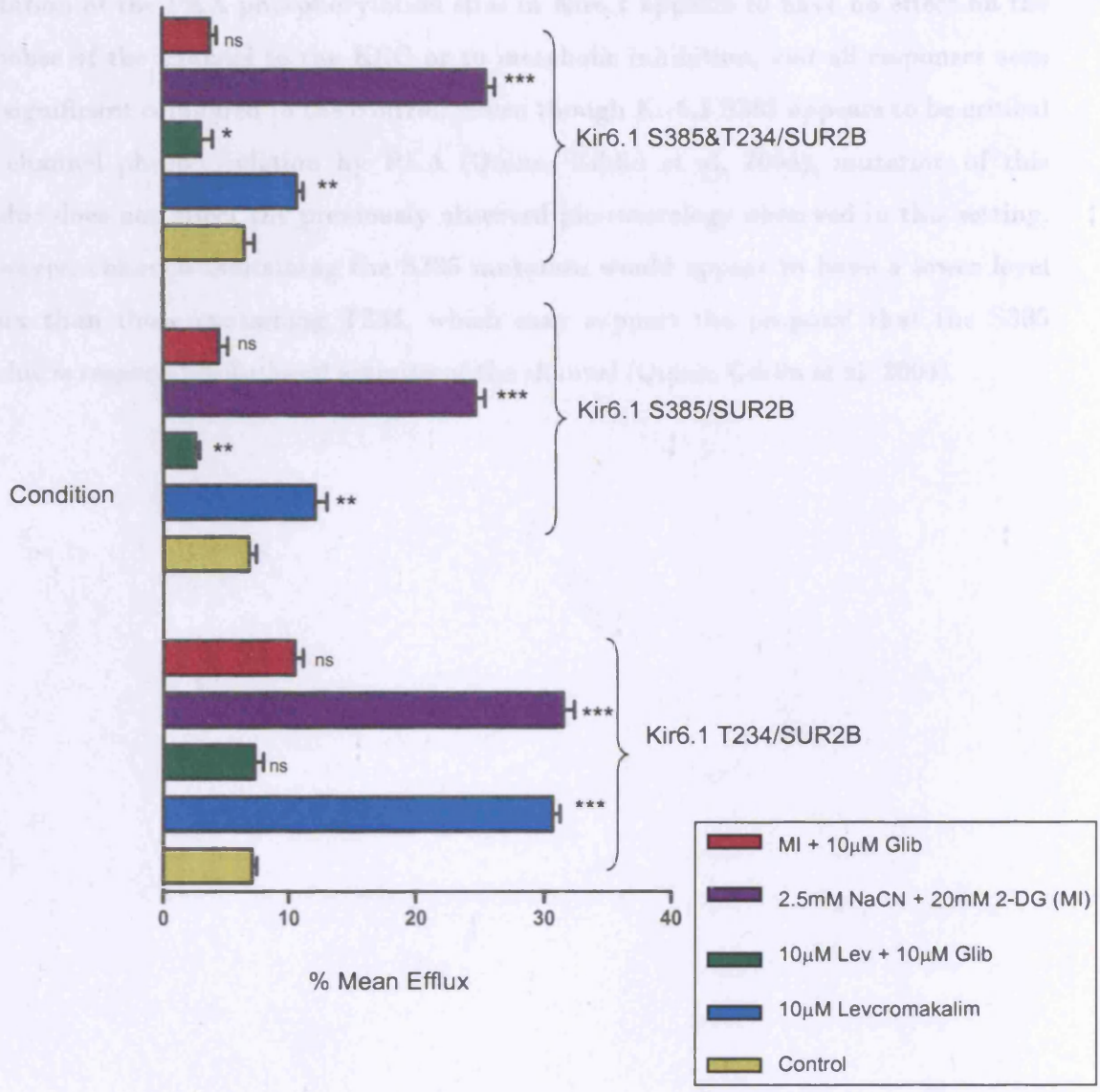

Figure 3.11: The effect of point mutations on the PKA consensus sites T234 and S385 in Kir6.1 on the functionality of Kir6.1/SUR2B as shown by $^{86}Rb^{+}$ efflux. The mutations were expressed alone or in combination. Efflux was measured 15 minutes after the addition of drugs, and was calculated as % efflux of initial $^{86}Rb^{+}$ content. The control represents DMSO diluted in HBS. Data are shown as +/- SEM, whereby n=9. *** P<0.001 compared to control, ** P=0.001-0.01 compared to control, * P=0.01-0.05 compared to control, (ns) P>0.05 compared to control.

Mutation of the PKA phosphorylation sites in Kir6.1 appears to have no effect on the response of the channel to the KCO or to metabolic inhibition, and all responses seen are significant compared to the control. Even though Kir6.1 S385 appears to be critical for channel phosphorylation by PKA (Quinn, Giblin et al. 2004), mutation of this residue does not affect the previously observed pharmacology observed in this setting. However, channels containing the S385 mutation would appear to have a lower level efflux than those containing T234, which may support the proposal that the S385 residue is responsible for basal activity of the channel (Quinn, Giblin et al. 2004).

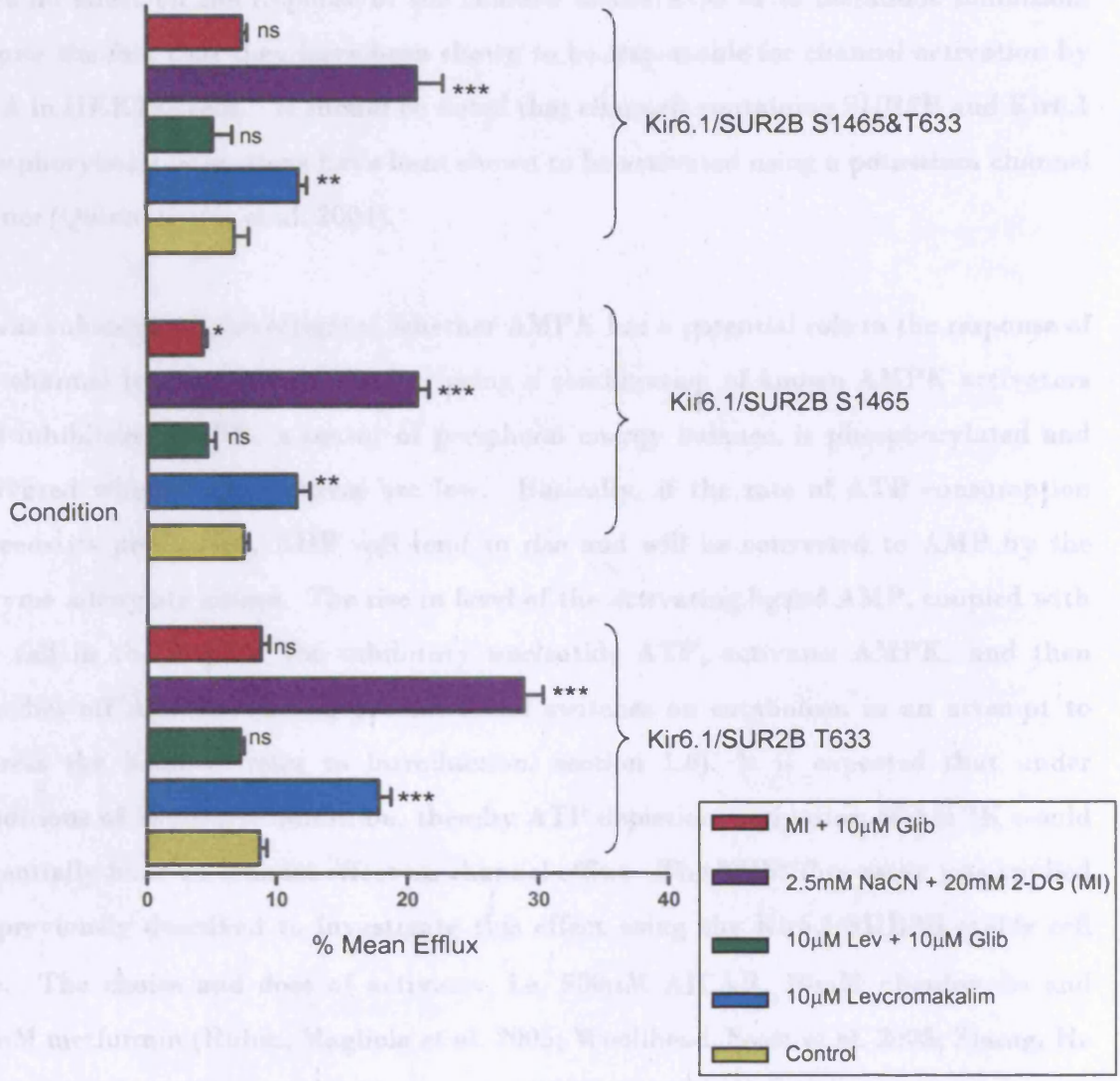

Figure 3.12: The effect of point mutations on the PKA consensus sites T633 and S1465 in SUR2B on the functionality of Kir6.1/SUR2B as shown by $^{86}Rb^{+}$ efflux. The mutations were expressed alone or in combination. Efflux was measured 15 minutes after the addition of drugs, and was calculated as % efflux of initial $^{86}Rb^{+}$ content. The control represents DMSO diluted in HBS. Data are shown as +/- SEM, whereby n=9. *** P<0.001 compared to control, ** P=0.001-0.01 compared to control, * P=0.01-0.05 compared to control, (ns) P>0.05.

Again, mutation of the identified PKA phosphorylation sites in SUR2B appears to have no effect on the response of the channel to the KCO or to metabolic inhibition, despite the fact that they have been shown to be responsible for channel activation by PKA in HEK293 cells. It should be noted that channels containing SUR2B and Kir6.1 phosphorylation mutations have been shown to be activated using a potassium channel opener (Quinn, Giblin et al. 2004).

It was subsequently investigated whether AMPK has a potential role in the response of the channel to metabolic inhibition, using a combination of known AMPK activators and inhibitors. AMPK, a sensor of peripheral energy balance, is phosphorylated and activated when energy sources are low. Basically, if the rate of ATP consumption exceeds its production, ADP will tend to rise and will be converted to AMP by the enzyme adenylate kinase. The rise in level of the activating ligand AMP, coupled with the fall in the level of the inhibitory nucleotide ATP, activates AMPK, and then switches off ATP consuming processes and switches on catabolism in an attempt to redress the balance (refer to introduction, section 1.6). It is expected that under conditions of metabolic inhibition, thereby ATP depletion, activation of AMPK would potentially have an indirect effect on channel efflux. The $^{86}Rb^{+}$ flux assay was applied as previously described to investigate this effect using the Kir6.1/SUR2B stable cell line. The choice and dose of activator, i.e. 500μM AICAR, 10mM phenformin and 10mM metformin (Rubin, Magliola et al. 2005; Woollhead, Scott et al. 2005; Zhang, He et al. 2007) or inhibitor, 200nM Compound C, 200μM C75, 1μM iodotubericidin and 50nM staurosporine (Fluckiger-Isler and Walter 1993; Massillon, Stalmans et al. 1994; Meggio, Donella Deana et al. 1995; Lee, Hwang et al. 2003; Kim, Miller et al. 2004; Landree, Hanlon et al. 2004; McCullough, Zeng et al. 2005)were chosen on the basis of literature searches. Generally these compounds are not specific in the targeting of AMPK activity, especially Staurosporine, and affect a variety of protein kinases. It was necessary to apply a dose of inhibitor/activator that would target AMPK without disrupting the activity of other signalling pathways. The data displayed in *Figure 3.13* was obtained from a preliminary experiment to deduce if the applied doses of these

compounds affected Kir6.1/SUR2B efflux induced via metabolic inhibition. Similar results were obtained for both 15 and 30 minutes of pre-incubation of AMPK activator/inhibitor prior to incubation with metabolic inhibitors. Those for the former are shown.

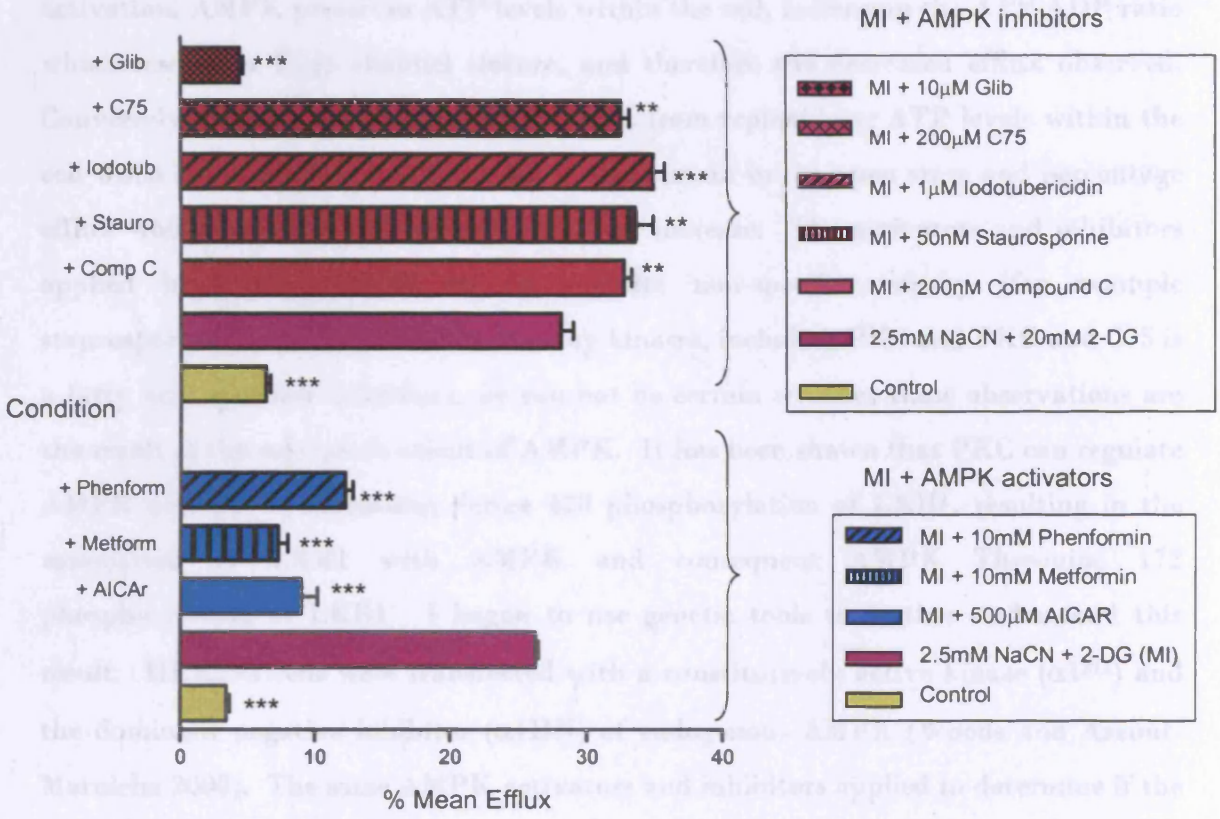

Figure 3.13: The effect of AMPK activators (AICAR, metformin, phenformin) and inhibitors (staurosporine, iodotubericidin, C75, compound C) on the response of the K_{ATP} channel Kir6.1/SUR2B to metabolic inhibition as shown by $^{86}Rb^+$ efflux. Efflux was measured after incubation with activator/inhibitor for 15 minutes, followed by incubation with metabolic inhibitors for 15 minutes, and was calculated as % efflux of initial $^{86}Rb^+$ content. The control represents DMSO diluted in HBS. Data are shown as +/- SEM, whereby n=6. *** P<0.001, ** P=0.001-0.01, * P=0.01-0.05 compared to metabolic inhibition.

These initial observations would indicate that all three AMPK activators applied significantly reverse the response of the channel to metabolic inhibition, i.e. decrease efflux ($P<0.001$), whereas the AMPK inhibitors increase the effect of the channel to metabolic inhibition. The response of the channel to metabolic inhibition after the application of glibenclamide is also shown as a control. It is expected that upon activation, AMPK preserves ATP levels within the cell, increasing the ATP/ADP ratio which results in K_{ATP} channel closure, and therefore the decreased efflux observed. Conversely, inhibition would prevent AMPK from replenishing ATP levels within the cell when depleted, therefore channels would remain in the open state and percentage efflux would remain at the same level if not increase. The activators and inhibitors applied have been known to demonstrate non-specific activity (for example staurosporine is a potent inhibitor of many kinases, including PKC and PKG and C75 is a fatty acid synthase inhibitor); we can not be certain whether these observations are the result of the sole involvement of AMPK. It has been shown that PKC can regulate AMPK activity by increasing Serine 428 phosphorylation of LKB1, resulting in the association of LKB1 with AMPK and consequent AMPK Threonine 172 phosphorylation of LKB1. I began to use genetic tools to further understand this result. HEK293 cells were transfected with a constitutively active kinase ($\alpha1^{312}$) and the dominant negative inhibitor ($\alpha1DN$) of endogenous AMPK (Woods and Azzout-Marniche 2000). The same AMPK activators and inhibitors applied to determine if the result observed in *Figure 3.13* held true, whereby it was speculated that any variation of this result would indicate that AMPK does indeed influence K_{ATP} channel regulation. However, the result obtained was inconclusive.

To summarise, the K_{ATP} channels Kir6.1/SUR2B and Kir6.2/SUR2B were shown to be metabolically responsive. i.e. open on $[ATP]_i$ depletion, via both the rubidium flux assay and the perforated patch-clamp method. HEK293 cells stably expressing the channel were shown to be the best system on which to apply the $^{86}Rb^+$ flux assay and observe a pharmacological response. In the other cell systems there would appear to be

considerable background noise from other native K^+ channels, and if another system was to be considered to observe native K_{ATP} channel efflux in future experiments, one would probably have to block the basal efflux of other native K^+ channels to reduce background noise. Even though cellular signalling factors have been shown to be involved in Kir6.1/SUR2B regulation, it is not clear from my experiments whether they contribute to the metabolic regulation of the channel. With reference to the Chapter one, *section 1.6*, this may be the case in the native setting, but it is clear from the data I have shown so far, that the channel is intrinsically metabolically sensitive. Therefore, in subsequent chapters I have primarily chosen to look at the regulation of the channel at the level of the channel- i.e. the intrinsic role that the pore-forming subunit and the sulphonylurea receptor play in the metabolic response of the channel.

Chapter Four

Determination of the functionality and surface expression of Kir6.1/SUR2B after truncation of the N- and C-terminus of the pore-forming subunit

Chapter Four: Results

Determination of the functionality and surface expression of Kir6.1/SUR2B after truncation of the N- and C-terminus of the pore-forming subunit

It has previously been shown that co-expression of SUR and Kir6.*x* is necessary to generate significant plasmalemmal K^+ currents (Inagaki, Tsuura et al. 1995; Tucker, Gribble et al. 1997; Aguilar-Bryan and Bryan 1999; Zerangue, Schwappach et al. 1999), and this observation triggered a number of studies on the cell biology of channel complex formation (Makhina and Nichols 1998; Zerangue, Schwappach et al. 1999). Mutant forms of Kir6.2 with a C-terminal truncation of 26 (Kir6.2ΔC26) or 36 amino acids (Kir6.2ΔC36) produce currents in the absence of SUR1 subunits (Tucker, Gribble et al. 1997). This was shown by the currents recorded from oocytes injected with mRNA encoding Kir6.2ΔC36/ΔC26, and it was deduced that they were not only capable of independent expression, but that they were also intrinsically sensitive to metabolically induced changes in cytosolic nucleotide levels. Kir6.2ΔC26/ΔC36 has since served as a useful tool to understand the role of each subunit in channel gating by nucleotides and pharmacological agents (Gribble, Tucker et al. 1997; Babenko, Gonzalez et al. 1999; Koster, Sha et al. 1999; Proks, Gribble et al. 1999; Reimann, Tucker et al. 1999; Cui, Tinker et al. 2003; Saraya, Yokokura et al. 2004; Lu, Hong et al. 2005). The knowledge that Kir6.2ΔC36 could be forced to express channel activity independently of SUR (Tucker, Gribble et al. 1997), together with an assay that was capable of detecting surface expression of K_{ATP} channels in *Xenopus oocytes*, was used to map an ER localization signal in Kir6.2 and then in SUR1 (Zerangue, Schwappach et al. 1999). Similar signals are also found in Kir6.1 (Zerangue, Schwappach et al. 1999) and SUR2 (Konstas, Dabrowski et al. 2002). This RKR motif either prevents the export of the protein from the ER and/or retrieves it from the golgi. Deletion of this motif allows each protein to express independently (Tucker, Gribble et al. 1997; Zerangue, Schwappach et al. 1999).

However, it was not certain if it was possible to express Kir6.1 independently. Constructs were previously made by Yi Cui in which the C-terminal 48 and 61 amino acids were truncated (removing the RXR motif), and these constructs were only shown to be functional when expressed with SUR2B. It was thought necessary to investigate this further.

Additionally, deletion of the N-terminus of Kir6.1 when expressed in combination with SUR1 has been found to increase basal activity, i.e. that occurring in the absence of nucleotide diphosphate (Babenko and Bryan 2001). N-terminal truncation of Kir6.1 was not found to compromise the response to Mg-nucleotide-dependent stimulation by SUR1, and progressively larger deletions (ΔN13, ΔN21 and ΔN33) increased the open probability, with maximal effect seen with ΔN33 (Babenko and Bryan 2001).

Based on this existing evidence, various ΔN-Kir6.1-ΔC truncation mutants were made to delineate if Kir6.1ΔC is indeed only functional in the presence of a sulphonylurea receptor, or if Kir6.1ΔC shows intrinsic ATP/metabolic sensitivity in the absence of SUR. It was also of interest to deduce whether Kir6.1ΔN could further increase any basal activity observed. N- and C-terminal truncation mutants were made via conventional PCR. A plasmid encoding Kir6.1 with an HA epitope introduced into the extracellular M1 and H5 domains (Kir6.1-eHA) was kindly provided by Dr LY Jan. and sub-cloned into the mammalian expression vector pcDNA3.1/Zeo prior to my experiments. The HA epitope is a nine amino acid sequence (YPYDVPDYA) present in the human influenza virus hemagglutinin protein, and is recognized by the high affinity rat monoclonal isolate (3F10, *Roche*). With reference to *Figure 4.1*, pre-optimised PCR conditions were applied to generate the various truncation mutants from Kir6.1-eHA using the primers listed in Chapter 2.

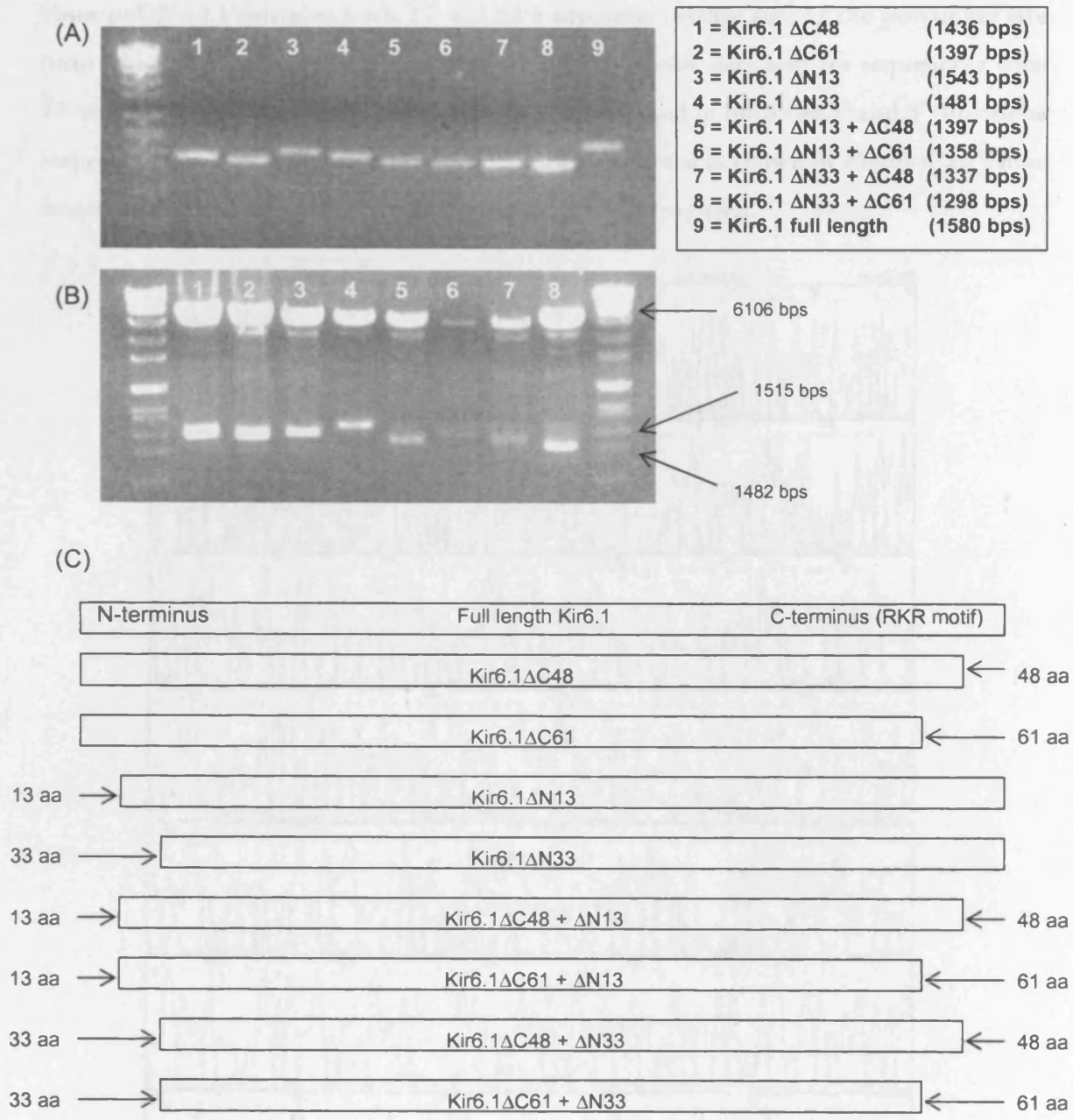

Figure 4.1: Generation of the ΔN-Kir6.1-eHA-ΔC truncation mutants via conventional PCR. (A) Analysis of PCR products via agarose gel electrophoresis. Full length Kir6.1-eHA was generated as a positive control (Lane 9). A standard DNA Molecular Weight Marker VII (0.359, 0.492, 0.710, 0.992, 1.164, 1.482, 1.515, 1.882, 1.953, 2.799, 3.639, 4.899, 6.106, 7.427, 8.576 kbp) was used to determine the length of the fragments (*Roche, UK*). The length of each PCR fragment is indicated in the text box (B) Restriction digest of truncated PCR fragments sub-cloned into pcDNA3.1 using the restriction enzymes BamH1 and Xba1. (C) Diagram to compare each of successive truncations with full length Kir6.1 and to depict the number of amino acids removed in each case. Deletion of the C-terminus removes the RKR motif.

Since pcDNA3.1 contains both T7 and SP6 promoters either side of the polylinker site (into which the mutants were inserted), individual clones were sent for sequencing with T7 and SP6 primers (therefore the sequence was checked in both the 5' and 3' directions respectively). An example of a sequencing trace obtained is shown in *Figure 4.2*. These results confirmed that the correct truncations were introduced.

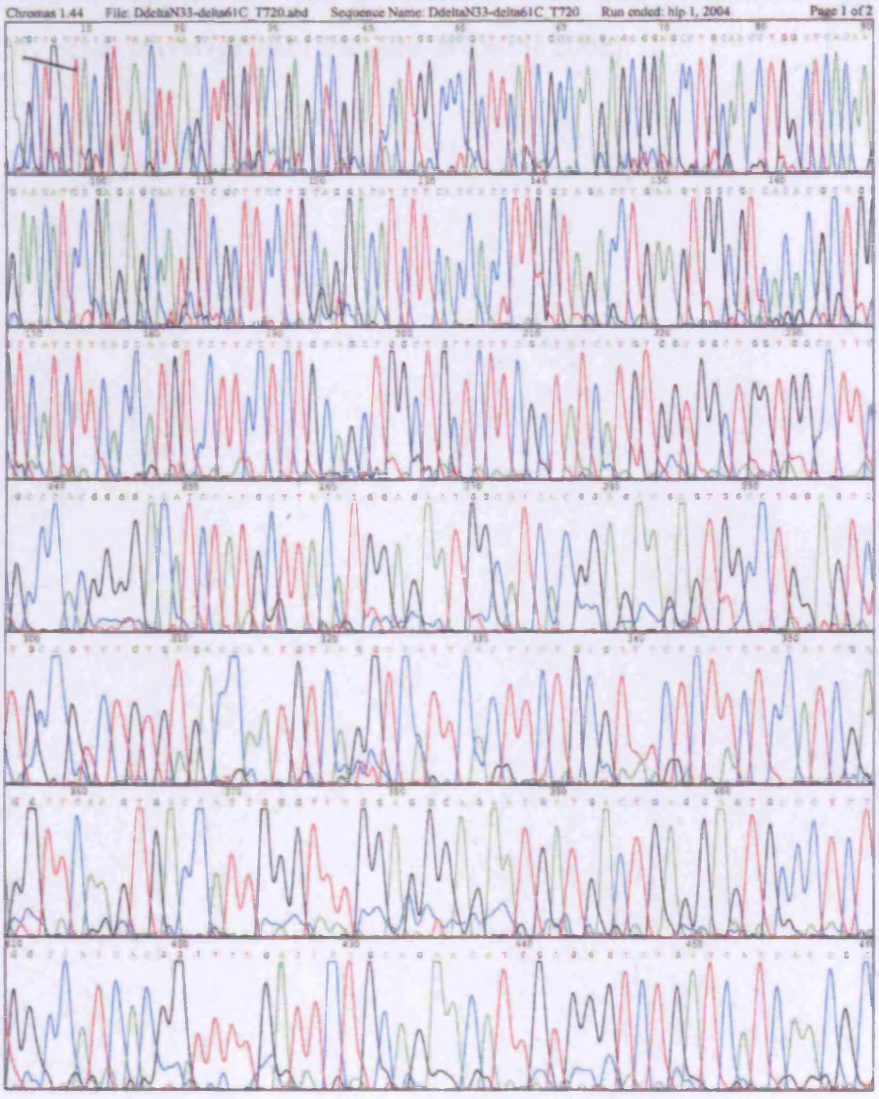

Figure 4.2: An example chromatogram result that was opened with the software programme Chromas to confirm the generation of a truncated Kir6.1 mutant, in this case Kir6.1ΔN33 (cloned into pcDNA3.1) that was sequenced using a T7 primer. A clean sequence was indicated by peaks that were evenly spaced with each only having one colour. This example result indicated that the quality of the template and primer was good. The Chromas programme enabled conversion of the sequence into FASTA format, enabling a nucleotide-nucleotide blast search to be conducted on the NCBI website (http://www.ncbi.nlm.nih.gov).

Prior to testing the functionality of the ΔN-Kir6.1-ΔC truncation mutants, I wanted to determine whether removal of the C-terminus of Kir6.1 enabled its independent expression. Immunofluorescent staining was performed in permeabilised and non-permeabilised cells according to published protocols (Cui, Tran et al. 2002; Giblin, Quinn et al. 2002; Muzyamba, Farzaneh et al. 2007). CHO-K1 cells were used, since the assay did not appear to work in HEK293 cells. This phenomenon has also been described by other investigators (Margeta-Mitrovic 2002).

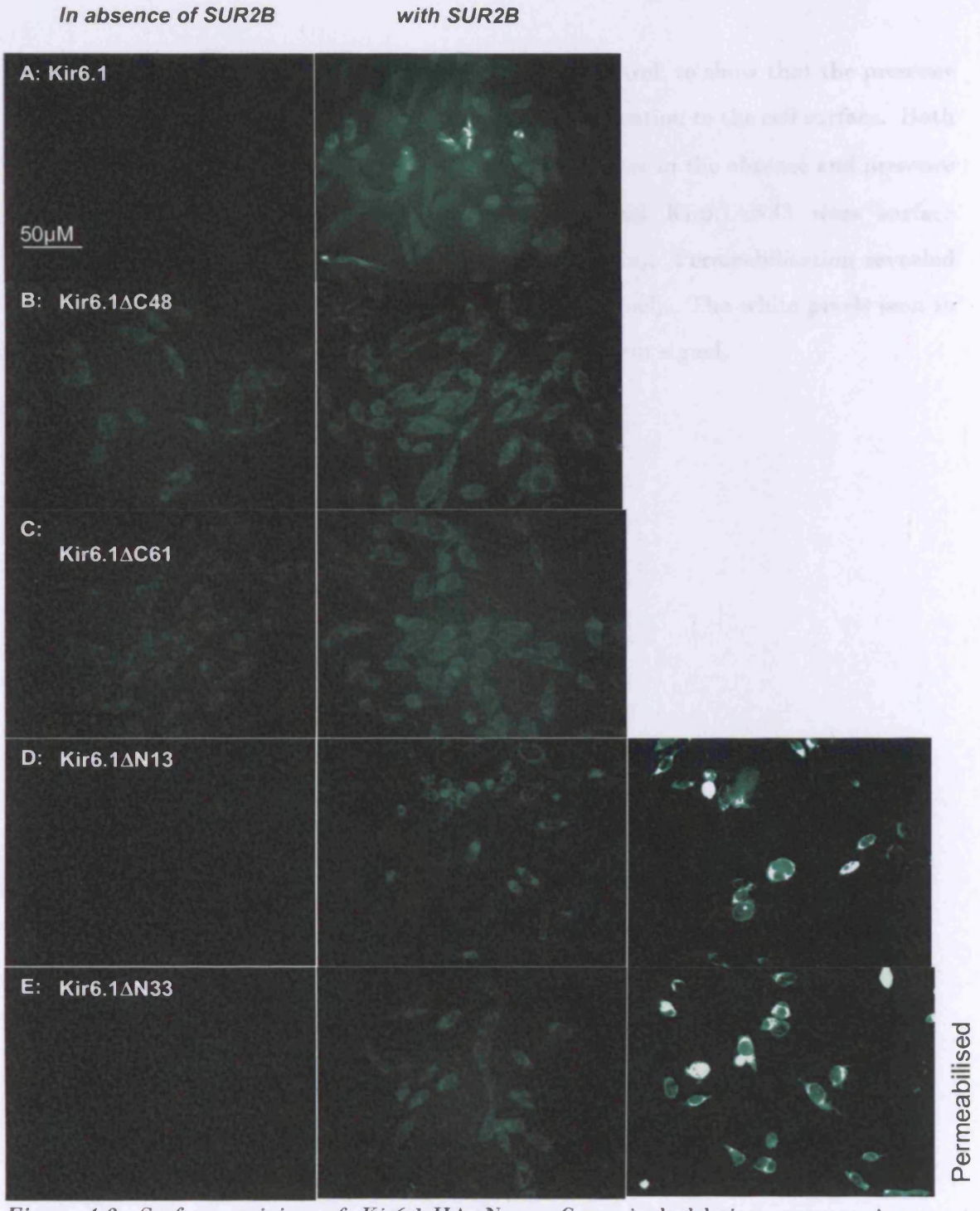

Figure 4.3: Surface staining of Kir6.1-HA N- or C-terminal deletion mutants in non-permeabilised cells, expressed with (left panel) and without (middle panel) SUR2B. Images of permeabilised cells in which Kir6.1ΔN13/ΔN33 (E&D) were overexpressed in the absence of SUR2B are also shown as a control (indicative that recombinant protein was retained intracellularly). All images were captured at the same exposure (1 second) and magnification (400×), and were not subject to any other form of enhancement other than the addition of green pseudocolour when opened in Adobe Photoshop. The white scale bar represents 50μm.

Kir6.1 was expressed with and without SUR2B as a control, to show that the presence of the sulphonylurea receptor was required for its translocation to the cell surface. Both Kir6.1ΔC48 and Kir6.1ΔC61 translocated to the cell surface in the absence and presence of SUR2B (*Figure 4.3b&c*), however Kir6.1ΔN13 and Kir6.1ΔN33 were surface expressed only in the presence of SUR2B (*Figure 4.3d&e*). Permeabilisation revealed the presence of channel protein (*Figure 4.3d&e* right panel). The white pixels seen in the permeabilised images represent saturation of fluorescent signal.

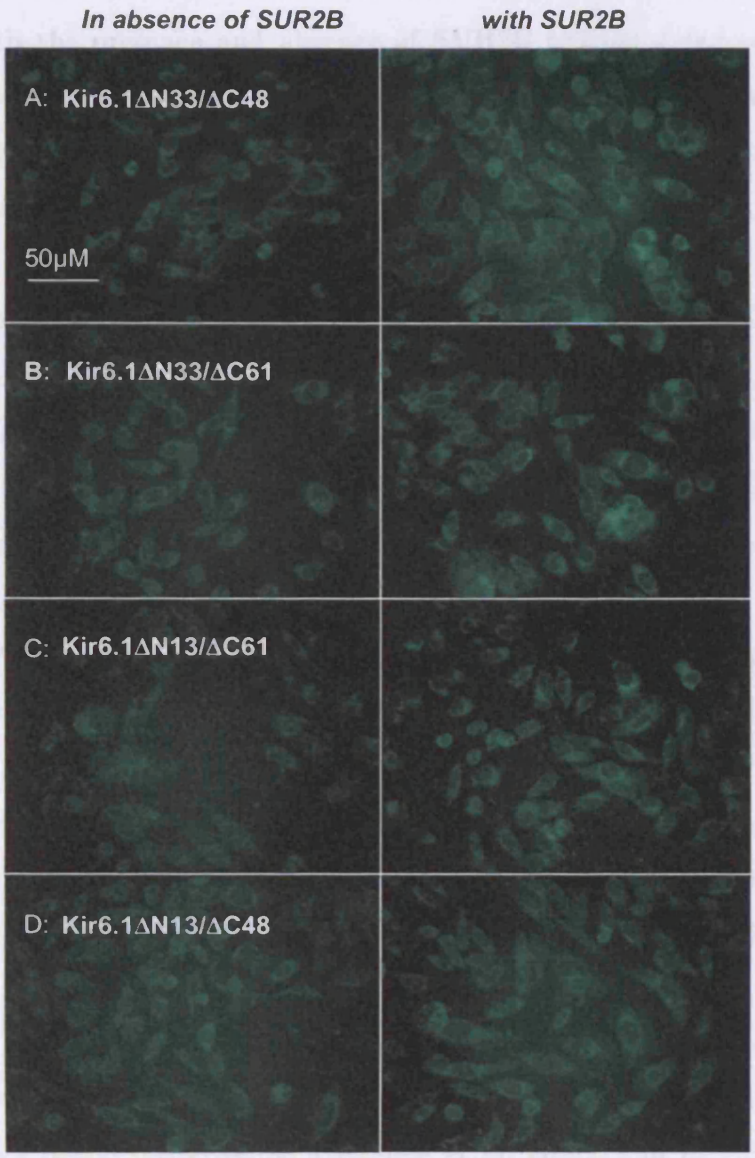

Figure 4.4: Surface staining of Kir6.1-HA N- and C-terminal deletion mutants in non-permeabilised cells, expressed with (left panel) and without (right panel) SUR2B. All images were captured at the same exposure (1 second) and magnification (400×), and were not subject to any other form of enhancement other than the addition of green pseudocolour when opened in Adobe Photoshop. The white scale bar represents 50μm.

All four double N- and C- terminus truncated mutants of Kir6.1 translocated to the cell surface in both the presence and absence of SUR2B (*Figure 4.4a,b,c&d*). It is also interesting to note that, despite the non-quantitative nature of this assay, the sulphonylurea receptor appears to increase surface expression of the Kir6.1 mutants that are able to traffic independently.

The results obtained in *Figures 4.3 & 4.4* were expected. In Kir6.1ΔN13 and Kir6.1ΔN33 the RKR motif is still present, therefore the channel is only surface expressed in the presence of SUR2B (whereby this motif is masked). Representative permeabilised images are shown for Kir6.1ΔN13 and Kir6.1ΔN33 to show that on rupture of the cell membrane reconstituted channel protein is detected, and hence that the blank images shown are not the result of failure of the transfection procedure. For all other Kir6.1 truncations the RKR motif is absent, hence the channel pore is expressed both in the presence and absence of SUR2B in non-permeabilised cells.

Before proceeding to look at the functionality of the various ΔN-Kir6.1-ΔC mutations, I have side-tracked slightly, and have discussed a recently published study in which this immunohistochemistry assay was applied (Muzyamba, Farzaneh et al. 2007).

Experiments were performed to support the localization observed in confocal microscopy studies of mutant Kir6.2/SUR1 complexes which result in congenital hyperinsulinism (CHI) (Muzyamba, Farzaneh et al. 2007), and to validate the assay and hence the data shown in the previous two figures.

Kir6.2 and SUR1 are encoded by the genes *ABCC8* and *KCNJ11* respectively, mutations in which lead to CHI (also known as Persistent Hyperinsulinaemic Hypoglycaemia of Infancy (PHHI) and formerly known as Nesidioblastosis)(Kane, Shepherd et al. 1996). Under normal circumstances, high levels of glucose in the cell result release of insulin from pancreatic ß-cells. However, ß-cells in individuals with CHI secrete insulin despite low blood glucose levels (Aguilar-Bryan and Bryan 1999;

Miki, Nagashima et al. 1999). It is thought that the β-cell is persistently depolarized because of abnormally modulated or absent K_{ATP} channels (Thomas, Cote et al. 1995; Dunne, Cosgrove et al. 2004). Mutations in SUR1 and Kir6.2 that lead to a loss of channel function have also been shown to be major causes of CHI (Sharma, Crane et al. 2000; Huopio, Shyng et al. 2002), and defective trafficking of channel protein is one mechanism whereby some SUR1 mutations lead to loss of channel function and consequently onset of this disease. SUR1 mutations that cause trafficking defects located within or downstream of NBD2 have been reported (Sharma, Crane et al. 1999; Cartier, Conti et al. 2001; Partridge, Beech et al. 2001; Taschenberger, Mougey et al. 2002), as have mutations located in the first transmembrane domain (TM0). The latter can be corrected by sulfonylureas, and the rescued channels are fully functional.

Previous studies of channel mutations that were isolated from patients and expressed in various systems, indicate that a majority of described mutations lead to nonfunctional channels, and that this is in part because the channel protein fails to traffic properly (Kane, Shepherd et al. 1996; Otonkoski, Ammala et al. 1999; Sharma, Crane et al. 1999; Partridge, Beech et al. 2001).

Recently, two patients were identified with complex DNA mutations. The first was homozygous for two mutations in SUR1, D1193V (TMD2) and R1436Q (located in NBD2) resulting in typical diffuse CHI and severe hyperinsulinism. A second patient had inherited two SUR1 mutations from his father, G228D (CL3) and D1471N (NBD2), and mutation V1572I (NBD2) from his mother, resulting in focal CHI. Hamster SUR1 and mouse Kir6.2 clones were used to introduce the desired mutations using the Stratagene QuikChange kit, since the lab has expertise in manipulating them. To mimic the fact that the patients had mutations on the same chromosome, the SUR1 mutations D1193V and R1436Q (SUR1 D1193V/R1436Q) and G228D and D1471 (SUR1 G228D/D1471N) were made in the same cDNA construct. These were engineered by Dr Muzyamba.

As part of a study to determine the consequences of DNA variations on K_{ATP} channel function, immunohistochemistry was performed on cells expressing the mutant channel protein to observe if there was any membrane delivery of the channel complex (Muzyamba, Farzaneh et al. 2007). The individual SUR1 mutants were expressed with mouse Kir6.2-HA (Kir6.2 with an extracellular antigenic haemagglutinin epitope tag engineered between the H5 segment and TMD1), which was a gift from Dr Jan (John. Monck et al. 1998; Zerangue, Schwappach et al. 1999).

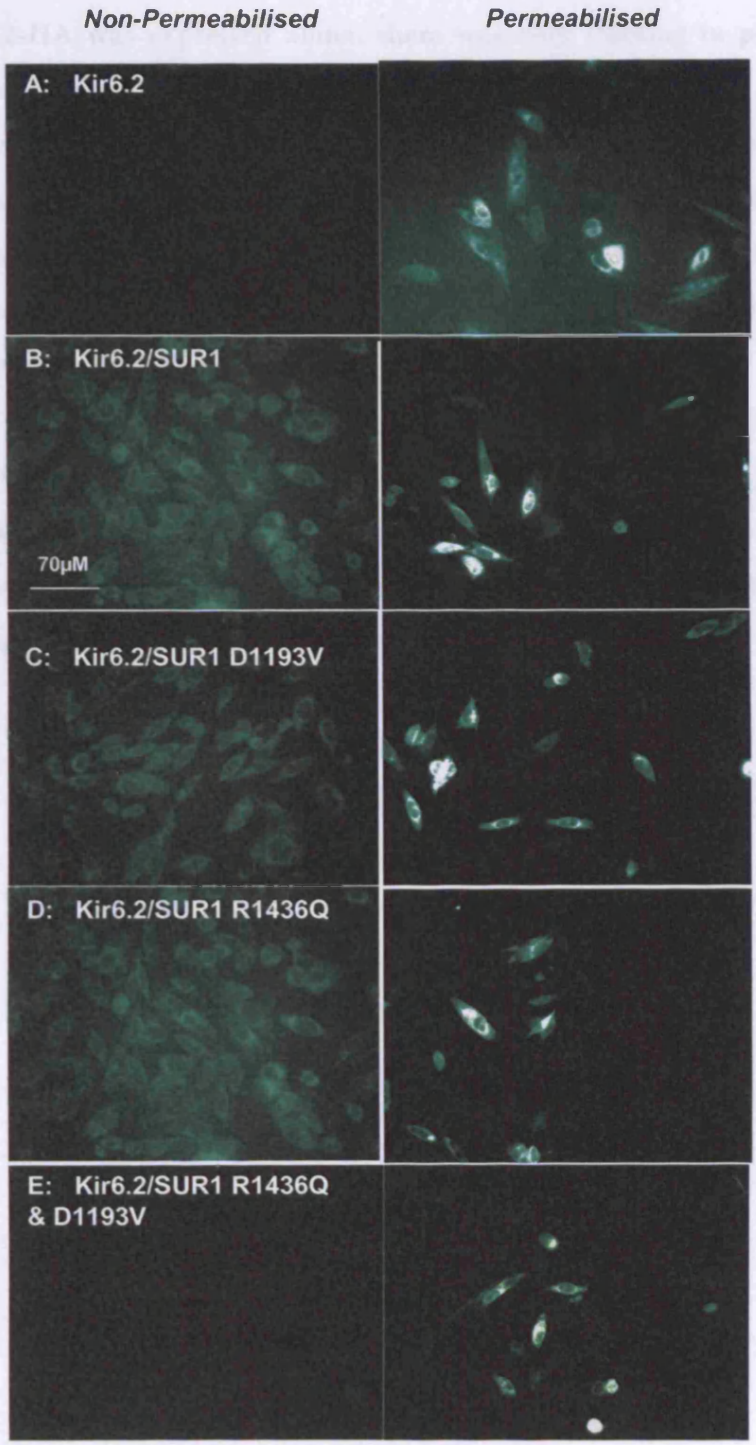

Figure 4.5: Surface staining of wild-type and mutant Kir6.2/SUR1 K_{ATP} channel complexes in permeabilised (left panel) and non-permeabilised (right panel) CHO-K1 cells (refer to methods). Mutations reside in SUR1 at R1436Q and D1193V, and are expressed alone or in combination. All images were captured at the same exposure (1 second) and magnification (400×), and were not subject to any other form of enhancement other than the addition of green pseudocolour when opened in Photoshop. The white scale bar represents 70μm.

When Kir6.2-HA was expressed alone, there was only staining in permeabilised cells (*Figure 4.5a*). However, when expressed with SUR1, there was staining in both permeabilised and non-permeabilised cells, indicating significant membrane delivery of the complex (*Figure 4.5b*). The single SUR1 D1193V and SUR1 R1436Q translocated Kir6.2-HA to the plasma membrane, as indicated by staining in non-permeabilised cells (*Figure 4.5c&d*). However, the double mutant failed to do so, as indicated by staining in permeabilised cells only (*Figure 4.5e*).

These observations confirmed the data obtained by confocal microscopy co-localization experiments, whereby SUR1 D1193V and SUR1 R1436Q translocated Kir6.2-GFP to the plasma membrane, whereas the double mutant failed to do so and Kir6.2-GFP was located intracellularly (Muzyamba, Farzaneh et al. 2007).

Figure 4.6: Surface staining of wild-type and mutant Kir6.2/SUR1 K_{ATP} channel complexes in permeabilised (left panel) and non-permeabilised (right panel) CHO-K1 cells. Mutations reside in SUR1 at G228D and D1471N (expressed alone or in combination) and at V15721. All images were captured at the same exposure (1 second) and magnification (400×), and were not subject to any other form of enhancement other than the addition of green pseudocolour when opened in Adobe Photoshop. The white scale bar represents 70μm.

SUR1 G228D, SUR1 D1471N and SUR1 G228D/D1471N all failed to translocate Kir6.2-HA to the cell surface (*Figure 4.6a,b&c*), whereas the coexpression of SUR1 VI572I with Kir6.2-HA led to staining in both permeabilised and non-permeabilised cells (*Figure 4.6d*).

Again, these observations are consistent with the co-localization experiments in which SUR1 G228D, SUR1 D1471N and SUR1 G228D/D1471N all failed to translocate Kir6.2-GFP to the plasma membrane, whereas SUR1 V1572I did (Muzyamba, Farzaneh et al. 2007).

It should be emphasized that the conditions used for permeabilization led to a number of cells detaching, which accounts for the lower apparent density seen with the permeabilised samples. Transfection efficiency was high in both permeabilised and non-permeabilised cell samples (~70%) as determined by parallel transfection of the reconstituted channel DNA with GFP. Since the results from this assay and the confocal microscopy studies were consistent (Muzyamba, Farzaneh et al. 2007), it was deemed to be a valid method of monitoring surface expression of channel complexes.

Since I was confident that truncation of the C-terminus of Kir6.1 removed the RKR motif, allowing it to be expressed independently of SUR2B, the previously described N- and C-terminal truncation mutants were initially expressed with SUR2B, and channel functionality tested with the $^{86}Rb^{+}$ flux assay.

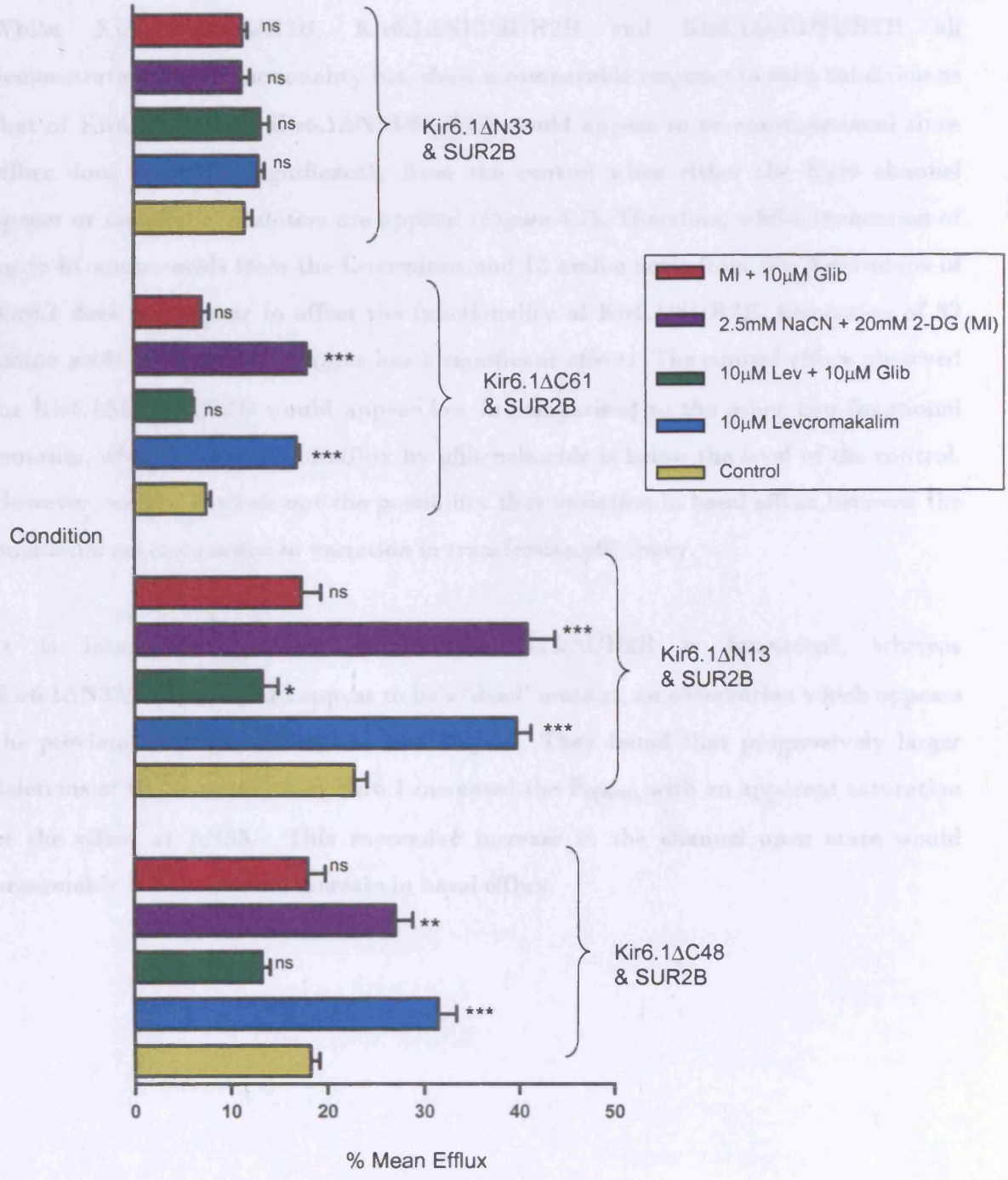

Figure 4.7: The effect of truncation of either the N or C terminus of Kir6.1 on the function of the Kir6.1/SUR2B as shown by $^{86}Rb^{+}$ efflux. Efflux was measured 15 minutes after the addition of drugs, and was calculated as % efflux of initial $^{86}Rb^{+}$ content. The control represents DMSO diluted in HBS. Data are shown as +/- SEM, whereby n=9. *** P<0.001 compared to control, ** P=0.001-0.01 compared to control, * P=0.01-0.05 compared to control, (ns) P>0.05 compared to control.

Whilst Kir6.1ΔC48/SUR2B, Kir6.1ΔN13/SUR2B and Kir6.1ΔC61/SUR2B all demonstrate normal functionality (i.e. show a comparable response to each condition as that of Kir6.1/SUR2B), Kir6.1ΔN33/SUR2B would appear to be non-functional since efflux does not differ significantly from the control when either the K_{ATP} channel opener or metabolic inhibitors are applied (*Figure 4.7*). Therefore, whilst truncation of up to 61 amino acids from the C-terminus and 13 amino acids from the N-terminus of Kir6.1 does not appear to affect the functionality of Kir6.1/SUR2B, truncation of 33 amino acids from the N-terminus has a significant effect. The control efflux observed for Kir6.1ΔC61/SUR2B would appear low in comparison to the other two functional mutants, whereby reversal of efflux by glibenclamide is below the level of the control. However, we can not rule out the possibility that variation in basal efflux between the functional mutants is due to variation in transfection efficiency.

It is interesting to note that Kir6.1ΔN13/SUR2B is functional, whereas Kir6.1ΔN33/SUR2B would appear to be a 'dead' mutant, an observation which opposes the previous findings of Babenko and Bryan. They found that progressively larger deletions of the N-terminus of Kir6.1 increased the $P_{0(max)}$, with an apparent saturation of the effect at ΔN33. This successive increase in the channel open state would presumably infer a gradual increase in basal efflux.

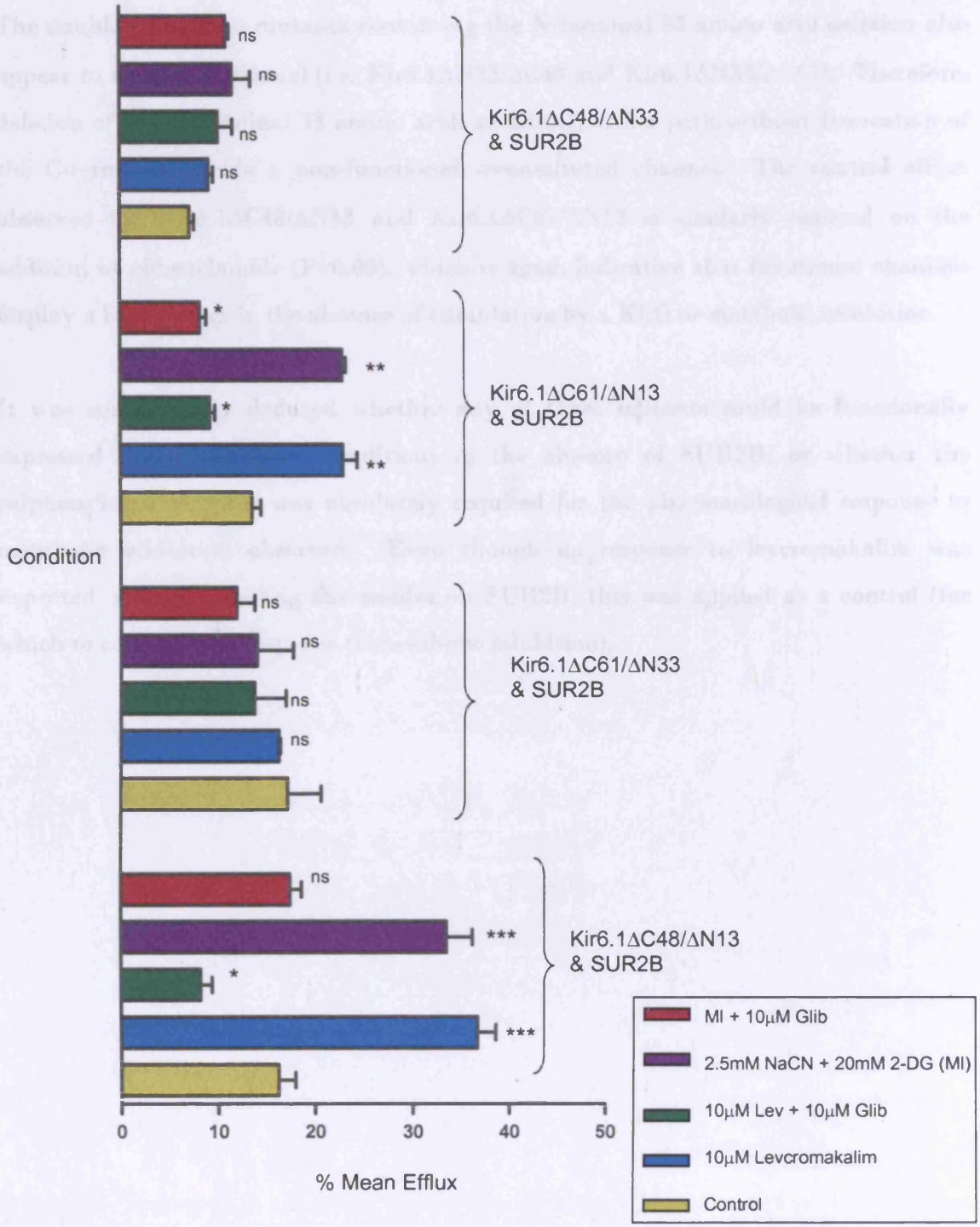

Figure 4.8: The effect of truncation of both the C&N terminus of Kir6.1 on the function of the Kir6.1/SUR2B as shown by $^{86}Rb^{+}$ efflux. Efflux was measured 15 minutes after the addition of drugs, and was calculated as % efflux of initial $^{86}Rb^{+}$ content. The control represents DMSO diluted in HBS. The data represent means +/- SEM for three different experiments performed in triplicate (n=9). *** P<0.001 compared to control, ** P=0.001-0.01 compared to control, * P=0.01-0.05 compared to control, (ns) P>0.05 compared to control.

The double truncation mutants containing the N-terminal 33 amino acid deletion also appear to be non-functional (i.e. Kir6.1ΔN33/ΔC48 and Kir6.1ΔN33/ΔC61). Therefore, deletion of the N-terminal 33 amino acids of Kir6.1, either with/without truncation of the C-terminus, yields a non-functional reconstituted channel. The control efflux observed for Kir6.1ΔC48/ΔN13 and Kir6.1ΔC61/ΔN13 is similarly reduced on the addition of glibenclamide ($P<0.05$), which is again indicative that functional channels display a basal efflux in the absence of stimulation by a KCO or metabolic inhibition.

It was subsequently deduced whether any of these mutants could be functionally expressed under the same conditions in the absence of SUR2B, or whether the sulphonylurea receptor was absolutely required for the pharmacological response to metabolic inhibition observed. Even though no response to levcromakalim was expected, since its binding site resides on SUR2B, this was applied as a control (for which to compare the response to metabolic inhibition).

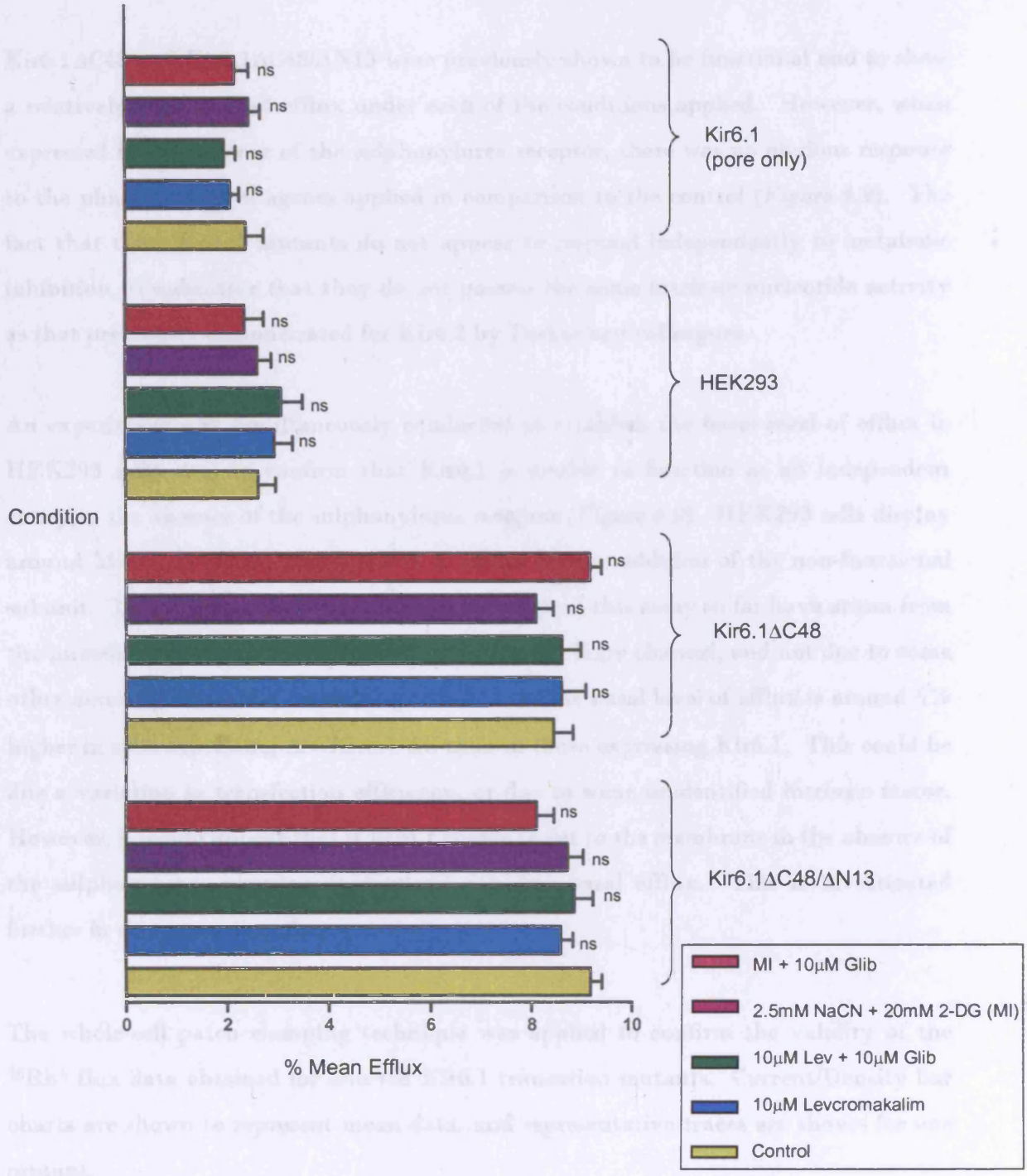

Figure 4.9: Deduction of the functionality of Kir6.1ΔC48/ΔN13 and Kir6.1ΔC48 expressed in HEK293 minus the sulphonylurea receptor. Efflux is also compared with that in untransfected HEK293 cells and cells transfected with Kir6.1, whereby the same conditions were applied to elicit a response. Efflux was measured 15 minutes after the addition of drugs, and was calculated as % efflux of initial $^{86}Rb^{+}$ content. The control represents DMSO diluted in HBS. The data represent means +/- SEM for three different experiments performed in triplicate (n=9).

Kir6.1ΔC48 and Kir6.1ΔC48/ΔN13 were previously shown to be functional and to show a relatively high level of efflux under each of the conditions applied. However, when expressed in the absence of the sulphonylurea receptor, there was no obvious response to the pharmacological agents applied in comparison to the control (*Figure 4.9*). The fact that these Kir6.1 mutants do not appear to respond independently to metabolic inhibition, is indicative that they do not possess the same intrinsic nucleotide activity as that previously demonstrated for Kir6.2 by Tucker and colleagues.

An experiment was simultaneously conducted to establish the basal level of efflux in HEK293 cells, and to confirm that Kir6.1 is unable to function as an independent entity in the absence of the sulphonylurea receptor (*Figure 4.9*). HEK293 cells display around 3% basal efflux, which is not amplified on the addition of the non-functional subunit. This suggests that the results obtained from this assay so far have arisen from the introduction of recombinant DNA encoding the K_{ATP} channel, and not due to some other anomaly. It is also interesting to note that the basal level of efflux is around 6% higher in cells expressing ΔN-Kir6.1-ΔC than in those expressing Kir6.1. This could be due a variation in transfection efficiency, or due to some unidentified intrinsic factor. However, it would appear that if Kir6.1 is able to get to the membrane in the absence of the sulphonylurea receptor, it displays a higher basal efflux. This is investigated further in the proceeding chapter.

The whole-cell patch clamping technique was applied to confirm the validity of the $^{86}Rb^{+}$ flux data obtained for selected Kir6.1 truncation mutants. Current/Density bar charts are shown to represent mean data, and representative traces are shown for one mutant.

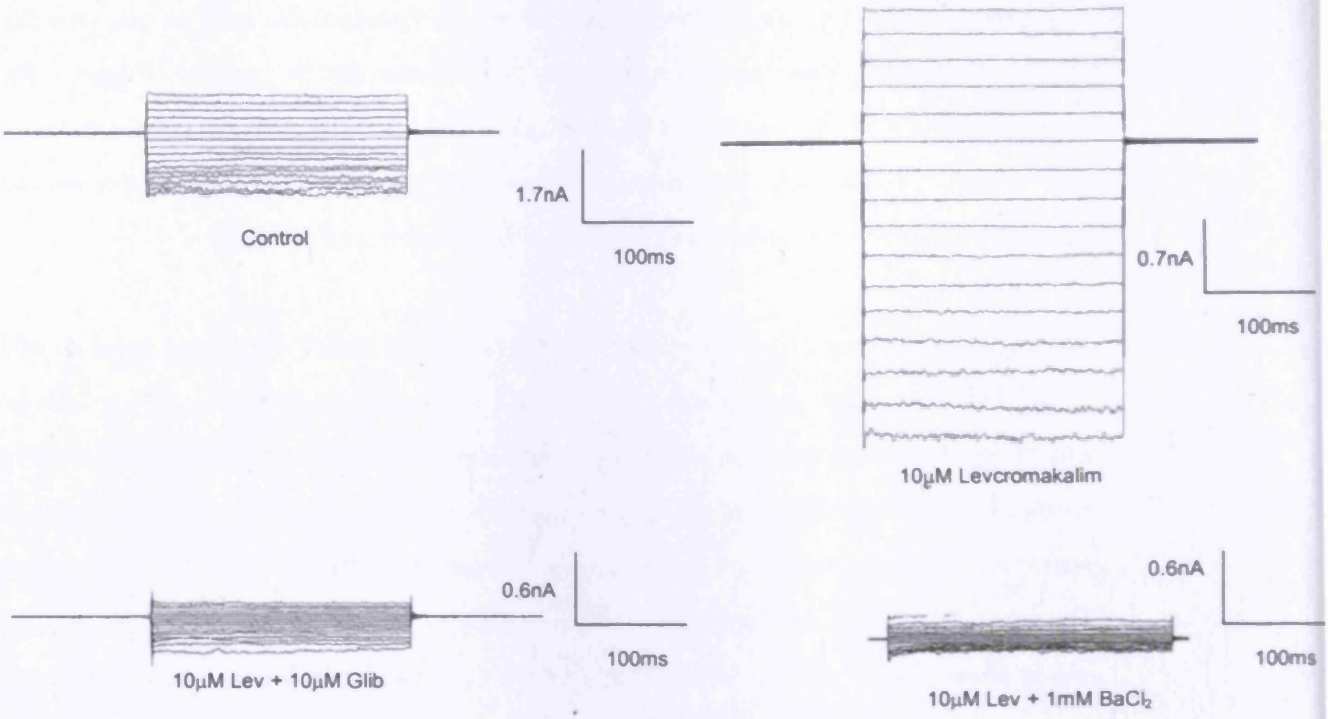
1.7nA
100ms
Control
0.7nA
100ms
10μM Levcromakalim
0.6nA
100ms
10μM Lev + 10μM Glib
0.6nA
100ms
10μM Lev + 1mM BaCl2

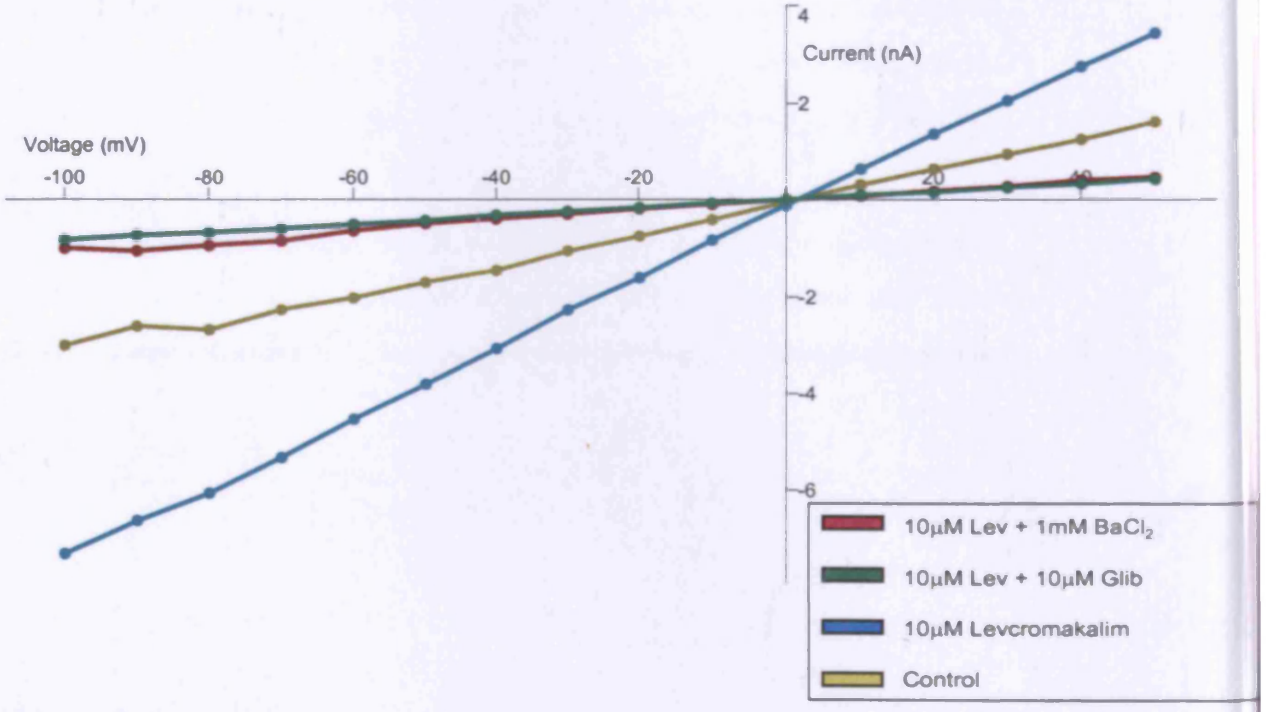
Current (nA)
Voltage (mV)
-100
-80
-60
-40
-20
20
40
4
2
-2
-4
-6
10μM Lev + 1mM BaCl2
10μM Lev + 10μM Glib
10μM Levcromakalim
Control

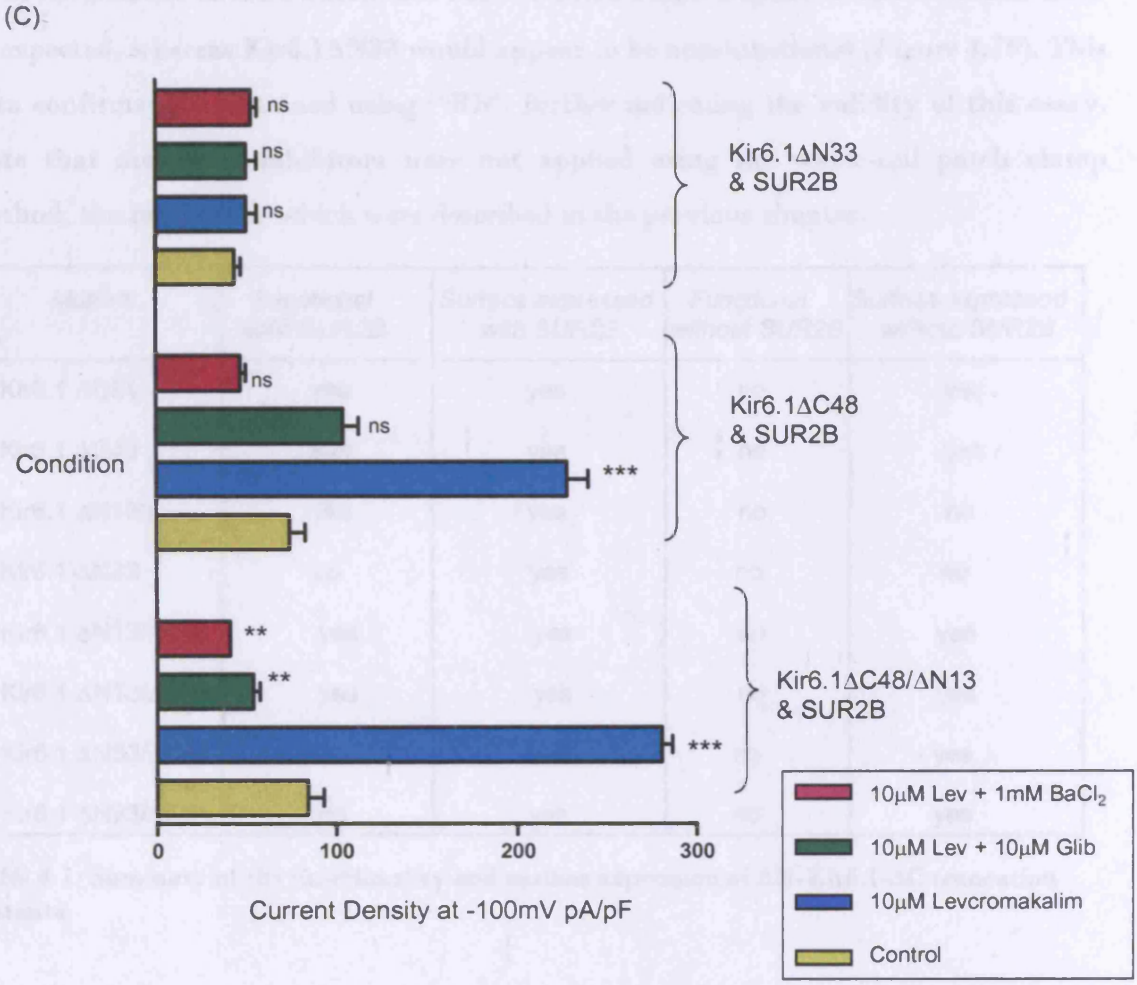

Figure 4.10: Data to represent patch clamp recordings obtained from HEK293 cells transiently transfected with Kir6.1ΔC48/ΔN13 & SUR2B, Kir6.1ΔC48 & SUR2B and Kir6.1ΔN33 & SUR2B. Voltage clamp recordings were obtained under symmetrical K^+ conditions, and were evoked during 200ms voltage steps between -100mV and +50mV in 10mV increments from a holding potential of 0mV (A) Representative traces for each of the conditions for Kir6.1ΔC48. Traces are shown for the control current (external solution with DMSO), 10μM levcromakalim, 10μM levcromakalim and 10μM glibenclamide and 10μM levcromakalim with 1mM $BaCl_2$ (B) Representative I/V traces (pA/pF) for Kir6.1ΔC48 under each condition, whereby each trace crosses the holding potential at 0mV (C) Current/Density bar chart to represent mean data for the response of Kir6.1ΔC48 & SUR2B, Kir6.1ΔC48/ΔN13 & SUR2B and Kir6.1ΔN33 & SUR2B to the applied KCO and KCBs. The data represent means +/- SEM (n=6) *** P<0.001 compared to control, ** P=0.001-0.01 compared to control, (ns) P>0.05 compared to control.

Both Kir6.1ΔC48/ΔN13/SUR2B and Kir6.1ΔC48/SUR2B respond to the KCO and KCB as expected, whereas Kir6.1ΔN33 would appear to be non-functional (*Figure 4.10*). This data confirms that obtained using $^{86}Rb^{+}$, further indicating the validity of this assay. Note that metabolic inhibitors were not applied using the whole-cell patch clamp method, the reasons for which were described in the previous chapter.

Mutant	*Functional with SUR2B*	*Surface expressed with SUR2B*	*Functional without SUR2B*	*Surface expressed without SUR2B*
Kir6.1 ΔC61	yes	yes	no	yes
Kir6.1 ΔC48	yes	yes	no	yes
Kir6.1 ΔN13	yes	yes	no	no
Kir6.1 ΔN33	no	yes	no	no
Kir6.1 ΔN13/ΔC48	yes	yes	no	yes
Kir6.1 ΔN13/ΔC61	yes	yes	no	yes
Kir6.1 ΔN33/ΔC48	no	yes	no	yes
Kir6.1 ΔN33/ΔC61	no	yes	no	yes

Table 4.1: Summary of the functionality and surface expression of ΔN-Kir6.1-ΔC truncation mutants

The table summarizes the key findings obtained from the Kir6.1 truncation mutants. All were surface expressed in the presence of SUR2B. Those that were surface expressed in the absence of the sulphonylurea receptor and functional in its presence were Kir6.1ΔC61, Kir6.1ΔC48, Kir6.1ΔC48/ΔN13 and Kir6.1ΔC61/ΔN13. Kir6.1ΔC48 and Kir6.1ΔC48/ΔN13 were unable to function independently, suggesting a lack of intrinsic ATP sensitivity. However, since they demonstrated increased basal activity, their pharmacology was subsequently investigated using the K_{ATP} channel pore blockers $BaCl_2$ and PNU-37883A. In fact, the latter proved to be a useful tool to study metabolic regulation of the K_{ATP} channel, this being the focus of the next chapter.

Chapter Five

The application of K_{ATP} channel inhibitors to infer the role of the pore-forming subunit in channel regulation under metabolic inhibition

Chapter Five: Results

The application of K_{ATP} channel inhibitors to infer the role of the pore-forming subunit in channel regulation under metabolic inhibition

PNU-37883A is a novel non-sulphonylurea K_{ATP} channel inhibitor, which although was originally developed on the basis of its weak diuretic effects, showed some selectivity for the vascular K_{ATP} channel (Humphrey, Smith et al. 1996). Early experiments in rat mesenteric artery showed that PNU-37883A inhibited blood vessel relaxation induced by KCOs (Meisheri, Humphrey et al. 1993), and *in vitro* experiments showed that it significantly reversed hypotension produced by cromakalim, pinacidil and minoxidil in rats, cats and dogs (Meisheri, Humphrey et al. 1993). Furthermore, electrophysiological experiments demonstrated that even though PNU-37883A was not able to inhibit current in cardiac and skeletal myocytes, it was able to selectively inhibit K_{ATP} currents activated by levcromakalim in single smooth muscle cells isolated from rat mesenteric artery (Wellman, Barrett-Jolley et al. 1999).

Subsequent experiments were designed to more directly address the issue of the site of action of PNU-37883A (Cui, Tinker et al. 2003), whereby its effects on four types of cloned K_{ATP} channels stably expressed in the HEK-293 cell line were investigated via the whole-cell configuration of the patch-clamp technique. Its effect on the current generated by Kir6.2ΔC26 was also examined. Inhibition of the putative smooth muscle clones Kir6.1/SUR2B and Kir6.2/SUR2B (IC_{50} 6μM and 15μM respectively) was significantly greater than inhibition with either the pancreatic or β cell or cardiac clones, whereby the SUR receptor affects drug binding to the pore. PNU-37883A inhibited currents generated by expressing Kir6.2ΔC26 alone (IC_{50} 5μM), but when expressed with SUR2B this was increased to 38μM. These findings are further confirmation that PNU-37883A has a degree of vascular sensitivity, providing evidence for a heteromeric channel structure, with the channel pore composed of Kir6.1 and Kir6.2 subunits (Teramoto 2003).

PNU-37883A was therefore deemed as a useful means of investigating the functionality of the ΔN-Kir6.1-ΔC mutants generated, particularly the basal efflux observed in Chapter 4 (*Figure 4.9*) when expressed in HEK293 cells. A dose-response experiment was initially conducted on HEK293 cells stably expressing Kir6.1/SUR2B using the $^{86}Rb^{+}$ flux assay. PNU-37883A had not been applied in this setting before, and it was necessary to determine the dose required to significantly reduce channel efflux, whereby efflux was induced by 10μm levcromakalim.

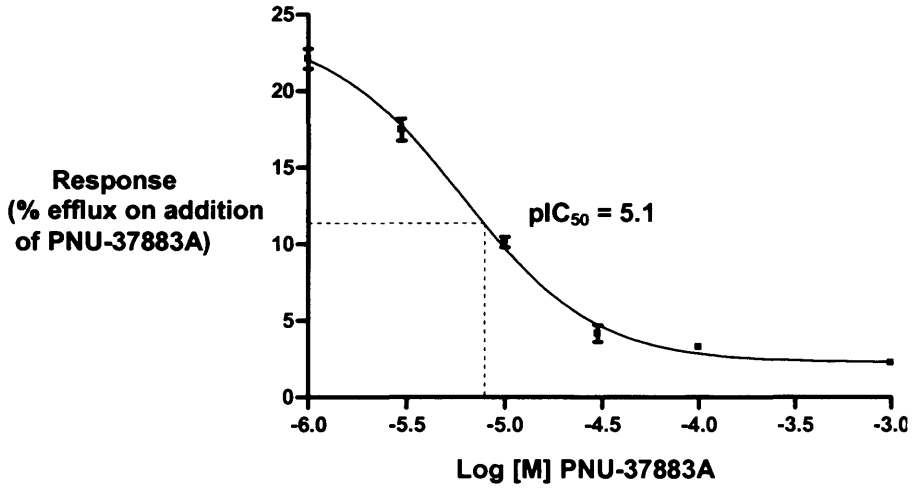

Figure 5.1: Dose response curve to determine concentration at which the potassium channel inhibitor, PNU-37883A, results in maximal inhibition of Kir6.1 conductance. Efflux was induced by the application of the KCO levcromakalim (10μM). $^{86}Rb^{+}$ efflux, plotted as a percentage efflux on application of PNU-37883A, was measured 15 minutes after the addition of 1μM, 3μM, 10μM, 30μM, 100μM and 1mM respectively to HEK293 cells stably transfected with Kir6.1/SUR2B. Data are shown as +/- SEM, whereby (n) = 9 and $pIC_{50} = 5.1$

The % initial efflux observed on the application of the KCO was approximately 22%, and is comparable with previous data (*Figure 3.2*). Maximal inhibition of mean Kir6.1/SUR2B efflux was seen after the addition of 100μM PNU-37883A (hence this was the applied dose in subsequent experiments), whereby the drug potency was determined via the IC_{50} value for current inhibition (~10μM). This is similar to the IC_{50} of PNU-37883A inhibition on the Kir6.2/SUR2B and Kir6.1/SUR2B cell lines previously determined via patch clamping (Cui, Tinker et al. 2003). $BaCl_2$ also interacts

with the pore-forming subunits, but shows less selectivity between the K_{ATP} channel subtypes. 1mM $BaCl_2$ was applied since this pore-forming subunit inhibitor has been in wide use in a number of different systems, and it has previously been shown by a former member of the lab, Quinn KV, that this is an optimal concentration to efficiently block the K_{ATP} channel current in the whole-cell patch clamp mode at a hyperpolarised potential. $BaCl_2$ is less potent in comparison with glibenclamide in blocking K_{ATP} channels and a relatively high concentration is required for significant blocking (Nelson and Quayle 1995). Barium block of Kir currents increases with membrane hyperpolarisation. On increasing the membrane to a more hyperpolarised voltage in the presence of barium, the increase in block by barium occurs over several hundred milliseconds (Quayle, McCarron et al. 1993). It is thought that barium binds to a site in the pore to prevent K^+ movement through the channel. Assuming that the binding site lies within the membrane voltage field, membrane hyperpolarisation will favour binding of positively charged ions to the site. The simplest explanation is that the barium binding site lies within the channel pore (Quayle, McCarron et al. 1993).

Based on the evidence discussed, both barium chloride and PNU-37883A were applied to ΔN-Kir6.1-ΔC to determine if any basal current observed via efflux could be reversed.

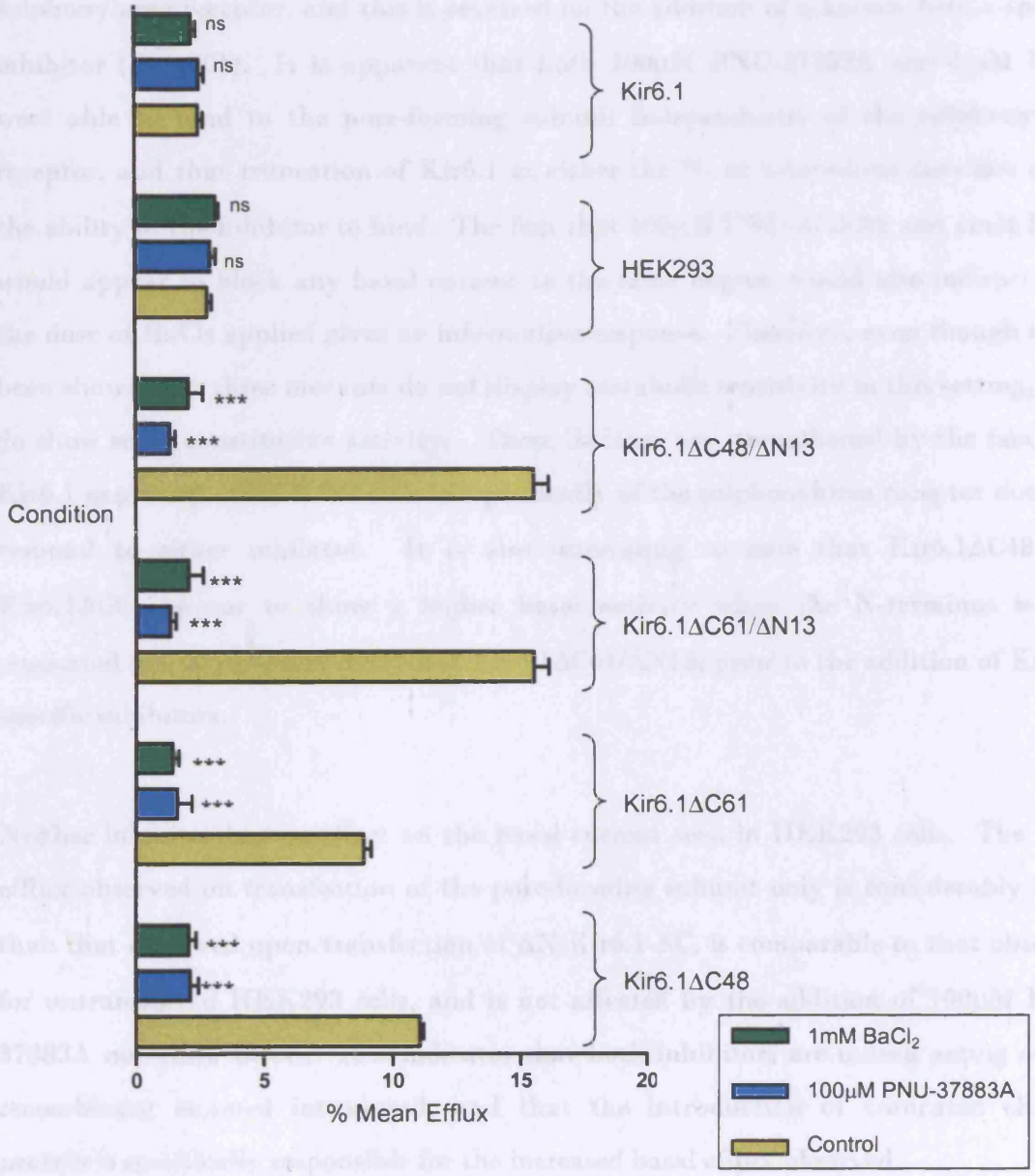

Figure 5.2: Effect of potassium channel inhibitors on HEK293 cells transfected with Kir6.1 truncated mutants. These are compared with experiments to establish the effect of 100μM PNU-37883A and 1mM $BaCl_2$ on the basal flux in untransfected HEK293 cells, and cells transfected with Kir6.1. Mean $^{86}Rb^+$ efflux of HEK293 cells transiently transfected with Kir6.1 or ΔN-Kir6.1-ΔC terminal truncated mutants (minus sulphonylurea receptor) 15 minutes after addition of drugs. Efflux was calculated as % efflux of initial $^{86}Rb^+$ content. The control represents DMSO diluted in HBS. Data are shown as +/- SEM, whereby n = 9. *** $P<0.001$ compared to control, (ns) $P>0.05$ compared to control.

All four truncation mutants display basal activity when expressed in the absence of the sulphonylurea receptor, and this is reversed on the addition of a known Kir6.*x*-specific inhibitor ($P<0.001$). It is apparent that both 100μM PNU-37883A and 1mM $BaCl_2$ were able to bind to the pore-forming subunit independently of the sulphonylurea receptor, and that truncation of Kir6.1 at either the N- or C-terminus does not affect the ability of the inhibitor to bind. The fact that 100μM PNU-37883A and 1mM $BaCl_2$ would appear to block any basal current to the same degree, would also indicate that the dose of $BaCl_2$ applied gives an informative response. Therefore, even though it has been shown that these mutants do not display metabolic sensitivity in this setting, they do show some constitutive activity. These findings are strengthened by the fact that Kir6.1 expressed in HEK293 cells independently of the sulphonylurea receptor does not respond to either inhibitor. It is also interesting to note that Kir6.1ΔC48 and Kir6.1ΔC61 appear to show a higher basal activity when the N-terminus is also truncated (i.e. Kir6.1ΔC48/ΔN13 and Kir6.1ΔC61/ΔN13) prior to the addition of Kir6.*x*-specific inhibitors.

Neither inhibitor has an effect on the basal current seen in HEK293 cells. The basal efflux observed on transfection of the pore-forming subunit only is considerably lower than that observed upon transfection of ΔN-Kir6.1-ΔC, is comparable to that observed for untransfected HEK293 cells, and is not affected by the addition of 100μM PNU-37883A nor 1mM $BaCl_2$. This indicates that both inhibitors are indeed acting on the recombinant channel introduced, and that the introduction of truncated channel protein is specifically responsible for the increased basal efflux observed.

Both Kir6.1ΔC48 and Kir6.1ΔC48/ΔN13 were subsequently expressed with SUR2B, and the ability of PNU-37883A and $BaCl_2$ to reverse efflux observed on the addition of KCO and metabolic inhibitors deduced. It was interesting to determine whether a pore blocker could substitute for 10μM glibenclamide, which acts on the sulphonylurea receptor, to produce the result observed in *Figures 4.7 and 4.8*. Since it has also been

shown that the potency of PNU-37883A was seven-fold greater on Kir6.2ΔC26 than Kir6.2ΔC26/SUR2B, it was also of interest to determine whether the sulphonylurea receptor could modulate the response of ΔN-Kir6.1-ΔC.

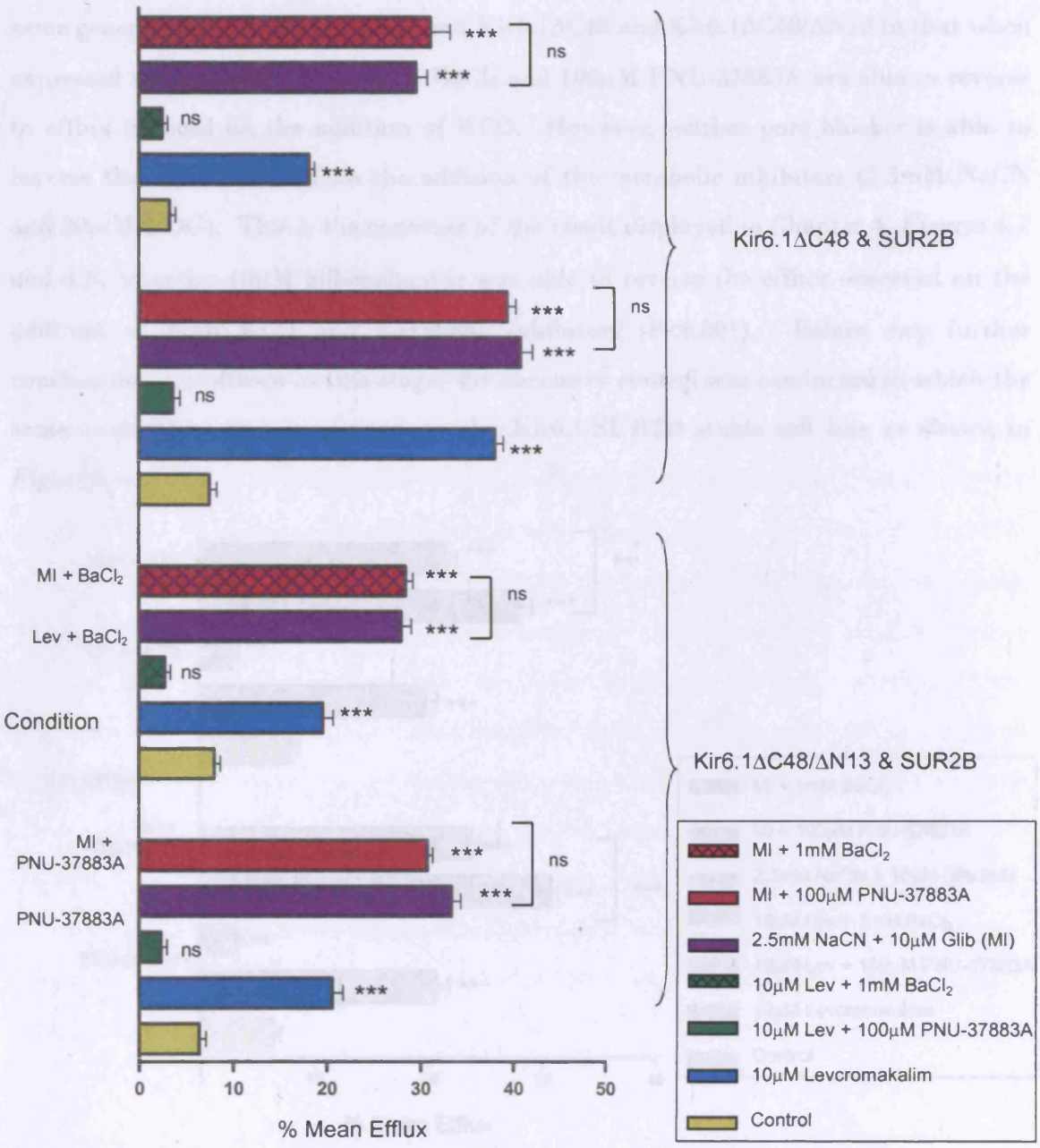

Figure 5.3: Effect of potassium channel blockers on ΔN-Kir6.1-ΔC truncation mutants expressed with SUR2B. Mean $^{86}Rb^{+}$ efflux of HEK293 cells transiently transfected with either Kir6.1ΔC48/SUR2B or Kir6.1ΔC48/ΔN13/SUR2B measured 15 minutes after addition of drugs. The efflux was calculated as % efflux of initial $^{86}Rb^{+}$ content. The control represents DMSO diluted in HBS. Data are shown as +/- SEM, whereby n = 9. *** P<0.001 compared to control, ** P 0.001-0.01compared to control, (ns) P>0.05 compared to control. The ability of both PNU-37883A and $BaCl_2$ to reverse the efflux observed on metabolic inhibition of the channel are also directly compared.

The result displayed in *Figure 5.3* is very interesting, and somewhat unexpected. The same general result is observed for both Kir6.1ΔC48 and Kir6.1ΔC48/ΔN13 in that when expressed with SUR2B, both 1mM $BaCl_2$ and 100μM PNU-37883A are able to reverse to efflux induced on the addition of KCO. However, neither pore blocker is able to reverse the efflux induced on the addition of the metabolic inhibitors (2.5mM NaCN and 20mM 2-DG). This is the converse of the result displayed in Chapter 4, *Figures 4.7 and 4.8*, whereby 10μM glibenclamide was able to reverse the efflux observed on the addition of both KCO and metabolic inhibitors ($P<0.001$). Before any further conclusions were drawn as this stage, the necessary control was conducted in which the same experiment was conducted on the Kir6.1/SUR2B stable cell line as shown in *Figure 5.4*.

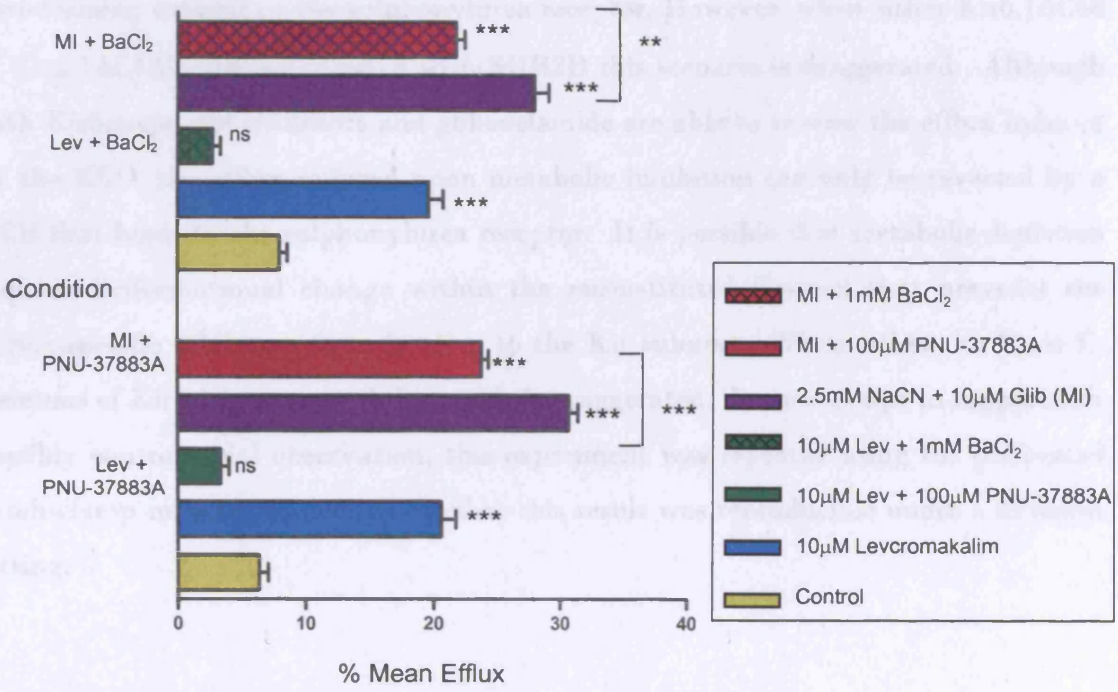

Figure 5.4: Effect of potassium channel inhibitors on the Kir6.1/SUR2B stable cell line. The ability 100μM PNU-37883A and 1mM $BaCl_2$ to reverse the efflux previously shown to be induced with a KCO and metabolic inhibitors was investigated. Mean $^{86}Rb^+$ efflux was measured 15 minutes after addition of drugs. Efflux was calculated as % efflux of initial $^{86}Rb^+$ content. The control represents DMSO diluted in HBS. Data are shown as +/- SEM, whereby n = 9. *** $P<0.001$ compared to control, (ns) $P>0.05$ compared to control. The ability of both PNU-37883A and $BaCl_2$ to reverse the efflux observed on metabolic inhibition of the channel are also directly compared.

The application of 100μM PNU-37883A and 1mM $BaCl_2$ reduced the efflux observed on the addition of KCO to the Kir6.1/SUR2B stable cell line to a similar extent as that observed for glibenclamide. Neither the application of 100μM PNU-37883A nor 1mM $BaCl_2$ showed a reduction of efflux induced by the addition of metabolic inhibitors to a similar extent as that observed for glibenclamide (*Figure 3.2*). Therefore, when the cloned equivalent of the vascular K_{ATP} channel, Kir6.1/SUR2B, is expressed in HEK293 cells the increase in efflux (compared to the basal level observed) induced by both the KCO and metabolic inhibitors is reversed by both glibenclamide, but to a lesser degree via inhibitors that bind to the pore-forming subunit (there appears to be around a 20% reduction). Therefore, the degree of reversal of efflux induced via metabolic inhibition depends on where the inhibitor binds to the K_{ATP} channel, i.e. the pore-forming subunit or the sulphonylurea receptor. However, when either Kir6.1ΔC48 or Kir6.1ΔC48/ΔN13 is expressed with SUR2B this scenario is exaggerated. Although both Kir6.*x*-specific inhibitors and glibenclamide are able to reverse the efflux induced by the KCO, the efflux induced upon metabolic inhibition can only be reversed by a KCB that binds to the sulphonylurea receptor. It is possible that metabolic depletion induces conformational change within the reconstituted channel that prevents the Kir6.*x*-specific inhibitors from binding to the Kir subunit. When either the N- or C-terminus of Kir6.1 is truncated this result is exaggerated. In an attempt to support this possibly controversial observation, this experiment was repeated using the perforated patch-clamp method, to deduce whether this result was reproducible under a different setting.

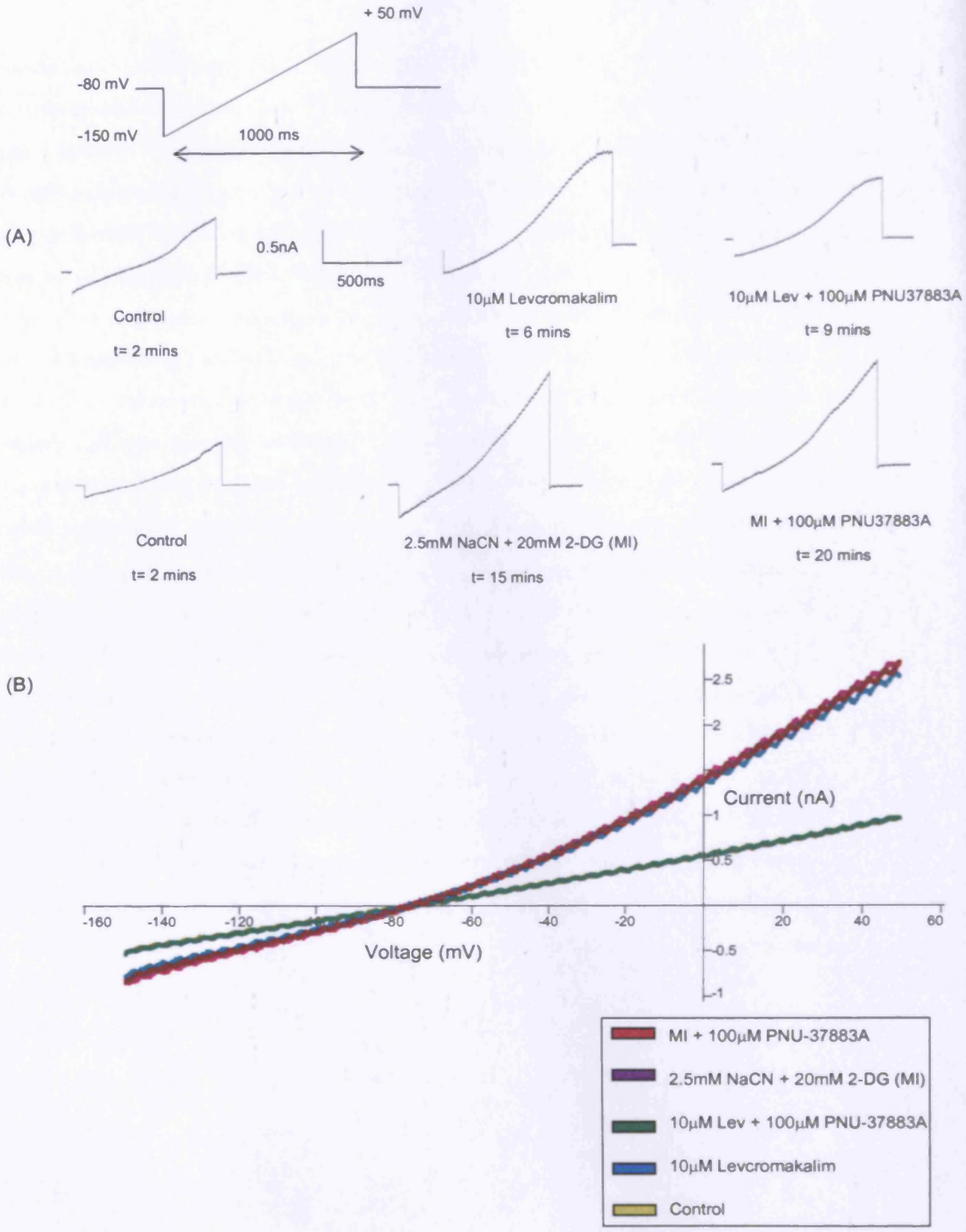
(A)
+ 50 mV
-80 mV
-150 mV
1000 ms
0.5nA
500ms
Control
t= 2 mins
10μM Levcromakalim
t= 6 mins
10μM Lev + 100μM PNU37883A
t= 9 mins
Control
t= 2 mins
2.5mM NaCN + 20mM 2-DG (MI)
t= 15 mins
MI + 100μM PNU37883A
t= 20 mins
(B)
Current (nA)
Voltage (mV)
-160
-140
-120
-80
-60
-40
-20
20
40
60
2.5
2
1
0.5
-0.5
-1
MI + 100μM PNU-37883A
2.5mM NaCN + 20mM 2-DG (MI)
10μM Lev + 100μM PNU-37883A
10μM Levcromakalim
Control

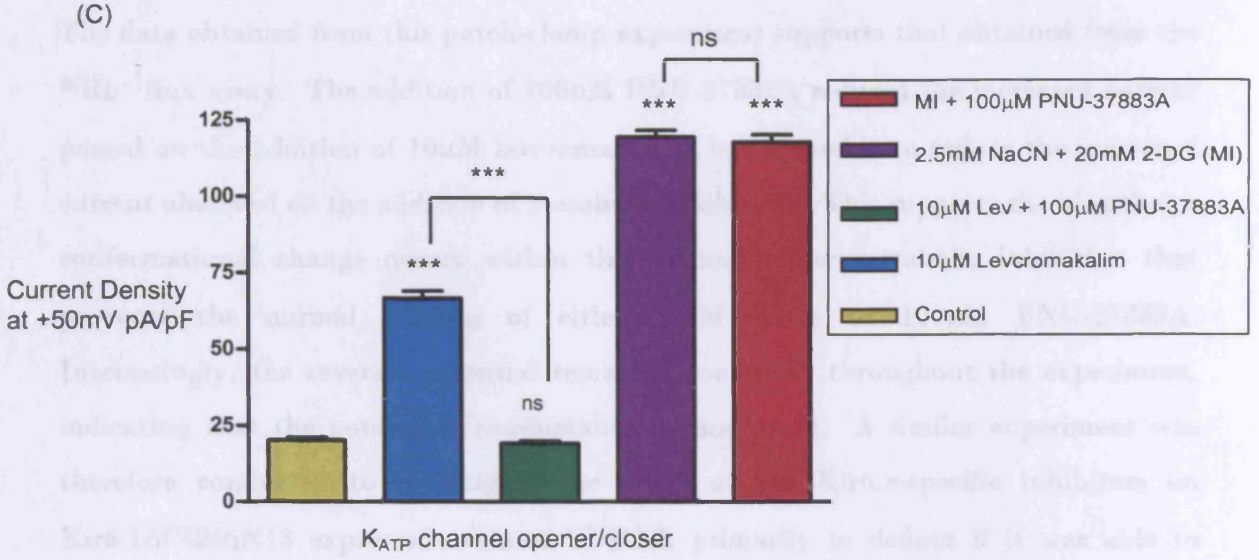

Figure 5.5: The effect of the K_{ATP} channel inhibitor PNU-37883A on the reconstituted channel Kir6.1ΔC48/ΔN13/SUR2B in the presence of a KCO and metabolic inhibitors, as demonstrated by the perforated patch-clamp method. Currents were evoked via voltage clamp recordings over 1000ms voltage steps between -150mV and +50mV from a holding potential of -80mV, with 15s between sweep starts. (A) Representative traces for each of the conditions: external solution with DMSO, 10μM Levcromakalim, 10μM Levcromakalim with 100μM PNU-37883A, metabolic inhibitors (2.5mM NaCN and 20mM 2-DG) and metabolic inhibitors with 100μM PNU-37883A. The time taken to achieve a response in relation to the control is given (note that glibenclamide was flushed out before the addition of metabolic inhibitors). (B) Representative I/V traces for each of the conditions (pA/pF), whereby each trace crosses the holding potential at -80mV. (C) Current/Density bar chart to represent mean data of the reconstituted channel currents under each condition *** $P<0.001$ compared to control, (ns) implies $P>0.05$ compared to control (n=6). The ability of PNU-37883A to reverse the efflux observed on the addition of metabolic inhibitors and KCO of the channel are also directly compared.

The data obtained from this patch-clamp experiment supports that obtained from the $^{86}Rb^{+}$ flux assay. The addition of 100μM PNU-37883A reduced the increased current passed on the addition of 10μM levcromakalim, but is unable to reduce the increased current observed on the addition of metabolic inhibitors. This supports the idea that a conformational change occurs within the channel under metabolic inhibition that prevents the normal binding of either 1mM $BaCl_2$ or 100μM PNU-37883A. Interestingly, the reversal potential remained consistent throughout the experiment, indicating that the potassium conductance is unaffected. A similar experiment was therefore conducted to investigate the effect of the Kir6.*x*-specific inhibitors on Kir6.1ΔC48/ΔN13 expressed without SUR2B, primarily to deduce if it was able to reduce any basal current observed.

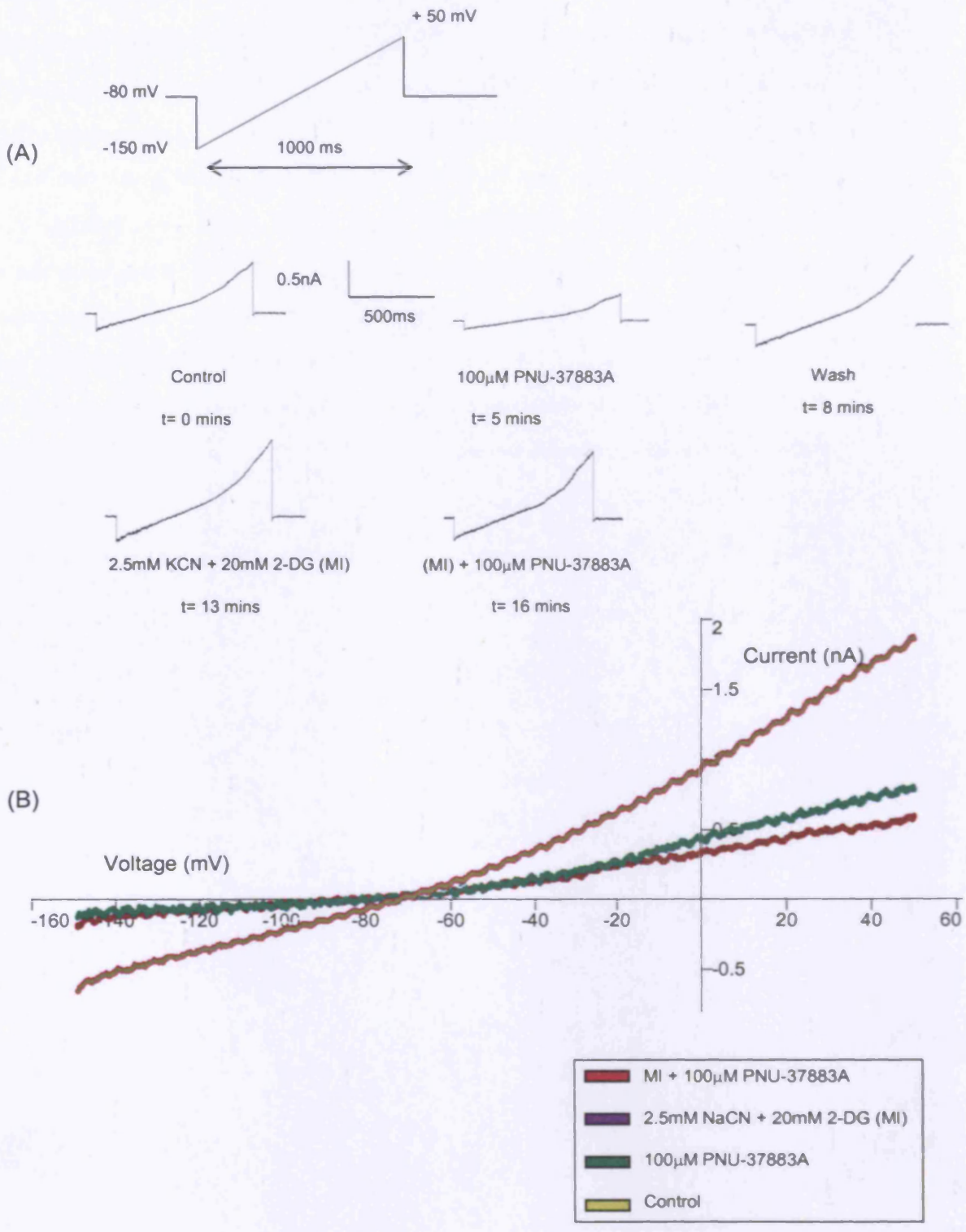
(A)
+ 50 mV
-80 mV
-150 mV
1000 ms
0.5nA
500ms
Control
t= 0 mins
100μM PNU-37883A
t= 5 mins
Wash
t= 8 mins
2.5mM KCN + 20mM 2-DG (MI)
t= 13 mins
(MI) + 100μM PNU-37883A
t= 16 mins
(B)
Current (nA)
Voltage (mV)
2
1.5
-0.5
-160
-120
-100
-80
-60
-40
-20
20
40
60
MI + 100μM PNU-37883A
2.5mM NaCN + 20mM 2-DG (MI)
100μM PNU-37883A
Control

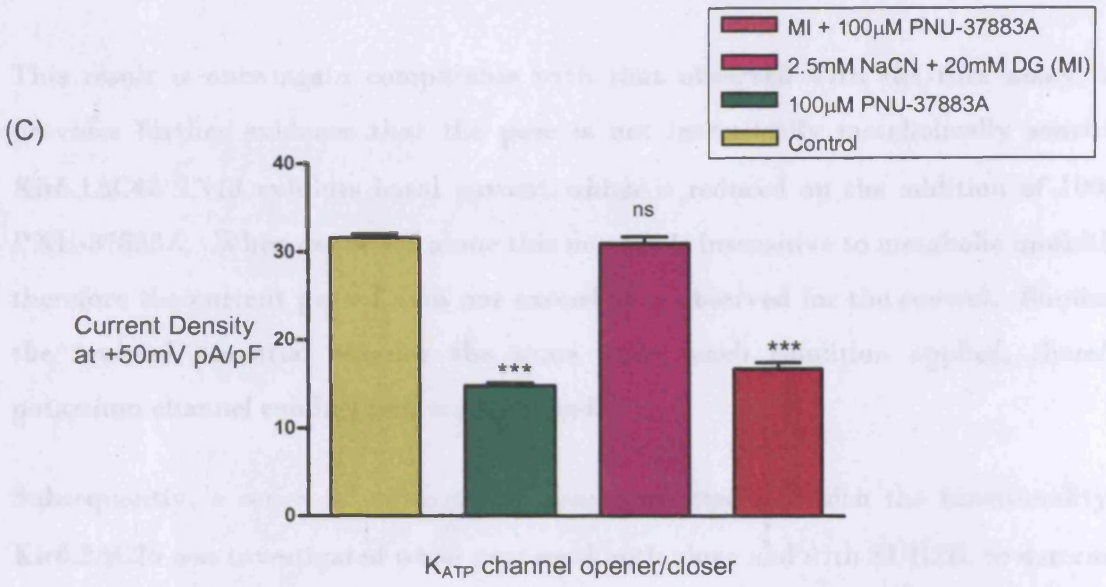

Figure 5.6: The effect of the K_{ATP} channel inhibitor PNU-37883A on the reconstituted channel Kir6.1ΔC48/ΔN13. The ability of 100μM PNU-37883A to reverse basal efflux and that induced by metabolic inhibitors was investigated using the perforated patch-clamp method. Currents were evoked via voltage clamp recordings during 1000ms voltage steps between -150mV and +50mV from a holding potential of -80mV, with 15s between sweep starts. (A) Representative traces for each of the conditions: Control (external solution with DMSO), 100μM PNU-37883A, metabolic inhibitors (2.5mM NaCN and 20mM 2-DG) and metabolic inhibitors with 100μM PNU-37883A. The time taken to achieve a response in relation to the control is given (B) Representative I/V traces for each of the conditions (pA/pF), whereby each trace crosses the holding potential at -80mV. (C) Current/Density bar chart to represent mean data of the reconstituted channel currents under each condition *** $P<0.001$ compared to control. (ns) $P>0.05$ (n=6)

This result is once again comparable with that observed with the flux assay, and provides further evidence that the pore is not intrinsically metabolically sensitive. Kir6.1ΔC48/ΔN13 exhibits basal current which is reduced on the addition of 100μM PNU-37883A. When expressed alone this mutant is insensitive to metabolic inhibition, therefore the current passed does not exceed that observed for the control. Similarly, the reversal potential remains the same under each condition applied, therefore potassium channel conductance is unaffected.

Subsequently, a series of experiments were conducted in which the functionality of Kir6.2ΔC26 was investigated when expressed both alone and with SUR2B, to determine how the response of a mutant known to express current at the membrane in the absence of SUR, compared to Kir6.1ΔC48/ΔN13. Kir6.2ΔC26 was previously engineered by Yi Cui by introducing a stop codon into Kir6.2 using site-directed mutagenesis.

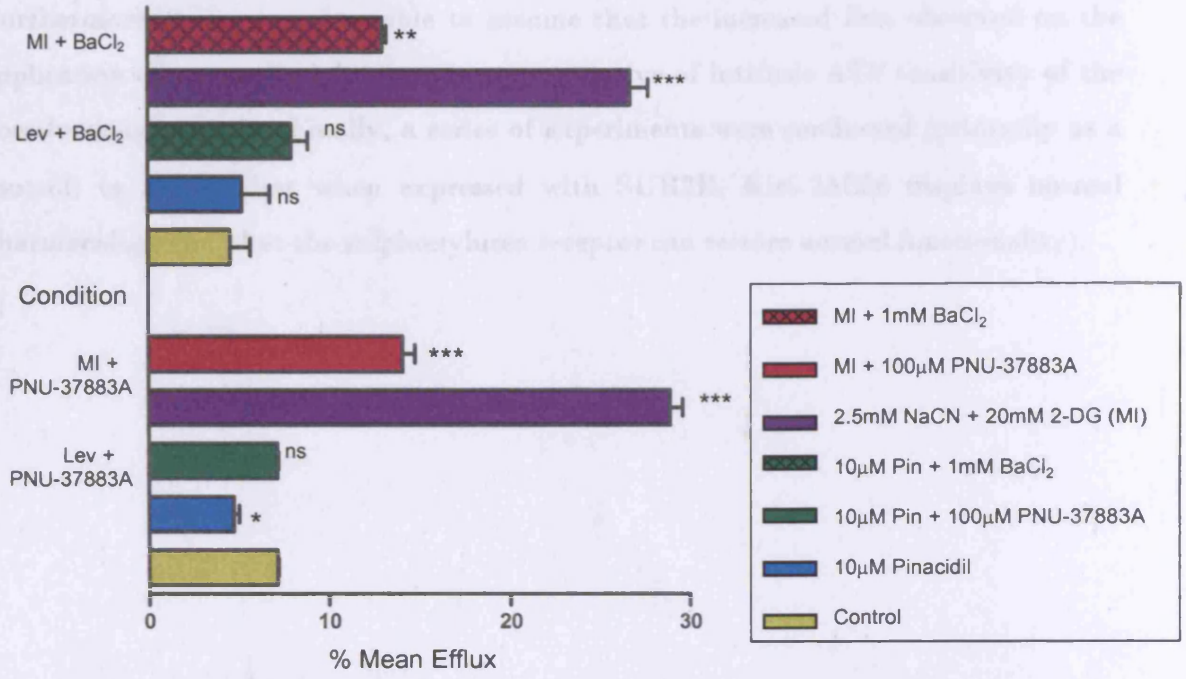

Figure 5.7: Effect of potassium channel Kir6.*x*-specific inhibitors on HEK293 cells transfected with Kir6.2ΔC26. The ability 100µM PNU-37883A and 1mM $BaCl_2$ to reverse the efflux induced with a KCO and metabolic inhibitors was investigated. Mean $^{86}Rb^+$ efflux was measured 15 minutes after addition of drugs. Efflux was calculated as % efflux of initial $^{86}Rb^+$ content. The control represents DMSO diluted in HBS. Data are shown as +/- SEM, whereby n = 9. *** P<0.001, ** P 0.001-0.01 compared to control, *P =0.01-0.05 compared to control, (ns) P>0.05 compared to control.

When Kir6.2ΔC26 was expressed alone, no response to the KCO pinacidil was observed (which is not surprising due to the absence of a sulphonylurea receptor to which it binds). However, significant response to the metabolic inhibitors 2.5mM NaCN and 20mM 2-DG was observed, which was reduced on the addition of either 1mM $BaCl_2$ or 100µM PNU-37883A (P<0.001). This correlates with the previous observation that Kir6.2ΔC26 has intrinsic metabolic sensitivity (Tucker, Gribble et al. 1997) and that PNU-37883A is able to inhibit current generated by expressing Kir6.2ΔC26 alone (Cui, Tinker et al. 2003). Comparison of this result with the perforated-patch data displayed in *Figure 5.6*, and the $^{86}Rb^+$ flux data displayed in *Figure 4.9*, indicates that there is a

difference in metabolic sensitivity between Kir6.1ΔC48/ΔN13 and Kir6.2ΔC26. Furthermore, it is now reasonable to assume that the increased flux observed on the application of metabolic inhibitors is representative of intrinsic ATP sensitivity of the pore-forming subunit. Finally, a series of experiments were conducted (primarily as a control) to ensure that when expressed with SUR2B, Kir6.2ΔC26 displays normal pharmacology (i.e. that the sulphonylurea receptor can restore normal functionality).

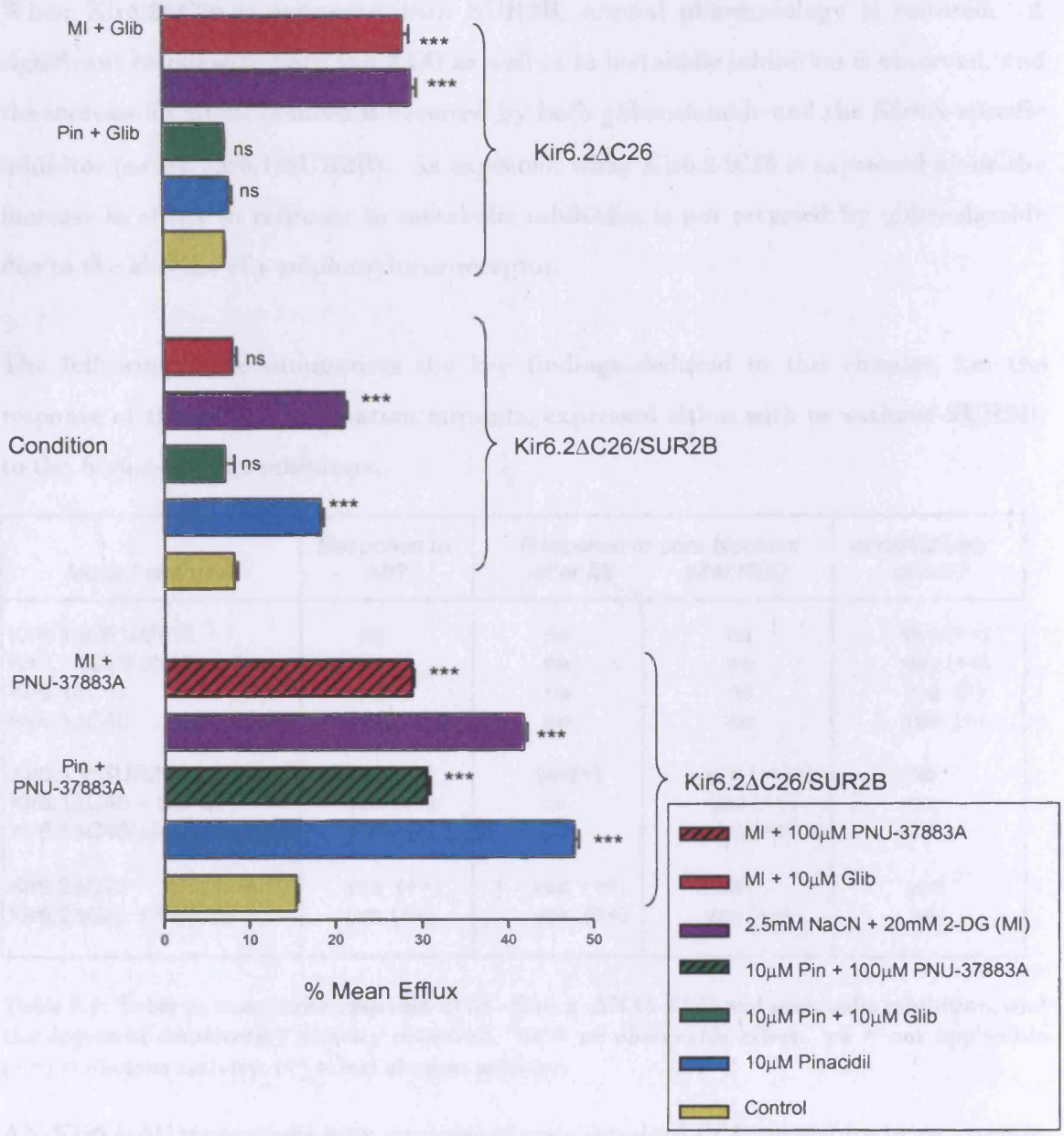

Figure 5.8: The effect of a KCO and metabolic inhibitors on HEK293 cells transiently expressing Kir6.2ΔC26 both with and without SUR2B. Mean $^{86}Rb^{+}$ efflux was measured 15 minutes after addition of drugs. Efflux was calculated as % efflux of initial $^{86}Rb^{+}$ content. The control represents DMSO diluted in HBS. Data are shown as +/- SEM, whereby n = 9. *** $P<0.001$, (ns) $P>0.05$ compared to control.

When Kir6.2ΔC26 is expressed with SUR2B, normal pharmacology is restored. A significant response to both the KCO as well as to metabolic inhibition is observed, and the increase in efflux induced is reversed by both glibenclamide and the Kir6.*x*-specific inhibitor (as for Kir6.1/SUR2B). As expected, when Kir6.2ΔC26 is expressed alone the increase in efflux in response to metabolic inhibition is not reversed by glibenclamide due to the absence of a sulphonylurea receptor.

The following table summarises the key findings deduced in this chapter, i.e. the response of the various truncation mutants, expressed either with or without SUR2B, to the Kir6.*x*-specific inhibitors.

Mutant channel	*Response to MI?*	*Response to pore blockers after MI*	*after KCO*	*constitutively active?*
Kir6.1ΔC61/ΔN13	ne	ne	ne	yes (++)
Kir6.1ΔC48/ΔN13	ne	ne	ne	yes (++)
Kir6.1ΔC61	ne	ne	ne	yes (+)
Kir6.1ΔC48	ne	ne	ne	yes (+)
Kir6.1 + SUR2B	yes (++)	yes(+)	yes (++)	na
Kir6.1ΔC48 + SUR2B	yes (++)	ne	yes (++)	na
Kir6.1ΔC48/ΔN13 + SUR2B	yes (++)	ne	yes (++)	na
Kir6.2ΔC26	yes (++)	yes (++)	na	yes
Kir6.2ΔC26 + SUR2B	yes (++)	yes (++)	yes (++)	na

Table 5.1: Table to summarise response of ΔC-Kir6.*x* -ΔN to KCO and metabolic inhibition, and the degree of constitutive activity observed. ne = no observable effect. na = not applicable (++) = obvious activity, (+) = less obvious activity.

ΔN-Kir6.1-ΔC truncations were engineered via a standard PCR procedure in an attempt to create a mutant of the pore-forming subunit of the channel which displayed intrinsic ATP sensitivity in the absence of the sulphonylurea receptor, as is the case for Kir6.2ΔC26. This was made on the premise that it would serve as a useful tool for determining whether drugs that act on K_{ATP} channels do so by interacting with Kir6.2 or with SUR1, and for examining functional interaction between Kir6.2 and SUR1.

In the previous chapter it was shown that Kir6.1ΔC48 and Kir6.1ΔC48/ΔN13 did not display efflux in response to the applied metabolic inhibitors in the absence of a sulphonylurea receptor. However, they displayed a relatively high basal efflux. In this chapter it was shown that this basal efflux was effectively reduced by the K_{ATP} channel inhibitors PNU-37883A and $BaCl_2$. Interestingly, Kir6.1ΔC48/ΔN13 and Kir6.1ΔC61/ΔN13 passed a higher basal efflux than when the C-terminus alone was truncated, indicating that deletion of the N-terminus enhanced the ability of the Kir6.1ΔC48 (expressed without SUR2B) to pass current. It was for this reason that the ability of the functionality of Kir6.1ΔC48/ΔN13 was investigated via the perforated patch-clamp method when expressed alone and with SUR2B.

Kir6.1ΔC48/ΔN13/SUR2B showed an increase in efflux on the application of KCO and metabolic inhibitors, but the later was not reduced on the application of pore blockers. This is the converse of the earlier observation in which glibenclamide was able to reverse efflux induced from either KCO or metabolic inhibitors. In comparison, neither PNU-37883A nor $BaCl_2$ reduced the current passed by Kir6.1/SUR2B when metabolically inhibited to the same extent as that previously observed by glibenclamide. Therefore, both data obtained from $^{86}Rb^+$ flux and patch clamping would indicate under conditions of ATP depletion, the channel undergoes conformational change that prevents efficient binding of both $BaCl_2$ and PNU-37883A. but does not affect binding of glibenclamide to the sulphonylurea receptor. Deletion of the N- and C-terminus attenuates this observation, in that both $BaCl_2$ and PNU-37883A do not appear to interact with the channel, or interact but do not affect the ability of the channel to pass current.

We observe a different scenario for Kir6.2ΔC26, which when expressed in the absence of SUR2B was responsive to metabolic inhibition, which was reversed by both $BaCl_2$ and PNU-37883A. This confirms the previously observed constitutive activity of Kir6.2ΔC26, and emphasizes the difference between Kir6.1ΔC48 and Kir6.2ΔC26 in

their intrinsic sensitivity to metabolically induced changes in cytosolic nucleotide levels. The efflux passed by Kir6.2ΔC26/SUR2B under metabolic inhibition was reversed by PNU-37883A, but likewise not as effectively as glibenclamide, but the effect was more pronounced than for Kir6.1ΔC48/ΔN13.

There is obviously a difference in the role that the pore-forming subunits Kir6.1 and Kir6.2 play in the metabolic sensitivity of the reconstituted K_{ATP} channel, and it would appear that the sulphonylurea receptor has a greater importance in the regulation of Kir6.1/SUR2B than Kir6.2/SUR2B. The importance of the sulphonylurea receptor in channel regulation is the focus of the next chapter.

Chapter Six

The role of the Sulphonylurea receptor in K_{ATP} channel regulation

Chapter Six: Results

The role of the Sulphonylurea receptor in K_{ATP} channel regulation

My previous studies have focused on the consequences of truncation of the pore-forming subunit on the functionality of the K_{ATP} channel, whereby Kir6.1ΔC48 and Kir6.1ΔC48/ΔN13 were surface expressed in the absence of the sulphonylurea receptor, but did not respond to MI when expressed independently. This was suggestive of an absence of intrinsic ATP sensitivity; the converse of that observed by Tucker and colleagues for Kir6.2. The importance of the sulphonylurea receptor as a regulatory subunit was discussed in the Introductory chapter, section 1.1 (the ABC Superfamily). With specific reference to *Figure 1.5*, I switched my attention to the role that SUR2B plays in the functionality of Kir6.1 and Kir6.2-containing channels. It was of interest to begin to understand the molecular mechanisms of how nucleotides regulate Kir6.1 containing complexes and to possibly delineate the region involved.

To investigate the roles of the individual NBDs of SUR2B, Yi Cui had previously employed site-directed mutagenesis to exchange the lysine residue in the W_A motif of either NBD1 or NBD2 with alanine (K708A and K1349M respectively). In other ABC transporters, these mutations were shown to abolish ATP binding and/or hydrolysis (Azzaria, Schurr et al. 1989; Carson and Welsh 1995; Ko and Pedersen 1995; Ueda, Inagaki et al. 1997; Ueda, Komine et al. 1999). In SUR1, these mutations prevent activation by Mg-nucleotides (Gribble, Tucker et al. 1997; Shyng, Ferrigni et al. 1997).

It was subsequently deemed desirable to engineer a double NBD mutant to observe the simultaneous effect of exchanging both lysines in the W_A motifs on the functionality of Kir6.1/SUR2B. SUR2B K708A (contained in pcDNA3.1) was used as a template to introduce the K1349M mutation, and SUR2B K1349M (again contained in pcDNA3.1) was used as a template to introduce K708A. Both mutations were introduced via site-directed mutagenesis, and were sequenced to ensure that the correct constructs had

been engineered. The data in *Figure 6.1* shows the initial assessment, via $^{86}Rb^{+}$efflux, of the effect of expressing these SUR2B NBD mutants with Kir6.1 on channel functionality.

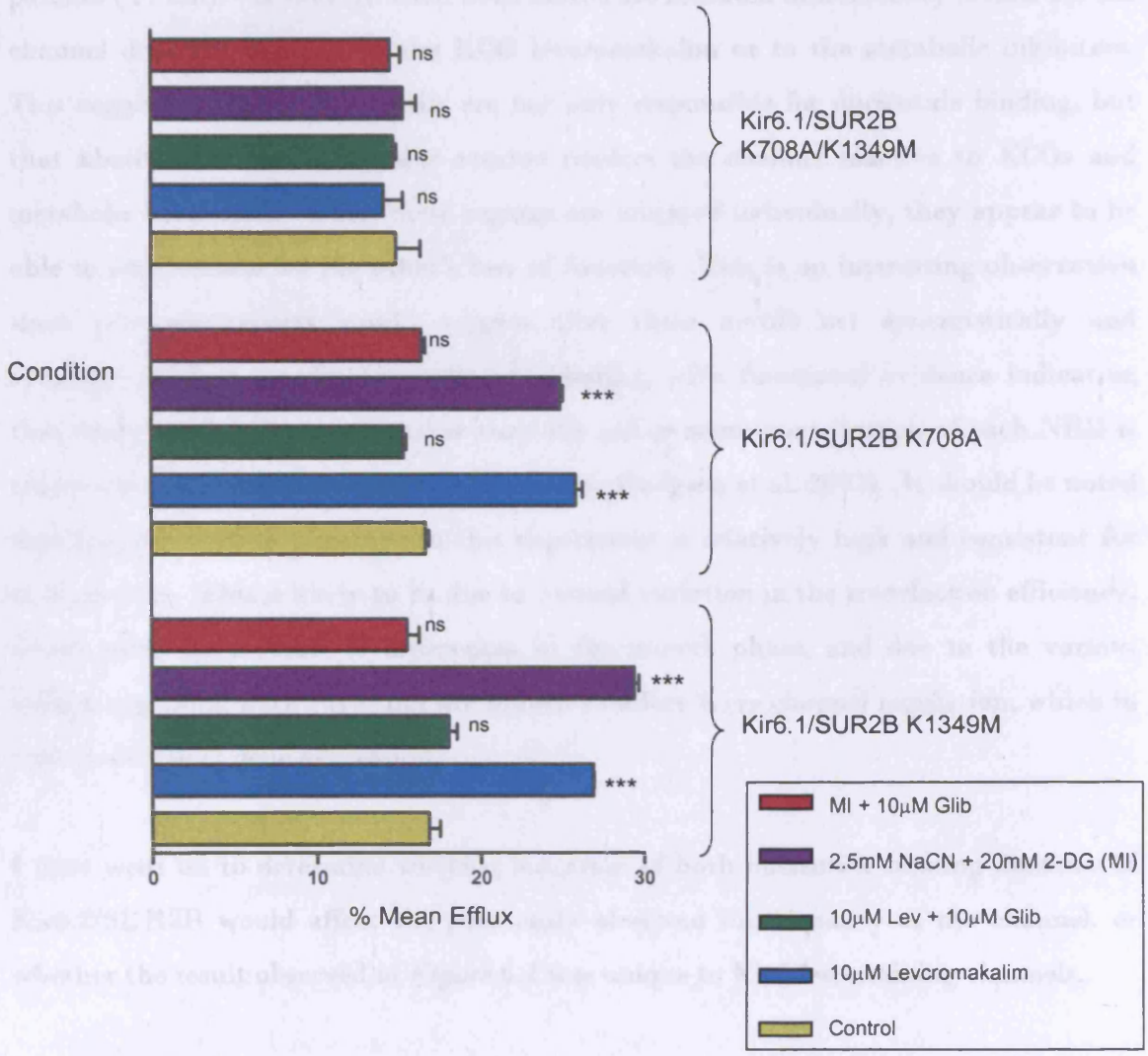

Figure 6.1: The effect of mutating the W_A motif lysine of NBDs 1 and 2 of the sulphonylurea receptor on the functionality of the K_{ATP} channel Kir6.1/SUR2B. Mean $^{86}Rb^{+}$ efflux of HEK293 cells transiently transfected with Kir6.1 and with SUR2B K708A/SUR2B K1349M or with SUR2B K708A/K1349M 15 minutes after the addition of drugs. Efflux was calculated as % efflux of initial $^{86}Rb^{+}$ content. The control represents DMSO diluted in HBS. Data are shown as +/- SEM, whereby n = 9. *** $P<0.001$ compared to control, (ns) $P>0.05$ compared to control.

It is evident that when only one of the Walker motifs is mutated, Kir6.1/SUR2B displays normal functionality. This is in line with previous evidence that SUR2B K1349M gives consistently low level activity when expressed with Kir6.1 in inside-out patches (Yi Cui). However, when both motifs are mutated functionality is lost, i.e. the channel does not respond to the KCO levcromakalim or to the metabolic inhibitors. This suggests that the W_A motifs are not only responsible for nucleotide binding, but that abolition of the key lysine residue renders the channel inactive to KCOs and metabolic inhibition. When these regions are mutated individually, they appear to be able to compensate for the other's loss of function. This is an interesting observation since previous reports would suggest that these motifs act synergistically and symmetrically to coordinate nucleotide binding, with functional evidence indicating that cooperative interaction rather than the independent contribution of each NBD is critical for K_{ATP} channel regulation (Zingman, Hodgson et al. 2002). It should be noted that the basal efflux observed in this experiment is relatively high and consistent for each mutant. This is likely to be due to natural variation in the transfection efficiency, which could be a result of differences in the growth phase, and due to the various cellular signaling pathways that are known to affect K_{ATP} channel regulation, which in turn could affect gene expression.

I then went on to determine whether mutation of both nucleotide binding domains in Kir6.2/SUR2B would affect the previously observed functionality of the channel, or whether the result observed in *Figure 6.1* was unique to Kir6.1-containing channels.

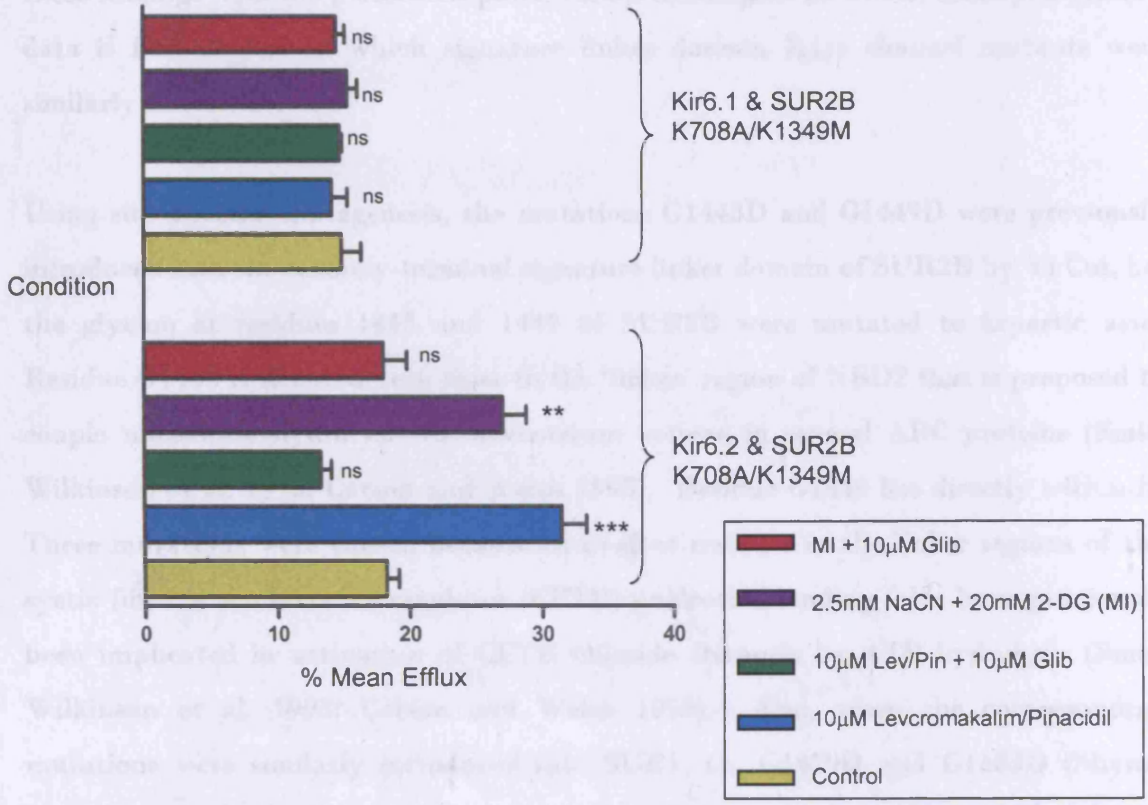

Figure 6.2: Comparison of the functionality of Kir6.1/SUR2B and Kir6.2/SUR2B, whereby SUR2B contains mutations in both the W_A motif lysines of both NBD1 and NBD2. Mean $^{86}Rb^+$ efflux of HEK293 cells transiently transfected with the reconstituted channel 15 minutes after the addition of drugs. Efflux was calculated as % efflux of initial $^{86}Rb^+$ content. The KCOs Pinacidil and Levcromakalim were applied to the Kir6.2-containing and Kir6.1-contianing channels respectively. The control represents DMSO diluted in HBS. Data are shown as +/- SEM, whereby n = 9. *** $P<0.001$ compared to control, (ns) $P>0.05$ compared to control.

Interestingly, when the double NBD mutant is expressed with Kir6.2, the channel would appear to function normally (data for Kir6.1 & SUR2B K708A/K1349M is shown as a direct comparison). Therefore, the W_A motif lysines do not appear to play the same level of importance in the regulation of Kir6.1 and Kir6.2 containing channels. Bearing in mind that Kir6.2 is functional in the absence of SUR (Tucker, Gribble et al. 1997), it is possible that Kir6.2 has some unique intrinsic property that compensates for the loss of these residues despite their previously demonstrated importance (Azzaria, Schurr et al. 1989; Carson and Welsh 1995; Ko and Pedersen 1995; Gribble, Tucker et al. 1997; Shyng, Ferrigni et al. 1997; Ueda, Inagaki et al. 1997). It was necessary to confirm

these findings with the perforated-patch clamp technique. However, some preliminary data is first shown, in which signature linker domain K_{ATP} channel mutants were similarly screened.

Using site-directed mutagenesis, the mutations G1443D and G1449D were previously introduced into the carboxy-terminal signature linker domain of SUR2B by Yi Cui, i.e. the glycine at residues 1443 and 1449 of SUR2B were mutated to aspartic acid. Residue G1443 is situated very close to the 'linker' region of NBD2 that is proposed to couple nucleotide hydrolysis to downstream actions in several ABC proteins (Smit, Wilkinson et al. 1993; Carson and Welsh 1995). Residue G1449 lies directly within it. These mutations were chosen because equivalent residues in the linker regions of the cystic fibrosis conductance regulator (CFTR) nucleotide binding folds have previously been implicated in activation of CFTR chloride channels by ATP hydrolysis (Smit, Wilkinson et al. 1993; Carson and Welsh 1995). Also, when the corresponding mutations were similarly introduced into SUR1, i.e. G1479D and G1485D (Shyng, Ferrigni et al. 1997), they failed to respond to activation by diazoxide and stimulation by MgADP. In turn, the observations that stimulation of K_{ATP} channels by ADP and by diazoxide both require Mg^{2+} and hydrolysable nucleotides (Findlay 1988; Lederer and Nichols 1989) suggest that the two processes may share common molecular mechanisms. Both diazoxide and MgADP activate K_{ATP} channels in the presence of inhibitor concentrations of ATP, and both processes require Mg^{2+} and hydrolysable nucleotides (Findlay 1988; Lederer and Nichols 1989). It was as such thought that G1479D and G1485 may affect channel activity, presumably by affecting binding and/or hydrolysis of ATP, or by affecting the transduction of nucleotide binding and hydrolysis to channel opening and closing (Shyng, Ferrigni et al. 1997). In the preliminary experiments shown, both Kir6.1 and Kir6.2 were expressed with SUR2B G1443D and SUR2B G1449D to observe the effect of these mutations on the response of the channel to the KCO and metabolic inhibition.

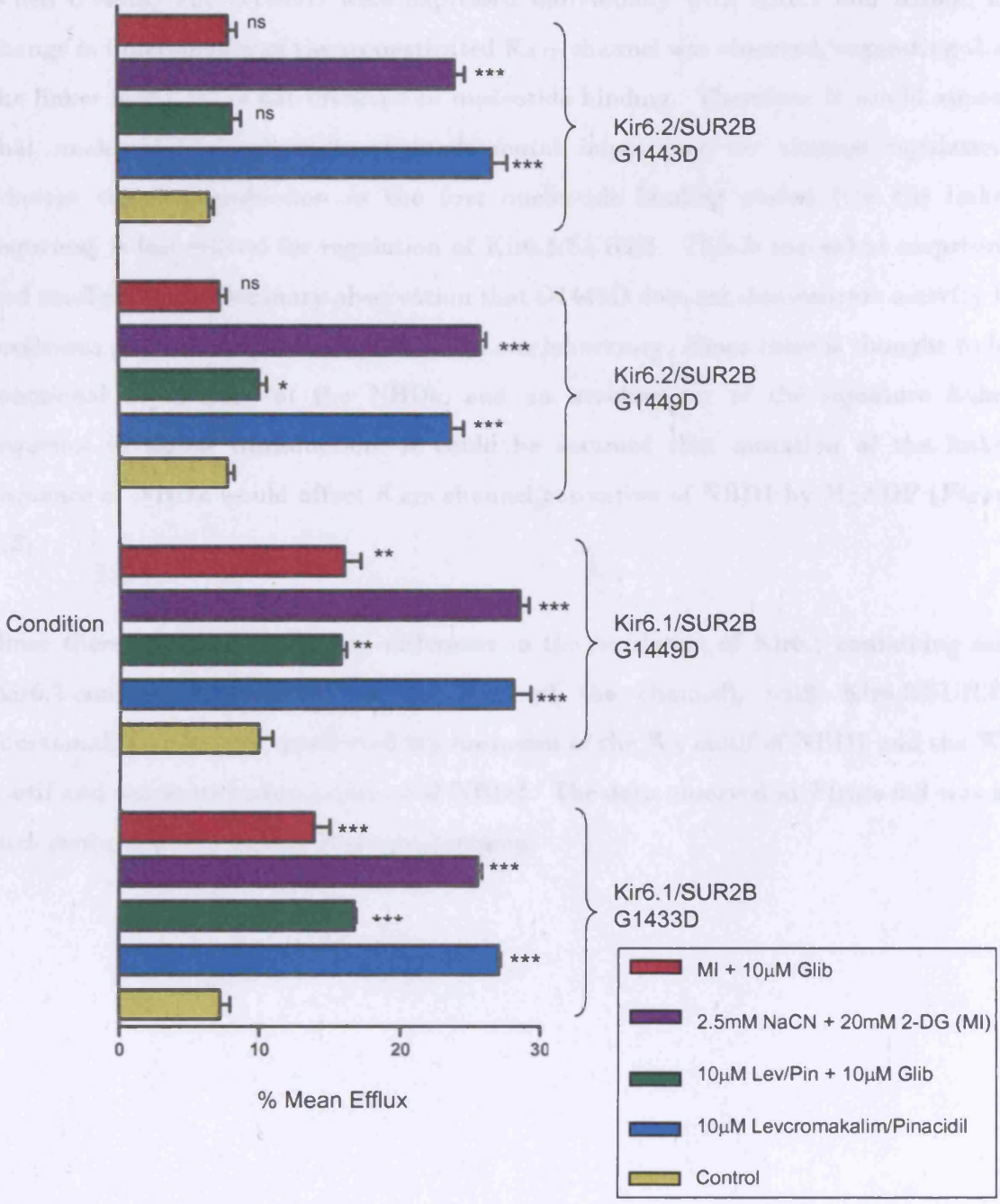

Figure 6.3: The effect of introducing a single mutation into the linker domains of the sulphonylurea receptor on the functionality of the K_{ATP} channel Kir6.1/SUR2B and Kir6.2/SUR2B. Mean $^{86}Rb^+$ efflux of HEK293 cells transiently transfected with Kir6.1 and SUR2B G1449D or G1443D or with Kir6.2 and SUR2B G1449D or G1443D 15 minutes after the addition of drugs. Efflux was calculated as % efflux of initial $^{86}Rb^+$ content. The KCOs Pinacidil and Levcromakalim were applied to Kir6.2-containing and Kir6.1-containing channels respectively. The control represents DMSO diluted in HBS. Data are shown as +/- SEM, whereby n = 9. *** $P<0.001$ compared to control, (ns) $P>0.05$ compared to control.

When G1443D and G1449D were expressed individually with Kir6.1 and Kir6.2, no change in functionality of the reconstituted K_{ATP} channel was observed, suggesting that the linker in NBD2 is not involved in nucleotide binding. Therefore, it would appear that nucleotide hydrolysis is of fundamental importance for channel regulation, whereas signal transduction in the first nucleotide binding pocket (via the linker sequence) is less critical for regulation of Kir6.1/SUR2B. This is somewhat surprising and conflicts the preliminary observation that G1449D does not demonstrate activity in inside-out patches, as previously shown in our laboratory. Since there is thought to be functional asymmetry of the NBDs, and an involvement of the signature linker sequence in signal transduction, it could be assumed that mutation of the linker sequence of NBD2 would affect K_{ATP} channel activation of NBD1 by MgADP (*Figure 6.2*).

Since there appears to be a key difference in the regulation of Kir6.1-containing and Kir6.2-containing channels (at the level of the channel), with Kir6.2/SUR2B functionality seemingly unaffected my mutation of the W_A motif of NBD1 and the W_A motif and signature linker sequence of NBD2. The data observed in *Figure 6.3* was as such confirmed via perforated patch-clamping.

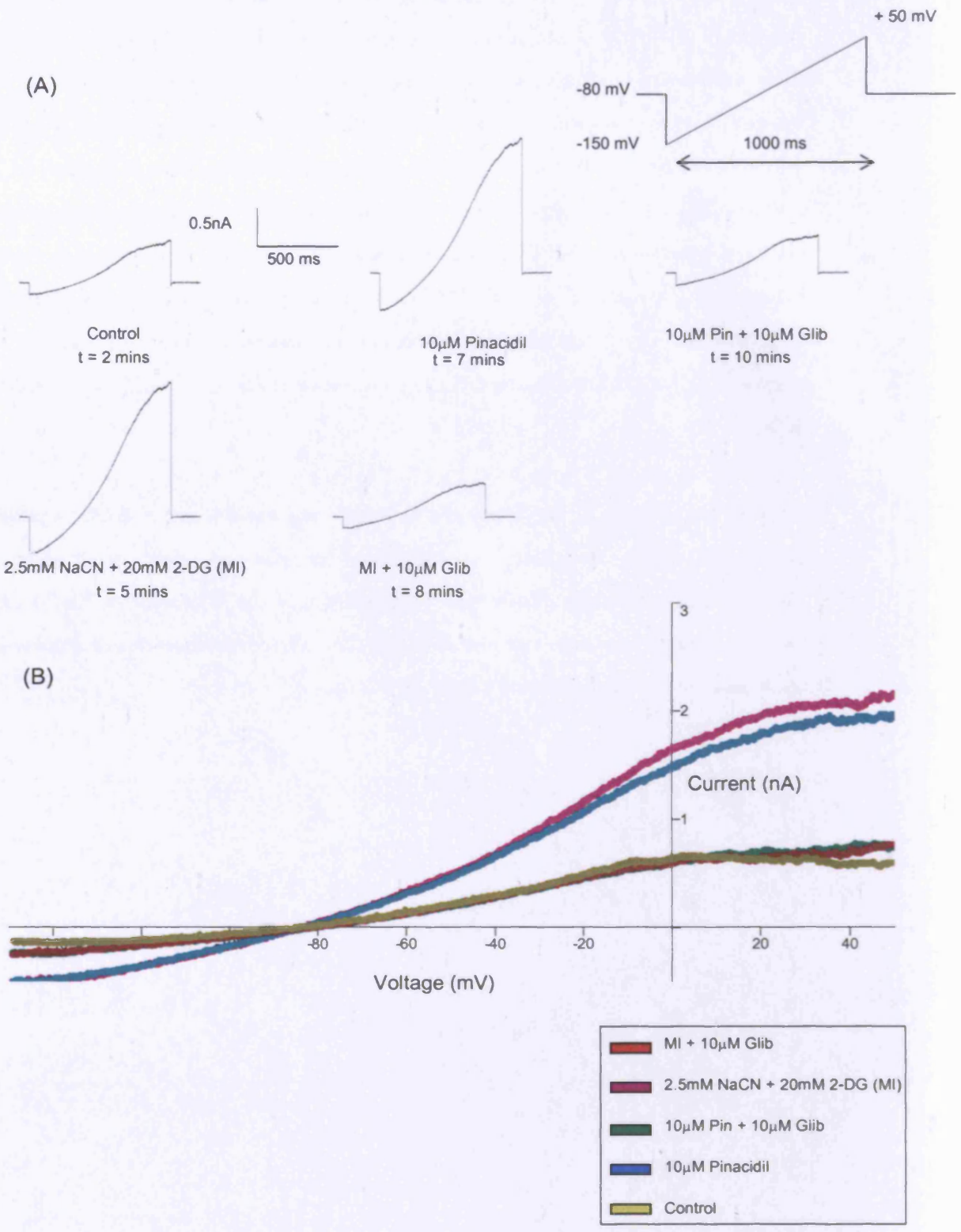
(A)
+ 50 mV
-80 mV
-150 mV
1000 ms
0.5nA
500 ms
Control
t = 2 mins
10μM Pinacidil
t = 7 mins
10μM Pin + 10μM Glib
t = 10 mins
2.5mM NaCN + 20mM 2-DG (MI)
t = 5 mins
MI + 10μM Glib
t = 8 mins
(B)
Current (nA)
Voltage (mV)
MI + 10μM Glib
2.5mM NaCN + 20mM 2-DG (MI)
10μM Pin + 10μM Glib
10μM Pinacidil
Control

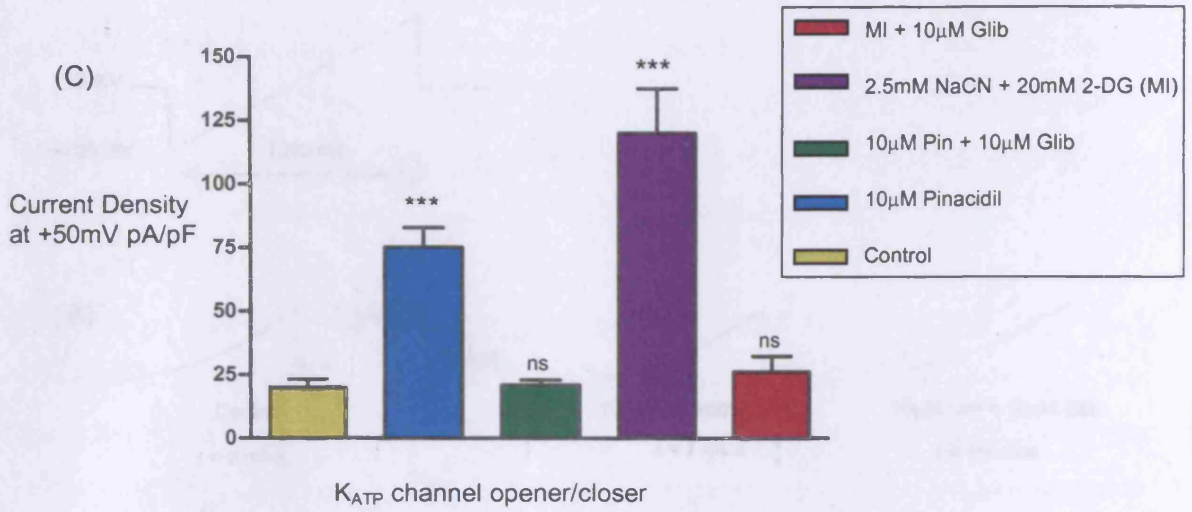

Figure 6.4: The effect of mutating both the W_A motifs of the K_{ATP} channel Kir6.2/SUR2B on channel functionality (i.e. Kir6.2 & SUR2B K1349M/K708A) as demonstrated by the perforated patch-clamp method. Currents were evoked via voltage clamp recordings were evoked over 1000ms voltage steps between -150mV and +50mV in 1mV increments from a holding potential of -80mV, with 15s between sweep starts. (A) Representative traces for each of the conditions: external solution with DMSO, 10μM Levcromakalim, 10μM Levcromakalim with 100μM PNU-37883A, metabolic inhibitors (2.5mM NaCN and 20mM 2-DG) and metabolic inhibitors with 100μM PNU-37883A. The time taken from perforation to the current recorded under each condition is given (note that that the KCO and KCB were washed out prior to the induction of metabolic inhibition). (B) Representative I/V traces for each of the conditions (pA/pF), whereby each trace crosses the holding potential at -80mV. (C) Current/Density bar chart to represent mean data of the reconstituted channel currents under each condition *** $P<0.001$, (ns) implies $P>0.05$ compared to control (n=5)

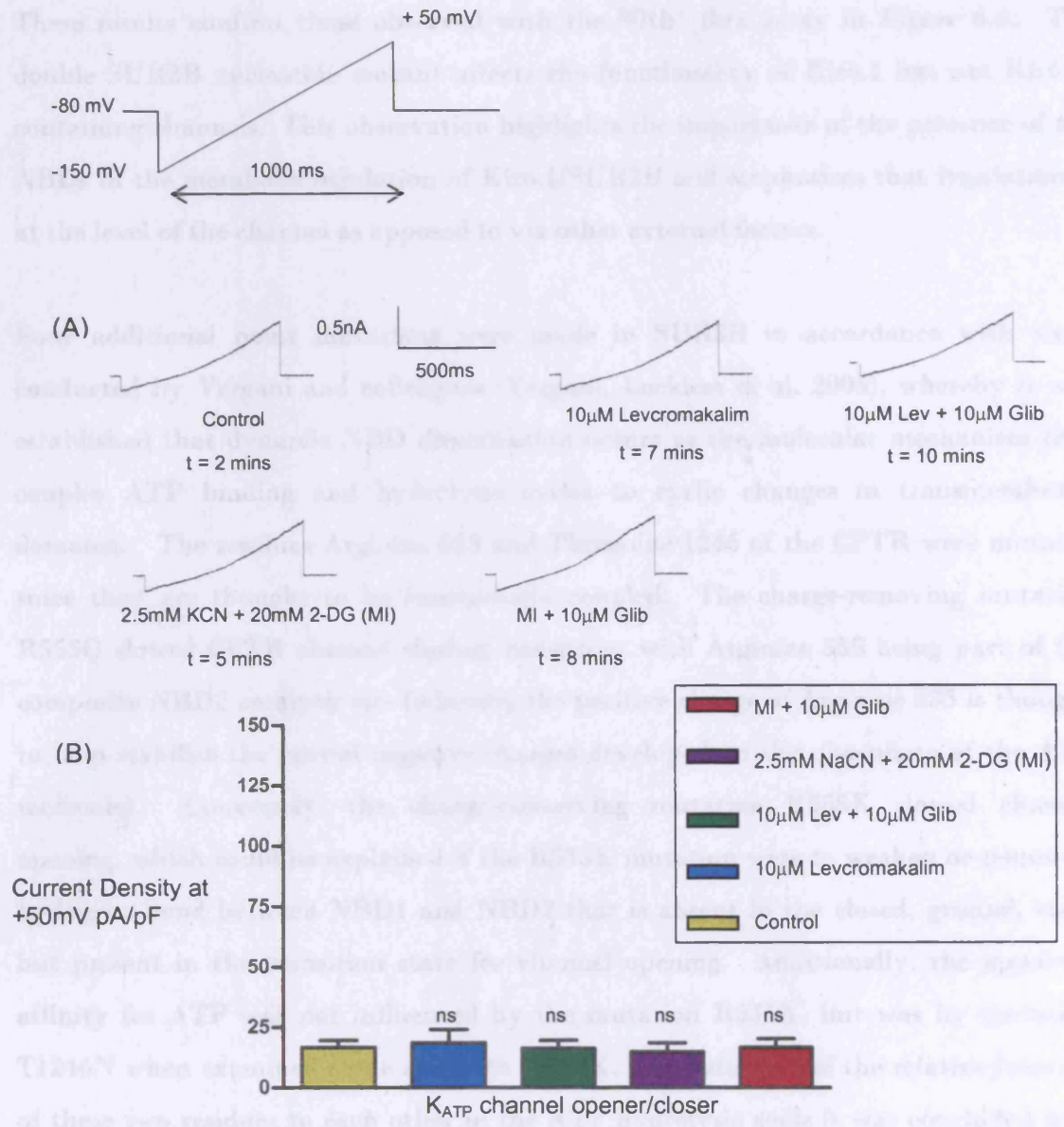

Figure 6.5: The effect of mutating both the W_A motifs of the K_{ATP} channel Kir6.1/SUR2B (i.e. Kir6.1 & SUR2B K1349M/K708A) on channel functionality as demonstrated by the perforated patch-clamp method. Currents were evoked via voltage clamp recordings were evoked during 1000ms voltage steps between -150mV and +50mV in 1mV increments from a holding potential of -80mV, with 15s between sweep starts. (A) Representative traces for each of the conditions: external solution with DMSO, 10μM Levcromakalim, 10μM Levcromakalim with 100μM PNU-37883A, metabolic inhibitors (2.5mM NaCN and 20mM 2-DG) and metabolic inhibitors with 100μM PNU-37883A. The time taken from perforation to the current recorded under each condition is given (note that that the KCO and KCB were removed before the induction of metabolic inhibition). (B) Current/Density bar chart to represent mean data of the reconstituted channel currents under each condition *** P<0.001, (ns) implies P>0.05 (n=6)

These results confirm those observed with the $^{86}Rb^{+}$ flux assay in *Figure 6.2.* The double SUR2B nucleotide mutant affects the functionality of Kir6.1 but not Kir6.2-containing channels. This observation highlights the importance of the presence of the NBDs in the metabolic regulation of Kir6.1/SUR2B and emphasizes that regulation is at the level of the channel as opposed to via other external factors.

Four additional point mutations were made in SUR2B in accordance with work conducted by Vergani and colleagues (Vergani, Lockless et al. 2005), whereby it was established that dynamic NBD dimerization occurs as the molecular mechanism that couples ATP binding and hydrolysis cycles to cyclic changes in transmembrane domains. The residues Arginine 555 and Threonine 1246 of the CFTR were mutated since they are thought to be functionally coupled. The charge-removing mutation R555Q slowed CFTR channel closing, consistent with Arginine 555 being part of the composite NBD2 catalytic site (whereby the positive charge of Arginine 555 is thought to help stabilize the partial negative charges developed on the phosphate of the ATP molecule). Conversely, the charge-conserving mutation R555K slowed channel opening, which could be explained if the R555K mutation were to weaken or remove a hydrogen bond between NBD1 and NBD2 that is absent in the closed, ground, state but present in the transition state for channel opening. Additionally, the apparent affinity for ATP was not influenced by the mutation R555K, but was by mutation T1246N when examined alone and with R555K. On deduction of the relative location of these two residues to each other in the ATP hydrolysis cycle it was concluded that ATP binding occurs before the formation of a closely apposed NBD1-NBD2 dimer (Vergani, Lockless et al. 2005).

Based on these observations, the corresponding mutations were introduced into SUR2B via site-directed mutagenesis. These were R816Q, R816K and T1345N. Finally, in other ABC-ATPases, mutating the key lysine in the W_A motif to arginine drastically reduces or abolishes hydrolysis. CFTR channels carrying the corresponding mutation, K1250R, have prolonged open burst duration. This is indicative of slowed hydrolysis at

the CFTR's NBD2 catalytic site. As such, the corresponding mutation was also introduced into SUR2B (K1349R). Preliminary data, in which these mutants were screened using the $^{86}Rb^{+}$ flux assay to assess abolition of functionality in preparation for further analysis, is shown in *Figure 6.6.*

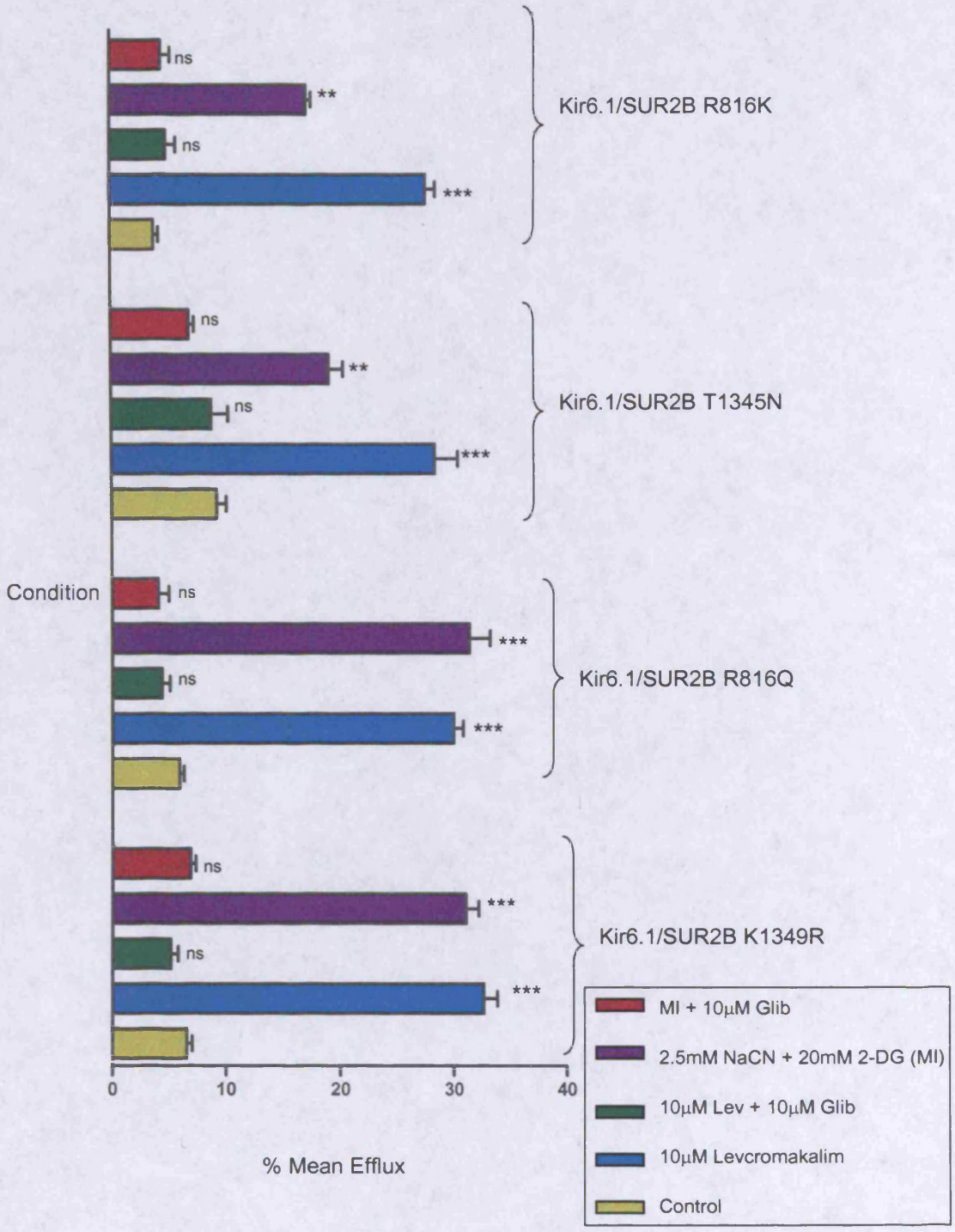

Figure 6.6: The effect of mutating Arg 816, Thr 1345 and Lys 1349 of the sulphonylurea receptor on the functionality of the K_{ATP} channel Kir6.1/SUR2B. Mean $^{86}Rb^{+}$ efflux of HEK293 cells transiently transfected with Kir6.1 and SUR2B K1349R/R816Q/R816K/T1345N 15 minutes after the addition of drugs. Efflux was calculated as % efflux of initial $^{86}Rb^{+}$ content. The control represents DMSO diluted in HBS. Data are shown as +/- SEM, whereby n = 6. *** $P<0.001$ compared to control, (ns) $P>0.05$ compared to control.

Mutation of Arginine 816 (R816K or R816Q), residing three positions after the signature linker sequence in the NBD1 tail, does not appear to affect the functionality of Kir6.1/SUR2B. Mutation of Threonine 1345 (residing in the W_A phosphate-binding loop in the NBD2 head) or Lysine 1349 (residing in the W_A motif, specifically the phosphate binding loop to arginine) similarly does not appear to affect pharmacology. This is consistent with the previous result, whereby mutation of Lysine 1349 to Methionine did not abolish the functionality of Kir6.1/SUR2B (*Figure 6.2*). On visual observation it would appear that there may be a slight reduction in the response to metabolic inhibition on the introduction of R816K or T1455N, indicating that ATP binding or hydrolysis may be affected to a degree. However, this would need to be investigated further, possibly by conducting similar experiments to those of Vergani and colleagues (Vergani, Lockless et al. 2005).

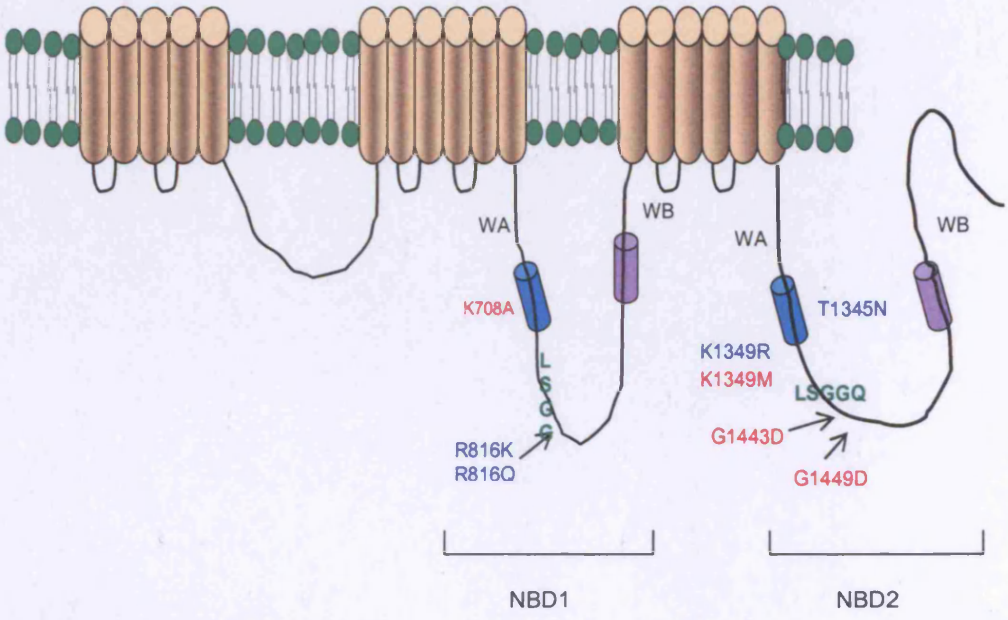

Figure 6.7: Diagram depicting the sulphonylurea receptor to indicate the mutations that were introduced into NBD1 and NBD2. K708A represents mutation of the lysine in the W_A motif of NBD1, and K1349R/K1349M and T1345N mutation of the lysine and threonine respectively of the W_A motif. R816K/R816Q and G1443D/G1449D represent mutations affecting the signature linker sequence of NBD1 and NBD2 respectively.

Figure 6.7 summarizes the mutations that were screened in this chapter to further understand the importance of the sulphonylurea receptor in the metabolic regulation of the K_{ATP} channel. Only simultaneous mutation of K708A and K1349M SUR2B affected the functionality of Kir6.1-containing channels. The fact that the individual mutations of NBD1 and NBD2, and mutations in the linker sequence did not appear to affect the normal response to the various pharmacological agents goes against the previous evidence that there is functional asymmetry of the NBDs. However, it is possible that the residues mutated were not of key importance to the catalytic cycle in the NBD sites in both Kir6.1/SUR2B and Kir6.2/SUR2B. This is discussed further in the subsequent chapter.

Chapter Seven

Discussion

Chapter Seven: Discussion

To introduce this chapter, I would like to highlight that all-in-all this thesis has highlighted the usefulness of the $^{86}Rb^{+}$ flux assay as a technique, with a high enough sensitivity and specificity to screen for ion channel functionality (on condition that the transfection efficiency of recombinant ion channels was at least 80%). It proved useful in the screening of a variety of recombinant ion channels relatively quickly, and since the results that I deemed to the most significant were confirmed via either whole-cell or perforated patch-clamping, we can assume that the data obtained is an accurate depiction of the way in which the recombinant K_{ATP} channels respond to the various pharmacological agents applied. Undoubtedly, patch clamping is the gold standard for determining ion-channel functionality, providing high quality and physiologically relevant data of ion channel function at the single cell or single channel level (Hamill, Marty et al. 1981). No other existing technology can provide such a direct, precise and detailed measurement of the activity of an ion channel down to the single-molecule level. However, it has a relatively low throughput and reproducibility. There are many automated recording techniques under development, for example the Port-a-Patch (an automated electrophysiology work station). This is based on a planar, microstructured glass chip, and enables automatic whole cell patch-clamp measurements (Brueggemann, George et al. 2004). It is conceivable that with time, such technologies will replace the use of radioactive assays. In the meantime, I am confident that $^{86}Rb^{+}$ flux is an accurate screening tool.

7.1 Rationale for conducting these studies

The objective of this thesis was to assess the metabolic sensitivity of the K_{ATP} channel Kir6.1/SUR2B, and to begin to understand the molecular mechanism responsible for this. It was originally hypothesised that Kir6.1 would be a hormonal rather than a predominant metabolic sensor. It has frequently been observed that smooth muscle contains a current that is less sensitive to changes in metabolism and the channels responsible are directed by hormonal inputs and protein kinase activity. The opening

of these channels is absolutely dependent on the presence of nucleotide diphosphates and the inhibition by ATP is much less marked. This has been described as the K_{NDP} current. In native vascular smooth muscle tissues, vasodilators such as CGRP activate analogous currents through a PKA dependent mechanism, and this modulation accounts for a substantial portion of the vasodilatation (Quayle and Standen 1994). In contrast vasoconstrictors, in particular angiotensin II, inhibit the channel by activating protein kinase C (Kubo, Quayle et al. 1997). It was proposed that Kir6.1/SUR2B is the molecular counterpart of vascular smooth muscle ATP-sensitive K^+ channel, with properties analogous to that of the K_{NDP} current. It appears, from the work that has been conducted in both our and other laboratories, that Kir6.1/SUR2B may indeed constitute the K_{ATP}/K_{NDP} channel in the vascular smooth muscle.

A number of studies had previously addressed the molecular mechanisms of nucleotide regulation of the 'metabolically sensitive' Kir6.2 containing channel complexes (predominantly Kir6.2/SUR1 and Kir6.2/SUR2A) (Shyng and Nichols 1997; Babenko, Gonzalez et al. 1999; Ueda, Komine et al. 1999; Dong, Tang et al. 2005). In contrast, little was known of the molecular details of how nucleotides regulate Kir6.1 containing complexes.

To recap, there are some interesting paradoxes. At the functional level, Kir6.1/SUR2B is less ATP sensitive: ATP stimulates channel activity at submillimolar concentrations, with activity peaking at 1mM, and only moderate inhibition occurring above this (Yamada, Isomoto et al. 1997). Channel opening is absolutely dependent on the provision of nucleotide diphosphates and does not occur in their absence. However, at the biochemical level, fluorescent derivatives of ATP can bind with similar affinities to the C-termini of Kir6.1, Kir6.2 and Kir1.1 (Vanoye, MacGregor et al. 2002). Overall, there is a fundamental gap in our understanding of what accounts for these profound differences given the commonality of the expressed sulphonylurea receptor and the high homology between Kir6.1 and Kir6.2.

Vascular and non-vascular smooth muscle may express Kir6.2 in addition to Kir6.1 and SUR2B, and Yi Cui reported that the diverse range of unitary conductance reported for smooth muscle K_{ATP} channels may be due to co-assembly of Kir6.1 and Kir6.2 to form channels, with different combinations of the pore-forming subunits and their associated SUR2B subunits (Cui, Tinker et al. 2003). Therefore, in this thesis I set out to assess if Kir6.1/SUR2B displays any metabolic sensitivity and to compare the metabolic regulation of Kir6.1/SUR2B with that of Kir6.2/SUR2B. I wanted to elucidate if the pore-forming subunit accounted for any differences in regulation at the molecular level (given the commonality of the sulphonylurea receptor, SUR2B).

Using both the $^{86}Rb^{+}$ flux assay and the perforated patch-clamp technique, I deduced that Kir6.1/SUR2B was indeed metabolically responsive (*Figures 3.2 & 3.8*). Inhibition of both oxidative metabolism and glycolysis depleted $[ATP]_i$ levels and increased ADP levels to a sufficient level to induce channel opening (*Figure 3.3*). Since Kir6.1-containing channels have been reported not to be activated by depletion of ATP (Yamada, Isomoto et al. 1997), this was an interesting result in itself. Because the role that cellular signalling pathways (as assessed via the involvement of AMPK, adenosine and PKA) did not appear to be so clear-cut, I placed more emphasis on the regulation of Kir6.1/SUR2B at the metabolic level (i.e. directly by ATP and MgADP) as opposed to regulation by protein kinases.

ATP and non-hydrolysable derivatives bind to determinants in the N- and C-terminus of Kir6.2 to result in channel inhibition (Koster, Sha et al. 1999; Vanoye, MacGregor et al. 2002). In contrast, MgADP is known to interact with the nucleotide binding domains of SUR at the W_A and W_B motifs in a complex fashion to increase the activity of the channel complex (Shyng, Ferrigni et al. 1997; Ueda, Komine et al. 1999). Therefore, I looked at the role that both the pore-forming and sulphonylurea receptor subunits play in the metabolic regulation of the channel. It would appear from these combinative results that Kir6.1 is not primarily responsible for metabolic sensitivity of the channel, but that SUR2B is likely to be.

7.2 The role of the pore-forming subunit in channel regulation

-Studies involving removal of the N- and C-terminus to allow independent expression

It was found that Kir6.2ΔC26 can be expressed and function independently, and that this makes it a useful tool for determining whether drugs act on K_{ATP} channels do so by interacting with Kir6.2 or with SUR1, and for examining the functional interaction between Kir6.2 and SUR1 (Tucker, Gribble et al. 1997). Therefore, I similarly deleted the C-terminus (hence removal of the RKR motif) of Kir6.1 to allow its independent expression. The N-terminus of Kir6.1 was also deleted, since this was thought to increase basal activity when expressed in combination with SUR2B in the absence of nucleotide diphosphate (Babenko and Bryan 2001).

Surface staining revealed that removal of the RKR motif of Kir6.1 did indeed allow independent surface expression, whereas when present the pore was not trafficked to the cell membrane (*Figure 4.3*), which was the case for Kir6.1 and Kir6.1-ΔN. Deletion of the C-terminus did not obliterate functionality when Kir6.1 was expressed with the sulphonylurea receptor, however this did not allow its independent functional expression (*Figure 4.9*), i.e. Kir6.1-ΔC did not display intrinsic ATP sensitivity as was previously shown by Tucker and Colleagues for Kir6.2-ΔC (Tucker, Gribble et al. 1997).

Another key observation was that Kir6.1-ΔN33/SUR2B was non-functional (*Figure 4.7 & Figure 4.10*). It has been reported that N-terminal truncation of Kir6.1 was not found to compromise the response to Mg-nucleotide-dependent stimulation by the sulphonylurea receptor, and that progressively larger deletions (ΔN13, ΔN21 and ΔN33) increased the open probability, with maximal effect seen with ΔN33 (Babenko and Bryan 2001). The data displayed in *Figures 4.6 and 4.9* would indicate that this is not necessarily the case.

It has also been shown that the deletion of residues 2-10 and 20-30 of N-terminus of Kir6.2 are associated with a significant increase in open probability in absence of ATP,

but that intrinsic ATP sensitivity was not affected in co-expressed channels (Koster, Sha et al. 1999). It is thought that the normal role of N-terminus may be to destabilise the open state under the influence of SUR1. This action may be blocked by physical tethering of the N-terminus to SUR1, and is therefore absent both after deletion of the Kir6.2 N-terminus, or upon expression of Kir6.2 without SUR1. This would explain lack of additivity of the effect of N- and C-terminal deletions expressed without SUR1 (Koster, Sha et al. 1999). Similarly, it has been shown that deletion of more than half of the N-terminus of Kir6.2 has no effect on intraburst kinetics, and that the rate of transition which terminates a burst and decreases fraction of time channel spends in interburst closed states (Babenko, Gonzalez et al. 1999) is decreased. N-terminal Kir6.2 mutants have been shown to have an extremely high open probability in absence of nucleotides. They also demonstrate a decreased apparent ATP-sensitivity, which is consistent with the involvement of the N-terminus in a transition to an interburst closed state that preferentially binds inhibitory ATP (Babenko, Gonzalez et al. 1999).

All-in-all previous data has demonstrated that the two cytoplasmic domains of Kir6.2 make additive contributions to ATP-inhibitory gating via different mechanisms; the N-terminus controls the transition to an ATP-sensitive interburst state, the C-terminus interacts with ATP. Deletions of the C-terminus do not affect intrinsic ATP sensitivity of the channel, but allow generation of functional channels in absence of SUR1. Deletions of N-terminus, do not generate functional channels without SUR1, but stabilise the open channel, leading to apparent reduction in ATP sensitivity in absence of SUR1. In fact, the N-terminus may function to transduce a destabilizing effect of SUR1 on open state. It is therefore somewhat surprising that both $^{86}Rb^{+}$ flux and patch-clamp data indicate that Kir6.1ΔN33/SUR2B is non-functional. Even though it has been shown that truncations of 40 amino acids or beyond of Kir6.2 did not generate functional channels in the presence of SUR1 (Koster, Sha et al. 1999), and that Kir6.2ΔN53 failed to produce functional channels when expressed with SUR1 (Babenko, Gonzalez et al. 1999), one would assume that the high open probability of

Kir6.1ΔN33/SUR1 seen by Babenko and Bryan in 2001 would correspond to a high basal flux.

It is possible that these differing observations are due to the fact that Kir6.1-ΔN was expressed with a different sulphonylurea receptor. In may be possible that N-terminus of Kir6.1 does not play the same destabilising role in SUR2B-containing channels as Kir6.1/SUR1. This would need to be investigated further; however the data that I obtained is convincing and consistent: deletion of the N-terminal 33 amino acids reduces functionality of both Kir6.1 and Kir6.1-ΔC when expressed with SUR2B.

-Studies using K_{ATP} channel inhibitors specific to Kir6.x

Even though Kir6.1-ΔC48 did not display intrinsic metabolic sensitivity, it displayed significant basal efflux in comparison to HEK293 cells or to those expressing Kir6.1 alone (*Figure 4.9*). The same was also true for Kir6.1ΔC48/ΔN13. Therefore, truncated pore-forming subunits that were found to be expressed at the cell membrane in the absence of the sulphonylurea receptor would also appear to display a higher basal efflux. This basal efflux was reduced by the drugs which bind to the Kir6.*x* subunit, i.e. $BaCl_2$ and PNU-37883A, indicating that the pore was still able to pass a small amount of current even though it was not able to 'sense' changes in nucleotide levels. PNU-37883A has also been shown to block current passed by Kir6.2ΔC26 (Cui, Tinker et al. 2003). Therefore, truncation of the pore-forming subunit would not appear to affect the ability of inhibitors specific to Kir6.*x* to bind to Kir6.2-containing channels.

Kir6.1, Kir6.1ΔC48 and Kir6.1ΔC48/ΔN13 were subsequently expressed with SUR2B, and the ability of and $BaCl_2$ to reverse efflux induced upon metabolic inhibition, and via the application of a KCO investigated. Both Kir6.*x* inhibitors were able to reverse metabolically induced flux as seen for glibenclamide, and truncation of reconstituted channel completely abolished reversal (*Figures 5.3, 5.4 and 5.5*). Therefore, under conditions of nucleotide depletion, the ability of the inhibitors to bind to Kir6.1 would

appear to be disrupted, and truncation of the pore at the N- and C-terminus enhances this effect. Both PNU-37883A and $BaCl_2$ are still able to bind to the pore when expressed with the sulphonylurea receptor in this system, since they are able to reverse efflux induced by the KCO. This was a very interesting observation, and both $^{86}Rb^+$ flux and the perforated patch-clamp method yielded a consistent result (*Figure 5.5*). This may be an example whereby enhancement/inhibition of ligand binding to one subunit is affected by co-expression with another subunit. It should also be considered that the presence/absence of nucleotides influences ligand binding. Since the nucleotide pool is significantly depleted under metabolic inhibition, this may explain the discrepancy in this result. I believe the most likely scenario to explain this result is that nucleotide depletion affects the sterical conformation of the NBDs, affecting the overall conformation of the sulphonylurea receptor, which in turn affects the conformation of the pore-forming subunit and the ability of inhibitors specific to Kir6.*x* to bind. Truncation of the pore-forming subunit influences conformational change 'transmitted' to the pore. It is interesting that Kovalev and colleagues showed in their experiments using the *Xenopus oocyte* system that PNU-37883A sensitivity was not affected by KCOs or metabolic inhibition (Kovalev, Quayle et al. 2004). However, they also showed that PNU-37883A shows selectivity for channels containing Kir6.1, whereas I have shown (*Figure 5.7 & Figure 5.6*), as have Cui and colleagues, that Kir6.2-containing channels do show some sensitivity for PNU-37883A (Cui, Tinker et al. 2003). Since we both used the HEK293 expression system, it is possible that the oocyte system affected PNU-37883A sensitivity.

Yi Cui observed that Kir6.2ΔC26 shows a greater sensitivity to PNU-37883A when expressed alone than when expressed with SUR2B (Cui, Tinker et al. 2003). The potency of the drug was seven-fold greater on Kir6.2ΔC26 current than Kir6.2ΔC26/SUR2B. The presence of SUR may in some way hinder access to, or modify the conformation of a drug binding site on the pore-forming subunit. It is also interesting to note that the SUR subunit can also have an effect on the potency of PNU-37883A, with the IC_{50} ranging from about 5μm with SUR2B to 32μm with SUR1

(Surah-Narwal, Xu et al. 1999). It is possible that SUR2B conferred a lower potency of PNU-37883A to the pore than when it was expressed alone. It would be interesting to co-express SUR1 with the truncated Kir6.1 pore-forming subunit to determine whether the result observed remained true. We should bear in mind that that the dependence of SUR is seen for the inhibitory potency of ATP on K_{ATP} channels, even though Kir6.*x* has clearly been identified as the site of inhibitory ATP action (Tucker, Gribble et al. 1997). Similar enhancements have also been observed, whereby the co-expression of Kir6.1 with SUR2B increases SUR2B affinity for PNU-99963 via interaction between these two types of subunits (Cui, Tinker et al. 2003). Also, SUR2B expressed with Kir6.1 has a higher affinity for glibenclamide than SUR2B alone (Russ, Hambrock et al. 1999).

Since a dose-response curve was conducted to assess the ability of PNU-37883A to reverse Kir6.1/SUR2B efflux induced by a KCO, we can assume that the potency of PNU-37883A was not an influencing factor, and that high enough dose of PNU-37883A was applied to observe the ability of PNU-37883A to reverse any efflux passed when the pore was expressed alone, or with SUR2B. However, we should not rule out the possibility that a higher dose of Kir6.*x* inhibitor is required to inhibit the channel under conditions of metabolic inhibition.

I observed a different scenario for Kir6.2ΔC26, which when expressed in the absence of SUR2B was responsive to metabolic inhibition, and for which efflux induced on metabolic inhibition was reversed by both Kir6.*x*-specific inhibitors (*Figure 5.7*). When Kir6.2ΔC26 was expressed with SUR2B, efflux induced by both metabolic inhibition and the KCO was reversed, but again this was not as pronounced as when glibenclamide was applied (*Figure 5.8*). This may be indicative that any sterical change that may occur within the channel when the nucleotide level is depleted is consistent for Kir6.1 and Kir6.2-containing channels. In any case, the data obtained confirms the previously observed constitutive activity of Kir6.2ΔC26, and emphasizes the difference between

Kir6.1ΔC48 and Kir6.2ΔC26 in their intrinsic sensitivity to metabolically induced changes in cytosolic nucleotide levels (*Figure 5.7 & Figure 5.6*).

7.3 The Role of the Sulphonylurea receptor in channel regulation

Perhaps the most interesting, and somewhat controversial, result obtained in this thesis was obtained via assessing the functionality of Kir6.1/SUR2B engineered to contain a mutation within the W_A motifs of NBD1 and NBD2 (*Figure 6.1*). In other ABC transporters, the mutation of these residues has been shown to abolish ATP binding and/or hydrolysis (Azzaria, Schurr et al. 1989; Carson and Welsh 1995; Ko and Pedersen 1995; Ueda, Inagaki et al. 1997; Ueda, Komine et al. 1999), and in SUR1, these mutations prevent activation by Mg-nucleotides (Gribble, Tucker et al. 1997; Shyng, Ferrigni et al. 1997; Gribble, Tucker et al. 1998).

Campbell and colleagues recently built a NBD dimer model of SUR1 (Campbell, Sansom et al. 2003). In this model, the W_A motif of both NBDs interacted with the β-phosphate of ATP. Consistent with this finding, high-affinity ATP binding to site 1 of SUR1 or MRP1 has been shown to be abolished by mutation of the W_A lysine in NBD1, and mutation of the W_A lysine in NBD2 prevented the ability of MgADP to stabilize ATP binding at NBD1 (Ueda, Inagaki et al. 1997). Similarly, the independent or combined mutation of the lysine residues in the W_A motif of NBD1 and NBD2 of SUR1 (K719 and K1384 respectively), abolished channel activation by both MgADP and MgATP (Gribble, Tucker et al. 1997; Shyng, Ferrigni et al. 1997). This loss of MgADP binding and activation can be explained by the fact that the W_A lysine interacts with the β-phosphate of the nucleotide in the NBD dimer model (Campbell, Sansom et al. 2003). The model also suggests that both ATP binding at NBD1 and MgADP binding at site 2 are essential for nucleotide activation of SUR1.

In Chapter 6, it was deduced via $^{86}Rb^+$ flux, and confirmed by the perforated patch-clamp method, that both NBDs need to be mutated simultaneously to obliterate normal functionality of Kir6.1/SUR2B (*Figure 6.1 & Figure 6.5*). When the

corresponding mutations were introduced into Kir6.2/SUR2B, channel functionality was not affected (*Figure 6.2 & Figure 6.4*). With reference to the introductory chapter, *Figure 1.9*, this data does not support the previous model proposed by Matsuo and colleagues, whereby the synergistic action of the NBDs of SUR is required for the nucleotide action of the K_{ATP} channels by SUR subunits (Matsuo, Kimura et al. 2005).

Reimann and colleagues reported that the W_A mutation of NBD2 of SUR2A (K1348A) abolished the channel activation by MgADP, whereas the corresponding mutation of NBD1 (K707A) did not. This supports the idea that NBD2 of SUR is essential for MgADP activation by SUR (Reimann, Gribble et al. 2000). On the other hand, Gribble and colleagues reported that both W_A mutations (K719A and K1345A) are required to abolish channel activation by MgADP (Gribble, Tucker et al. 1997). It was subsequently found that the K708A mutation of SUR1 affects 8-azido-ATP binding not only to NBD1 but also NBD2 (Matsuo, Kimura et al. 2005). Therefore, nucleotide binding at NBD1 could also be important for MgADP activation by affecting nucleotide binding at NBD2, and vice-versa. In fact, nucleotide binding experiments have revealed that when MgADP directly binds to NBD2, or is produced upon hydrolysis of bound MgATP, a conformational change in NBD2 transduces another conformational change in NBD1, to stabilize ATP-binding at NBD1 (Matsuo, Kimura et al. 2005). Similar cooperativity has been found for nucleotide binding to the two NBDs of SUR2A and SUR2B (Matsuo, Tanabe et al. 2000). It is somewhat surprising therefore, that individual mutation of the W_A motifs of NBD1 and NBD2 of SUR2B does not affect the response of the channel to metabolic inhibition (*Figure 6.1*).

It is also interesting that mutation of the glycine residue both within and just outside the signature linker sequence of NBD2 of SUR2B did not affect channel functionality (*Figure 6.3*), considering that there is thought to be functional asymmetry of the NBDs and an involvement of the signature linker sequence in signal transduction. Also, when the corresponding mutations were introduced into SUR1, i.e. G1479D and G1485D (Shyng, Ferrigni et al. 1997), they failed to respond to activation by diazoxide and

stimulation by MgADP. Mutation of the conserved serine in the signature linker sequence of either NBD1 or NBD2 (S830 and S1482 respectively), has been shown to reduce (S830) and abolish (S1482) K_{ATP} channel activation by MgADP (Matsuo, Dabrowski et al. 2002). This is further evidence that the signature linker sequence is involved in signal transduction, and is further evidence for the proposed functional asymmetry of the NBDs. In the model proposed by Campbell and colleagues, the linker serine interacts with the β-phosphate of ATP and the backbone of the W_A glycine in both NBDs (Campbell, Sansom et al. 2003).

On the whole, given the previous evidence discussed, the data obtained from mutation of the NBDs and signature linker sequence is surprising (*Figures 6.1-6.5*). The NBD dimer model created by Campbell and colleagues was created for SUR1, and it is possible that the key residues involved in nucleotide interaction and transduction differ in SUR2B. It would also appear that replacement of Kir6.2 with Kir6.1 in SUR2B-containing channels influences the residues in the Walker motifs that are involved in the catalytic ATPase cycle (Matsuo, Kimura et al. 2005). A preliminary experiment was conducted in which the same W_A lysine was mutated to arginine (K1349R), and threonine 1345 in the W_A phosphate-binding loop in the NBD2 head was mutated to asparagine, and similarly Kir6.1/SUR2B functionality was unaffected (*Figure 6.7*). Since mutation of lysine at position 1349 to either arginine or methionine (i.e. a positively charged or non-polar amino acid) does not affect channel functionality, this may be further indication that ATP does not bind here. Mutation of Arginine 816, residing three positions after the signature linker sequence in the NBD1 tail, to either lysine or glutamine (R816K or R816Q) did not affect channel functionality either (*Figure 6.7*). The mutations screened in *Figure 6.7* were engineered because recent work demonstrated by Vergani and colleagues would indicate that the equivalent residues are involved in dynamic NBD dimerization in the CFTR (Vergani, Lockless et al. 2005). However, this would not necessarily appear to be the case for SUR2B.

Differences in sensitivity between SUR1, SUR2A and SUR2B in the interaction with adenine nucleotides have been reported to exist. The affinities of NBD1 of SUR1 for ATP and ADP (especially ATP) are significantly higher than those of SUR2A and SUR2B. The affinity of NBD2 for ATP is significantly higher than that of SUR2A, and the affinities of NBD2 of SUR2B for ATP and ADP are significantly higher than those of SUR2A. It is possible that these differences in nucleotide binding affinities of SUR subunits are possibly related to differential regulation of K_{ATP} channels. Structural modeling has revealed that seven residues at the central portion of the C-terminal 42 amino acids localize near the W_A motif of NBD2 (Matsushita, Kinoshita et al. 2002). The polar and charged residues in the segment are located within a distance that allows their electrostatic interaction with Arg1344 on the Walker-A loop of NBD2. It is thought that the C-terminal region may alter the sensitivity of K_{ATP} channels to adenine nucleotides by affecting the affinity and/or ATP hydrolysis of NBDs of the sulphonylurea receptor (Babenko, Gonzalez et al. 1999). It is possible, that as well as affecting the strength of nucleotide interaction with the residues in the Walker motifs, these key residues in the C-terminal 42 amino acids influence the exact residues that are involved via slight sterical differences that may be induced between sulphonylurea receptor subtypes. It was recently shown that syntaxin-1A was shown to inhibit K_{ATP} channel by interaction with NBD1 of SUR1. It is possible that other cellular systems or ligands modify the nucleotide binding and/or ATP hydrolysis of each SUR subtype in a different way (Pasyk, Kang et al. 2004).

7.4 Possible extension of these studies

There are a number of issues in continuation of the work presented here that could be addressed in the future. Photoaffinity labelling and scanning with sulfhydryl group reagents accomplished via mutagenesis identified that both N-and C-termini of the pore-forming subunit contribute to recognition of ATP (Trapp, Haider et al. 2003). The most recently developed model implicates two Kir6.2 subunits in the coordination of one ATP molecule. While K185 and R201 in the C-terminus of one subunit and R50 in the N-terminus of another Kir6.2 have been directly implicated in the interaction of the

γ- and β-phosphate of ATP, respectively, the adenine ring interacts with E179 and R301 of the second subunit (Alekseev, Hodgson et al. 2005). It would of interest to mutate the corresponding residues of Kir6.1 to understand the mechanism of ATP inhibition of the pore in Kir6.1/SUR2B channel complexes, and in turn metabolic regulation. It would also be of interest to make chimeras between Kir6.1 and Kir6.2 containing deletion mutants that remove that RKR motif (Kir6.1-Δ48 and Kir6.2-Δ36). Splicing by overlap extension could be applied to swap the N-termini, whole C-terminus and distal C-terminus between Kir6.1 and Kir6.2. Other investigators have found that a number of these are functional in the presence of the coexpressed sulphonylurea receptor (Kondo, Repunte et al. 1998; Takano, Xie et al. 1998). The use of a Kir6.1 chimera has also proved to be a useful technique in the determination of PNU-37883A sensitivity (Kovalev, Quayle et al. 2004). It would be interesting to swap residues of Kir6.2 that confer ATP sensitivity with those of Kir6.1 to determine if sensitivity would be abolished, and to identify if there are residues or structural determinants outside the region exchanged that also make a contribution.

The introduction of mutations into the W_B motif would also prove useful. Mutation of the invariant W_B aspartate of either NBD at either S853 or D1505 of SUR1 has been shown to abolish channel activation by MgADP (Gribble, Tucker et al. 1997; Shyng, Ferrigni et al. 1997), and mutations in NBD1 abolish ATP binding (Ueda, Inagaki et al. 1997). These results are therefore similar to those reported for the W_A lysine. The model proposed by Campbell and colleagues suggests that the W_B aspartate is 6Å away from the ATP molecule; therefore its exact role is not clear. It may be that the structural effects of these mutations disrupt the electrostatic coordination of the ATP molecule, and it would be interesting to see if the same holds true for SUR2B.

I have already begun to subclone SUR2B into two fragments (containing NBD1 and NBD2) into the vectors pEYFP and pECFP (which encode enhanced versions of the green fluorescent protein (GFP) and an enhanced cyan fluorescent protein respectively) and pcDNA3.1. This will enable future Fluorescence Resonance Energy Transfer

(FRET) experiments to be conducted in the future to determine if the two fragments co-localise when expressed with Kir6.1-GFP or Kir6.2-GFP, and to identify which SUR2B fragment interacts with the pore-forming subunit via observation of any conformational change.

It Chapter 3, *Figure 3.13*, it was demonstrated that AMPK may play an indirect response of the channel to metabolic inhibition. It would be of interest to investigate the role of AMPK in native tissue, since the result obtained would obviously be more representative of how AMPK regulates the K_{ATP} channel in a physiological setting.

Ultimately, 3D models and crystallography studies of K_{ATP} channel subunits have been demonstrated to reveal an abundance of information with respect to the function of the channel and the residues involved in nucleotide interaction (Campbell, Sansom et al. 2003; Ashcroft 2005; Mikhailov, Campbell et al. 2005; Ashcroft 2006). Such studies have so far focussed on Kir6.2 and SUR1, and the application of the modelling programs applied to SUR2B will identify any key structural differences, and hopefully enhance our understanding of the metabolic regulation of Kir6.1/SUR2B and clarify the key observations that I have discussed.

Bibliography

Bibliography

Abraham, M. R., V. A. Selivanov, et al. (2002). "Coupling of cell energetics with membrane metabolic sensing. Integrative signaling through creatine kinase phosphotransfer disrupted by M-CK gene knock-out." J Biol Chem 277(27): 24427-34.

Aguilar-Bryan, L. and J. Bryan (1999). "Molecular biology of adenosine triphosphate-sensitive potassium channels." Endocr Rev 20(2): 101-35.

Aguilar-Bryan, L., C. G. Nichols, et al. (1995). "Cloning of the beta cell high-affinity sulfonylurea receptor: a regulator of insulin secretion." Science 268(5209): 423-6.

Akao, M., H. Otani, et al. (1997). "Myocardial ischemia induces differential regulation of K_{ATP} channel gene expression in rat hearts." J Clin Invest 100(12): 3053-9.

Alekseev, A. E., D. M. Hodgson, et al. (2005). "ATP-sensitive K^+ channel channel/enzyme multimer: metabolic gating in the heart." J Mol Cell Cardiol 38(6): 895-905.

Allikmets, R., B. Gerrard, et al. (1996). "Characterization of the human ABC superfamily: isolation and mapping of 21 new genes using the expressed sequence tags database." Hum Mol Genet 5(10): 1649-55.

Amoroso, S., H. Schmid-Antomarchi, et al. (1990). "Glucose, sulfonylureas, and neurotransmitter release: role of ATP-sensitive K_+ channels." Science 247(4944): 852-4.

Antcliff, J. F., S. Haider, et al. (2005). "Functional analysis of a structural model of the ATP-binding site of the K_{ATP} channel Kir6.2 subunit." Embo J 24(2): 229-39.

Ashcroft, F. M. (1988). "Adenosine 5'-triphosphate-sensitive potassium channels." Annu Rev Neurosci 11: 97-118.

Ashcroft, F. M. (2005). "ATP-sensitive potassium channelopathies: focus on insulin secretion." J Clin Invest 115(8): 2047-58.

Ashcroft, F. M. (2006). "From molecule to malady." Nature 440(7083): 440-7.

Ashcroft, F. M. (2006). "K(ATP) channels and insulin secretion: a key role in health and disease." Biochem Soc Trans 34(Pt 2): 243-6.

Ashcroft, F. M. and F. M. Gribble (1998). "Correlating structure and function in ATP-sensitive K^+ channels." Trends Neurosci 21(7): 288-94.

Ashcroft, F. M. and F. M. Gribble (2000). "Tissue-specific effects of sulfonylureas: lessons from studies of cloned K(ATP) channels." J Diabetes Complications 14(4): 192-6.

Ashcroft, F. M., D. E. Harrison, et al. (1984). "Glucose induces closure of single potassium channels in isolated rat pancreatic beta-cells." Nature 312(5993): 446-8.

Ashcroft, F. M. and P. Rorsman (1989). "Electrophysiology of the pancreatic beta-cell." Prog Biophys Mol Biol 54(2): 87-143.

Ashcroft, S. J. and F. M. Ashcroft (1990). "Properties and functions of ATP-sensitive K-channels." Cell Signal 2(3): 197-214.

Ashfield, R., F. M. Gribble, et al. (1999). "Identification of the high-affinity tolbutamide site on the SUR1 subunit of the K(ATP) channel." Diabetes 48(6): 1341-7.

Ashford, M. L., N. C. Sturgess, et al. (1988). "Adenosine-5'-triphosphate-sensitive ion channels in neonatal rat cultured central neurones." Pflugers Arch 412(3): 297-304.

Azzaria, M., E. Schurr, et al. (1989). "Discrete mutations introduced in the predicted nucleotide-binding sites of the mdr1 gene abolish its ability to confer multidrug resistance." Mol Cell Biol 9(12): 5289-97.

Babenko, A. P., L. Aguilar-Bryan, et al. (1998). "A view of sur/KIR6.X, K_{ATP} channels." Annu Rev Physiol 60: 667-87.

Babenko, A. P. and J. Bryan (2001). "A conserved inhibitory and differential stimulatory action of nucleotides on K(IR)6.0/SUR complexes is essential for excitation-metabolism coupling by K(ATP) channels." J Biol Chem 276(52): 49083-92.

Babenko, A. P. and J. Bryan (2002). "SUR-dependent modulation of K_{ATP} channels by an N-terminal KIR6.2 peptide. Defining intersubunit gating interactions." J Biol Chem 277(46): 43997-4004.

Babenko, A. P., G. Gonzalez, et al. (1999). "The N-terminus of KIR6.2 limits spontaneous bursting and modulates the ATP-inhibition of K_{ATP} channels." Biochem Biophys Res Commun 255(2): 231-8.

Babenko, A. P., G. Gonzalez, et al. (2000). "Pharmaco-topology of sulfonylurea receptors. Separate domains of the regulatory subunits of K(ATP) channel isoforms are required for selective interaction with K(+) channel openers." J Biol Chem 275(2): 717-20.

Babenko, A. P., G. C. Gonzalez, et al. (2000). "Hetero-concatemeric KIR6.X4/SUR14 channels display distinct conductivities but uniform ATP inhibition." J Biol Chem 275(41): 31563-6.

Bank, A. J., R. Sih, et al. (2000). "Vascular ATP-dependent potassium channels, nitric oxide, and human forearm reactive hyperemia." Cardiovasc Drugs Ther 14(1): 23-9.

Baraldi, P. G., R. Romagnoli, et al. (2006). "Ligands for A2B adenosine receptor subtype." Curr Med Chem 13(28): 3467-82.

Baraldi, P. G., M. A. Tabrizi, et al. (2003). "Recent developments in the field of A2A and A3 adenosine receptor antagonists." Eur J Med Chem 38(4): 367-82.

Baukrowitz, T. and B. Fakler (2000). "K_{ATP} channels gated by intracellular nucleotides and phospholipids." Eur J Biochem 267(19): 5842-8.

Baukrowitz, T., U. Schulte, et al. (1998). "PIP2 and PIP as determinants for ATP inhibition of K_{ATP} channels." Science 282(5391): 1141-4.

Beech, D. J., H. Zhang, et al. (1993). "K channel activation by nucleotide diphosphates and its inhibition by glibenclamide in vascular smooth muscle cells." Br J Pharmacol 110(2): 573-82.

Belardinelli, L., J. C. Shryock, et al. (1996). "Binding of the novel nonxanthine A2A adenosine receptor antagonist [3H]SCH58261 to coronary artery membranes." Circ Res 79(6): 1153-60.

Belardinelli, L., J. C. Shryock, et al. (1998). "The A2A adenosine receptor mediates coronary vasodilation." J Pharmacol Exp Ther 284(3): 1066-73.

Bienengraeber, M., A. E. Alekseev, et al. (2000). "ATPase activity of the sulfonylurea receptor: a catalytic function for the K_{ATP} channel complex." Faseb J 14(13): 1943-52.

Blau, H. M., C. Webster, et al. (1985). "Evidence for defective myoblasts in Duchenne muscular dystrophy." Adv Exp Med Biol 182: 85-110.

Bonev, A.D. and M.T. Nelson (1993). "ATP-sensitive potassium channels in smooth muscle cells from guinea pig urinary bladder." Am J Physiol 264 (5 Pt 1): C1190-200

Bradley, K. K., J. H. Jaggar, et al. (1999). "Kir2.1 encodes the inward rectifier potassium channel in rat arterial smooth muscle cells." J Physiol 515 (Pt 3): 639-51.

Brayden, J. E. (2002). "Functional roles of K_{ATP} channels in vascular smooth muscle." Clin Exp Pharmacol Physiol 29(4): 312-6.

Bruch, L., S. Rubel, et al. (1998). "Pituitary adenylate cyclase activating peptides relax human pulmonary arteries by opening of K_{ATP} and KCa channels." Thorax 53(7): 586-7.

Brueggemann, A., M. George, et al. (2004). "Ion channel drug discovery and research: the automated Nano-Patch-Clamp technology." Curr Drug Discov Technol 1(1): 91-6.

Bryan, J. and L. Aguilar-Bryan (1999). "Sulfonylurea receptors: ABC transporters that regulate ATP-sensitive K(+) channels." Biochim Biophys Acta 1461(2): 285-303.

Bryan, J., W. H. Vila-Carriles, et al. (2004). "Toward linking structure with function in ATP-sensitive K^+ channels." Diabetes 53 Suppl 3: S104-12.

Budas, G. R., S. Jovanovic, et al. (2004). "Hypoxia-induced preconditioning in adult stimulated cardiomyocytes is mediated by the opening and trafficking of sarcolemmal K_{ATP} channels." Faseb J 18(9): 1046-8.

Butler, A., A. G. Wei, et al. (1989). "A family of putative potassium channel genes in Drosophila." Science 243(4893): 943-7.

Campbell, J. D., M. S. Sansom, et al. (2003). "Potassium channel regulation." EMBO Rep 4(11): 1038-42.

Cao, K., G. Tang, et al. (2002). "Molecular basis of ATP-sensitive K^+ channels in rat vascular smooth muscles." Biochem Biophys Res Commun 296(2): 463-9.

Carling, D. (2004). "The AMP-activated protein kinase cascade--a unifying system for energy control." Trends Biochem Sci 29(1): 18-24.

Carrasco, A. J., P. P. Dzeja, et al. (2001). "Adenylate kinase phosphotransfer communicates cellular energetic signals to ATP-sensitive potassium channels." Proc Natl Acad Sci U S A 98(13): 7623-8.

Carson, M. R. and M. J. Welsh (1995). "Structural and functional similarities between the nucleotide-binding domains of CFTR and GTP-binding proteins." Biophys J 69(6): 2443-8.

Cartier, E. A., L. R. Conti, et al. (2001). "Defective trafficking and function of K_{ATP} channels caused by a sulfonylurea receptor 1 mutation associated with persistent hyperinsulinemic hypoglycemia of infancy." Proc Natl Acad Sci U S A 98(5): 2882-7.

Chan, K. W., H. Zhang, et al. (2003). "N-terminal transmembrane domain of the SUR controls trafficking and gating of Kir6 channel subunits." Embo J 22(15): 3833-43.

Chutkow, W. A., J. C. Makielski, et al. (1999). "Alternative splicing of sur2 Exon 17 regulates nucleotide sensitivity of the ATP-sensitive potassium channel." J Biol Chem 274(19): 13656-65.

Chutkow, W. A., J. Pu, et al. (2002). "Episodic coronary artery vasospasm and hypertension develop in the absence of Sur2 K(ATP) channels." J Clin Invest 110(2): 203-8.

Chutkow, W. A., M. C. Simon, et al. (1996). "Cloning, tissue expression, and chromosomal localization of SUR2, the putative drug-binding subunit of cardiac, skeletal muscle, and vascular K_{ATP} channels." Diabetes 45(10): 1439-45.

Clapp, L. H. and A. Tinker (1998). "Potassium channels in the vasculature." Curr Opin Nephrol Hypertens 7(1): 91-8.

Claycomb, W. C., N. A. Lanson, Jr., et al. (1998). "HL-1 cells: a cardiac muscle cell line that contracts and retains phenotypic characteristics of the adult cardiomyocyte." Proc Natl Acad Sci U S A 95(6): 2979-84.

Clement, J. P. t., K. Kunjilwar, et al. (1997). "Association and stoichiometry of K(ATP) channel subunits." Neuron 18(5): 827-38.

Cohen, M. M., Jr. (2003). "Persistent hyperinsulinemic hypoglycemia of infancy." Am J Med Genet A 122(4): 351-3.

Cole, W. C. and O. Clement-Chomienne (2003). "ATP-sensitive K^+ channels of vascular smooth muscle cells." J Cardiovasc Electrophysiol 14(1): 94-103.

Cole, W. C., T. Malcolm, et al. (2000). "Inhibition by protein kinase C of the K(NDP) subtype of vascular smooth muscle ATP-sensitive potassium channel." Circ Res 87(2): 112-7.

Conti, L. R., C. M. Radeke, et al. (2001). "Transmembrane topology of the sulfonylurea receptor SUR1." J Biol Chem 276(44): 41270-8.

Cook, D. L. and C. N. Hales (1984). "Intracellular ATP directly blocks K^+ channels in pancreatic B-cells." Nature 311(5983): 271-3.

Cook, D. L., L. S. Satin, et al. (1988). "ATP-sensitive K^+ channels in pancreatic beta-cells. Spare-channel hypothesis." Diabetes 37(5): 495-8.

Crawford, R. M., G. R. Budas, et al. (2002). "M-LDH serves as a sarcolemmal K(ATP) channel subunit essential for cell protection against ischemia." Embo J 21(15): 3936-48.

Crawford, R. M., S. Jovanovic, et al. (2003). "Chronic mild hypoxia protects heart-derived H9c2 cells against acute hypoxia/reoxygenation by regulating expression of the SUR2A subunit of the ATP-sensitive K^+ channel." J Biol Chem 278(33): 31444-55.

Crawford, R. M., H. J. Ranki, et al. (2002). "Creatine kinase is physically associated with the cardiac ATP-sensitive K^+ channel in vivo." Faseb J 16(1): 102-4.

Cui, Y., J. P. Giblin, et al. (2001). "A mechanism for ATP-sensitive potassium channel diversity: Functional coassembly of two pore-forming subunits." Proc Natl Acad Sci U S A 98(2): 729-34.

Cui, Y., A. Tinker, et al. (2003). "Different molecular sites of action for the K_{ATP} channel inhibitors, PNU-99963 and PNU-37883A." Br J Pharmacol 139(1): 122-8.

Cui, Y., S. Tran, et al. (2002). "The molecular composition of K(ATP) channels in human pulmonary artery smooth muscle cells and their modulation by growth." Am J Respir Cell Mol Biol 26(1): 135-43.

D'Hahan, N., C. Moreau, et al. (1999). "Pharmacological plasticity of cardiac ATP-sensitive potassium channels toward diazoxide revealed by ADP." Proc Natl Acad Sci U S A 96(21): 12162-7.

Dart, C. and N. B. Standen (1993). "Adenosine-activated potassium current in smooth muscle cells isolated from the pig coronary artery." J Physiol 471: 767-86.

Dart, C. and N. B. Standen (1995). "Activation of ATP-dependent K^+ channels by hypoxia in smooth muscle cells isolated from the pig coronary artery." J Physiol 483 (Pt 1): 29-39.

Davies, S. P., H. Reddy, et al. (2000). "Specificity and mechanism of action of some commonly used protein kinase inhibitors." Biochem J 351(Pt 1): 95-105.

Dean, M., Y. Hamon, et al. (2001). "The human ATP-binding cassette (ABC) transporter superfamily." J Lipid Res 42(7): 1007-17.

Dhar-Chowdhury, P., M. D. Harrell, et al. (2005). "The glycolytic enzymes, glyceraldehyde-3-phosphate dehydrogenase, triose-phosphate isomerase, and pyruvate kinase are components of the K(ATP) channel macromolecular complex and regulate its function." J Biol Chem 280(46): 38464-70.

Dong, K., L. Q. Tang, et al. (2005). "Novel nucleotide-binding sites in ATP-sensitive potassium channels formed at gating interfaces." Embo J 24(7): 1318-29.

Drain, P., L. Li, et al. (1998). "K_{ATP} channel inhibition by ATP requires distinct functional domains of the cytoplasmic C terminus of the pore-forming subunit." Proc Natl Acad Sci U S A 95(23): 13953-8.

Du, Q., S. Jovanovic, et al. (2006). "Overexpression of SUR2A generates a cardiac phenotype resistant to ischemia." Faseb J 20(8): 1131-41.

Duflot, S., B. Riera, et al. (2004). "ATP-sensitive K(+) channels regulate the concentrative adenosine transporter CNT2 following activation by A(1) adenosine receptors." Mol Cell Biol 24(7): 2710-9.

Dugravot, S., F. Grolleau, et al. (2003). "Dimethyl disulfide exerts insecticidal neurotoxicity through mitochondrial dysfunction and activation of insect K(ATP) channels." J Neurophysiol 90(1): 259-70.

Duncker, D. J., H. H. Oei, et al. (2001). "Role of K(ATP)(+) channels in regulation of systemic, pulmonary, and coronary vasomotor tone in exercising swine." Am J Physiol Heart Circ Physiol 280(1): H22-33.

Duncker, D. J., N. S. Van Zon, et al. (1993). "Role of K^+ATP channels in coronary vasodilation during exercise." Circulation 88(3): 1245-53.

Duncker, D. J., N. S. van Zon, et al. (1995). "Endogenous adenosine mediates coronary vasodilation during exercise after K(ATP)+ channel blockade." J Clin Invest 95(1): 285-95.

Dunne, M. J., K. E. Cosgrove, et al. (2004). "Hyperinsulinism in infancy: from basic science to clinical disease." Physiol Rev 84(1): 239-75.

Dunne, M. J. and O. H. Petersen (1991). "Potassium selective ion channels in insulin-secreting cells: physiology, pharmacology and their role in stimulus-secretion coupling." Biochim Biophys Acta 1071(1): 67-82.

Enkvetchakul, D., G. Loussouarn, et al. (2000). "The kinetic and physical basis of K(ATP) channel gating: toward a unified molecular understanding." Biophys J 78(5): 2334-48.

Enkvetchakul, D. and C. G. Nichols (2003). "Gating mechanism of K_{ATP} channels: function fits form." J Gen Physiol 122(5): 471-80.

Faivre, J. F. and I. Findlay (1989). "Effects of tolbutamide, glibenclamide and diazoxide upon action potentials recorded from rat ventricular muscle." Biochim Biophys Acta 984(1): 1-5.

Faraci, F. M. and C. G. Sobey (1998). "Role of potassium channels in regulation of cerebral vascular tone." J Cereb Blood Flow Metab 18(10): 1047-63.

Findlay, I. (1988). "Effects of ADP upon the ATP-sensitive K^+ channel in rat ventricular myocytes." J Membr Biol 101(1): 83-92.

Findlay, I. and M. J. Dunne (1986). "ATP maintains ATP-inhibited K^+ channels in an operational state." Pflugers Arch 407(2): 238-40.

Fluckiger-Isler, R. E. and P. Walter (1993). "Stimulation of rat liver glycogen synthesis by the adenosine kinase inhibitor 5-iodotubercidin." Biochem J 292 (Pt 1): 85-91.

Fox, J. E., L. Jones, et al. (2005). "Identification and pharmacological characterization of sarcolemmal ATP-sensitive potassium channels in the murine atrial HL-1 cell line." J Cardiovasc Pharmacol 45(1): 30-5.

Fredholm, B. B., I. J. AP, et al. (2001). "International Union of Pharmacology. XXV. Nomenclature and classification of adenosine receptors." Pharmacol Rev 53(4): 527-52.

Fujita, A. and Y.Kurachi (2000). "Molecular aspects of ATP-sensitive K^+ channels in the cardiovascular system and K^+ channel openers." Pharmacol Ther 85(1): 39-53

Fujita, H., T. Ogura, et al. (2006). "A key role for the subunit SUR2B in the preferential activation of vascular K_{ATP} channels by isoflurane." Br J Pharmacol 149(5): 573-80.

Garland, J. G. and G. A. McPherson (1992). "Evidence that nitric oxide does not mediate the hyperpolarization and relaxation to acetylcholine in the rat small mesenteric artery." Br J Pharmacol 105(2): 429-35.

Ghosh, A., P. Ronner, et al. (1991). "The role of ATP and free ADP in metabolic coupling during fuel-stimulated insulin release from islet beta-cells in the isolated perfused rat pancreas." J Biol Chem 266(34): 22887-92.

Giblin, J. P., J. L. Leaney, et al. (1999). "The molecular assembly of ATP-sensitive potassium channels. Determinants on the pore forming subunit." J Biol Chem 274(32): 22652-9.

Giblin, J. P., K. Quinn, et al. (2002). "The cytoplasmic C-terminus of the sulfonylurea receptor is important for K_{ATP} channel function but is not key for complex assembly or trafficking." Eur J Biochem 269(21): 5303-13.

Glitsch, H. G. and A. Tappe (1993). "The $Na+/K^+$ pump of cardiac Purkinje cells is preferentially fuelled by glycolytic ATP production." Pflugers Arch 422(4): 380-5.

Gottesman, M. M. (1988). "Multidrug resistance during chemical carcinogenesis: a mechanism revealed?" J Natl Cancer Inst 80(17): 1352-3.

Gribble, F. M. and F. Reimann (2003). "Sulphonylurea action revisited: the post-cloning era." Diabetologia 46(7): 875-91.

Gribble, F. M., S. J. Tucker, et al. (1997). "The essential role of the Walker A motifs of SUR1 in K-ATP channel activation by Mg-ADP and diazoxide." Embo J 16(6): 1145-52.

Gribble, F. M., S. J. Tucker, et al. (1998). "MgATP activates the beta cell K_{ATP} channel by interaction with its SUR1 subunit." Proc Natl Acad Sci U S A 95(12): 7185-90.

Hambrock, A., C. Loffler-Walz, et al. (1999). "ATP-Sensitive K^+ channel modulator binding to sulfonylurea receptors SUR2A and SUR2B: opposite effects of MgADP." Mol Pharmacol 55(5): 832-40.

Hamill, O. P., A. Marty, et al. (1981). "Improved patch-clamp techniques for high-resolution current recording from cells and cell-free membrane patches." Pflugers Arch 391(2): 85-100.

Hardie, D. G. and D. Carling (1997). "The AMP-activated protein kinase--fuel gauge of the mammalian cell?" Eur J Biochem 246(2): 259-73.

Hardie, D. G., S. A. Hawley, et al. (2006). "AMP-activated protein kinase--development of the energy sensor concept." J Physiol 574(Pt 1): 7-15.

Hayabuchi, Y., N. B. Standen, et al. (2001). "Angiotensin II inhibits and alters kinetics of voltage-gated K(+) channels of rat arterial smooth muscle." Am J Physiol Heart Circ Physiol 281(6): H2480-9.

Helling RB, G. H., Boyer HW (1974). "Analysis of R.EcoRI fragments of DNA from lamboid bacteriophages and other viruses by agarose-gel electrophoresis." J.Virol 14: 1235-1244.

Higgins, C. F. (1992). "ABC transporters: from microorganisms to man." Annu Rev Cell Biol 8: 67-113.

Higgins, C. F. and K. J. Linton (2004). "The ATP switch model for ABC transporters." Nat Struct Mol Biol 11(10): 918-26.

Hilgemann, D. W. and R. Ball (1996). "Regulation of cardiac Na+,Ca2+ exchange and K_{ATP} potassium channels by PIP2." Science 273(5277): 956-9.

Hille, B. (1992). "Ionic channels of excitable cells." Sinauer, Massachusetts: 1-20.

Ho, K., C. G. Nichols, et al. (1993). "Cloning and expression of an inwardly rectifying ATP-regulated potassium channel." Nature 362(6415): 31-8.

Hopfner, K. P., A. Karcher, et al. (2000). "Structural biology of Rad50 ATPase: ATP-driven conformational control in DNA double-strand break repair and the ABC-ATPase superfamily." Cell 101(7): 789-800.

Humphrey, S. J., M. P. Smith, et al. (1996). "Cardiovascular effects of the K-ATP channel blocker U-37883A and structurally related morpholinoguanidines." Methods Find Exp Clin Pharmacol 18(4): 247-60.

Hung, L. W., I. X. Wang, et al. (1998). "Crystal structure of the ATP-binding subunit of an ABC transporter." Nature 396(6712): 703-7.

Hunter, M. and G. Giebisch (1988). "Calcium-activated K-channels of Amphiuma early distal tubule: inhibition by ATP." Pflugers Arch 412(3): 331-3.

Huopio, H., S. L. Shyng, et al. (2002). "K(ATP) channels and insulin secretion disorders." Am J Physiol Endocrinol Metab 283(2): E207-16.

Hyde, S. C., P. Emsley, et al. (1990). "Structural model of ATP-binding proteins associated with cystic fibrosis, multidrug resistance and bacterial transport." Nature 346(6282): 362-5.

Inagaki, N., T. Gonoi, et al. (1996). "A family of sulfonylurea receptors determines the pharmacological properties of ATP-sensitive K^+ channels." Neuron 16(5): 1011-7.

Inagaki, N., T. Gonoi, et al. (1997). "Subunit stoichiometry of the pancreatic beta-cell ATP-sensitive K^+ channel." FEBS Lett 409(2): 232-6.

Inagaki, N. and S. Seino (1998). "ATP-sensitive potassium channels: structures, functions, and pathophysiology." Jpn J Physiol 48(6): 397-412.

Inagaki, N., Y. Tsuura, et al. (1995). "Cloning and functional characterization of a novel ATP-sensitive potassium channel ubiquitously expressed in rat tissues, including pancreatic islets, pituitary, skeletal muscle, and heart." J Biol Chem 270(11): 5691-4.

Ishibashi, Y., D. J. Duncker, et al. (1998). "ATP-sensitive K^+ channels, adenosine, and nitric oxide-mediated mechanisms account for coronary vasodilation during exercise." Circ Res 82(3): 346-59.

Isomoto, S., C. Kondo, et al. (1997). "Inwardly rectifying potassium channels: their molecular heterogeneity and function." Jpn J Physiol 47(1): 11-39.

Isomoto, S., C. Kondo, et al. (1996). "A novel sulfonylurea receptor forms with BIR (Kir6.2) a smooth muscle type ATP-sensitive K^+ channel." J Biol Chem 271(40): 24321-4.

Itani T, A. H., Yamaguchi N, Tadakuma T, Yasuda T. (1987). "A simple and efficient liposome method for transfection of DNA into mammalian cells grown in suspension." Gene 56: 267-276.

Jackson, W. F. (2000). "Hypoxia does not activate ATP-sensitive K^+ channels in arteriolar muscle cells." Microcirculation 7(2): 137-45.

Jackson, W. F. (2005). "Potassium channels in the peripheral microcirculation." Microcirculation 12(1): 113-27.

John, S. A., J. R. Monck, et al. (1998). "The sulphonylurea receptor SUR1 regulates ATP-sensitive mouse Kir6.2 K^+ channels linked to the green fluorescent protein in human embryonic kidney cells (HEK 293)." J Physiol 510 (Pt 2): 333-45.

Jovanovic, S., Q. Du, et al. (2005). "Glyceraldehyde 3-phosphate dehydrogenase serves as an accessory protein of the cardiac sarcolemmal K(ATP) channel." EMBO Rep 6(9): 848-52.

Kahn, B. B., T. Alquier, et al. (2005). "AMP-activated protein kinase: ancient energy gauge provides clues to modern understanding of metabolism." Cell Metab 1(1): 15-25.

Kamei, K., S. Yoshida, et al. (1994). "Regional and species differences in glyburide-sensitive K+ channels in airway smooth muscles as estimated from actions of KC 128 and levcromakalim." Br J Pharmacol 113(3): 889-97.

Kamouchi, M., K. Van Den Bremt, et al. (1997). "Modulation of inwardly rectifying potassium channels in cultured bovine pulmonary artery endothelial cells." J Physiol 504 (Pt 3): 545-56.

Kane, C., R. M. Shepherd, et al. (1996). "Loss of functional K_{ATP} channels in pancreatic beta-cells causes persistent hyperinsulinemic hypoglycemia of infancy." Nat Med 2(12): 1344-7.

Kane, G. C., C. F. Lam, et al. (2006). "Gene knockout of the KCNJ8-encoded Kir6.1 K(ATP) channel imparts fatal susceptibility to endotoxemia." Faseb J 20(13): 2271-80.

Kang, Y., B. Ng, et al. (2006). "Syntaxin-1A actions on sulfonylurea receptor 2A can block acidic pH-induced cardiac K(ATP) channel activation." J Biol Chem 281(28): 19019-28.

Kerr, I. D. (2002). "Structure and association of ATP-binding cassette transporter nucleotide-binding domains." Biochim Biophys Acta 1561(1): 47-64.

Ketchum, K. A., W. J. Joiner, et al. (1995). "A new family of outwardly rectifying potassium channel proteins with two pore domains in tandem." Nature 376(6542): 690-5.

Kim, E. K., I. Miller, et al. (2004). "C75, a fatty acid synthase inhibitor, reduces food intake via hypothalamic AMP-activated protein kinase." J Biol Chem 279(19): 19970-6.

Kingsbury, M. P., H. Robinson, et al. (2001). "Investigation of mechanisms that mediate reactive hyperaemia in guinea-pig hearts: role of K(ATP) channels, adenosine, nitric oxide and prostaglandins." Br J Pharmacol 132(6): 1209-16.

Kleppisch, T. and M. T. Nelson (1995). "Adenosine activates ATP-sensitive potassium channels in arterial myocytes via A2 receptors and cAMP-dependent protein kinase." Proc Natl Acad Sci U S A 92(26): 12441-5.

Kleta, R. and D. Bockenhauer (2006). "Bartter syndromes and other salt-losing tubulopathies." Nephron Physiol 104(2): p73-80.

Klinger, M., M. Freissmuth, et al. (2002). "Adenosine receptors: G protein-mediated signalling and the role of accessory proteins." Cell Signal 14(2): 99-108.

Ko, Y. H. and P. L. Pedersen (1995). "The first nucleotide binding fold of the cystic fibrosis transmembrane conductance regulator can function as an active ATPase." J Biol Chem 270(38): 22093-6.

Kondo, C., V. P. Repunte, et al. (1998). "Chimeras of Kir6.1 and Kir6.2 reveal structural elements involved in spontaneous opening and unitary conductance of the ATP-sensitive K^+ channels." Receptors Channels 6(2): 129-40.

Konstas, A. A., M. Dabrowski, et al. (2002). "Intrinsic sensitivity of Kir1.1 (ROMK) to glibenclamide in the absence of SUR2B. Implications for the identity of the renal ATP-regulated secretory K^+ channel." J Biol Chem 277(24): 21346-51.

Koster, J. C., Q. Sha, et al. (1999). "ATP inhibition of K_{ATP} channels: control of nucleotide sensitivity by the N-terminal domain of the Kir6.2 subunit." J Physiol 515 (Pt 1): 19-30.

Kovalev, H., J. M. Quayle, et al. (2004). "Molecular analysis of the subtype-selective inhibition of cloned K_{ATP} channels by PNU-37883A." Br J Pharmacol 141(5): 867-73.

Kubo, M., J. M. Quayle, et al. (1997). "Angiotensin II inhibition of ATP-sensitive K^+ currents in rat arterial smooth muscle cells through protein kinase C." J Physiol 503 (Pt 3): 489-96.

Kubo, Y., T. J. Baldwin, et al. (1993). "Primary structure and functional expression of a mouse inward rectifier potassium channel." Nature 362(6416): 127-33.

Landree, L. E., A. L. Hanlon, et al. (2004). "C75, a fatty acid synthase inhibitor, modulates AMP-activated protein kinase to alter neuronal energy metabolism." J Biol Chem 279(5): 3817-27.

Landry, D. W. and J. A. Oliver (2001). "The pathogenesis of vasodilatory shock." N Engl J Med 345(8): 588-95.

Lawrence, K. M., A. Chanalaris, et al. (2002). "K(ATP) channel gene expression is induced by urocortin and mediates its cardioprotective effect." Circulation 106(12): 1556-62.

Lederer, W. J. and C. G. Nichols (1989). "Nucleotide modulation of the activity of rat heart ATP-sensitive K^+ channels in isolated membrane patches." J Physiol 419: 193-211.

Lee, M., J. T. Hwang, et al. (2003). "AMP-activated protein kinase activity is critical for hypoxia-inducible factor-1 transcriptional activity and its target gene expression under hypoxic conditions in DU145 cells." J Biol Chem 278(41): 39653-61.

Lee, W. S., Y. J. Kwon, et al. (1993). "Disturbances in autoregulatory responses of rat pial arteries by sulfonylureas." Life Sci 52(19): 1527-34.

Lesage, F., R. Reyes, et al. (1996). "Dimerization of TWIK-1 K^+ channel subunits via a disulfide bridge." Embo J 15(23): 6400-7.

Li, L., J. Wang, et al. (2000). "The I182 region of k(ir)6.2 is closely associated with ligand binding in K(ATP) channel inhibition by ATP." Biophys J 79(2): 841-52.

Li, L., J. Wu, et al. (2003). "Differential expression of Kir6.1 and SUR2B mRNAs in the vasculature of various tissues in rats." J Membr Biol 196(1): 61-9.

Light, P. E., C. Bladen, et al. (2000). "Molecular basis of protein kinase C-induced activation of ATP-sensitive potassium channels." Proc Natl Acad Sci U S A 97(16): 9058-63.

Lin, Y. W., T. Jia, et al. (2003). "Stabilization of the activity of ATP-sensitive potassium channels by ion pairs formed between adjacent Kir6.2 subunits." J Gen Physiol 122(2): 225-37.

Linton, K. J. and C. F. Higgins (1998). "The Escherichia coli ATP-binding cassette (ABC) proteins." Mol Microbiol 28(1): 5-13.

Linton, K.J. (2007). "Structure and Function of ABC Transporters". Physiology (Bethesda) 22: 122-130.

Liu, Y., W. D. Gao, et al. (1996). "Cell-type specificity of preconditioning in an in vitro model." Basic Res Cardiol 91(6): 450-7.

Liu, Y., W. D. Gao, et al. (1997). "Priming effect of adenosine on K(ATP) currents in intact ventricular myocytes: implications for preconditioning." Am J Physiol 273(4 Pt 2): H1637-43.

Locher, K. P., A. T. Lee, et al. (2002). "The E. coli BtuCD structure: a framework for ABC transporter architecture and mechanism." Science 296(5570): 1091-8.

Lu, T., M. P. Hong, et al. (2005). "Molecular determinants of cardiac K(ATP) channel activation by epoxyeicosatrienoic acids." J Biol Chem 280(19): 19097-104.

MacGregor, G. G., K. Dong, et al. (2002). "Nucleotides and phospholipids compete for binding to the C terminus of K_{ATP} channels." Proc Natl Acad Sci U S A 99(5): 2726-31.

Makhina, E. N. and C. G. Nichols (1998). "Independent trafficking of K_{ATP} channel subunits to the plasma membrane." J Biol Chem 273(6): 3369-74.

Margeta-Mitrovic, M. (2002). "Assembly-dependent trafficking assays in the detection of receptor-receptor interactions." Methods 27(4): 311-7.

Markworth, E., C. Schwanstecher, et al. (2000). "ATP4- mediates closure of pancreatic beta-cell ATP-sensitive potassium channels by interaction with 1 of 4 identical sites." Diabetes 49(9): 1413-8.

Masia, R., D. Enkvetchakul, et al. (2005). "Differential nucleotide regulation of K_{ATP} channels by SUR1 and SUR2A." J Mol Cell Cardiol 39(3): 491-501.

Massillon, D., W. Stalmans, et al. (1994). "Identification of the glycogenic compound 5-iodotubercidin as a general protein kinase inhibitor." Biochem J 299 (Pt 1): 123-8.

Matsuo, M., M. Dabrowski, et al. (2002). "Mutations in the linker domain of NBD2 of SUR inhibit transduction but not nucleotide binding." Embo J 21(16): 4250-8.

Matsuo, M., Y. Kimura, et al. (2005). "K_{ATP} channel interaction with adenine nucleotides." J Mol Cell Cardiol 38(6): 907-16.

Matsuo, M., K. Tanabe, et al. (2000). "Different binding properties and affinities for ATP and ADP among sulfonylurea receptor subtypes, SUR1, SUR2A, and SUR2B." J Biol Chem 275(37): 28757-63.

Matsushita, K., K. Kinoshita, et al. (2002). "Intramolecular interaction of SUR2 subtypes for intracellular ADP-Induced differential control of K(ATP) channels." Circ Res 90(5): 554-61.

Mattheakis, L. C. and A. Savchenko (2001). "Assay technologies for screening ion channel targets." Curr Opin Drug Discov Devel 4(1): 124-34.

McCullough, L. D., Z. Zeng, et al. (2005). "Pharmacological inhibition of AMP-activated protein kinase provides neuroprotection in stroke." J Biol Chem 280(21): 20493-502.

McDonald, T. F. and D. P. MacLeod (1973). "Metabolism and the electrical activity of anoxic ventricular muscle." J Physiol 229(3): 559-82.

Meggio, F., A. Donella Deana, et al. (1995). "Different susceptibility of protein kinases to staurosporine inhibition. Kinetic studies and molecular bases for the resistance of protein kinase CK2." Eur J Biochem 234(1): 317-22.

Meisheri, K. D., S. J. Humphrey, et al. (1993). "4-morpholinecarboximidine-N-1-adamantyl-N'-cyclohexylhydrochloride (U-37883A): pharmacological characterization of a novel antagonist of vascular ATP-sensitive K^+ channel openers." J Pharmacol Exp Ther 266(2): 655-65.

Melamed-Frank, M., A. Terzic, et al. (2001). "Reciprocal regulation of expression of pore-forming K_{ATP} channel genes by hypoxia." Mol Cell Biochem 225(1-): 145-50.

Melchert, P. J., D. J. Duncker, et al. (1999). "Role of K(+)(ATP) channels and adenosine in regulation of coronary blood flow in the hypertrophied left ventricle." Am J Physiol 277(2 Pt 2): H617-25.

Mikhailov, M. V., J. D. Campbell, et al. (2005). "3-D structural and functional characterization of the purified K_{ATP} channel complex Kir6.2-SUR1." Embo J 24(23): 4166-75.

Mikhailov, M. V., E. A. Mikhailova, et al. (2000). "Investigation of the molecular assembly of beta-cell K(ATP) channels." FEBS Lett 482(1-2): 59-64.

Mikhailov, M. V., E. A. Mikhailova, et al. (2001). "Molecular structure of the glibenclamide binding site of the beta-cell K(ATP) channel." FEBS Lett 499(1-2): 154-60.

Miki, T., K. Nagashima, et al. (1999). "The structure and function of the ATP-sensitive K^+ channel in insulin-secreting pancreatic beta-cells." J Mol Endocrinol 22(2): 113-23.

Miki, T., M. Suzuki, et al. (2002). "Mouse model of Prinzmetal angina by disruption of the inward rectifier Kir6.1." Nat Med 8(5): 466-72.

Miwa, A., K. Ueda, et al. (1997). "Protein kinase C-independent correlation between P-glycoprotein expression and volume sensitivity of Cl- channel." J Membr Biol 157(1): 63-9.

Miyoshi, H., Y. Nakaya, et al. (1994). "Nonendothelial-derived nitric oxide activates the ATP-sensitive K^+ channel of vascular smooth muscle cells." FEBS Lett 345(1): 47-9.

Moreau, C., H. Jacquet, et al. (2000). "The molecular basis of the specificity of action of K(ATP) channel openers." Embo J 19(24): 6644-51.

Moritz, W., C. A. Leech, et al. (2001). "Regulated expression of adenosine triphosphate-sensitive potassium channel subunits in pancreatic beta-cells." Endocrinology 142(1): 129-38.

Murphy, M. E. and J. E. Brayden (1995). "Nitric oxide hyperpolarizes rabbit mesenteric arteries via ATP-sensitive potassium channels." J Physiol 486 (Pt 1): 47-58.

Muzyamba, M., T. Farzaneh, et al. (2007). "Complex ABCC8 DNA variations in congenital hyperinsulinism: lessons from functional studies." Clin Endocrinol (Oxf) 67(1): 115-24.

Nakashima, M. and P. M. Vanhoutte (1995). "Isoproterenol causes hyperpolarization through opening of ATP-sensitive potassium channels in vascular smooth muscle of the canine saphenous vein." J Pharmacol Exp Ther 272(1): 379-84.

Nelson, M. T., Y. Huang, et al. (1990). "Arterial dilations in response to calcitonin gene-related peptide involve activation of K^+ channels." Nature 344(6268): 770-3.

Nelson, M. T. and J. M. Quayle (1995). "Physiological roles and properties of potassium channels in arterial smooth muscle." Am J Physiol 268(4 Pt 1): C799-822.

Nichols, C. G. (2006). "K_{ATP} channels as molecular sensors of cellular metabolism." Nature 440: 470-466.

Nichols, C. G. and W. J. Lederer (1991). "Adenosine triphosphate-sensitive potassium channels in the cardiovascular system." Am J Physiol 261(6 Pt 2): H1675-86.

Nichols, C. G. and A. N. Lopatin (1997). "Inward rectifier potassium channels." Annu Rev Physiol 59: 171-91.

Nichols, C. G., S. L. Shyng, et al. (1996). "Adenosine diphosphate as an intracellular regulator of insulin secretion." Science 272(5269): 1785-7.

Noma, A. (1983). "ATP-regulated K^+ channels in cardiac muscle." Nature 305(5930): 147-8.

Novellino, E., B. Cosimelli, et al. (2005). "2-(Benzimidazol-2-yl)quinoxalines: a novel class of selective antagonists at human A(1) and A(3) adenosine receptors designed by 3D database searching." J Med Chem 48(26): 8253-60.

O'Brien Aj, T. G., Cui Y, Singer M, Clapp LH (2002). "Inhibition of the pore-vlocking subunit of the K_{ATP} channel partially reverses endotoxin-induced vascular hyporeactivity in rat superior mesenteric artery." Br J Pharmacol 135.

Ohno-Shosaku, T., B. J. Zunkler, et al. (1987). "Dual effects of ATP on K^+ currents of mouse pancreatic beta-cells." Pflugers Arch 408(2): 133-8.

Okuyama, Y., M. Yamada, et al. (1998). "The effects of nucleotides and potassium channel openers on the SUR2A/Kir6.2 complex K^+ channel expressed in a mammalian cell line, HEK293T cells." Pflugers Arch 435(5): 595-603.

Oswald, C., I. B. Holland, et al. (2006). "The motor domains of ABC-transporters. What can structures tell us?" Naunyn Schmiedebergs Arch Pharmacol 372(6): 385-99.

Otonkoski, T., C. Ammala, et al. (1999). "A point mutation inactivating the sulfonylurea receptor causes the severe form of persistent hyperinsulinemic hypoglycemia of infancy in Finland." Diabetes 48(2): 408-15.

Park, W. S., N. Kim, et al. (2006). "Angiotensin II inhibits inward rectifier K+ channels in rabbit coronary arterial smooth muscle cells through protein kinase Calpha." Biochem Biophys Res Commun 341(3): 728-35.

Partridge, C. J., D. J. Beech, et al. (2001). "Identification and pharmacological correction of a membrane trafficking defect associated with a mutation in the sulfonylurea receptor causing familial hyperinsulinism." J Biol Chem 276(38): 35947-52.

Pasyk, E. A., Y. Kang, et al. (2004). "Syntaxin-1A binds the nucleotide-binding folds of sulphonylurea receptor 1 to regulate the K_{ATP} channel." J Biol Chem 279(6): 4234-40.

Paulusma, C. C., P. J. Bosma, et al. (1996). "Congenital jaundice in rats with a mutation in a multidrug resistance-associated protein gene." Science 271(5252): 1126-8.

Ploug, K. B., L. Edvinsson, et al. (2006). "Pharmacological and molecular comparison of K(ATP) channels in rat basilar and middle cerebral arteries." Eur J Pharmacol 553(1-3): 254-62.

Proks, P. and F. M. Ashcroft (1997). "Phentolamine block of K_{ATP} channels is mediated by Kir6.2." Proc Natl Acad Sci U S A 94(21): 11716-20.

Proks, P., F. M. Gribble, et al. (1999). "Involvement of the N-terminus of Kir6.2 in the inhibition of the K_{ATP} channel by ATP." J Physiol 514 (Pt 1): 19-25.

Puck, T. T. (1957). "The genetics of somatic mammalian cells." Adv Biol Med Phys 5: 75-101.

Quayle, J. M., J. G. McCarron, et al. (1993). "Inward rectifier K^+ currents in smooth muscle cells from rat resistance-sized cerebral arteries." Am J Physiol 265(5 Pt 1): C1363-70.

Quayle, J. M., M. T. Nelson, et al. (1997). "ATP-sensitive and inwardly rectifying potassium channels in smooth muscle." Physiol Rev 77(4): 1165-232.

Quayle, J. M. and N. B. Standen (1994). "K_{ATP} channels in vascular smooth muscle." Cardiovasc Res 28(6): 797-804.

Quayle, J. M., M. R. Turner, et al. (2006). "Effects of hypoxia, anoxia, and metabolic inhibitors on K_{ATP} channels in rat femoral artery myocytes." Am J Physiol Heart Circ Physiol 291(1): H71-80.

Quinn, K. V., Y. Cui, et al. (2003). "Do anionic phospholipids serve as cofactors or second messengers for the regulation of activity of cloned ATP-sensitive K^+ channels?" Circ Res 93(7): 646-55.

Quinn, K. V., J. P. Giblin, et al. (2004). "Multisite phosphorylation mechanism for protein kinase A activation of the smooth muscle ATP-sensitive K^+ channel." Circ Res 94(10): 1359-66.

Raab-Graham, K. F., L. J. Cirilo, et al. (1999). "Membrane topology of the amino-terminal region of the sulfonylurea receptor." J Biol Chem 274(41): 29122-9.

Rainbow, R. D., M. James, et al. (2004). "Proximal C-terminal domain of sulphonylurea receptor 2A interacts with pore-forming Kir6 subunits in K_{ATP} channels." Biochem J 379(Pt 1): 173-81.

Ranki, H. J., R. M. Crawford, et al. (2002). "Ageing is associated with a decrease in the number of sarcolemmal ATP-sensitive K^+ channels in a gender-dependent manner." Mech Ageing Dev 123(6): 695-705.

Ray, P., F. L. Monroe, et al. (1991). "Cyanide sensitive and insensitive bioenergetics in a clonal neuroblastoma x glioma hybrid cell line." Neurochem Res 16(10): 1121-4.

Reid, J. M., D. J. Paterson, et al. (1993). "The effect of tolbutamide on cerebral blood flow during hypoxia and hypercapnia in the anaesthetized rat." Pflugers Arch 425(3-4): 362-4.

Reimann, F., M. Dabrowski, et al. (2003). "Analysis of the differential modulation of sulphonylurea block of beta-cell and cardiac ATP-sensitive K^+ (K(ATP)) channels by Mg-nucleotides." J Physiol 547(Pt 1): 159-68.

Reimann, F., F. M. Gribble, et al. (2000). "Differential response of K(ATP) channels containing SUR2A or SUR2B subunits to nucleotides and pinacidil." Mol Pharmacol 58(6): 1318-25.

Reimann, F., P. Proks, et al. (2001). "Effects of mitiglinide (S 21403) on Kir6.2/SUR1, Kir6.2/SUR2A and Kir6.2/SUR2B types of ATP-sensitive potassium channel." Br J Pharmacol 132(7): 1542-8.

Reimann, F., S. J. Tucker, et al. (1999). "Involvement of the n-terminus of Kir6.2 in coupling to the sulphonylurea receptor." J Physiol 518 (Pt 2): 325-36.

Ren, Y., X. Xu, et al. (2003). "Altered mRNA expression of ATP-sensitive and inward rectifier potassium channel subunits in streptozotocin-induced diabetic rat heart and aorta." J Pharmacol Sci 93(4): 478-83.

Repunte, V. P., H. Nakamura, et al. (1999). "Extracellular links in Kir subunits control the unitary conductance of SUR/Kir6.0 ion channels." Embo J 18(12): 3317-24.

Ribalet, B., S. A. John, et al. (2000). "Regulation of cloned ATP-sensitive K channels by phosphorylation, MgADP, and phosphatidylinositol bisphosphate (PIP(2)): a study of channel rundown and reactivation." J Gen Physiol 116(3): 391-410.

Ribalet, B., S. A. John, et al. (2003). "Molecular basis for Kir6.2 channel inhibition by adenine nucleotides." Biophys J 84(1): 266-76.

Riordan, J. R., J. M. Rommens, et al. (1989). "Identification of the cystic fibrosis gene: cloning and characterization of complementary DNA." Science 245(4922): 1066-73.

Rorsman, P. and G. Trube (1985). "Glucose dependent K^+-channels in pancreatic beta-cells are regulated by intracellular ATP." Pflugers Arch 405(4): 305-9.

Rovetto, M. J. (1979). "Energy metabolism in the ischemic heart." Tex Rep Biol Med 39: 397-407.

Rubin, L. J., L. Magliola, et al. (2005). "Metabolic activation of AMP kinase in vascular smooth muscle." J Appl Physiol 98(1): 296-306.

Russ, U., A. Hambrock, et al. (1999). "Coexpression with the inward rectifier K(+) channel Kir6.1 increases the affinity of the vascular sulfonylurea receptor SUR2B for glibenclamide." Mol Pharmacol 56(5): 955-61.

Rutter, G. A., G. Da Silva Xavier, et al. (2003). "Roles of 5'-AMP-activated protein kinase (AMPK) in mammalian glucose homoeostasis." Biochem J 375(Pt 1): 1-16.

Sakura, H., C. Ammala, et al. (1995). "Cloning and functional expression of cDNA encoding a novel ATP-sensitive potassium channel subunit expressed in pancreatic beta-cells, brain, heart and skeletal muscle." FEBS Lett 377(3): 338-44.

Salzman, A. L., A. Vromen, et al. (1997). "K(ATP)-channel inhibition improves hemodynamics and cellular energetics in hemorrhagic shock." Am J Physiol 272(2 Pt 2): H688-94.

Sambrook J, F. E., Maniatis T (1989). "A laboratory manual. Second Edition. Cold Spring Harbour Laboratory Press ed."

Sanger, F., S. Nicklen, et al. (1977). "DNA sequencing with chain-terminating inhibitors." Proc Natl Acad Sci U S A 74(12): 5463-7.

Saraya, A., M. Yokokura, et al. (2004). "Effects of fluoroquinolones on insulin secretion and beta-cell ATP-sensitive K^+ channels." Eur J Pharmacol 497(1): 111-7.

Satoh, E., M. Yamada, et al. (1998). "Intracellular nucleotide-mediated gating of SUR/Kir6.0 complex potassium channels expressed in a mammalian cell line and its modification by pinacidil." J Physiol 511 (Pt 3): 663-74.

Schwappach, B., N. Zerangue, et al. (2000). "Molecular basis for K(ATP) assembly: transmembrane interactions mediate association of a K^+ channel with an ABC transporter." Neuron 26(1): 155-67.

Seino, S. (1999). "ATP-sensitive potassium channels: a model of heteromultimeric potassium channel/receptor assemblies." Annu Rev Physiol 61: 337-62.

Seino, S. and T. Miki (2003). "Physiological and pathophysiological roles of ATP-sensitive K^+ channels." Prog Biophys Mol Biol 81(2): 133-76.

Selivanov, V. A., A. E. Alekseev, et al. (2004). "Nucleotide-gated K_{ATP} channels integrated with creatine and adenylate kinases: amplification, tuning and sensing of energetic signals in the compartmentalized cellular environment." Mol Cell Biochem 256-257(1-2): 243-56.

Sharma, N., A. Crane, et al. (1999). "The C terminus of SUR1 is required for trafficking of K_{ATP} channels." J Biol Chem 274(29): 20628-32.

Sharma, N., A. Crane, et al. (2000). "Familial hyperinsulinism and pancreatic beta-cell ATP-sensitive potassium channels." Kidney Int 57(3): 803-8.

Shi, N. Q., B. Ye, et al. (2005). "Function and distribution of the SUR isoforms and splice variants." J Mol Cell Cardiol 39(1): 51-60.

Shibasaki, T., Y. Sunaga, et al. (2004). "Interaction of ATP sensor, cAMP sensor, Ca2+ sensor, and voltage-dependent Ca2+ channel in insulin granule exocytosis." J Biol Chem 279(9): 7956-61.

Shyng, S., T. Ferrigni, et al. (1997). "Regulation of K_{ATP} channel activity by diazoxide and MgADP. Distinct functions of the two nucleotide binding folds of the sulfonylurea receptor." J Gen Physiol 110(6): 643-54.

Shyng, S., T. Ferrigni, et al. (1998). "Functional analyses of novel mutations in the sulfonylurea receptor 1 associated with persistent hyperinsulinemic hypoglycemia of infancy." Diabetes 47(1): 1145-51.

Shyng, S. and C. G. Nichols (1997). "Octameric stoichiometry of the K_{ATP} channel complex." J Gen Physiol 110(6): 655-64.

Shyng, S. L., C. A. Cukras, et al. (2000). "Structural determinants of PIP(2) regulation of inward rectifier K(ATP) channels." J Gen Physiol 116(5): 599-608.

Shyng, S. L. and C. G. Nichols (1998). "Membrane phospholipid control of nucleotide sensitivity of K_{ATP} channels." Science 282(5391): 1138-41.

Smit, L. S., D. J. Wilkinson, et al. (1993). "Functional roles of the nucleotide-binding folds in the activation of the cystic fibrosis transmembrane conductance regulator." Proc Natl Acad Sci U S A 90(21): 9963-7.

Sorrentino, R., R. d'Emmanuele di Villa Bianca, et al. (1999). "Involvement of ATP-sensitive potassium channels in a model of a delayed vascular hyporeactivity induced by lipopolysaccharide in rats." Br J Pharmacol 127(6): 1447-53.

Spruce, A. E., N. B. Standen, et al. (1985). "Voltage-dependent ATP-sensitive potassium channels of skeletal muscle membrane." Nature 316(6030): 736-8.

Standen, N. B. (2003). "K_{ATP} Channels in Vascular Smooth Muscle: Structure, Regulation and Functional Roles." J Clin Basic Cardiol 6: 7-14.

Standen, N. B., J. M. Quayle, et al. (1989). "Hyperpolarizing vasodilators activate ATP-sensitive K^+ channels in arterial smooth muscle." Science 245(4914): 177-80.

Stutts, M. J., C. M. Canessa, et al. (1995). "CFTR as a cAMP-dependent regulator of sodium channels." Science 269(5225): 847-50.

Sukhodub, A., S. Jovanovic, et al. (2007). "AMP-activated protein kinase mediates preconditioning in cardiomyocytes by regulating activity and trafficking of sarcolemmal ATP-sensitive K(+) channels." J Cell Physiol 210(1): 224-36.

Sun, X., K. Cao, et al. (2004). "Selective expression of Kir6.1 protein in different vascular and non-vascular tissues." Biochem Pharmacol 67(1): 147-56.

Surah-Narwal, S., S. Z. Xu, et al. (1999). "Block of human aorta Kir6.1 by the vascular K_{ATP} channel inhibitor U37883A." Br J Pharmacol 128(3): 667-72.

Suzuki, M., R. A. Li, et al. (2001). "Functional roles of cardiac and vascular ATP-sensitive potassium channels clarified by Kir6.2-knockout mice." Circ Res 88(6): 570-7.

Suzuki, M., N. Sasaki, et al. (2002). "Role of sarcolemmal K(ATP) channels in cardioprotection against ischemia/reperfusion injury in mice." J Clin Invest 109(4): 509-16.

Takano, M., D. Y. Qin, et al. (1990). "ATP-dependent decay and recovery of K^+ channels in guinea pig cardiac myocytes." Am J Physiol 258(1 Pt 2): H45-50.

Takano, M., L. H. Xie, et al. (1998). "Cytoplasmic terminus domains of Kir6.x confer different nucleotide-dependent gating on the ATP-sensitive K^+ channel." J Physiol 512 (Pt 2): 395-406.

Tanabe, K., S. J. Tucker, et al. (1999). "Direct photoaffinity labeling of the Kir6.2 subunit of the ATP-sensitive K^+ channel by 8-azido-ATP." J Biol Chem 274(7): 3931-3.

Tarasov, A., J. Dusonchet, et al. (2004). "Metabolic regulation of the pancreatic beta-cell ATP-sensitive K^+ channel: a pas de deux." Diabetes 53 Suppl 3: S113-22.

Taschenberger, G., A. Mougey, et al. (2002). "Identification of a familial hyperinsulinism-causing mutation in the sulfonylurea receptor 1 that prevents normal trafficking and function of K_{ATP} channels." J Biol Chem 277(19): 17139-46.

Teramoto, N. (2003). "Molecular and electrophysiological investigation of ATP-sensitive K^+ channels in lower urinary tract function: the aims for clinical treatment of unstable detrusor." Nippon Yakurigaku Zasshi 121(5): 317-24.

Teramoto, N and A.F. Brading (1996). "Activation by levcromakalim and metabolic inhibition of glibenclamide-sensitive K channels in smooth muscle cells of pig proximal urethra". Br J Pharmacol 118(3): 635-42

Teramoto, N., K. E. Creed, et al. (1997). "Activity of glibenclamide-sensitive K^+ channels under unstimulated conditions in smooth muscle cells of pig proximal urethra." Naunyn Schmiedebergs Arch Pharmacol 356(3): 418-24.

Teramoto, N., G. McMurray, et al. (1997). "Effects of levcromakalim and nucleoside diphosphates on glibenclamide-sensitive K^+ channels in pig urethral myocytes." Br J Pharmacol 120(7): 1229-40.

Teramoto, N., T. Tomoda, et al. (2002). "Modification of ATP-sensitive K^+ channels by proteolysis in smooth muscle cells from pig urethra." Life Sci 72(4-5): 475-85.

Teramoto, N., T. Tomoda, et al. (2006). "Different glibenclamide-sensitivity of ATP-sensitive K^+ currents using different patch-clamp recording methods." Eur J Pharmacol 531(1-3): 34-40.

Terzic, A. and Y. Kurachi (1996). "Actin microfilament disrupters enhance K(ATP) channel opening in patches from guinea-pig cardiomyocytes." J Physiol 492 (Pt 2): 395-404.

Terzic, A., R. T. Tung, et al. (1994). "Nucleotide regulation of ATP sensitive potassium channels." Cardiovasc Res 28(6): 746-53.

Thomas, P. M., G. J. Cote, et al. (1995). "Mutations in the sulfonylurea receptor gene in familial persistent hyperinsulinemic hypoglycemia of infancy." Science 268(5209): 426-9.

Thorne, H. V. (1966). "Electrophoretic separation of polyoma virus DNA from host cell DNA." Virology 29(2): 234-9.

Thorneloe, K. S., Y. Maruyama, et al. (2002). "Protein kinase C modulation of recombinant ATP-sensitive K(+) channels composed of Kir6.1 and/or Kir6.2 expressed with SUR2B." J Physiol 541(Pt 1): 65-80.

Thorneloe, K. S. and M. T. Nelson (2005). "Ion channels in smooth muscle: regulators of intracellular calcium and contractility." Can J Physiol Pharmacol 83(3): 215-42.

Trapp, S., S. Haider, et al. (2003). "Identification of residues contributing to the ATP binding site of Kir6.2." Embo J 22(12): 2903-12.

Trapp, S., S. J. Tucker, et al. (1997). "Activation and inhibition of K-ATP currents by guanine nucleotides is mediated by different channel subunits." Proc Natl Acad Sci U S A 94(16): 8872-7.

Trube, G. and J. Hescheler (1984). "Inward-rectifying channels in isolated patches of the heart cell membrane: ATP-dependence and comparison with cell-attached patches." Pflugers Arch 401(2): 178-84.

Tucker, S. J., F. M. Gribble, et al. (1998). "Molecular determinants of K_{ATP} channel inhibition by ATP." Embo J 17(12): 3290-6.

Tucker, S. J., F. M. Gribble, et al. (1997). "Truncation of Kir6.2 produces ATP-sensitive K^+ channels in the absence of the sulphonylurea receptor." Nature 387(6629): 179-83.

Tung, R. T. and Y. Kurachi (1991). "On the mechanism of nucleotide diphosphate activation of the ATP-sensitive K^+ channel in ventricular cell of guinea-pig." J Physiol 437: 239-56.

Ueda, K., N. Inagaki, et al. (1997). "MgADP antagonism to Mg2+-independent ATP binding of the sulfonylurea receptor SUR1." J Biol Chem 272(37): 22983-6.

Ueda, K., J. Komine, et al. (1999). "Cooperative binding of ATP and MgADP in the sulfonylurea receptor is modulated by glibenclamide." Proc Natl Acad Sci U S A 96(4): 1268-72.

Unger, T., O. Chung, et al. (1996). "Angiotensin receptors." J Hypertens Suppl 14(5): S95-103.

Van Wagoner, D. R. and M. Lamorgese (1994). "Ischemia potentiates the mechanosensitive modulation of atrial ATP-sensitive potassium channels." Ann N Y Acad Sci 723: 392-5.

Vanoye, C. G., G. G. MacGregor, et al. (2002). "The carboxyl termini of K(ATP) channels bind nucleotides." J Biol Chem 277(26): 23260-70.

Vergani, P., S. W. Lockless, et al. (2005). "CFTR channel opening by ATP-driven tight dimerization of its nucleotide-binding domains." Nature 433(7028): 876-80.

Vivaudou, M. and C. Forestier (1995). "Modification by protons of frog skeletal muscle K_{ATP} channels: effects on ion conduction and nucleotide inhibition." J Physiol 486 (Pt 3): 629-45.

Weese-Mayer, D. E., M. J. Ackerman, et al. (2007). "Sudden Infant Death Syndrome: review of implicated genetic factors." Am J Med Genet A 143(8): 771-88.

Weiss B, J.-S. A., Live TR, Fareed GC, Richardson CC (1968). "Enzymatic breakage and joining of deoxyribonucleic acid. VI. Further purification and properties of polynucleotide ligase from *Escheria coli* infected with bacteriophage T4." J.Biol.Chem. 243: 4543-4555.

Weiss, J. N. and S. T. Lamp (1989). "Cardiac ATP-sensitive K^+ channels. Evidence for preferential regulation by glycolysis." J Gen Physiol 94(5): 911-35.

Wellman, G. C., R. Barrett-Jolley, et al. (1999). "Inhibition of vascular K(ATP) channels by U-37883A: a comparison with cardiac and skeletal muscle." Br J Pharmacol 128(4): 909-16.

Wilson, A. J., R. I. Jabr, et al. (2000). "Calcium modulation of vascular smooth muscle ATP-sensitive K(+) channels: role of protein phosphatase-2B." Circ Res 87(11): 1019-25.

Wilson, C. (1989). "Inhibition by sulphonylureas of vasorelaxation induced by K^+ channel activators in vitro." J Auton Pharmacol 9(1): 71-8.

Woods , A.D. Azzout-Marniche, et al. (2000). "Characterisation of the role of AMP-activated protein kinase in the regulation of glucose-activated gene expression using constitutively active and dominant negative forms of the kinase". Mol Cell Biol 20(18): 6704-11.

Woollhead, A. M., J. W. Scott, et al. (2005). "Phenformin and 5-aminoimidazole-4-carboxamide-1-beta-D-ribofuranoside (AICAR) activation of AMP-activated protein kinase inhibits transepithelial Na+ transport across H441 lung cells." J Physiol 566(Pt 3): 781-92.

Wu, C. C., C. Thiemermann, et al. (1995). "Glibenclamide-induced inhibition of the expression of inducible nitric oxide synthase in cultured macrophages and in the anaesthetized rat." Br J Pharmacol 114(6): 1273-81.

Xu, J., X. Wang, et al. (2001). "Ion-channel assay technologies: quo vadis?" Drug Discov Today 6(24): 1278-1287.

Xu, R. H., H. Pelicano, et al. (2005). "Inhibition of glycolysis in cancer cells: a novel strategy to overcome drug resistance associated with mitochondrial respiratory defect and hypoxia." Cancer Res 65(2): 613-21.

Yaffe, D. and O. Saxel (1977). "Serial passaging and differentiation of myogenic cells isolated from dystrophic mouse muscle." Nature 270(5639): 725-7.

Yamada, M., S. Isomoto, et al. (1997). "Sulphonylurea receptor 2B and Kir6.1 form a sulphonylurea-sensitive but ATP-insensitive K^+ channel." J Physiol 499 (Pt 3): 715-20.

Yamada, M. and Y. Kurachi (2004). "The nucleotide-binding domains of sulfonylurea receptor 2A and 2B play different functional roles in nicorandil-induced activation of ATP-sensitive K^+ channels." Mol Pharmacol 65(5): 1198-207.

Yamada, M. and Y. Kurachi (2005). "A functional role of the C-terminal 42 amino acids of SUR2A and SUR2B in the physiology and pharmacology of cardiovascular ATP-sensitive K(+) channels." J Mol Cell Cardiol 39(1): 1-6.

Yan, F., C. W. Lin, et al. (2004). "Sulfonylureas correct trafficking defects of ATP-sensitive potassium channels caused by mutations in the sulfonylurea receptor." J Biol Chem 279(12): 11096-105.

Yokoshiki, H., M. Sunagawa, et al. (1998). "ATP-sensitive K^+ channels in pancreatic, cardiac, and vascular smooth muscle cells." Am J Physiol 274(1 Pt 1): C25-37.

Zerangue, N., B. Schwappach, et al. (1999). "A new ER trafficking signal regulates the subunit stoichiometry of plasma membrane K(ATP) channels." Neuron 22(3): 537-48.

Zhang, H. and T. B. Bolton (1995). "Activation by intracellular GDP, metabolic inhibition and pinacidil of a glibenclamide-sensitive K-channel in smooth muscle cells of rat mesenteric artery." Br J Pharmacol 114(3): 662-72.

Zhang, H. L. and T. B. Bolton (1996). "Two types of ATP-sensitive potassium channels in rat portal vein smooth muscle cells." Br J Pharmacol 118(1): 105-14.

Zhang, L., H. He, et al. (2007). "Metformin and phenformin activate AMP-activated protein kinase in the heart by increasing cytosolic AMP concentration." Am J Physiol Heart Circ Physiol 293(1): H457-66.

Zhuo, M. L., Y. Huang, et al. (2005). "K_{ATP} channel: relation with cell metabolism and role in the cardiovascular system." Int J Biochem Cell Biol 37(4): 751-64.

Zingman, L. V., A. E. Alekseev, et al. (2001). "Signaling in channel/enzyme multimers: ATPase transitions in SUR module gate ATP-sensitive K^+ conductance." Neuron 31(2): 233-45.

Zingman, L. V., D. M. Hodgson, et al. (2002). "Tandem function of nucleotide binding domains confers competence to sulfonylurea receptor in gating ATP-sensitive K^+ channels." J Biol Chem 277(16): 14206-10.